

Republic of Iraq
Ministry of High Education
And Scientific Research
University of Technology
Department Of Production
And Metallurgy Eng.



Analysis and Application of Subdivision Surfaces

A thesis submitted

By
Mukdam Habib Shamoon kena

to the Department of Production and Metallurgy Engineering of
University of Technology
In partial fulfillment of the requirements for the degree of Master of
Science in Production Engineering

Supervised by:

Dr. Laith A. Mohammed

Dr. Kasim A. Khalaf

July 2007

*In the name of the Father, Son, and Holy Spirit,
one God Amen*

"No-one lights a lamp and puts it in a place where it will be hidden, or under a bowl. Instead he puts it on its stand, so that those who come in may see the light. Your eye is the lamp of your body. When your eyes are good, your whole body also is full of light.

But when they are bad, your body also is full of darkness. See to it, then, that light within you is not darkness. Therefore, if your whole body is full of light, and no part of it dark, it will be completely lighted, so when the light of lamp shines on you."

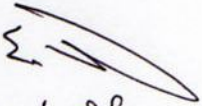
(LUKE 11:33-36)

Certificate of the Linguistic supervisor

I certify that this thesis entitled (*Analysis and Application of Subdivision Surfaces*) was prepared under my linguistic supervision.

Its language was amended to meet the style of the English language.

Signature:



Name: *Eyad Shamuldeen*

Date: *4 / 8 / 2007*

Supervisory Committee Approval

We, certify that this thesis entitled

Analysis and Application of Subdivision Surfaces

has been conducted under our supervision in a partial fulfillment of the requirements for the Master Degree at the Department of Production and Metallurgy Engineering of University of Technology, Baghdad.



Signature:

Dr. Laith A. Mohammed

*Dept. of Production and Metallurgy Engineering
University of Technology*

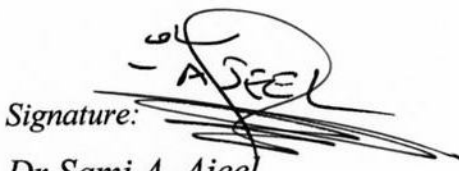


Signature:

Dr. Kasim A. Khalaf

*Dept. of Mechanical
University of Technology*

In view of the available recommendations I forward this thesis for debate by the Examining Committee.



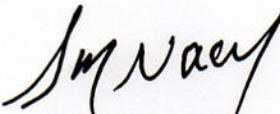
Signature:

Dr. Sami A. Ajeel

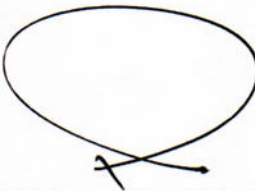
*Dept. of Production and Metallurgy Engineering
University of Technology*

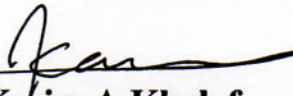
Certification of the Examination Committee

We certify that we have read the thesis entitled (*Analysis and Application of Subdivision Surfaces*) and as an examining committee, examined the student (*Mukdam Habib Shamooun Kena*) in its contents and that in what is connected with it, that in our opinion it meets the standard of thesis for the degree of master of Science in production Engineering.

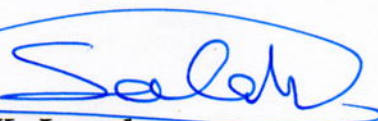
Signature: 
Ass. Prof. **Dr. Somer M. Nancy**
University of Baghdad
Date : 10/10/2007
(Chairman)

Signature: 
Ass. Prof. **Dr. Wathik Issa Mahdi**
University of Technology
Date : 10/10/2007
(Member)

Signature: 
Lecturer **Dr. Saad Kariem Shather**
University of Technology
Date : 10/10/2007
(Member)

Signature: 
Lecturer **Dr. Kasim A. Khalaf**
University of
Date : 10/10/2007
(Supervisor)

Approved by the Department of Production Engineering and Metallurgy,
University of Technology, Baghdad-Iraq.

Signature: 
Dr. Salah K. Jawad
Head of Department of Production and Metallurgy Engineering.
Date: 11/10/2007

Dedication

To my parents,
For their constant love and support.

Acknowledgement

I am deeply indebted to my advisor **Dr. Laith Abdullah** for his suggestions, supervision and guidance have been invaluable to the completion of this dissertation, and will long be treasured and greatly appreciated. No words in this world are adequate to express my gratitude.

With respect and gratitude, I wish to thank **Mr. Jan Philipp Hakenberg** for his support, encouragement and patience, he let me understand the guideline for the subdivision algorithm, explain the complex mathematical problem, and make programming for subdivision algorithm, toolpath generation, and the most programs on chapter five, and he work as guarantor when I negotiated with Technical University Darmstadt (Germany), that before he make search to find the best place to do the practical part for my thesis, the best word to describe this man is " the spiritual father for this thesis".

I'm very much obliged to the Head of Production Engineering and Metallurgy Department, for his assistance throughout the research. Also I express my gratefulness to the Department staff members for their help.

Researcher

Abstract

This thesis focuses on the computer aided design, manufacturing, (CAD/CAM), Subdivision algorithm, and the dies design theory like Constant Ratios of Successive Generalized Homogeneous Strain Increments (CRHS).

The representation of surfaces in smooth, parametric form is of central importance in mechanical engineering. In order to machine a shape using a computer, it is necessary to produce a computer-compatible description of that shape.

A comparison has been made between the surfaces generated by CRHS method and the surfaces generated by approximation techniques (Quartic Uniform B-spline technique and Quantic Uniform B-spline technique).

An Extrusion die profile is preliminary example which has been manufactured by CNC-milling process. The output surfaces from the Chaitian's subdivision algorithm which are employed in this thesis are highly efficient and accurate especially in 3D surfaces.

In this research, the Chaitian's Subdivision algorithm has been adopted and developed in Uniform B-spline technique case, to find the optimum cutter radius, so optimum cutter radius result (semi surface finishing process) for Die profile surface generated by CRHS method is (4mm), while for the surface generated by Quartic Uniform B-spline technique it is (5mm), and for the surface generated by Quantic Uniform B-spline technique it is (3mm), these results improve the surface accuracy of machining when the subdivision iteration increases, and that affects directly the side step design, which leads to change the toolpath length and design.

The interior data of the desired surfaces, designed by Matlab Software which have been transformed to Surfcam software to get the machining

process simulation and G-code programs for the three samples (designed by CRHS and approximation method); this G-code program has been designed to 3-axis FANUC 15 MB system.

The G-code programs have been implemented on CNC machine (Hermle C30U dynamic, 5-axis AC-kinematics, and the samples material is UREOL (Epoxy Resin), the machining process is achieved without a Lubricant.

Title	Page No.
Abstract	I
Contents	III
List of Abbreviations	VI
List of Symbols	VII
List of Figure	VIII
List of Table	XIII

Chapter One

Introduction

1.1 Introduction	1
1.2 CAD System	2
1.2.1 Surface Modeling	3
1.2.1.1 Polygon Mesh	3
1.2.1.2 Parametric Bicubic Patches	4
1.3 CAM System	7
1.4 Application of CAD/CAM in Metal Forming	7
1.5 Subdivision Algorithms	8
1.6 Constancy of the Ratio of the Successive Generalized Homogeneous Strain-increment (CRHS) Concept.	9
1.7 Aim of This Research	11

Chapter Two

Literature Survey

2.1 Introduction	12
2.2 Subdivision Algorithms	12
2.3 Analysis Subdivision Algorithms	18
2.4 Applications of Subdivision Algorithms	19
2.5 Listing the practical part for this thesis with respect to previous literature survey	21

Chapter Three

Bezier and Uniform B-spline Technology

3.1 Approximation of Curves and Surfaces	22
3.2 Bezier Curves	24
3.2.1 Bezier Curve Properties	25
3.3 Bezier Surfaces	32
3.4 B-spline Curve	38
3.4.1 B-spline Properties	39
3.5 B-spline Surfaces	41
3.6 Chapter Summary	45

Chapter Four

Subdivision Algorithms

4.1 Introduction	46
4.2 Curves Subdivision	47
4.2.1 Subdivision and Refinement Uniform B-spline Curve	47
4.2.2 Subdivision and Refinement of Bezier Curve	56
4.3 Uniform B-spline Surface Refinement	61
4.4 Bezier Surface Refinement	77
4.5 Loop Subdivision Scheme	85
4.6 The Butterfly Scheme	86
4.7 Hexagon Subdivision Surface	87
4.8 Catmull-Clark	89
4.9 Doo-Sabin	90
4.10 Chapter Summary	91

Chapter Five

Testing Subdivision Algorithm in Production Field

5.1 Dies Designed According Rational Concepts	94
5.1.1 Constant Ratios of Successive Generalized Homogeneous Strain Increments (CRHS)	95
5.2 Curvature Algorithm	100
5.3 Radius of Curvature	101
5.4 Toolpath Design	103
5.5 Cutting Conditions for Experiential Part	126

Chapter Six

Conclusions and Suggestions

For Future Work

6.1 Conclusions	129
6.2 Suggestion of Future Work	131

References	132
-------------------	-----

Appendices

Appendix A	137
Appendix B	145
Appendix C	149
Appendix D	152
Appendix E	155

Abbreviations	Definition
2D	Two Dimension.
3D	Three Dimension.
CAD	Computer-Aided Design.
CAM	Computer-Aided Manufacturing.
CAD/CAM	Computer-Aided Design and Manufacturing.
CNC	Computer Numerical Control.
IGES	Initial Graphics Exchange Specification.
STEP	Standard for the Exchange of Product Model Data.
NC	Numerical Control.
NURBS	Non-uniform rotational B-spline curves.
CRHS	Constancy of the Ratio of the successive generalized Homogeneous Strain-increment.
DCRHS	Decelerated Constancy of the Ratio of the successive generalized Homogeneous Strain-increment.
ACRHS	Accelerated Constancy of the Ratio of the successive generalized Homogeneous Strain-increment.
UCRHS	Uniform Constancy of the Ratio of the successive generalized Homogeneous Strain-increment.
PN	Point-normal.
EV	Extraordinary vertices.
ER	Extraordinary rules.
IFS	Iterated Function Systems.
FIN	Faired interpolating NURBS.
DXF	Data Exchange Format.
NCC	Numerical Control Code
HSS	High Speed Steel.
CMSR	The Constancy of the Mean Strain Rate.

Symbol	Definition
S	Rate of Deformation.
C_1	First surface continuity.
C_2	Second surface continuity.
n	Polynomial degree.
$B_{i,n}$	Bezier coefficient.
Δu	Incremental value in u-direction.
Δw	Incremental value in w-direction.
T	The number of knots.
K	B-spline order.
$N_{i,k}$	B-Spline coefficient.
$P_{i,j}$	Control points.
S_L	Splitting matrix for the left half of the curve or surface.
S_R	Splitting matrix for the right half of the curve or surface.
$\dot{\epsilon}$	The mean strain rate.
ϵ_{hn}	The homogeneous strain at any section (n) for die profile.
H	Mean curvature.
ρ_{min}	The minimum radius of curvature of the over all surface.
R_f	Radius of finishing cutter.
H	Scallop height.
s	The value of stepover
L	Distance from Die inlet.

Figure	Title	Pag.No.
(1.1.a)	3-D surface modeling (Polygon mesh).	4
(1.1.b)	3-D surface modeling (Hermite bicubic surface).	5
(1.1.c)	3-D surface modeling (Bezier bicubic surface).	5
(1.1.d)	3-D surface modeling (B-spline bicubic surface).	6
(1.2)	The compounds die (CRHS) surface profile along the die inlet-exit.	10
(3.1.a)	Bezier curve with three control points $n=2$ (regular control points).	26
(3.1.b)	Bezier curve with three control points $n=2$ (irregular control points).	26
(3.2.a)	Bezier curve with four control points $n=3$ (regular control points).	28
(3.2.b)	Bezier curve with four control points $n=3$ (regular control points).	28
(3.3)	Bezier curve with five control points $n=4$	29
(3.4)	Bezier curve with six control points $n=5$.	30
(3.5)	Bezier curve with seven control points $n=6$.	31
(3.6)	Block diagram of the proposed program depending on Bezier technique.	33
(3.7)	Flowchart of the proposed program depending on Bezier technique.	34
(3.8)	Bezier Surface (2nd degree), $n=2$, Matrix form (3x3).	35
(3.9)	Bezier Surface (3rd degree), $n=3$, Matrix form (4x4).	35
(3.10)	Bezier Surface (4th degree), $n=4$, Matrix form (5x5).	36
(3.11)	Bezier Surface (5th degree), $n=5$, Matrix form (6x6).	36
(3.12)	Bezier Surface (6 th degree), $n=6$, Matrix form (7x7) with Control points. a-Control polygon for Bezier surface with Matrix form (7x7). b-Bezier surface (6 th degree), $n=6$. c- Bezier Surface (6 th degree), $n=6$, with control polygon for Matrix form (7x7) with Control points.	37
(3.13)	B-spline curve (2nd degree), $k=3$, Matrix form (3x3) with Control points.	40
(3.14)	Block diagram of the proposed program depending on Uniform B-spline technique.	42
(3.15)	Flowchart of the proposed program depending on Uniform B-spline technique.	43
(3.16)	Uniform B-spline surface $k=3$, (3x3).	44

(3.17)	Uniform B-spline surface $k=4$, (4×4) .	44
(4.1)	Quadratic uniform B-spline curve (three control points).	48
(4.2)	The first subdivides stage for the control points to Uniform B-spline Curve	49
(4.3)	The Second subdivide stage for the control points to Uniform B-spline Curve	52
(4.4)	The Third subdivides stage for the control points to quadratic Uniform B-spline Curve.	54
(4.5)	The Fourth subdivides stage for the control points to quintic Uniform B-spline Curve.	55
(4.6)	Bezier curve before using the splitting matrixes to subdivide the control points.	58
(4.7)	Bezier curve after using the left splitting matrixes to subdivide the control points	59
(4.8)	Bezier curve after using the right splitting matrixes to subdivide the control points.	60
(4.9)	Bezier curve after using both (right and left) splitting matrixes to subdivide the control points.	60
(4.10)	Initial control polygon for the quadratic Uniform B-spline	62
(4.11)	Initial control polygon for the quadratic Uniform B-spline surface and the subdivide polygon when $u' = \frac{u}{2}$ and $w' = \frac{w}{2}$.	65
(4.12)	Subdivision masks	66
(4.13)	Initial control polygon for the cubic Uniform B-spline surface	68
(4.14)	Initial control polygon for the cubic Uniform B-spline surface, and the splitting control points (control polygon) with subdivide the cubic Uniform B-spline surface	72
(4.15)	Block diagram of the proposed program depending on refinement Uniform B-spline technique.	75
(4.16)	Flowchart of the proposed program depending on refinement Uniform B-spline Surfaces.	76
(4.17)	Initial control polygon for the cubic Bezier surface.	80
(4.18)	Initial control polygon for the cubic Bezier surface, and the splitting the left control polygon when used SL matrix.	80
(4.19)	Initial control polygon for the cubic Bezier surface, and the splitting the right control polygon when used SR matrix.	81
(4.20)	Initial control polygon for the cubic Bezier surface, and the splitting the right and left control polygon when used SL and SR matrix.	81
(4.21)	Block diagram of the proposed program depending on refinement Bezier technique.	83
(4.22)	Flowchart of the proposed program depending on refinement Bezier Surfaces.	84
(4.23)	Four steps in the subdivision of a triangle.	85
(4.24)	Rules for extraordinary vertices and boundaries.	86

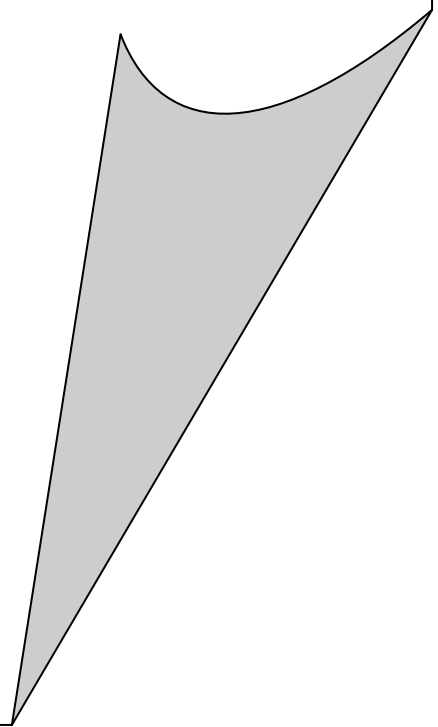
(4.25)	Situation around a newly inserted edge point for the interpolator Butterfly scheme	87
(4.26)	The position of the new point P is a weighted average of the points of the surrounding hexagon	88
(4.27)	Subdivision around a central vertex V_0 , showing surrounding control points (Q_i), edge points (E_i) and face points (F_i).	89
(4.28)	Left: An input polygon with surrounding edges. Right: The new faces created by one subdivision step of the Doo-Sabin algorithm.	90
(5.1)	The geometric shape (for the Forward Extrusion) dies profile designed by CRHS.	99
(5.2)	The shape for the Die, and the way to divide the Die profile to (n) sections (for Forward Extrusion), to design the Geometric shape for the Die by CRHS concepts	99
(5.3)	The sphere shape which explains the difference in the curvature value when the circles radius is different and the curvature has constant value at the same radius value.	101
(5.4)	The radius of curvature for some points on the designed profile	102
(5.5)	The tool-paths in XZ-plan (Front View)	103
(5.6)	Ball-end mill surface machining	105
(5.7)	Bezier surface $n=3$	106
(5.8: a, b)	Figure (5.8: a, b): Three dimension toolpath a- In U-direction. b- In w-direction.	107
(5.9)	Design the Geometric shape for the Die profile by CRHS concepts, the shape result is DCRHS, (for Forward Extrusion)	109
(5.10)	Geometric Die design for Forward Extrusion process depends on CRHS concepts with Die profile length 13mm	110
(5.11)	Drawing the Geometric shape for the Die profile which is designed by CRHS concepts, the shape result is DCRHS, (for Forward Extrusion), drawing by Quartic Subdivision for Uniform B-spline Curve.	110
(5.12)	Geometric Die design for Forward Extrusion process depends on CRHS concepts with Die profile length 13mm drawing by Quartic Subdivision for Uniform B-spline Curve.	111
(5.13)	Drawing the Geometric shape for the Die profile which is designed by CRHS concepts, the shape result is DCRHS, (for Forward Extrusion), drawing by Quintic Subdivision for Uniform B-spline Curve.	111
(5.14)	Geometric Die design for Forward Extrusion process depends on CRHS concepts with Die profile length 13mm drawing by Quintic Subdivision for Uniform B-spline Curve.	112

(5.15)	Find the difference in the shape geometry for these three curves (CRHS curve, Quartic Subdivision for Uniform B-spline Curve, and Quintic Subdivision for Uniform B-spline Curve)	112
(5.16)	The mean curvature. a- Main curvature for CRHS method. b- Main curvature for Quartic Subdivision for Uniform B-spline technical. c- Main curvature for Quintic Subdivision for Uniform B-spline technical.	114
(5.17)	The radius of curvature drawing. a- The radius of curvature for CRHS method. b- The radius of curvature for Quartic Subdivision for Uniform B-spline technical. c- The radius of curvature for Quintic Subdivision for Uniform B-spline technical.	115
(5.18)	Figure (5.18: a, b, and c): The toolpath generated. a- The toolpath for CRHS method. b- The toolpath for Quartic Subdivision for Uniform B-spline technical. c- The toolpath for Quintic Subdivision for Uniform B-spline technical.	116
(5.19)	The cutter ball dimension. a- The cutter dimension for CRHS method. b- The cutter dimension for Quartic Subdivision for Uniform B-spline technical. c- The cutter dimension for Quintic Subdivision for Uniform B-spline technical.	117
(5.20)	The deviation between the desired surface and surface after machined. a- The Deviation for surface generated by CRHS method. b- The Deviation for surface generated by Quartic Subdivision for Uniform B-spline technical. c- The Deviation for surface generated by Quintic Subdivision for Uniform B-spline technical.	118
(5.21)	The deviation between the desired surface and the machined surface at $x=5, 15,$ and 30 for surface generated by CRHS method.	119
(5.22)	The deviation between the desired surface and the machined surface at $x=5, 15,$ and 30 for surface generated by using Quartic subdivision algorithm to Uniform B-spline technical.	119
(5.23)	The deviation between the desired surface and the machined surface at $x=5, 15,$ and 30 for surface generated by using Quintic subdivision algorithm to Uniform B-spline technical.	120
(5.24)	The line segment for toolpath generated by CRHS method.	120
(5.25)	The line segment for toolpath generated by Quintic subdivision algorithm to uniform B-spline technical.	121

(5.26)	The line segment for toolpath generated by Quartic subdivision algorithm to uniform B-spline technical.	121
(5.27)	Import the DXF file extension to Surfam design file.	122
(5.28)	The stock base is XY-plane, the Z-direction is cutting direction, and the zero coordinates in the stock corner	124
(5.29)	Toolpath verification and G-code program for CRHS method die profile.	124
(5.30)	The semi finishing for the surfaces machined by Surfcam Software. a- The semi finishing surface generated by CRHS method. b-The semi finishing surface generated by Quartic Subdivision to Uniform B-spline technical. c-The semi finishing surface generated by Quintic Subdivision to Uniform B-spline technical.	125
(5.31)	CNC machine (Hermle C30U dynamic, 5-axis AC-kinematics) which belongs to UT Darmstadt University (Germany University)	126
(5.32)	The samples result from Machining process by CNC milling machine. a-Sample designed by CRHS method and machined with cutter radius R 4mm. b-Sample designed by Quintic Subdivision for Uniform B-spline technical and machined with cutter radius R 3mm. c-Sample designed by Quartic Subdivision for Uniform B-spline technical and machined with cutter radius R 5mm.	127
(5.33)	The samples result from Machining process by CNC milling machine. a-Sample designed by CRHS method and machined with cutter radius R 4mm. b-Sample designed by Quartic Subdivision for Uniform B-spline technical and machined with cutter radius R 5mm. c-Sample designed by Quintic Subdivision for Uniform B-spline technical and machined with cutter radius R 3mm.	128

Table	Title	Pag.No.
(1.1)	Make comparison between the surfaces (relation between the surface and the control points.)	6
(4.1)	Classification of the subdivision surface algorithm.	91
(5.1)	Calculate the R, Z, at every L for Forward Extrusion Die Profile by CRHS concept	109
(5.2)	The result Comparison between the surfaces presented above.	113
(5.3)	Surfcam cutting options summary sheet	123

CHAPTER ONE
INTRODUCTION



CHAPTER ONE

Introduction

1.1 Introduction

CAD/CAM (computer-aided design/computer-aided manufacturing) systems are an application to development of traditional design and manufacturing function. CAD is the part where the products are being designed with the help of computers, while CAM systems are those involving the efficient use of computer technology in the planning, management and control of the manufacturing function. The link between CAD/CAM is achieved with the use of computerized environment. The application of CAM in the manufacturing can be either "off-line" in which case the computer does not have direct connection with the process and the "On-line" in which the computer is directly connected with the process, controls the production, directs the machines and also receives information about current status, problems, breakdowns or needs^[1].

Computer - aided design "CAD" can be most simply described as "using a computer in the design process". It involves any type of design activity which makes use of the computer to develop, analyze or modify an engineering design.

A "CAD" system consists of three major parts:-

1. Hardware: - computer and input / output.
2. Operating system software.
3. Application software: - CAD package.

The graphics software such as "DXF format" used in this research is the collection of programs written to make it convenient for a user to operate the computer graphics system.

The most basic functions of AutoCAD are the 2D drafting functions. 2D geometry such as lines, circles, curves and so on can be defined. Precise 2D drawing capabilities and a full range of drafting functions such as "automatic dimensioning of drawings" provide powerful tools for

draftsmen in creating technical drawings or engineering plans. Also, the power of the computer in storing and manipulating large amounts of data can be used to replace large drawing vaults and archiving facilities with electronic forms of data storage, such as magnetic tapes ^[2].

1.2 CAD System

Computer-Aided Design system (CAD) is defined as the involvement of the computer into design activities and very often is associated with the use of interactive computer graphics system. There are many advantages in using a CAD system such as:

- It increases the productivity of the designer. CAD systems aid the designer to conceptualize the product more easily thus reducing the time needed for synthesizing.
- It improves the quality of the design by enabling the designer to perform more complicated engineering analysis and consider a larger number of design alternatives.
- It improves design documentation. The graphical output of a CAD system is superior to manual drafting, fewer errors and drawings standardization results in better documentation.
- It creates a manufacturing database during the creation of the product design documentation such as dimensions. Much of the required data base to manufacture the product is also created.

In the CAD system there are many processes that must be followed to design a new product; one of the processes related to this work is Geometric modeling ^[3].

1.2.1 Surface Modeling

Surface modeling is a graphical technique used to define and describe surfaces. A wire frame model can only describe the edges or boundaries of a part. Points between the boundaries of a part cannot be defined with wire frames. Surface models define not only the edges of a part, but also the surface between edges. Surface models are usually produced after the wire frame boundaries have been created. The surface between the wireframe boundaries is then defined. After the surface is defined it can be displayed with or without hidden lines. Each surface can be shaded in different tones of gray or colors. There are two basic approaches to 3-D surface modeling^[3]:

1. Polygon Mesh
2. Parametric Bicubic Patches.

1.2.1.1 Polygon Mesh

A Polygon mesh is a set of connected polygons which form bounded planar surfaces. Figure (1.1.a) illustrates polygon mesh. The exterior of most structures can be represented by a polygon mesh. The main disadvantage of this method is that the representation is only approximate. Polygon mesh is a collection of edges, vertices and polygons. Vertices are connected by edges, and the polygons can be thought of as sequences of edges or vertices. There are three ways of defining a polygon:

- a) By vertex coordinates
- b) By pointing into a vertex list
- c) By pointing into an edge list.

Among these, the third one is the best for consistency testing, since it contains the most information. The edges are shared in many structural models^[3].

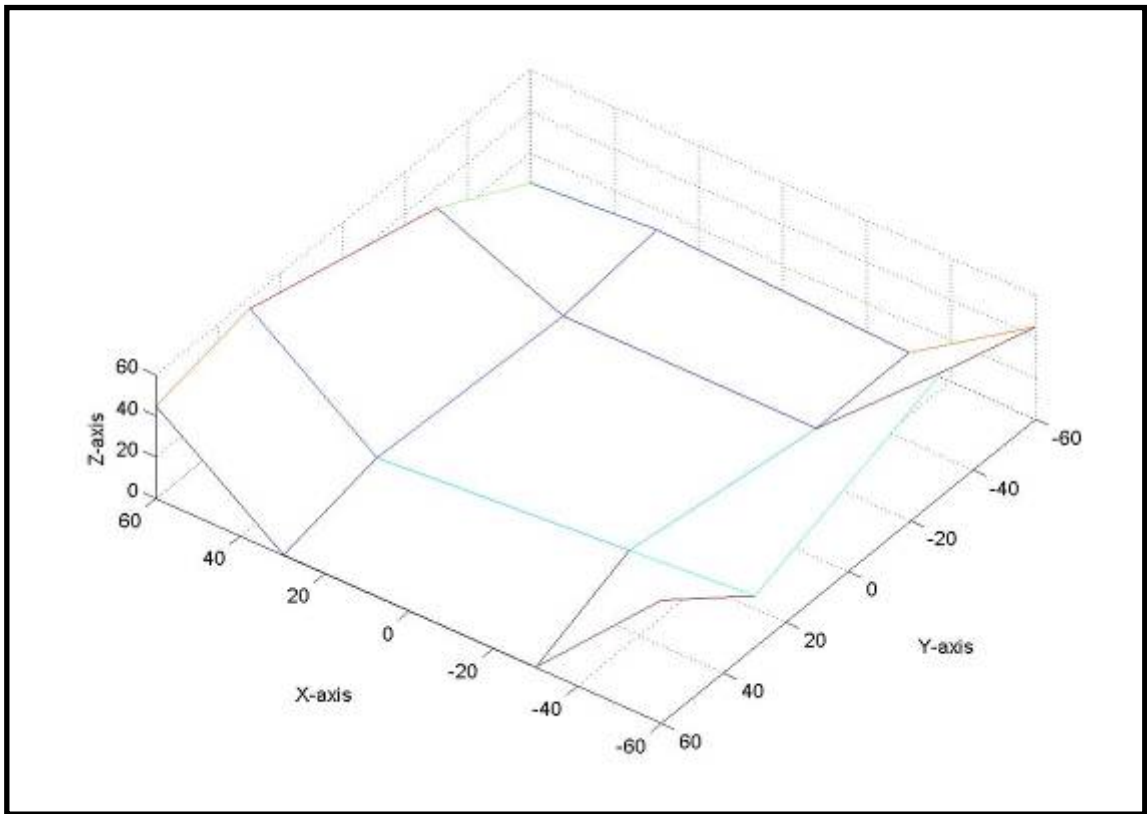


Figure (1.1.a): 3-D surface modeling (Polygon mesh).

1.2.1.2 Parametric Bicubic Patches

Parametric Bicubic Patches define the coordinates of points on a curved surface in terms of bicubic (two cubic) equations. The boundaries of the patch are parametric cubic curves. Fewer bicubic patches than polygonal patches are needed to represent curved surface for fixed accuracy.

- a) Interpolation method ^[3].
 $x = x, y = f(x), z = g(x)$
- b) Parametric representation ^[3].

$$\left. \begin{aligned}
 X(t) &= a_x t^3 + b_x t^2 + c_x t + d_x \\
 Y(t) &= a_y t^3 + b_y t^2 + c_y t + d_y \\
 Z(t) &= a_z t^3 + b_z t^2 + c_z t + d_z
 \end{aligned} \right\} \dots\dots\dots(1.2)$$

There are three important parametric cubic curves:

- Hermite Method. Figure (1.1.b) illustrates Hermite bicubic surface.
- Bezier Technique. Figure (1.1.c) illustrates Bezier bicubic surface.
- B-spline Method. Figure (1.1.d) illustrates B-Spline bicubic surface.

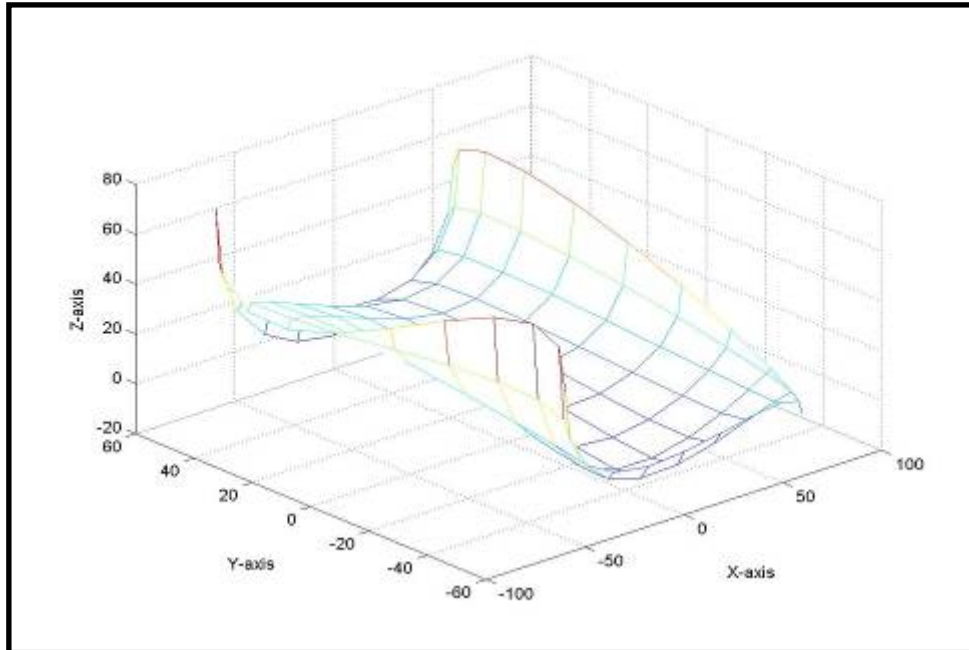


Figure (1.1.b) 3-D surface modeling (Hermite bicubic surface).

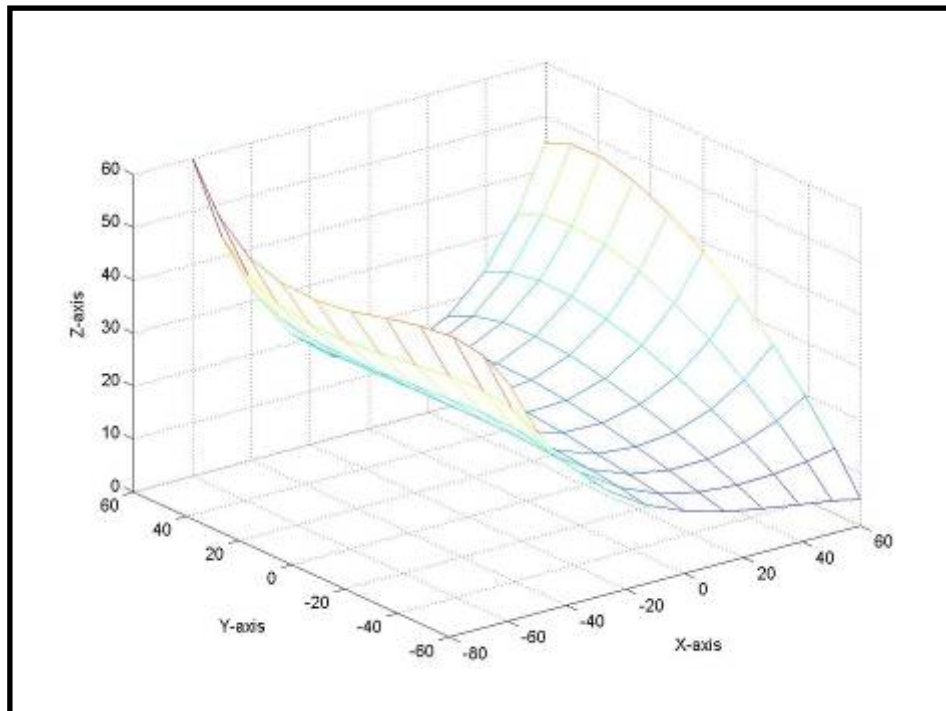


Figure (1.1.c): 3-D surface modeling (Bezier bicubic surface).

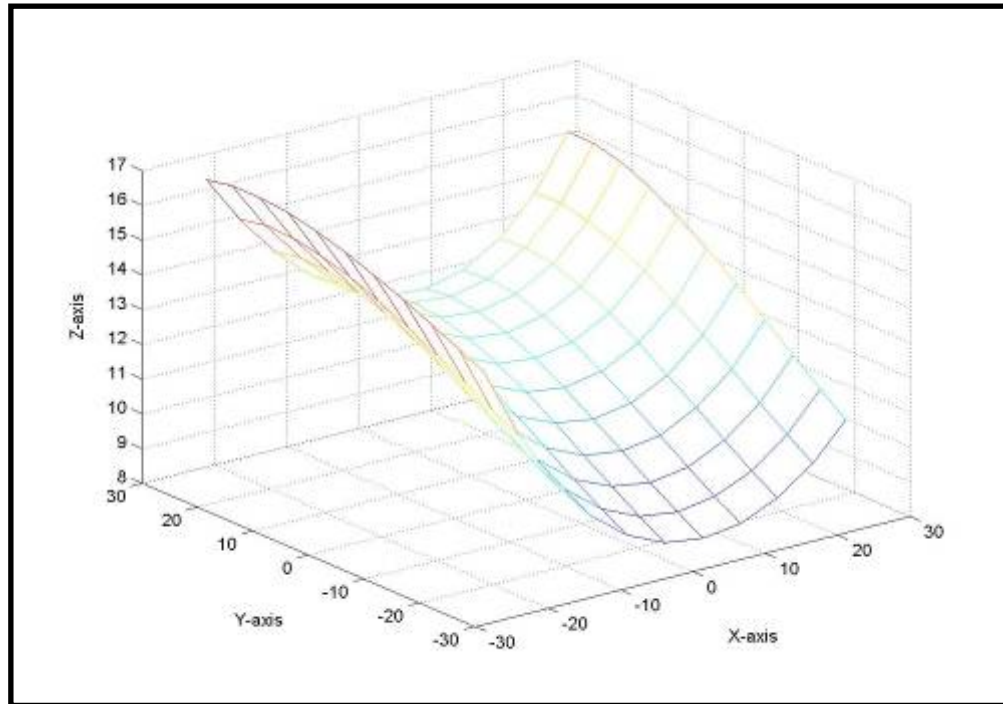


Figure (1.1.d): 3-D surface modeling (B-spline bicubic surface).

Table (1.1): Make comparison between the surfaces (relation between the surface and the control points.)

NO#	Surface type		
	Bezier	Uniform B-spline	Hermite
1	The surface follows the shape of the control point polygon and this point is sensitive in this surface type.	The curve follows the shape of the control point polygon and is constrained to lie in the convex hull of the control points.	The surface follows the shape of the control point polygon and this point is insensitive in this type.
2	The ability to estimate the surface shape from the control polygon is positive (So it is used in manufacturing and in CAD).	The ability to estimate the surface shape from the control polygon is Negative (So it was used with subdivision algorithm widely to decrease this negative point).	The ability to estimate the surface shape from the control polygon is Negative and depends on the first derivative for special control points.
3	The first and last control points are the end points of the curves segment	The surface didn't contact the control points while it was controlled by the control points coordinates.	In cubic case, the shape is oriented by the first and the last control points and the line tangent (first derivative for this first and last control point).

1.3 CAM system

The computer aided manufacturing (CAM) software tools found for manufacturing procedures that use computers to assist in the planning and production of manufacturing processes from inventory control to the programming of machine tools. The communication between computer-aided design and computer aided Manufacture has been developed. However, the possibility for the CAM user to inspect or revise the manufacturing systems capability description is very limited. Generally a CAM software user chooses a predefined standard machine and standard tools. The concept of such systems is based on the use of information and data from the CAD Process directly after necessary modification in the CAM procedures. The CAM system helps to generate cutter location data and post-process which creates part programming (G - Code) ^[4].

1.4 Application of CAD/CAM in Metal Forming

With the ongoing rapid improvements on the areas of Computer Aided design, Computer Aided Manufacturing some attempts for developing an integrated extrusion die design system have been made. The new and improved 3D design packages supply the designer with ample possibilities to create a realistic model of the die. All features on the die, even the smallest, can be defined completely. In a Computer Aided Manufacturing environment this allows for direct data transfer to the CNC-machines. the subdivision surfaces algorithm improve existing design rules, and develop new design rules or just improve the general understanding of the extrusion die design. Furthermore, the CNC-machines may be programmed with the help of the 3D model and the design application must incorporate the limitations and possibilities of the available machines and tools.

A computer based design application will help the experienced die designer to progress from the design of the profile to the design of the die by supplying him with the maximum support without limiting him in his

possibilities. The support should, among others, incorporate the maintenance of feature databases, the presentation of alternatives, calculation of mechanical properties and the maintenance and use of the knowledge database. The die designer or application manager must be able to incorporate new design insights into the application without much effort or the need to re-program the entire application.

1.5 Subdivision Algorithms

Subdivision curve and surface are valued in geometric modeling applications for their convenience and flexibility. They permit the representation of objects of arbitrary topological type in a form that is easy to design, render and manipulate. While they can be used to model smooth objects, they can also be extended to model objects with boundaries and sharp features ^[5].

Subdivision schemes that generalize B-spline representations are particularly useful. Although B-spline (and NURBS) surface representations are prevalent representation in geometric modeling, they cannot model objects of non-planar topology or objects possessing sharp features without cumbersome patch stitching and curve trimming. However, B-spline representations are easy to analyze because they are piecewise polynomials (or rational) in form. Subdivision surfaces, on the other hand, are defined as the limit of repeated refinement of a 3D control point mesh. In general, this limit does not result in a closed form representation. Therefore, conventional methods of analyzing surfaces are inadequate since they depend on representations such as polynomial or rational function.

There are also techniques for deriving exact formulas for points and normal on the limit surfaces.

The elegant simplicity and practical advantages of subdivision algorithms have made them useful for particular applications. For example, they are ideal for quickly rendering an object where a piecewise planar

model suffices. With the capability to calculate exact points and normal on the limit surface, subdivision algorithms are finding wider acceptance for applications that require smooth surfaces. With the added capability of creating sharp features, subdivision surfaces can be applied to represent even more realistic objects.

Subdivision surfaces are also making fundamental contributions to new application areas in geometric modeling. For example, they are a key element in the multiresolution representation for optimized surface fitting [5].

This thesis examines two topics related to subdivision surfaces. First, it has been shown how piecewise smooth subdivision scheme can be analyzed. Second it presents an engineering application.

1.6 Constancy of the Ratio of the Successive Generalized Homogeneous Strain-increment (CRHS) Concept.

This concept of tool design is based upon the basis of homogeneous strain for the metal forming operation, which represents a function of the physical dimensions of the engineering material to be formed. The die surface profile or tool profile can be produced by using this concept, because the forming pass is divided into number of sections (n) depending on the expression of CRHS through these sections, as follows [6]:

$$\frac{\varepsilon_{H_2} - \varepsilon_{H_1}}{\varepsilon_{H_1} - \varepsilon_{H_0}} = \frac{\varepsilon_{H_3} - \varepsilon_{H_2}}{\varepsilon_{H_2} - \varepsilon_{H_1}} = \dots \dots \dots \frac{\varepsilon_{H_n} - \varepsilon_{H_{n-1}}}{\varepsilon_{H_{n-1}} - \varepsilon_{H_{n-2}}} = \text{const} \tan t = S \quad \dots \dots \dots (1.3)$$

where (ε_{Hn}) is the value of homogeneous strain at the section (n) through the forming pass. But (S) is a constant called ‘Rate of Deformation’, it does not depend on the time because it is related to the deformation rate and has no relation to the strain rate. The value of (S) can be taken randomly, if it has a value:

$S < 1$: it means that the rate of deformation is (Decelerated), and it has a sign of (DCRHS).

$S=1$: the rate of deformation is (Uniform), and it has a sign of (UCRHS).

$S>1$: the rate of deformation is (Accelerated), and it has a sign of (ACRHS) as shown in Figure (1.2).

The constant (S) may take different values, but the experience in the metal forming tool design indicates that the range in between (0.8 –1.2) is sufficient for most applications. In this study, the value ($S = 0.8$) is considered as a decelerated rate of deformation, and the value ($S = 1.2$) for the accelerated rate ^[6].

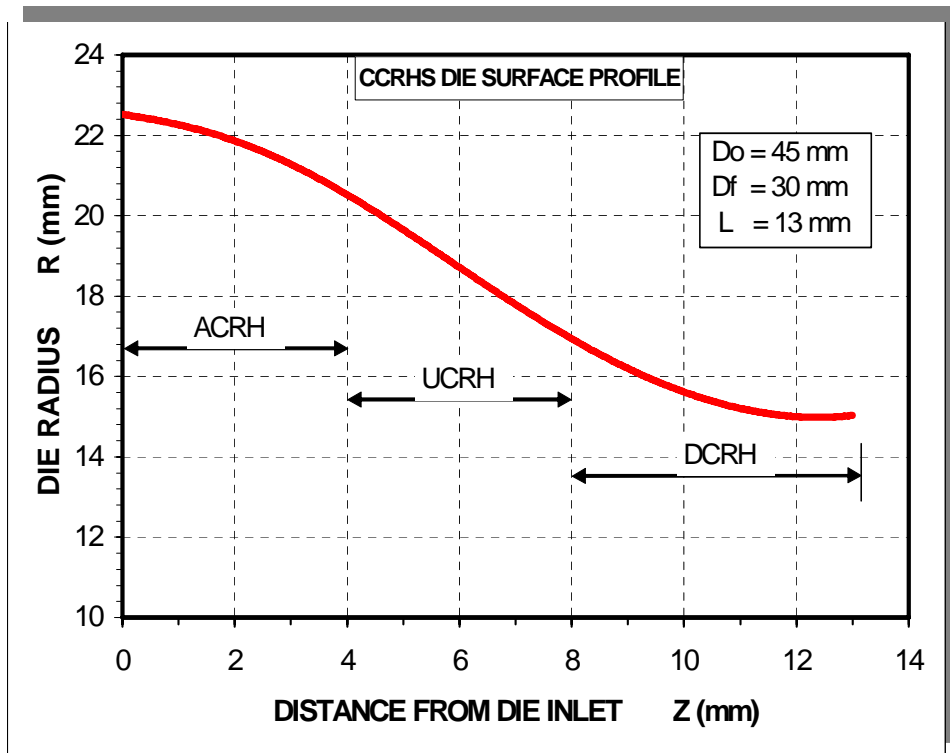


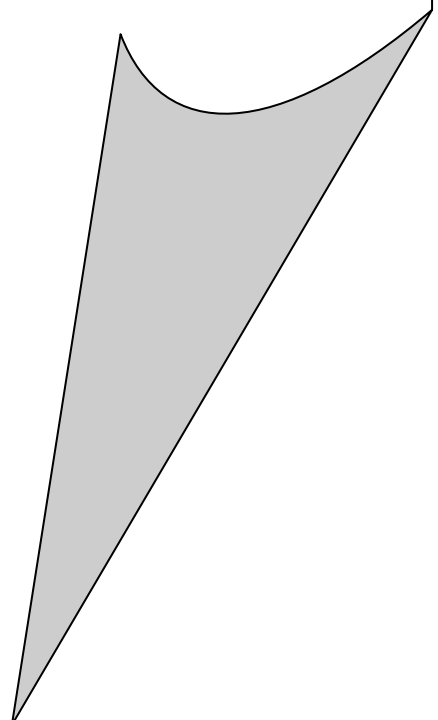
Fig. (1.2): The compounds die (CRHS) surface profile along the die inlet-exit ^[6].

1.7 Aim of this Research:

This aim of this research is:

1. Investigate subdivision surfaces such as Bezier, B-spline surface models by approximation technique, especially the Chaitian's Subdivision algorithm for Uniform B-spline technique, this technique could be used in reconstruction surface to produce smoother surface, then submit these curves and surfaces in production field.
2. Generate toolpath for milling process to CNC machine to make the die profile for Direct extrusion process and use the theoretical design like (CRHS) as guide to apply this algorithm, and make comparison between them, as well as find the deviation between the surface (Die profile shape) which is made by CRHS method, Quartic Uniform B-spline technique and Quintic Uniform B-spline technique which is developed from Chaitian's algorithm, and the surfaces after exposure to milling process.
3. The representation of surfaces in smooth, parametric form is of central importance in mechanical engineering. In order to machine a shape using a computer, it is necessary to produce a computer-compatible description of that shape.
4. These surfaces, for which the cutter contact points are generated for the proposed algorithms, are machined using CNC machine (Hermle C30U dynamic, 5-axis AC-kinematics) and then this data is used to generate cutter location data represented by G-Code format which is implemented on this CNC machining.

CHAPTER TWO
LITERATURE SURVEY



CHAPTER TWO**Literature Survey****2.1 Introduction:**

The researches published on the subject of Subdivision algorithms for the surfaces and curves is very important because it will give the researcher good background on his research and the sequence development of this research, this technique was invented in the 1978, it continues development, and the research has varied since then in more than one direction, and is more than one field, this direction is represented in these points:

1. Approximating (not interpolating original vertices).
2. Interpolating the original vertices.
3. Development of the subdivision surfaces and curves algorithm to service the field which they need.

For this purpose and to gain benefit, the researcher reviews the related literature as follows:

2.2 Subdivision Algorithms:

Hoppe, H., (1994); Introduces general method for automatic reconstruction of accurate, concise, piecewise smooth surfaces from unorganized 3D points.

Previous surface reconstruction methods have typically required additional knowledge, such as structure in the data, known surface genus, or orientation information. In contrast, the method outlined requires only the 3D coordinates of the data points.

This method is able to automatically infer the topological type of the surface, its geometry, and the presence and location of features such as boundaries, creases, and corners.

The reconstruction method has three major phases:

- 1) Initial surface estimation,
- 2) Mesh optimization.

3) Piecewise smooth surface optimization. A key ingredient in phase 3, and another principal contribution is the introduction of a new class of piecewise smooth representations based on subdivision.

The effectiveness of the three-phase reconstruction method is demonstrated on a number of examples using both simulated and real data ^[7].

Zorin, D., and Kristjansson, D. (2000) propose to use a different set of basis vectors for evaluation, which, unlike eigenvectors, depend continuously on the coefficients of the subdivision rules. The approach becomes possible to define evaluation for parametric families of rules without considering excessive number of special cases, while improving numerical stability of calculations it demonstrates how such bases are computed for a particular parametric family of subdivision rules extending Loop subdivision to meshes with boundary, and provides a detailed description of the evaluation algorithms ^[8].

Joy's, K. I. (2000) his paper basis depends on the binary subdivision of the uniform B-spline surface, which is defined by initial polygonal mesh, along with a subdivision (or refinement) operation which, given a polygonal mesh, will generate a new mesh that has a greater number of polygonal elements, and is hopefully “closer” to some resulting surface, by repetitively applying the subdivision procedure to the initial mesh, we generate a sequence of meshes that (hopefully) converges to a resulting surface ^[9].

Joy, K. I. (2000) introduces Subdivision methods for curve generation based upon a procedure which successively refines a control polygon into a sequence of control polygons that, in the limit, converges to a curve, and develop the refinement method for a quadratic uniform B-spline curve; the curves are commonly called subdivision curves as the refinement methods are based upon the binary subdivision of uniform B-spline curves ^[10].

Vlachos, A., Peters, J., Boyd, C., and Mitchell, J.L. ,(2001) introduce curved point-normal triangles, or short PN triangles, as an inexpensive

means of improving visual quality by smoothing out silhouette edges and providing more sample points for vertex shading operations. Specifically, PN triangle generation and sub-triangulation are to be inserted between the vertex-and-primitive-assembly stage and the vertex-shading stage of the graphics pipeline . The geometry of a PN triangle is defined as one cubic Bezier patch. The patch matches the point and normal information at the vertices of the flat triangle. Its normal is a separate linear or quadratic Bezier interpolate of the data ^[11].

Amresh, A., Farin, G., and Razdan, A., (2001) introduce two methods of adaptive subdivision for triangular meshes that make use of the Loop scheme or the Modified Butterfly scheme to get approximating or interpolating results respectively. The results are obtained at a lower cost when compared with those obtained by regular subdivision schemes. The first method uses the angles between the normal of a face and the normal of the adjacent faces to develop an adaptive method of subdivision. The other method relies on user input, i.e. the user specifies which parts of the mesh should be subdivided. This process can be automated by segmentation techniques, e.g. watershed segmentation, to get the areas in the mesh that need to be subdivided ^[12].

Bertram, M., and Hagen, H., (2001) propose a modified Loop subdivision surface scheme for the approximation of scattered data in the plane. Starting with a triangulated set of scattered data with associated function values, this scheme applies linear, stationary subdivision rules resulting in a hierarchy of triangulations that converge rapidly to a smooth limit surface. The novelty of this scheme is that it applies subdivision only to the ordinates of control points, whereas the triangulated mesh in the plane is fixed. The modified subdivision scheme defines locally supported, bivariate basis functions and provides multiple levels of approximation with triangles ^[13].

Claes, J. (2001) present a new modeling paradigm, providing the possibility of locally choosing an interpolating variant of the conventionally approximating subdivision scheme. His approach combines the advantages of approximating schemes with the precise control of interpolating schemes. Unlike other solutions that mostly focus on locally changing the weighting factors of the subdivision scheme, this thesis keeps the underlying uniform scheme intact. This method is based upon introducing additional control points on well-chosen locations, with optional interactive user control over the tangent plane (or surface normal) and the tension of the surface near the interpolating control points.

The same techniques used for surface modeling and editing are also adapted to implement a versatile free-form deformation tool, especially designed for 2D textured objects based on subdivision surfaces applied in 2D ^[14].

Stam, J. and Loop, C. (2002) provide new subdivision operator that unifies triangular and quadrilateral subdivision schemes. Designers often want the added flexibility of having both quads and triangles in their models. The new scheme is a generalization of the well known Catmull-Clark and Loop subdivision algorithms, and show that surfaces are G_1 everywhere and provide a proof that it is impossible to construct a G_2 scheme at the quad/triangle boundary. However, it provides rules that produce surfaces with bounded curvature at the regular quad/triangle boundary and provides optimal masks that minimize the curvature divergence elsewhere. It demonstrates the visual quality of the surfaces with several examples of categories and subject descriptors curve, surface, solid, and object representations ^[15].

Gross, N. (2004) introduces a new algorithm based on subdivision techniques which have been developed that efficiently interpolates a quadrilateral mesh of arbitrary topology with almost globally curvature

continuous fair NURBS surfaces. The Algorithm proposed is (faired interpolating NURBS) algorithm. The output of NURBS surfaces can be exported to commercial CAD systems in standards of data exchange, like IGES or STEP. This algorithm tackles the following problem:

1. Subdivision surfaces tend to have oscillations around extraordinary vertices and thus do not obtain a measure of surface fairness demanded in e.g. automotive design.
2. Subdivision techniques are not compatible with standards of data exchange, like IGES or STEP.
3. Approximating algorithms like the commonly used Catmull-Clark algorithm shrink in relationship to the input mesh.
4. Gaps between patch boundaries and discontinuous parameter lines are inherent to spline representation ^[16].

Barthe, L., and Kobbelt, L. (2004) extend the standard method to derive and optimize subdivision rules in the vicinity of extraordinary vertices (EV). Starting from a given set of rules for regular control meshes, we tune the extraordinary rules (ER) such that the necessary conditions for C_1 continuity are satisfied along with as many necessary C_2 conditions as possible. The approach sets up the general configuration around an EV by exploiting rotational symmetry and reformulating the subdivision rules in terms of the subdivision matrix's eigencomponents.

This method:

1. improves the curvature behavior around EVs.
2. optimizes several subdivision rules, i.e. not only the one for the EV itself but also the rules for its direct neighbors.
3. demonstrates capability to tune the ERs for the well-known Loop scheme and deriving ERs for a p3-type scheme based on 6-direction Box-spline ^[17].

Yvonnet, J. (2004) investigates the analysis of a piecewise smooth subdivision scheme, and applies the scheme to reconstruct the objects from non-uniformly sampled data points.

It extends the use of eigenanalysis and characteristic maps to analyze a piecewise smooth subdivision scheme that generalizes quartic triangular B-spline, and examines some topics related to subdivision surfaces:

1. It shows how a piecewise smooth subdivision scheme can be analyzed.
2. It derives formulas for points and tangents on the limit surface.
3. It presents an engineering application, and describes an algorithm for creating a surface that approximates an object from non-uniformly sampled data points and interpolates boundary curves ^[18].

Hakenberg, J. P. (2004) performed derive stationary subdivision rules on bi-uniform volumetric grids consisting of pair wise combinations of tetrahedral, octahedral, triangular prisms and cubes and refine the existing framework of quasi-interpolates so that weight stencils are obtained by algebraic manipulation. The joint spectral radius test proves that the combined schemes yield C_2 limit functions.

Furthermore, he presents an algorithm to subdivide an unstructured mesh consisting of the basic shapes enumerated above. The subdivision rules are generalized, such that smoothness is preserved across all faces and the effort of implementing the scheme remains low ^[19].

Seeger, S., Hormann, K., Hausler, G., and Greiner, G. (2005) studied how the well-known process of triangle mesh subdivision can be expressed in terms of the simplest mesh modification, namely the vertex split. Although this basic operation is capable of reproducing all common subdivision schemes if applied in the correct manner, they focus on Butterfly subdivision only for the purpose of perspicuity ^[20].

Schaefer, S., Levin, D., and Goldman, R. (2005) studied subdivision schemes generate self-similar curves and surfaces. Therefore there is a close connection between curves and surfaces generated by subdivision algorithms and self-similar fractals generated by Iterated Function Systems (IFS). It is demonstrated that this connection between subdivision schemes and fractals is even deeper by showing that curves and surfaces generated by subdivision are also attractors. they illustrate this fractal nature of subdivision, and present the derivatives which are associated with the curve type for many different subdivision curves and surfaces without extraordinary vertices, including B-splines, piecewise Bezier, interpolator four-point subdivision, bicubic subdivision, three-direction Quartic box-spline subdivision and Kobbelt's subdivision surfaces ^[21].

2.3 Analysis Subdivision Algorithms:

Claes, J. (2001) eigenanalysis is a handy tool to study the limit behavior of a subdivision curve scheme. A single step can be described in matrix form. In order to cope with endpoint conditions, the matrix formulation has the problem that the matrix should be double in size after every subdivision step. Therefore, usually a matrix of infinite dimensions is used. Such a matrix can either represent the subdivision of an infinite chain of points, or a closed curve. For many practical investigations, also a very limited matrix can also be used. In that case, the matrix represents a local environment that shrinks with every subdivision step.

As an example, is the subdivision scheme for cubic B-splines ^[14].

Schweitzer, J. E (2004) introduced theoretical basis for designing subdivision rules for various sharp surface features, and presents an analysis to determine properties of the limit surface for the rules that define a piecewise smooth subdivision surface. It shows that these surfaces are well-defined tangent plane, and behave as expected at singular points.

Analysis of the surface provides a more general framework for examining a subdivision scheme and accomplishes the specific tasks for the piecewise smooth subdivision scheme ^[5].

2.4 Applications for Subdivision Algorithms

Lounsbery, J.M. (1994) presents several applications of this work, including smooth level-of-detail control for graphics rendering, compression of geometric models, and animation previewing. The resulting algorithms are shown to run quite efficiently in most cases, and another application is in industrial design and computer animations ^[22].

Claes, J. (2001) gives an application of the subdivision techniques outside the world of surface modeling, where subdivision surfaces are used in 2D as a base for free-form deformations to fluently manipulating 2D animation objects, and it's also used in engineering applications, in combination with the finite element method. Not only the outer surface, but also the inner structure of an object is important, subdivision volumes are used ^[14].

Gross, N. (2004) introduces subdivision algorithms which have obvious advantages over spline representation also in the engineering area, as they can calculate arbitrary topological surfaces in a single calculation step. For example, they can eliminate problems with gaps between patch boundaries and discontinuous parameter lines inherent to spline representation. The new algorithms based on subdivision techniques have been developed that efficiently interpolate a quadrilateral mesh of arbitrary topology with almost globally curvature continuous fair NURBS surfaces. The Algorithm is called FIN (faired interpolating NURBS) algorithm. The output NURBS surfaces can be exported to commercial CAD systems in standards of data exchange, like IGES or STEP.

Some investigation has begun of subdivision surfaces which may serve as input to NCmilling. Even though the advantages of subdivision surfaces for this task have been recognized, the difficulty has been to date to calculate tool paths on the subdivision surface, as these algorithms have only been developed for spline surfaces in the past. This algorithm (FIN) combines the two surface representations; these former difficulties are inherently overcome. Tool-paths can be generated on the FIN surfaces with standard tools like Mastercam ^[16].

Schweitzer, J.E. (2004) in the interest of widening the application of subdivision surfaces, investigates a problem motivated by engineering practice, and addresses the reconstruction of an object from non-uniformly sampled 3D data.

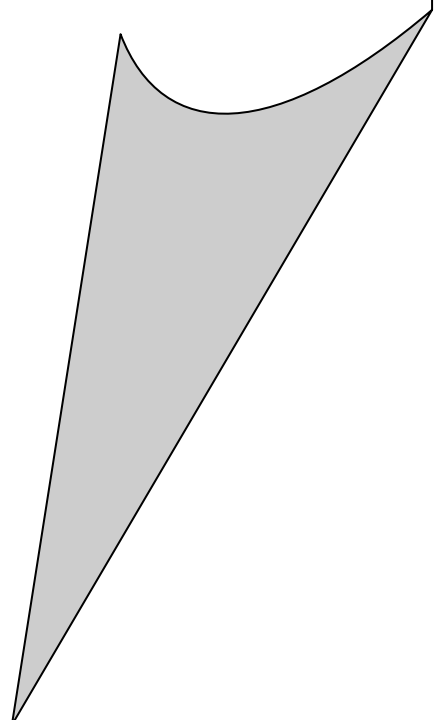
Created subdivision surfaces approximate object that have been sampled densely and uniformly. Costs associated with this data requirement include sampling time and expense, the difficulty of obtaining uniform samples from complex objects poses another problem. For example the physical dimensions of a scanner may make it impossible to reach certain regions such as in holes and pockets. There may also be regions that are occluded from the view of a scanner. For these reasons they developed an algorithm that reconstructs an object from non-uniform sampled data ^[5].

2.5 Listing the practical part for this thesis with respect to previous literature survey

1. This thesis it has used Chaitian's subdivision algorithm (Linear subdivision) for curves, and surfaces used (Bezier and Uniform B-spline techniques), then employees it in production field after making some analysis to this curves and surfaces.
2. This thesis reviews Doo and Sabian's algorithm (which use Quadrilaterals division), while another method reviews others like Loop algorithm (which use triangles division) used with many random and regular shapes by using the linear subdivision to these shape.
3. The proposed algorithm (Chaitian's subdivision algorithm) is developed in this thesis especially for Uniform B-spline curve after making more than one division iterations (Quartic Uniform B-spline, and Quantic Uniform B-spline techniques).
4. The refined B-spline technique has been used to create Die profile for direct extrusion shape by trial and error method and by moving the control points to arrive to the profile shape which is created before by theoretical design method like (CRHS). Comparison is made with the surface (Die shape) for these three surfaces.

CHAPTER THREE

BEZIER AND UNIFORM B-SPLINE TECHNOLOGY



CHAPTER THREE

Bezier and Uniform B-spline Technology

3.1 Approximation of Curves and Surfaces:

Many surfaces have mathematically complex or computationally expensive representations. For some applications, an approximation to these surfaces is adequate.

The problem of constructing surfaces from a set of points arises in numerous applications such as automobiles and ship hull design, scientific visualization, and geometric modeling. There are many variations of this problem, based on the form of data on extra information about the input, and requirements for the resulting surface.

This thesis focuses on the approximation of known surfaces. A surface will be approximated by sampling it first, and then building an approximating surface that interpolates the samples ^[23].

Computer-aided modeling techniques have been developed since the advent of NC milling machines in the late 40's. Since the early 60's Bezier and B-spline representations have evolved as the major tool to handle curves and surfaces ^[24].

These representations are geometrically intuitive and meaningful and they lead to constructive numerically robust algorithms.

The core concepts of Computer-aided Geometric Design (CAGD) with the intent to provide a clear and illustrative presentation of the basic principles as well as a treatment of advanced material, including multivariate splines, some subdivision techniques and constructions of arbitrarily smooth free-form surfaces.

One way to categorize surface fitting schemes is by locality of data used in constructing a portion of surface. A global scheme uses arbitrarily many of the data points in constructing each portion of the surface.

Whereas a local scheme only considers those data points near the portion of the surface being created, local schemes construct piecewise continuous surfaces, and ensure that adjacent surface patches meet "smoothly" [23].

By introducing a fourth parameter, (u), into the coordinate description of curve, we can express each of the three Cartesian coordinates in parametric form. Any point on the curve can then be represented by the vector function:

$$P(u) = (x(u), y(u), z(u)) \dots\dots\dots (3.1)$$

Usually, the parametric equations are set up so that parameter u is defined in the range from (0) to (1).

Parametric equations for surfaces are formulated with two parameters (u) and (w). Coordinate positions on a surface are then represented by the parametric vector function:

$$P(u, w) = (x(u, w), y(u, w), z(u, w)) \quad u, w \in [0, 1] \dots\dots\dots (3.2)$$

Many techniques exist for setting up polynomial parametric equations for curves and surfaces, given the coordinates for the control points. Basic methods for displaying curves specified with control points include the Bezier and B-spline curves [25].

In this chapter the Bezier and Uniform B-spline technique is studied in different freedom degrees as case study, with making all calculations, mathematical derivatives and drawing the curve and surface for the proposed technique.

3.2 Bezier Curves

In this setting every polynomial curve segment can be represented by its so-called Bezier polygon. The curve and its Bezier polygon are closely related. They have common end points and end tangents, the curve segment lies in the convex hull of its Bezier polygon, etc. Furthermore, one of the fastest and numerically most stable algorithms used to render a polynomial curve is based on the Bezier representation [24].

Mathematically a parametric Bezier curve is defined by [26]:

$$p(u) = \sum_{i=0}^n B_{n,i}(u)P_i \dots\dots\dots (3.3)$$

$$B_{n,i}(u) = c(n,i)u^i(i-u)^{n-i} \dots\dots\dots (3.4)$$

$$c(n,i) = \frac{n!}{i!(n-i)!} \dots\dots\dots (3.5)$$

In Matrix Form:

For the Bezier curve, when **n=2** equation (3.3) is rewritten in matrix form as:

$$p(u) = \begin{bmatrix} (1-2u+u^2) & (2u-2u^2) & u^2 \end{bmatrix} \begin{bmatrix} p_0 \\ p_1 \\ p_2 \end{bmatrix} \dots\dots\dots (3.6)$$

Or as

$$p(u) = \begin{bmatrix} u^2 & u & 1 \end{bmatrix} \begin{bmatrix} 1 & -2 & 1 \\ -2 & 2 & 0 \\ 1 & 0 & 0 \end{bmatrix} \begin{bmatrix} p_0 \\ p_1 \\ p_2 \end{bmatrix} \dots\dots\dots (3.7)$$

$$U = \begin{bmatrix} u^2 & u & 1 \end{bmatrix}, \quad p = \begin{bmatrix} p_0 & p_1 & p_2 \end{bmatrix}^T \dots\dots\dots (3.8)$$

$$M_{B(2)} = \begin{bmatrix} 1 & -2 & 1 \\ -2 & 2 & 0 \\ 1 & 0 & 0 \end{bmatrix} \dots\dots\dots (3.9)$$

This allows to rewrite the equation even more compactly as

$$P(u) = UM_{B(2)}P \dots\dots\dots (3.10)$$

3.2.1 Bezier Curve Properties:

1. A Bezier curve is a polynomial.

The degree of the polynomial is always one less than the number of control points. In computer graphics, we generally use degree (3). Quadratic curves are not flexible enough and going above degree (3) gives rises to complications and so the choice of cubic is the best compromise for most computer graphics applications.

2. The curve follows the shape of the control point polygon.

It is constrained within the convex hull formed by the control points.

3. The control points do not exert 'local' control.

Moving any control point affects the entire curve to a greater or lesser extent. All the basis functions are everywhere positive except at the point $u = 0$ and $u = 1$

4. The first and last control points are the end points of the curves segment

5. The tangent vectors to the curve at the end points are coincident with the first and last edge of the control point polygon.

6. Moving the control points alters the magnitude and direction of the tangent vectors.

This is the basis of the intuitive 'feel' of a Bezier curve interface.

7. Variation diminishing property

The curve does not oscillate about any straight line more often than the control point polygon.

8. The strange mix of points on and off the curve

9. Non localness

As soon as you move one control point, you affect the entire curve

10. Relationship between the degree of the curve and the number of control points ^[27].

Case Study (1)

Suppose the initial control points of the desired two curves are:

a) $p_1=(100,200,0)$, $p_2=(250,200,0)$,and $p_3=(250,100,0)$.

b) $p_1=(200,100,0)$, $p_2=(500,300,0)$,and $p_3=(400,250,0)$.

And $n=2$, draw the two Bezier Curves.

❖ Rearrange the control points in matrix form as follows:

a) $P_{11}=(100,200,0)$ $p_{12}=(250,200,0)$ $p_{13}=(250,100,0)$

b) $P_{11}=(200,100,0)$ $p_{12}=(500,300,0)$ $p_{13}=(400,250,0)$

❖ Use the equation (3.7) to determine $p(u)$

❖ Plot the control points and the curves result from equation (3.7) as shown in Figure (3.1: a, and b), with (u) ranging from (0) to (1).

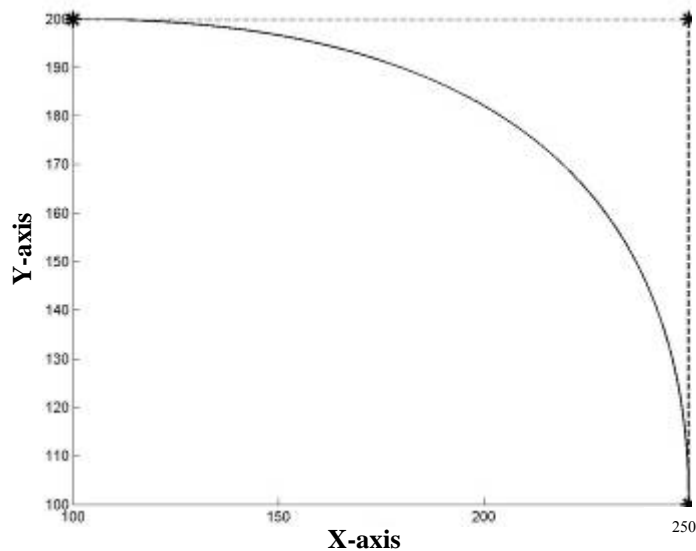


Figure (3.1.a) Bezier curve with three control points $n=2$ (regular control points).

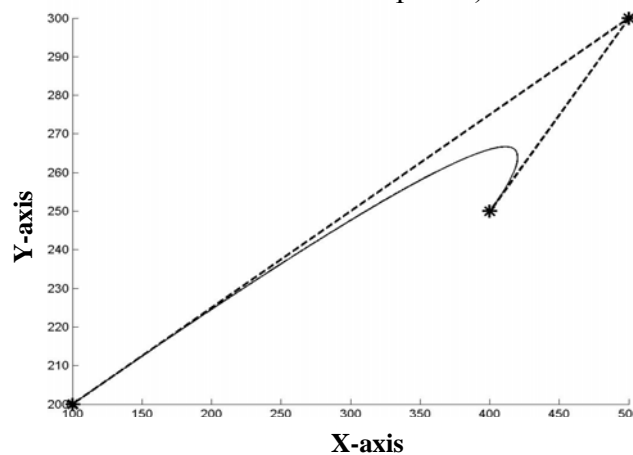


Figure (3.1.b) Bezier curve with three control points $n=2$ (irregular control points).

For a cubic Bezier curve, with **n=3**, equation (3.3) is rewriting in matrix form as:

$$p(u) = [(1-3u+3u^2-u^3) (3u-6u^2+3u^3) (3u^2-3u^3) u^3] \begin{bmatrix} p_0 \\ p_1 \\ p_2 \\ p_3 \end{bmatrix} \dots\dots (3.11)$$

Or as

$$p(u) = [u^3 \quad u^2 \quad u \quad 1] \begin{bmatrix} -1 & 3 & -3 & 1 \\ 3 & -6 & 3 & 0 \\ -3 & 3 & 0 & 0 \\ 1 & 0 & 0 & 0 \end{bmatrix} \begin{bmatrix} p_0 \\ p_1 \\ p_2 \\ p_3 \end{bmatrix} \dots\dots\dots (3.12)$$

Letting

$$U = [u^3 \quad u^2 \quad u \quad 1] , \quad p = [p_0 \quad p_1 \quad p_2 \quad p_3]^T \dots\dots\dots (3.13)$$

$$M_{B(3)} = \begin{bmatrix} -1 & 3 & -3 & 1 \\ 3 & -6 & 3 & 0 \\ -3 & 3 & 0 & 0 \\ 1 & 0 & 0 & 0 \end{bmatrix} \dots\dots\dots (3.14)$$

This allows to rewrite the equation even more compactly as

$$P(u) = UM_{B(3)}P \dots\dots\dots (3.15)$$

Case Study (2)

Suppose the initial control points of the desired two curves are:

- a) $p_1=(50,100,0), p_2=(200,100,0), p_3=(200,20,0),$ and $p_4=(450,20,0).$
- b) $p_1=(50,100,0), p_2=(100,200,0), p_3=(250,150,0),$ and $p_4=(150,50,0)$

And $n=3$, draw the two Bezier Curve.

- ❖ Rearrange the control points in matrix form as follows:
 - a) $P_{11}=(50,100,0) \quad p_{12}=(200,100,0) \quad p_{13}=(200,20,0) \quad p_{14}=(450,20,0)$
 - b) $P_{11}=(50,100,0) \quad p_{12}=(100,200,0) \quad p_{13}=(250,150,0) \quad p_{14}=(150,50,0)$
- ❖ Use the equation (3.12) to determine $p(u)$
- ❖ Plot the control points and the curves result from equation (3.12) as shown in Figure (3.2: a, and b), with (u) ranging from (0) to $(1).$

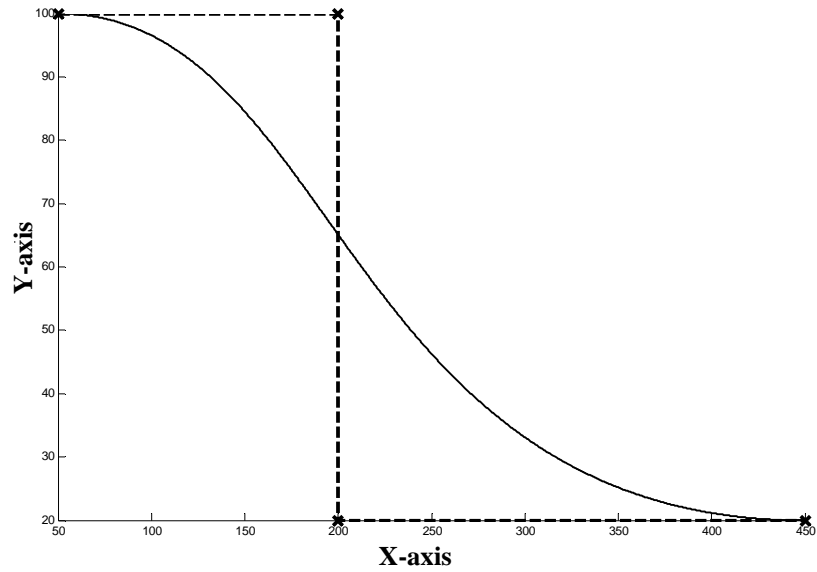


Figure (3.2.a) Bezier curve with four control points n=3 (regular control points).

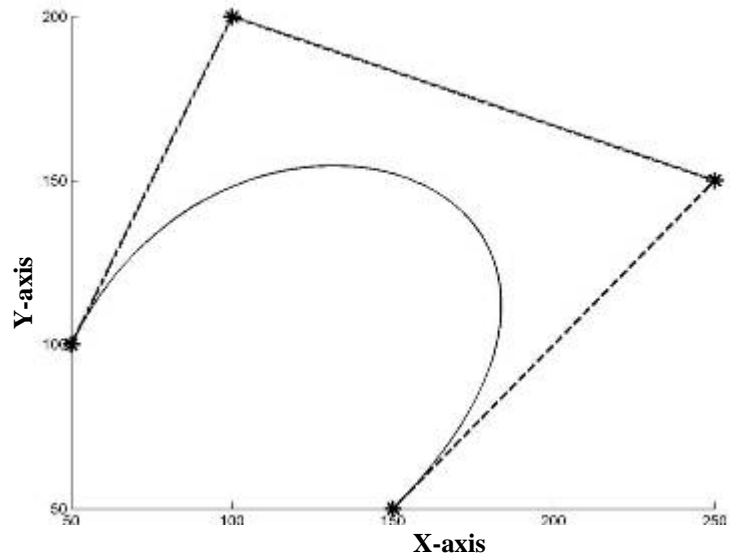


Figure (3.2.b) Bezier curve with four control points n=3 (irregular control points).

Obviously, the composition of these matrices varies with the number of vertices, n+1. So for **n=4**:

$$U = [u^4 \quad u^3 \quad u^2 \quad u \quad 1] \quad , \quad P = [p_0 \quad p_1 \quad p_2 \quad p_3 \quad p_4]^T \quad \dots\dots\dots (3.16)$$

$$M_{B(4)} = \begin{bmatrix} 1 & -4 & 6 & -4 & 1 \\ -4 & 12 & -12 & 4 & 0 \\ 6 & -12 & 6 & 0 & 0 \\ -4 & 4 & 0 & 0 & 0 \\ 1 & 0 & 0 & 0 & 0 \end{bmatrix} \quad \dots\dots\dots (3.17)$$

$$P(u) = UM_{B(4)}P \quad \dots\dots\dots (3.18)$$

Case Study (3)

Suppose the initial control points of the desired two curves are:

$p_1=(50,500,0)$, $p_2=(150,400,0)$, $p_3=(0,300,0)$, $p_4=(200,200,0)$, and $p_5=(120,100,0)$.

And $n=4$, draw the two Bezier Curve.

❖ Rearrange the control points in the matrix form as follows:

$P_{11}=(50,500,0)$ $p_{12}=(150,400,0)$ $p_{13}=(0,300,0)$ $p_{14}=(200,200,0)$
 $p_{15}=(120,100,0)$

❖ Use the equation (3.18) to determine $p(u)$

❖ Plot the control points and the curves result from equation (3.18) as shown in Figure (3.3), with (u) ranging from (0) to (1) .

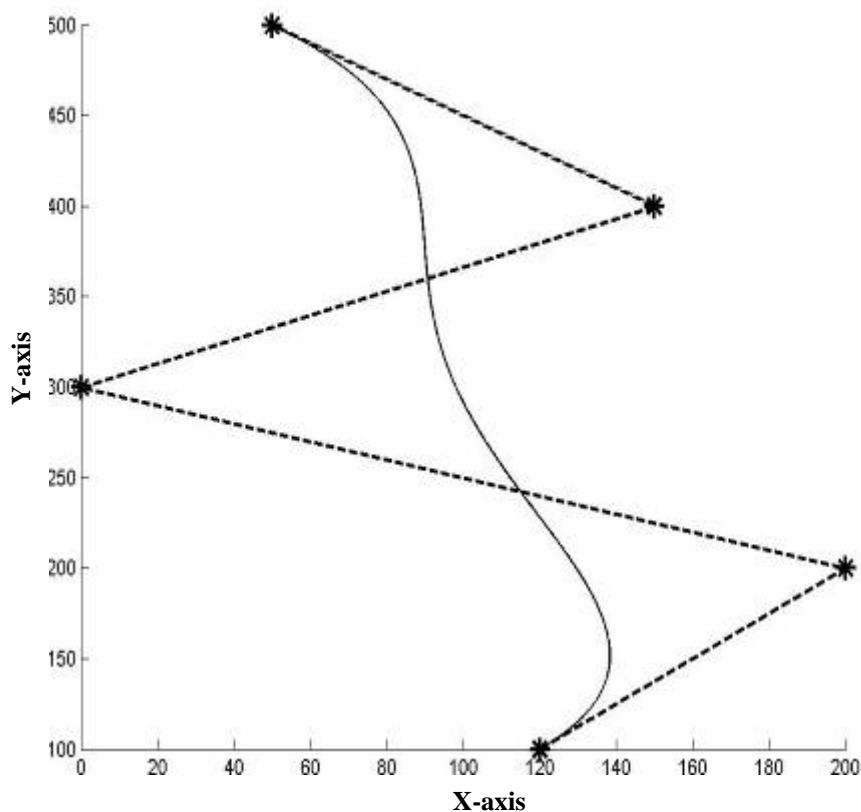


Figure (3.3) Bezier curve with five control points $n=4$.

The matrix form when $n=5$:

$$U = [u^5 \ u^4 \ u^3 \ u^2 \ u \ 1] \ , \ P = [p_0 \ p_1 \ p_2 \ p_3 \ p_4 \ p_5]^T \dots\dots\dots (3.19)$$

$$M_{B(5)} = \begin{bmatrix} -1 & 5 & -10 & 10 & -5 & 1 \\ 5 & -20 & 30 & -20 & 5 & 0 \\ -10 & 30 & -30 & 10 & 0 & 0 \\ 10 & -20 & 10 & 0 & 0 & 0 \\ -5 & 5 & 0 & 0 & 0 & 0 \\ 1 & 0 & 0 & 0 & 0 & 0 \end{bmatrix} \dots\dots\dots (3.20)$$

$$P(u) = UM_{B(5)}p \dots\dots\dots (3.21)$$

Case Study (4)

Suppose the initial control points of the desired two curves are:

$$p_1=(0,0,0), p_2=(50,500,0), p_3=(150,0,0), p_4=(250,400,0), p_5=(350,150,0),$$

And $p_6=(450,250,0)$.

And $n=5$, draw the two Bezier Curve.

❖ Rearrange the control points in the matrix form as follows:

$$P_{11}=(0,0,0) \ p_{12}=(50,500,0) \ p_{13}=(150,0,0) \ p_{14}=(250,400,0) \ p_{15}=(350,150,0),$$

$$p_{16}=(450,250,0)$$

❖ Use the equation (3.21) to determine $p(u)$

❖ Plot the control points and the curves result from equation (3.21) as shown in Figure (3.4), with (u) ranging from (0) to (1) .

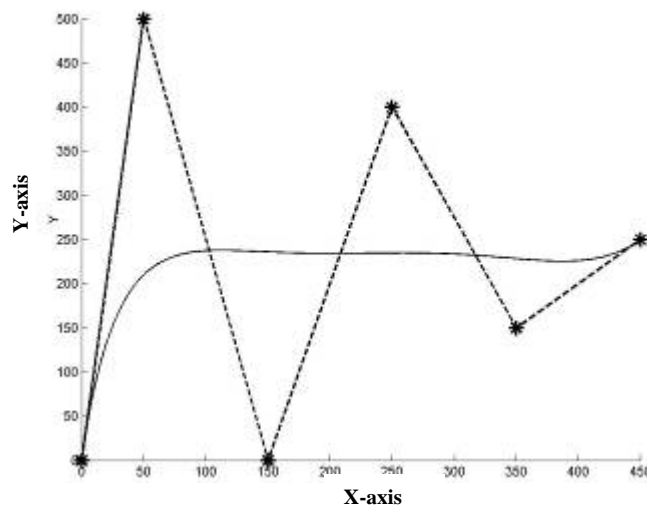


Figure (3.4) Bezier curve with six control points $n=5$.

The matrix form when $n=6$:

$$U = [u^6 \quad u^5 \quad u^4 \quad u^3 \quad u^2 \quad u \quad 1] \quad , \quad P = [p_0 \quad p_1 \quad p_2 \quad p_3 \quad p_4 \quad p_5 \quad p_6]^T$$

$$M_{B(6)} = \begin{bmatrix} 1 & -6 & 15 & -20 & 15 & -6 & 1 \\ -6 & 30 & -60 & 60 & -30 & 6 & 0 \\ 15 & -60 & 90 & -60 & 15 & 0 & 0 \\ -20 & 60 & -60 & 20 & 0 & 0 & 0 \\ 15 & -30 & 15 & 0 & 0 & 0 & 0 \\ -6 & 6 & 0 & 0 & 0 & 0 & 0 \\ 1 & 0 & 0 & 0 & 0 & 0 & 0 \end{bmatrix} \quad \dots\dots\dots (3.22)$$

$$P(u) = U M_{B(6)} P \quad \dots\dots\dots (3.23)$$

Case Study (5)

Suppose the initial control points of the desired two curves are:

$$p_1=(50,600,0), p_2=(100,500,0), p_3=(150,400,0), p_4=(0,300,0) ,$$

$$p_5=(300,150,0), p_6=(75,150,0), \text{and } p_7=(200,0,0).$$

And $n=6$, draw the two Bezier Curve.

❖ Rearrange the control points in the matrix form as follows:

$$P_{11}=(50,600,0) \quad P_{12}=(100,500,0) \quad p_{13}=(150,400,0) \quad p_{14}=(0,300,0)$$

$$p_{15}=(300,150,0) \quad p_{16}=(75,150,0) \quad p_{17}=(200,0,0)$$

❖ Use the equation (3.23) to determine $p(u)$

❖ Plot the control points and the curves result from equation (3.23) as shown in Figure (3.5), with (u) ranging from (0) to (1) .

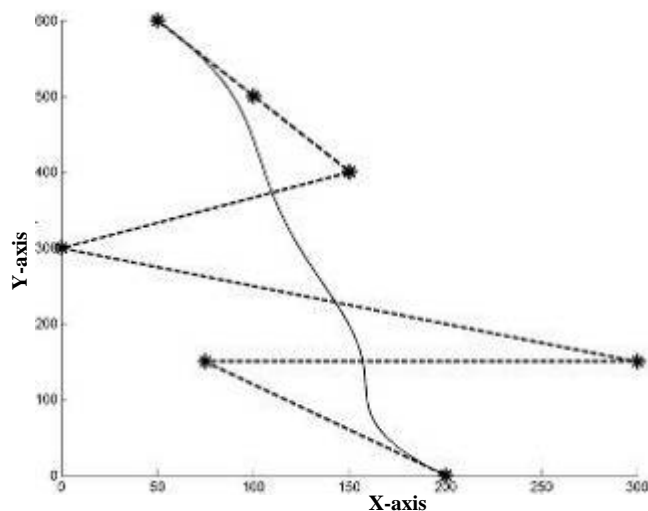


Figure (3.5) Bezier curve with seven control points $n=6$.

3.3 Bezier Surfaces

Bezier surfaces provide a flexible and powerful surface design tool. However practical usage suffers from the necessity of specifying precise, non intuitive mathematical information, e.g. position, tangent and twist vectors [26].

A Cartesian or tensor product Bezier surface is given by

$$p(u, w) = \sum_{i=0}^n \sum_{j=0}^m p_{ij} B_{i,n}(u) B_{j,m}(w) ; 0 \leq u \leq 1, 0 \leq w \leq 1 \dots\dots\dots (3.24)$$

$$B_{i,n}(u) = \frac{n!}{i!(n-i)!} u^i (1-u)^{n-i} \dots\dots\dots (3.25)$$

$$B_{j,m}(w) = \frac{m!}{j!(m-j)!} u^j (1-w)^{m-j} \dots\dots\dots (3.26)$$

The p_{ij} comprises an $(n+1) \times (m+1)$ rectangular array of control points defining the vortices of characteristic polyhedron of a Bezier patch.

So, the general matrix equation for Bezier patch is:

$$p(u, w) = U_{1 \times n} M_{B,n \times n} P_{n \times m} M_{B,m \times m}^T W_{m \times 1}^T \dots\dots\dots (3.27)$$

where the subscripts on the matrices indicate their dimensions for a bicubic Bezier patch (4x4).and expanded equation (3.27) becomes:

$$p(u, w) = [(1-u)^3 \quad 3u(1-u)^2 \quad 3u^2(1-u) \quad u^3] p \begin{bmatrix} (1-w)^3 \\ 3w(1-w)^2 \\ 3w^2(1-w) \\ w^3 \end{bmatrix} \dots\dots (3.28)$$

The matrix P is the matrix which contains the points that define the characteristic polyhedron [26].

$$p = \begin{bmatrix} p_{11} & p_{12} & p_{13} & p_{14} \\ p_{21} & p_{22} & p_{23} & p_{24} \\ p_{31} & p_{32} & p_{33} & p_{34} \\ p_{41} & p_{42} & p_{43} & p_{44} \end{bmatrix} \dots\dots\dots (3.29)$$

Implementing program to build the Bezier surface needs drawing the block diagram which is shown in Figure (3.6) and explaining the main

steps of the program while the detailed explanation of the proposed program has been given in the flowchart shown in Figure (3.7).

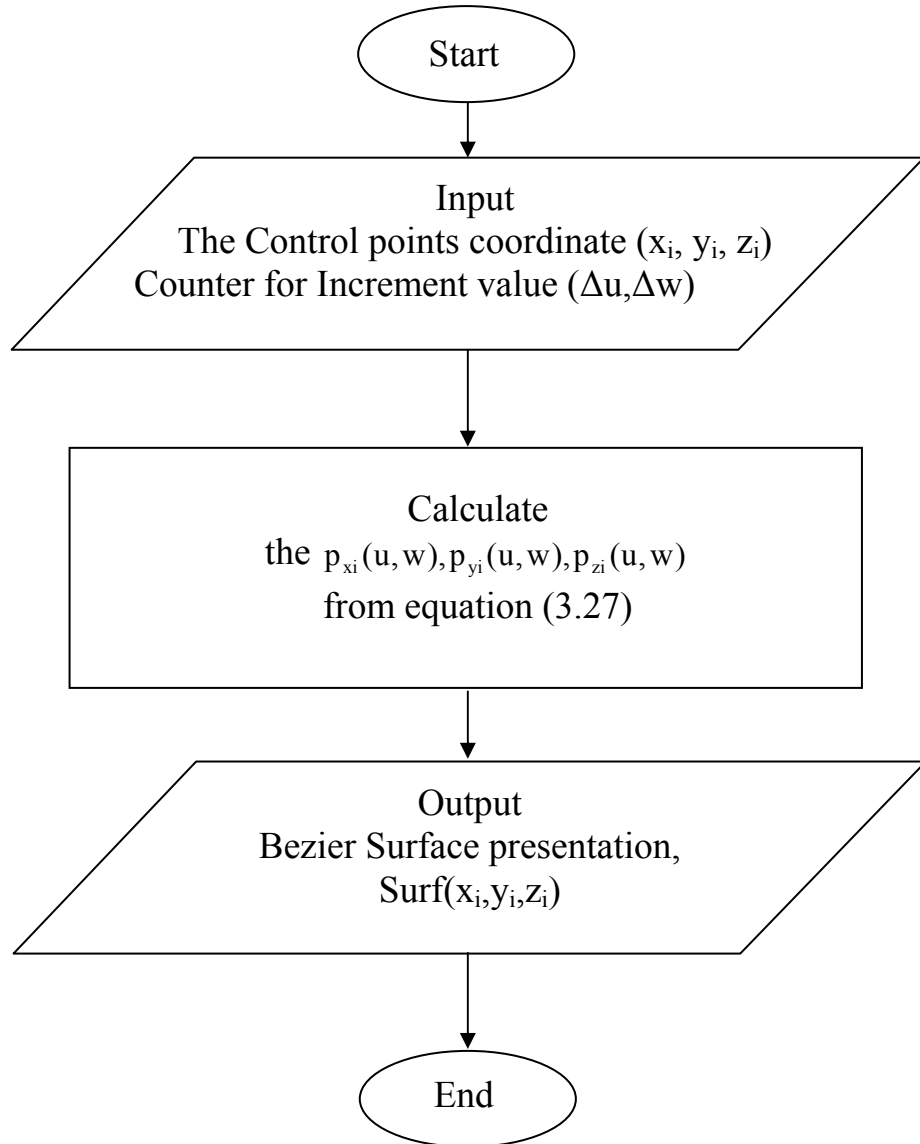


Figure (3.6): Block diagram of the proposed program depending on Bezier technique.

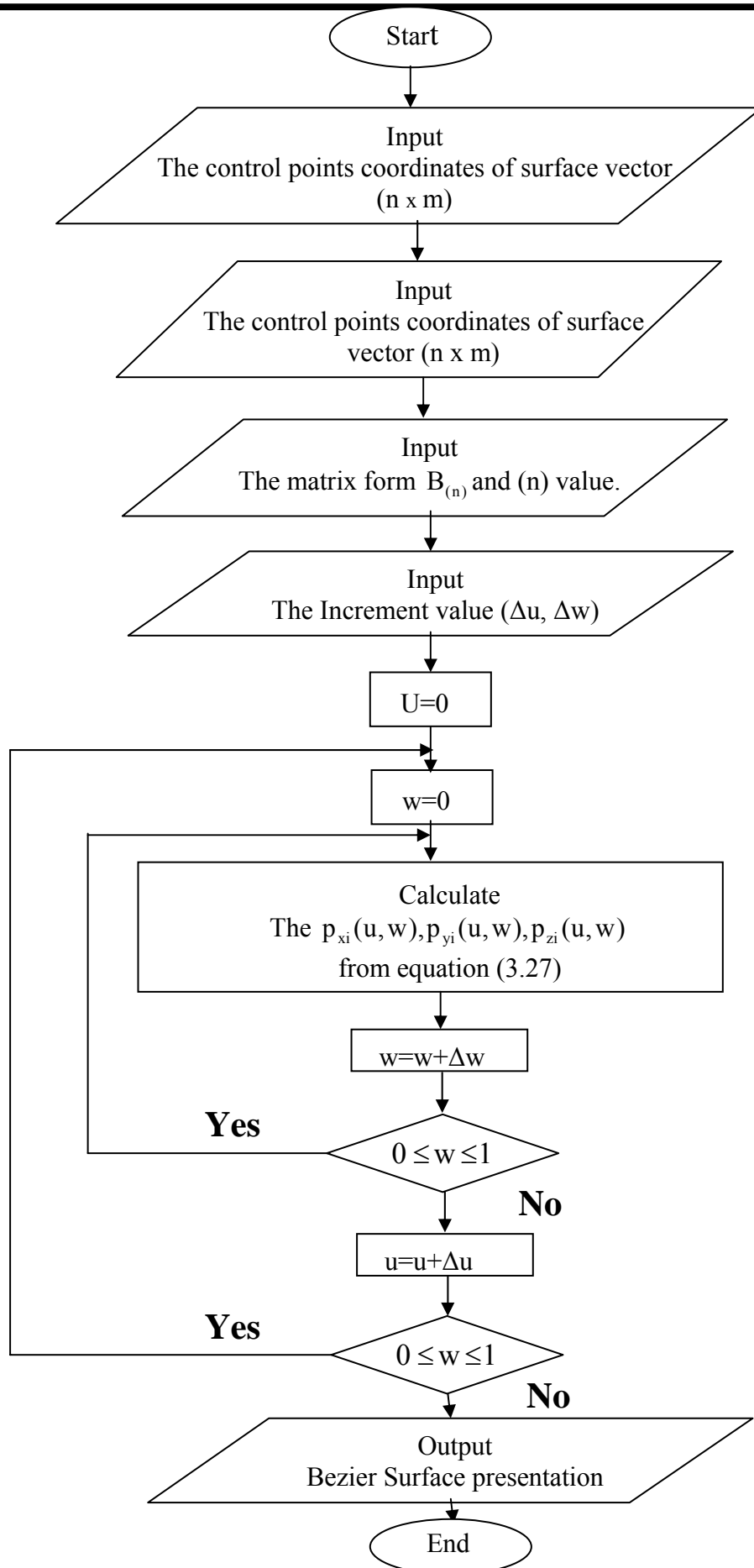


Figure (3.7): Flowchart of the proposed program depending on Bezier technique.

The proposed program can represent the surface in graphical mode with the software program Matlab (V7.0). Figures (3.8), (3.9), (3.10),(3.11),and (3.12) show a final result of practical application of our proposed program.

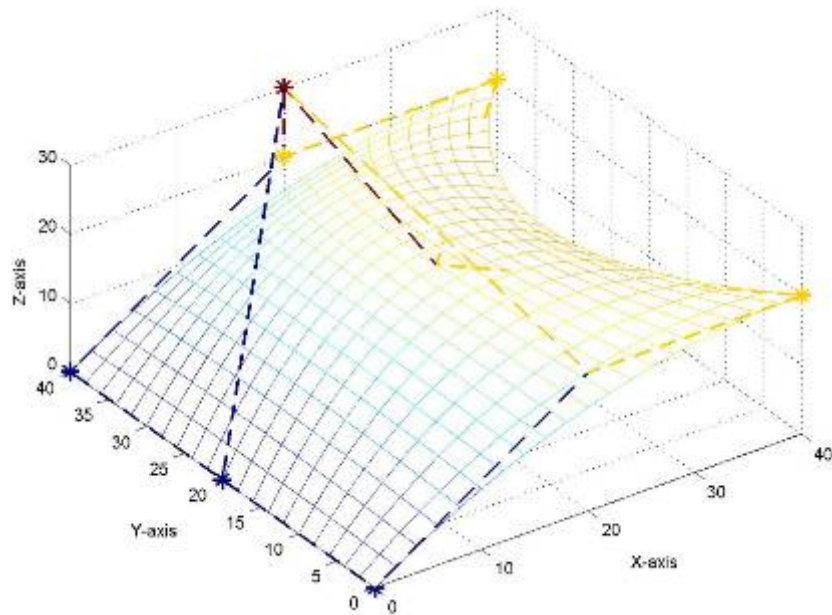


Figure (3.8) Bezier Surface (2nd degree), n=2, Matrix form (3x3).

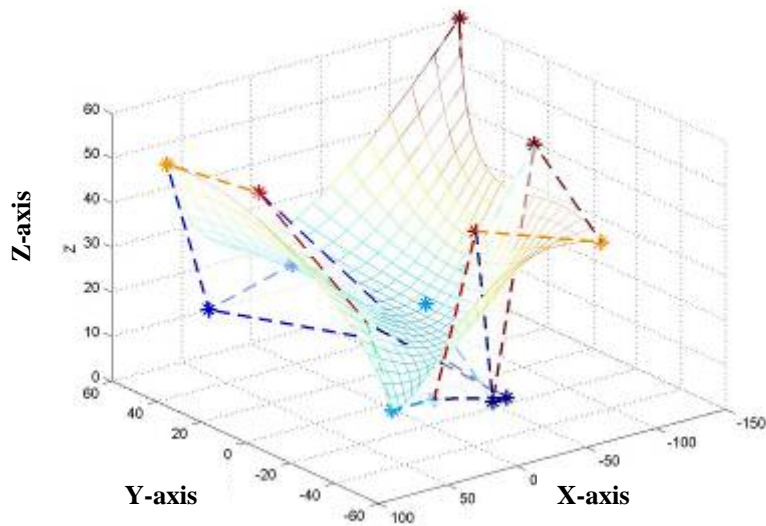


Figure (3.9) Bezier Surface (3rd degree), n=3, Matrix form (4x4).

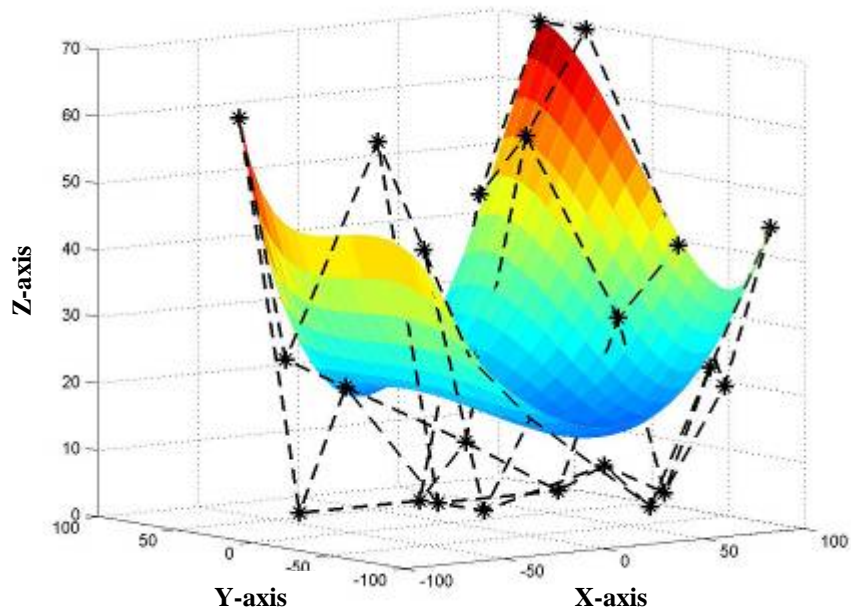


Figure (3.10) Bezier Surface (4th degree), $n=4$, Matrix form (5x5).

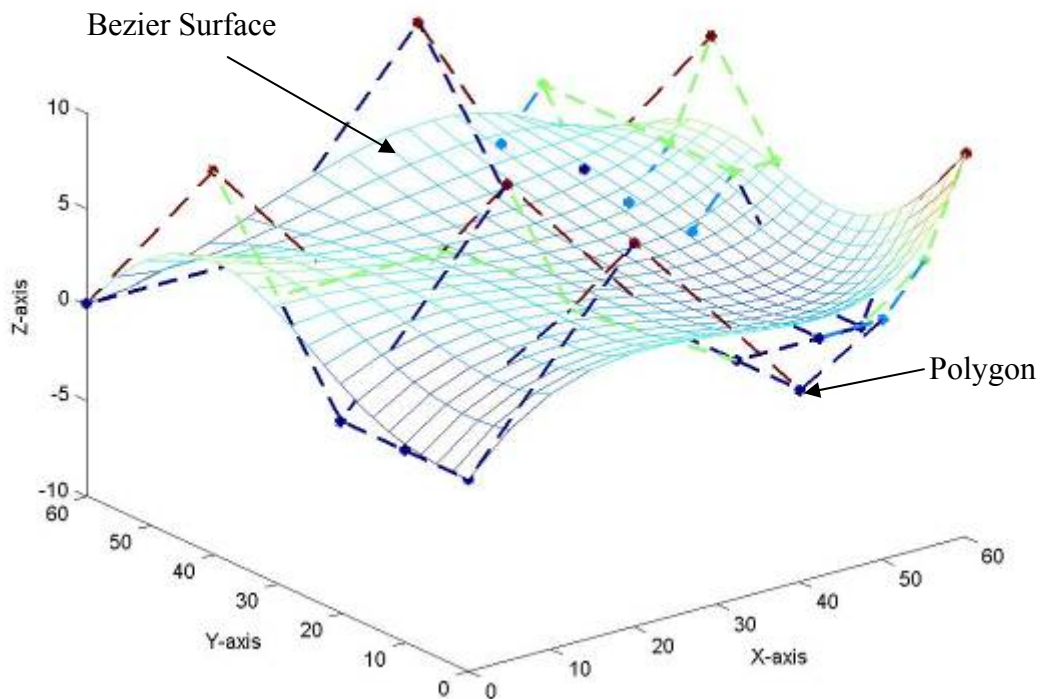
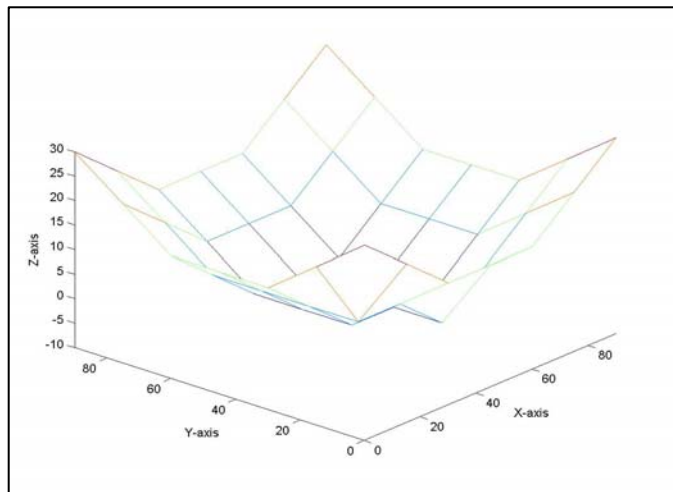
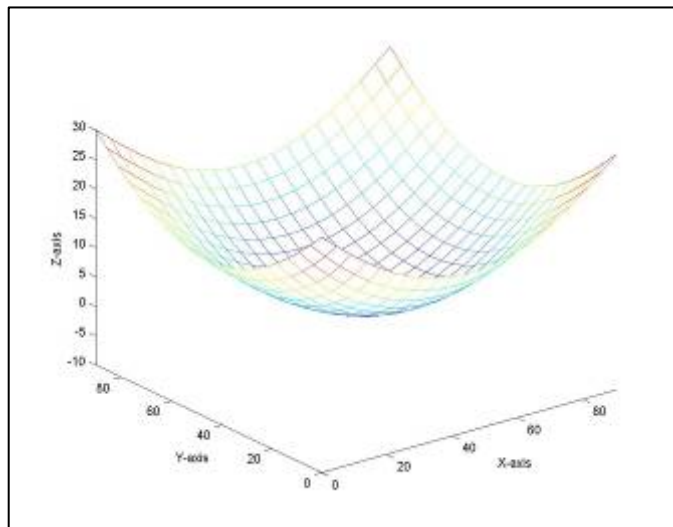


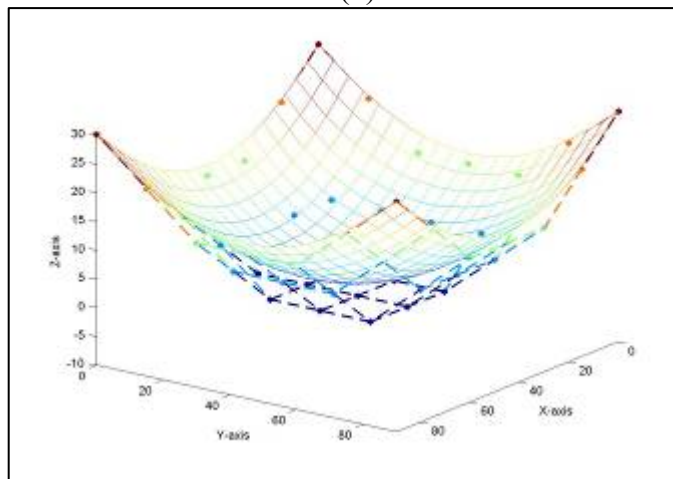
Figure (3.11) Bezier Surface (5th degree), $n=5$, Matrix form (6x6).



(a)



(b)



(c)

Figure (3.12: a, b, and c) Bezier Surface (6th degree), $n=6$, Matrix form (7x7) with Control points.

a-Control polygon for Bezier surface with Matrix form (7x7).

b-Bezier surface (6th degree), $n=6$.

c- Bezier Surface (6th degree), $n=6$, with control polygon for Matrix form (7x7) with Control points.

3.4 B-spline Curve

From the mathematical point of view, a curve generated by the vertices of a polygon is dependent on some approximation scheme to establish the relationship between the curve and the polygon.

The scheme is provided by choice of the basis function. Two characteristics of the Bernstein basis, however, limit the flexibility of the resulting curves. So, there is another basis, called the B-spline basis (from Basis spline), which contains the Bernstein basis as a special case. This basis is generally non-global. The non-global behavior of B-Spline curves is due to the fact that each vertex B_i is associated with a unique basis function, thus, each vertex affects the shape of curve only over a range of parameter values where the associated basis function is nonzero. The B-spline basis also allows the order of the basis function and hence the degree of the resulting curves to be changed without changing the number of defining polygon vertices.

The uniform basis functions are defined by the following expressions [26]:

$$N_{i,l}(u) = \begin{cases} 1 & \text{if } t_i \leq u \leq t_{i+1} \\ 0 & \text{other wise} \end{cases} \dots\dots\dots (3.30)$$

And

$$N_{i,k}(u) = \frac{(u-t_i)^{k-1} N_{i,k-1}(u)}{t_{i+k-1} - t_i} + \frac{(t_{i+k} - u)^{k-1} N_{i+1,k-1}(u)}{t_{i+k} - t_{i+1}} \dots\dots\dots (3.31)$$

where k controls the degree ($k-1$) of the resulting polynomial in u and also the continuity of the curve.

$$N+k+1=T \dots\dots\dots (3.32)$$

where T the number of knots.

The final equation of Uniform B-spline curve when $k=3$ is:

$$p_i(u) = \frac{1}{2} [(1-u)^2 p_i + (-2u^2 + 2u + 1)p_{i+1} + u^2 p_{i+2}] \dots\dots\dots (3.33)$$

3.4.1 B-spline Properties:

1. Controls points:

The curve follows the shape of the control point polygon and is constrained to lie in the convex hull of the control points.

2. Variation in diminishing property:

The curve does not oscillate about any straight line more often than the control point polygon.

3. Affine transformation compatibility:

The curve is transformed by applying any affine transformation (that is, any combination of linear transformations) to its control point representation.

4. Local Control:

A B-Spline curve exhibits local control - a control point is connected to four segments (in the case of a cubic) and moving a control point can influence only these segments ^[27].

And the special properties for the Uniform B-spline curve:

- ❖ The join point on the value of u between two segments is called the knot value.
- ❖ For uniform B-spline, knots are spaced at equal intervals in u .
- ❖ The blending functions are simple copies translated in u .
- ❖ In general uniform B-spline curves do not interpolate the end points ^[27].

Matrix Form:

When rewriting equation (3.33) using the matrix notation, Uniform B-spline with $k=3$ [29] is:

$$p_i(u) = \frac{1}{2} \begin{bmatrix} u^2 & u & 1 \end{bmatrix} \begin{bmatrix} 1 & -2 & 1 \\ -2 & 2 & 0 \\ 1 & 1 & 0 \end{bmatrix} \begin{bmatrix} p_{i-1} \\ p_i \\ p_{i+1} \end{bmatrix} ; i \in [1:n-1] \dots (3.34)$$

Case Study (6)

Suppose the initial control points of the desired two curves are:

$$p_1=(0,10,0), p_2=(20,30,20), p_3=(40,-5,20)$$

And $k=3$, draw the Uniform B-spline curve.

❖ Rearrange the control points in the matrix form as follows:

$$P_{11}=(0,10,0) \quad P_{12}=(20,30,20) \quad p_{13}=(40,-5,20)$$

Use the equation (3.34) to determine $p(u)$

Plot the control points and the curves result from equation (3.34) as shown in Figure (3.13), with (u) ranging from (0) to (1)

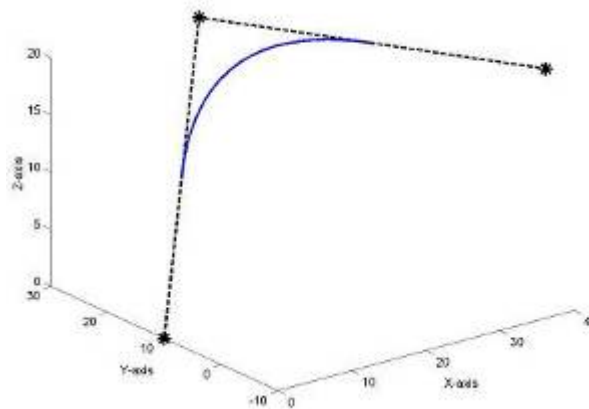


Figure (3.13) B-spline curve (2nd degree), $k=3$, Matrix form (3x3) with Control points.

And for cubic B-spline, when $k=4$ [29].

$$p_i(u) = \frac{1}{6} \begin{bmatrix} u^3 & u^2 & u & 1 \end{bmatrix} \begin{bmatrix} -1 & 3 & -3 & 1 \\ 3 & -6 & 3 & 0 \\ -3 & 0 & 3 & 1 \\ 1 & 4 & 1 & 0 \end{bmatrix} \begin{bmatrix} p_{i-1} \\ p_i \\ p_{i+1} \\ p_{i+2} \end{bmatrix} ; i \in [1:n-2] \dots (3.35)$$

Derivative of the Uniform B-Spline Basis Functions with $k=5$:

The derivative for uniform B-spline with $K=5$ is the same for cubic but with more complex solving equations (see Appendix A).

$$p_i'(u) = \frac{1}{24} [(u^4 - 4u^3 + 6u^2 - 4u + 1)p_i + (-4u^4 + 12u^3 - 6u^2 - 12u + 1)p_{i+1} + (5u^4 - 8u^3 + 9u^2 - 60u + 75)p_{i+2}]. \dots\dots\dots (3.36)$$

From equation(3.36)the Matrix form(M)is the result.

$$M = \frac{1}{24} \begin{bmatrix} 1 & -4 & 5 & 0 & 0 \\ -4 & 12 & -8 & 0 & 0 \\ 6 & -6 & 9 & 0 & 0 \\ -4 & -12 & -60 & 1 & 0 \\ 1 & 1 & 75 & 0 & 1 \end{bmatrix} \dots\dots\dots (3.37)$$

$$P_i(u) = \frac{1}{24} [u^4 \quad u^3 \quad u^2 \quad u \quad 1] \begin{bmatrix} 1 & -4 & 5 & 0 & 0 \\ -4 & 12 & -8 & 0 & 0 \\ 6 & -6 & 9 & 0 & 0 \\ -4 & -12 & -60 & 1 & 0 \\ 1 & 1 & 75 & 0 & 1 \end{bmatrix} \begin{bmatrix} p_{i-1} \\ p_i \\ p_{i+1} \\ p_{i+2} \\ p_{i+3} \end{bmatrix} \dots\dots (3.38)$$

3.5 B-spline Surfaces

The natural extension of the Bezier surface is the Cartesian product, B-spline surface is defined by

$$p(u, w) = \sum_{i=0}^m \sum_{j=0}^n p_{i,j} N_{i,k}(u) N_{j,l}(w) \dots\dots\dots (3.39)$$

$$p_{kl} = p_{ij}$$

$$i \in [s - 1 : s + k - 2]$$

$$j \in [t - 1 : t + l - 2]$$

The $p_{i,j}$ are control points and vertices of the characteristic polyhedron.

$N_{i,k}(u) : N_{j,l}(w)$: are the basis functions and they are the same as those of B-spline curves [26].

The equation (3.39) has been written as

$$p_{s,t}(u, w) = U M_s p M_s^T W^T \dots\dots\dots (3.40)$$

$$s \in [1 : m + 2 - k]$$

$$t \in [1 : n + 2 - l]$$

$$u, w \in [0,1]$$

Implementing the program to build the Uniform B-spline surface needs drawing the block diagram which is shown in Figure (3.14) and explaining the main steps of the program while the detailed explanation of the proposed program has been given in the flowchart that is shown in Figure (3.15).

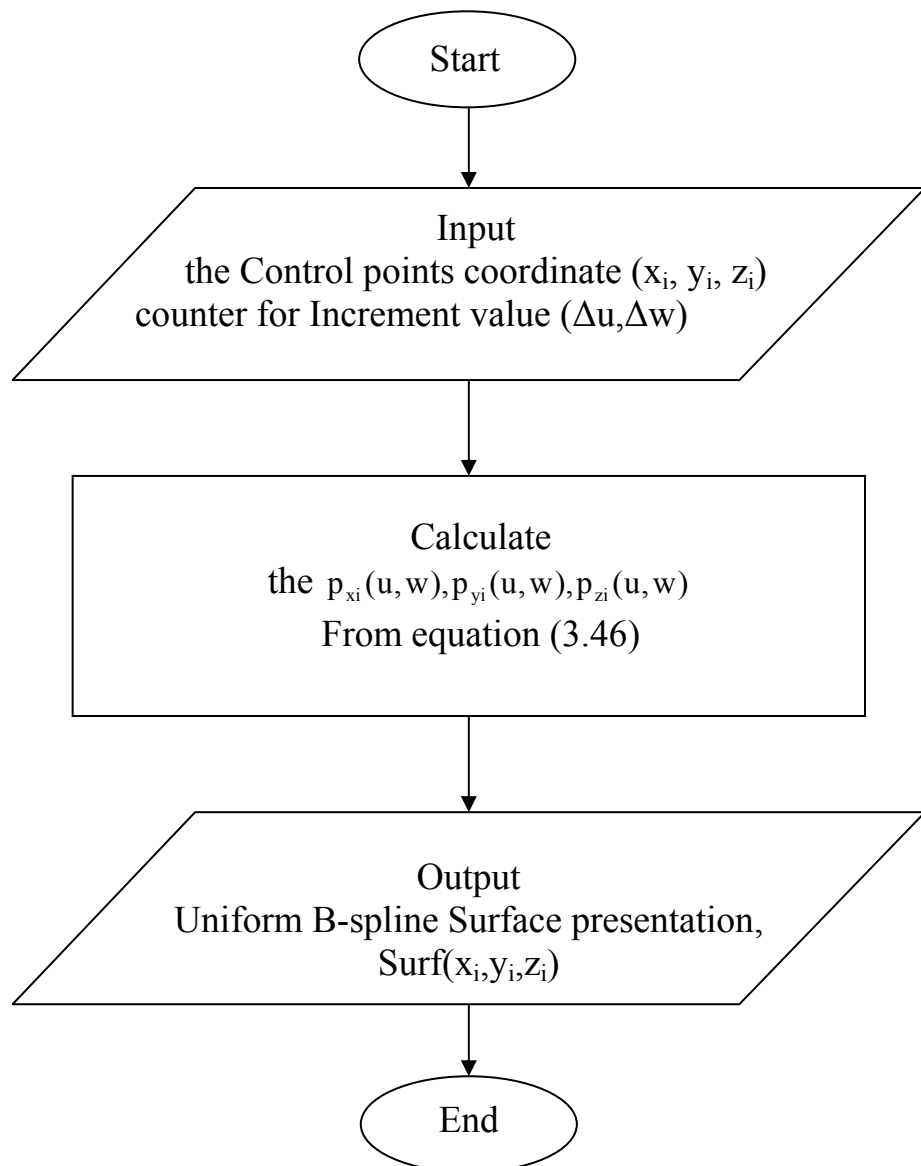


Figure (3.14): Block diagram of the proposed program depending on Uniform B-spline technique.

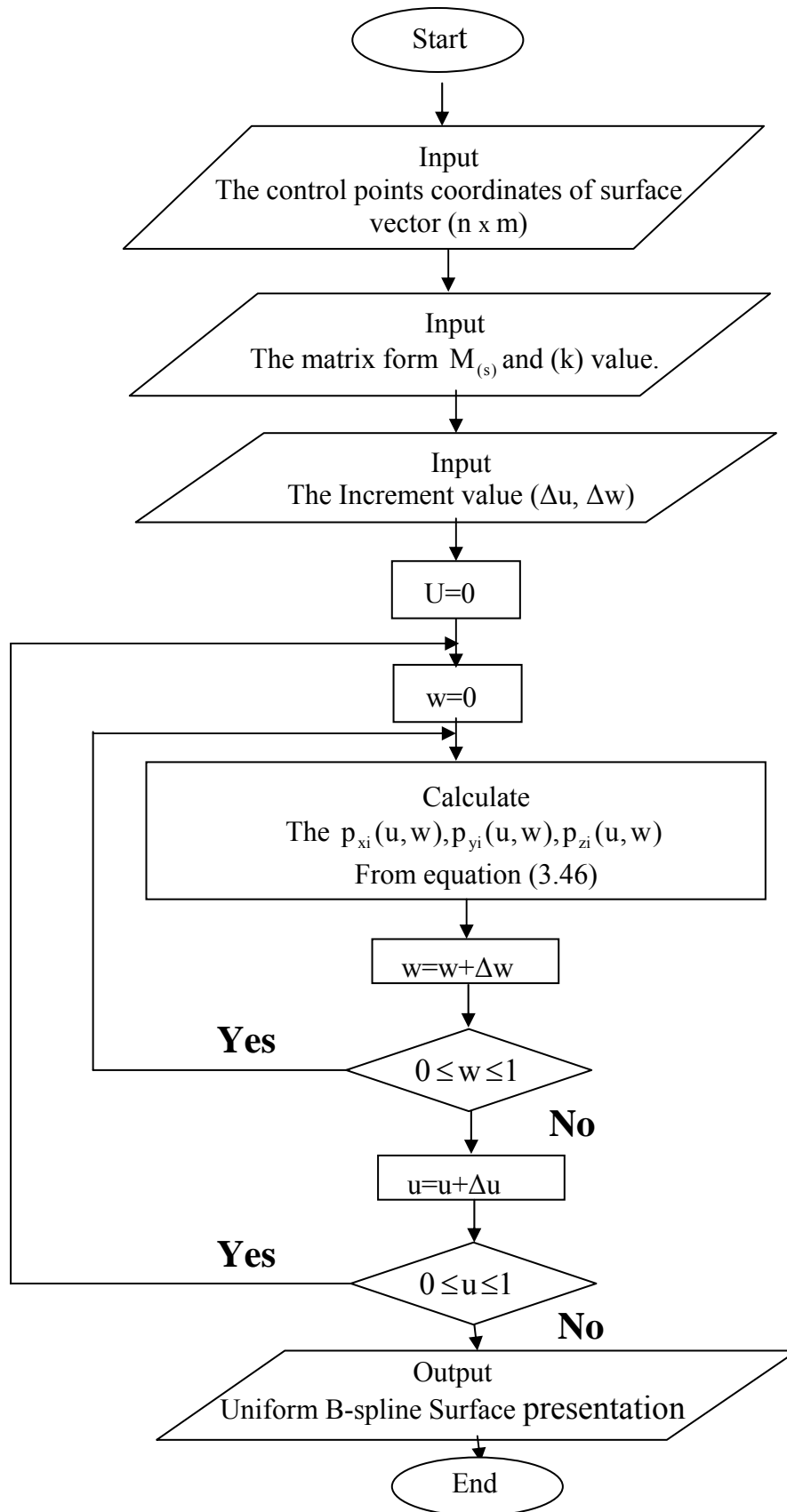


Figure (3.15): Flowchart of the proposed program depending on Uniform B-spline technique

The proposed program represents the surface in graphical mode with the software program Matlab (V7.0).Figures (3.16), and (3.17), show the final result of a practical application of proposed program.

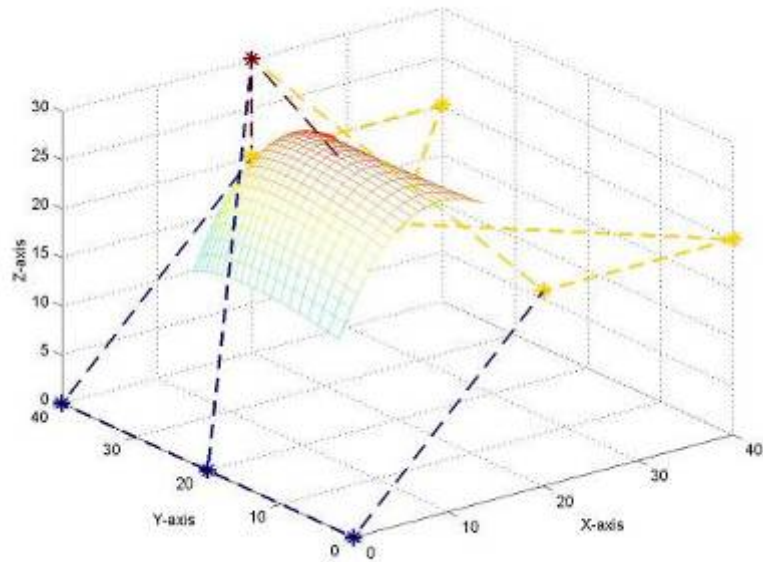


Figure (3.16): Uniform B-spline surface $k=3, (3 \times 3)$.

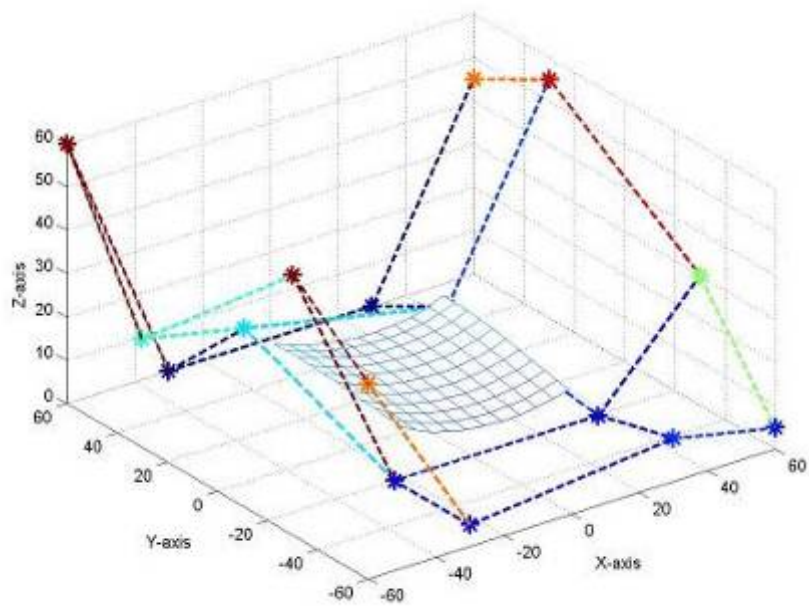


Figure (3.17): Uniform B-spline surface $k=4, (4 \times 4)$.

3.6 Chapter Summary

This chapter has focused on the approximation curves and surfaces for Bezier and Uniform B-spline technology.

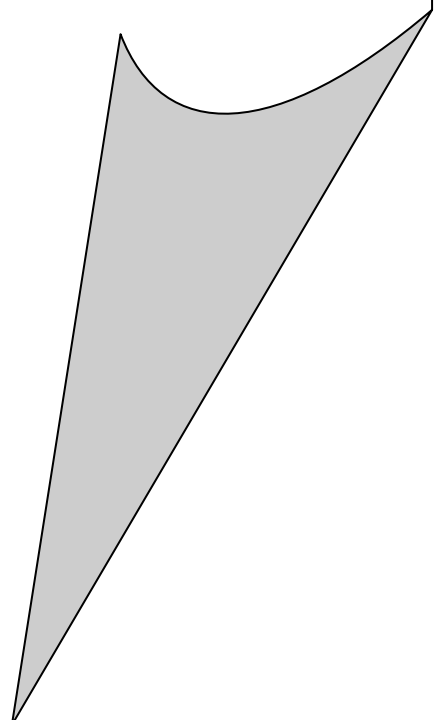
Firstly, it has reviewed the equation for the Bezier curve, and made some case studies to get several matrices forms M_s (Bezier) starting from $(n=2, \dots, 6)$ then reviewed the equation for the Bezier surface, so the block diagram, and Flowchart of the proposed program for Bezier technique is created.

Secondly, it has reviewed the equation for the Uniform B-spline curve and made some case studies to get several matrices forms M_s (Uniform B-spline) for $k=3,4$, and derivative of the matrix form for $K=5$, then reviewed the equation for the Uniform B-spline surface and this equation is solved to get Uniform B-spline surfaces for $K=3,4,5$, after that block diagram, and flowchart of the proposed program for Uniform B-spline technique are created.

However the aim of this chapter is to review the technique for Bezier and Uniform B-spline, and get the result as (M) matrices forms for both Bezier and Uniform B-spline in different freedom degrees, which will be used in the chapter four to implement the subdivision algorithm on these techniques.

CHAPTER FOUR

SUBDIVISION ALGORITHMS



CHAPTER FOUR

Subdivision algorithms

4.1 Introduction:

This thesis reviews the modeling of subdivision surfaces, although the theories behind subdivision surface schemes have been around for more than 20 years, only recently have they begun to get full attention.

For modeling surfaces such as the ones used in geometric modeling, there exist many good reasons to employ the subdivision paradigm. Subdivision schemes use simple rules to generate high-quality surfaces from coarse polygonal models.

Unlike most competing methods for generating surfaces, subdivision allows surfaces of arbitrary topology to be created using one single consistent paradigm. There is no need to stitch together different surface parts. This makes surface modeling much easier, as there is no fear of breaking the borders where patches are stitched together.

The most important implication for using subdivision algorithm is to vary the density of Control points over the surface. This permits the creation of small details and bodily limbs without the obligation to add numerous control points. Also important for subdivision surfaces is its extensive mathematical background, with important links to figure out multi-resolution analysis, which have proven their usefulness in many scientific fields. The divide-and-conquer approach, furthermore, allows for many applications in the field of simulating physical processes^[15].

Subdivision is a technique in computer aided geometric design for approximating a smooth surface by a sequence of increasingly faceted polyhedron. Subdivision schemes have several attributes that have motivated: The input that a designer or artist provides to the algorithm, usually a coarse mesh, is manageable in size and the subdivision iteration on the mesh, determined by a simple set of affine combinations, and typically results in a smooth surface^[19].

4.2 Curves Subdivision:

This chapter explains the concept of subdivision curves. Studying curve properties usually is much simpler than that of surfaces, making it easier to gain insights that later can be generalized to subdivision surfaces. Moreover, many subdivision surfaces schemes are directly or indirectly based on subdivision curve schemes^[14].

Subdivision methods for curve generation are based upon a procedure which successively refines a control polygon into a sequence of control polygons that is in the limit, or converges to a curve. The curves are commonly called subdivision curves as the refinement methods are based upon the binary subdivision of uniform B-spline curves by Chaitin’s method, or subdivision for Bezier curve^[30].

4.2.1 Subdivision and Refinement Uniform B-spline Curve:

For the Quadratic Uniform B-Spline Curve **k=3**, the equation for this curve with the matrix notation is calculated in chapter three in equation (3.34) and it could be rewritten in another form as shown in equation(4.1):

$$p(u) = \frac{1}{2} [1 \quad u \quad u^2] \begin{bmatrix} 1 & -2 & 1 \\ -2 & 2 & 0 \\ 1 & 1 & 0 \end{bmatrix} \begin{bmatrix} p_k \\ p_{k+1} \\ p_{k+2} \end{bmatrix} \dots\dots\dots(4.1)$$

For k = 0, 1, …, n - 2, and 0 ≤ t ≤ 1, and where

$$M_{(Quadratic\ B-spline)} = \frac{1}{2} \begin{bmatrix} 1 & -2 & 1 \\ -2 & 2 & 0 \\ 1 & 1 & 0 \end{bmatrix} \dots\dots\dots(4.2)$$

The matrix M in equation (4.2), when multiplied by [1 u u²] defines the quadratic uniform B-spline blending functions^[32].

Splitting and Refinement for the Quadratic Uniform B-Spline Curve

The binary subdivision of a quadratic uniform B-spline curve p(u) is defined by the control polygon {p₀, p₁, p₂} which is illustrated in Figure (4.1), containing only three points, and then this is extended to control polygons containing larger numbers of points.

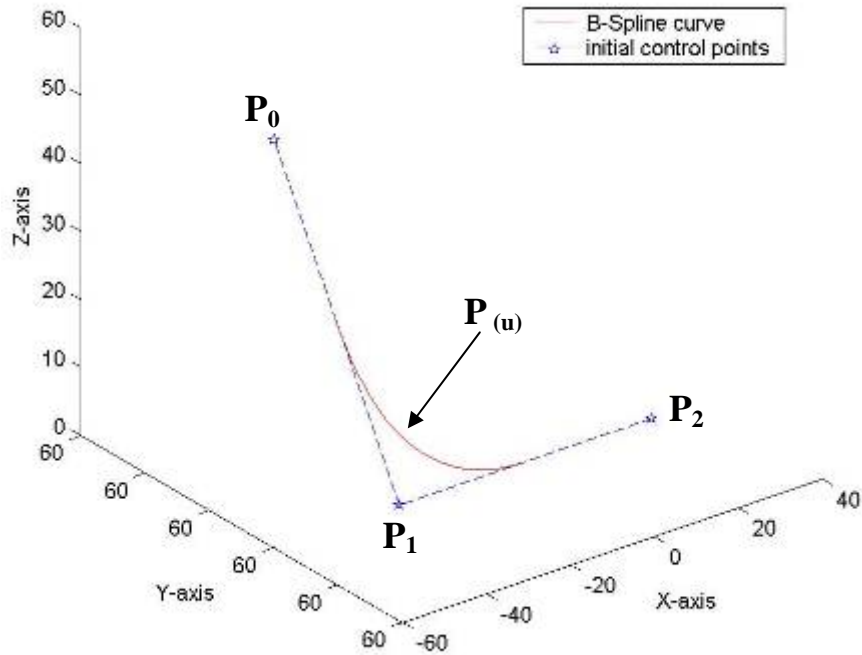


Figure (4.1) Quadratic uniform B-spline curve (three control points) [32].

A binary subdivision of the curve has been performed, by applying one of two splitting matrices in equations (4.4) and (4.5)

$$S_L = M^{-1} \begin{bmatrix} 1 & 0 & 0 \\ 0 & 1/2 & 0 \\ 0 & 0 & 1/4 \end{bmatrix} M \dots\dots\dots (4.3)$$

$$S_L = \frac{1}{4} \begin{bmatrix} 3 & 1 & 0 \\ 1 & 3 & 0 \\ 0 & 3 & 0 \end{bmatrix} \dots\dots\dots (4.4)$$

$$S_R = \frac{1}{4} \begin{bmatrix} 1 & 3 & 0 \\ 0 & 3 & 1 \\ 0 & 1 & 3 \end{bmatrix} \dots\dots\dots (4.5)$$

to the control polygon. When applied to the control polygon S_L gives the first half of the curve, and S_R gives the second half. As it turns out, several of the control points for the two subdivided components are the same. These matrices have been combined to create a (4×3) matrix in equation (4.6).

$$S_{(\text{Quadic B-spline})} = \frac{1}{4} \begin{bmatrix} 3 & 1 & 0 \\ 1 & 3 & 0 \\ 0 & 3 & 1 \\ 0 & 1 & 3 \end{bmatrix} \dots\dots\dots (4.6)$$

And it is applied to a control polygon in equation (4.7):

$$\begin{bmatrix} P_0^1 \\ P_1^1 \\ P_2^1 \\ P_3^1 \end{bmatrix} = \frac{1}{4} \begin{bmatrix} 3 & 1 & 0 \\ 1 & 3 & 0 \\ 0 & 3 & 1 \\ 0 & 1 & 3 \end{bmatrix} \begin{bmatrix} P_0 \\ P_1 \\ P_2 \end{bmatrix} = \begin{bmatrix} \frac{3}{4}P_0 + \frac{1}{4}P_1 \\ \frac{1}{4}P_0 + \frac{3}{4}P_1 \\ \frac{3}{4}P_1 + \frac{1}{4}P_2 \\ \frac{1}{4}P_1 + \frac{3}{4}P_2 \end{bmatrix} \dots\dots\dots (4.7)$$

And the refined curve has control points that are positioned as in the following illustration in Figure (4.2) i.e. at 1/4 and 3/4 along each of the lines of the control polygon. These are the same points as are developed in Chaitian's method [32].

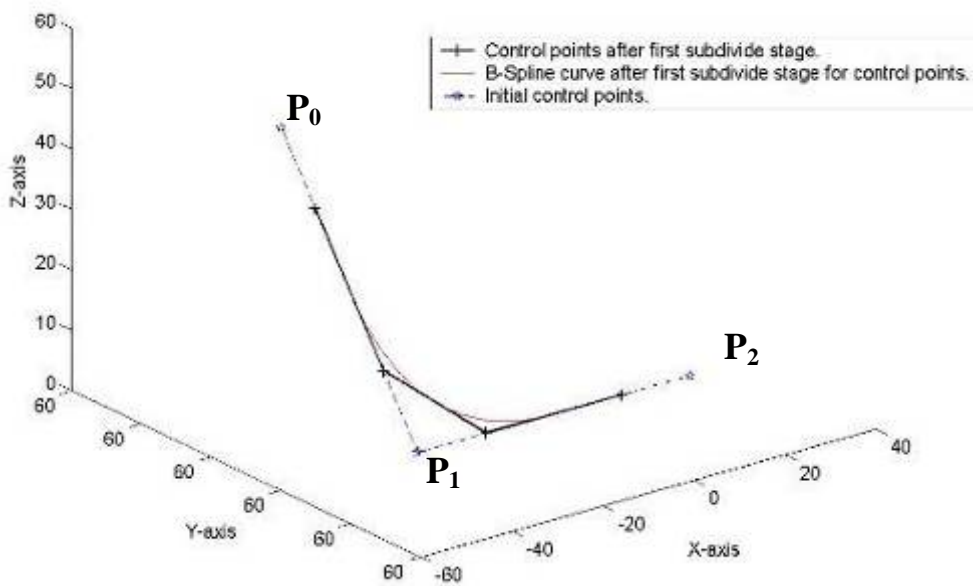


Figure (4.2) The first subdivides stage for the control points to Uniform B-spline Curve [32].

The general procedure is to give a control polygon; it has been generated by refinement of this set of points by constructing new points along each edge of the original polygon at a distance of 1/4 and 3/4 between the endpoints of the edge. The general idea behind subdivision curves is to assemble these points into a new control polygon which can then be used as

input to another refinement operation, generating a new set of points and another control polygon, and then this process continues until a refinement is reached that accurately represents the curve to a desired resolution [32].

For the cubic Uniform B-spline Curve $k=4$, the equation for this curve with the matrix notation is calculated in chapter three in equation (3.35) and it could be rewritten in another form in equation (4.8):

$$p(u) = \frac{1}{6} [1 \quad u \quad u^2 \quad u^3] \begin{bmatrix} 1 & 4 & 1 & 0 \\ -3 & 0 & 3 & 0 \\ 3 & -6 & 3 & 0 \\ -1 & 3 & -3 & 1 \end{bmatrix} \begin{bmatrix} p_k \\ p_{k+1} \\ p_{k+2} \\ p_{k+3} \end{bmatrix} \dots\dots\dots (4.8)$$

For $k = 0, 1, \dots, n - 3$, and $0 \leq t \leq 1$, and where

$$M_{(\text{cubic B-spline})} = \frac{1}{6} \begin{bmatrix} 1 & 4 & 1 & 0 \\ -3 & 0 & 3 & 0 \\ 3 & -6 & 3 & 0 \\ -1 & 3 & -3 & 1 \end{bmatrix} \dots\dots\dots (4.9)$$

The matrix M which is shown in equation (4.9), when multiplied by $[1 \quad u \quad u^2 \quad u^3]$ defines the cubic uniform B-spline blending functions.

Splitting and Refinement for the cubic Uniform B-Spline Curve

The binary subdivision of a cubic uniform B-spline curve $p(u)$ is defined by the control polygon $\{p_0, p_1, p_2, p_3\}$, containing only three points, and then this is extended to control polygons containing larger numbers of points. Let us consider the new control point in Figure (4.2) is the initial control point for the cubic uniform B-spline curve.

And the splitting matrix matrices can be calculated as shown in equations (4.10), (4.11) [30].

To gain more experience with this approach, three further examples of Chaitian (quadratic B-spline) subdivision are offered [31].

$$S_L = \frac{1}{8} \begin{bmatrix} 4 & 4 & 0 & 0 \\ 1 & 6 & 1 & 0 \\ 0 & 4 & 4 & 0 \\ 0 & 1 & 6 & 1 \end{bmatrix} \dots\dots\dots (4.10)$$

$$S_R = \frac{1}{8} \begin{bmatrix} 1 & 6 & 1 & 0 \\ 0 & 4 & 4 & 0 \\ 0 & 1 & 6 & 1 \\ 0 & 0 & 4 & 4 \end{bmatrix} \dots\dots\dots (4.11)$$

A binary subdivision of the curve is performed, by applying one of two splitting matrix S_L and S_R to control polygon. (When applied to the control polygon S_L gives the first half of the curve, and S_R gives the second half.)

As it turns out, several of the control points for the two subdivided components are the same. Thus, these matrices it have been combined, creating a (5×4) matrix as shown in equation (4.12).

$$S_{(CubicB-spline)} = \frac{1}{8} \begin{bmatrix} 4 & 4 & 0 & 0 \\ 1 & 6 & 1 & 0 \\ 0 & 4 & 4 & 0 \\ 0 & 1 & 6 & 1 \\ 0 & 0 & 4 & 4 \end{bmatrix} \dots\dots\dots (4.12)$$

And the new control point for the subdivide polygon is calculated in equation (4.13).

$$\begin{bmatrix} P_0^1 \\ P_1^1 \\ P_2^1 \\ P_3^1 \\ P_4^1 \end{bmatrix} = \frac{1}{8} \begin{bmatrix} 4 & 4 & 0 & 0 \\ 1 & 6 & 1 & 0 \\ 0 & 4 & 4 & 0 \\ 0 & 1 & 6 & 1 \\ 0 & 0 & 4 & 4 \end{bmatrix} \begin{bmatrix} P_0 \\ P_1 \\ P_2 \\ P_3 \end{bmatrix} \dots\dots\dots (4.13)$$

This generates a new control polygon which serves as the refinement of the original. The five control points of this new control polygon specify the two subdivision halves of the curve-and therefore specify the curve itself, This is illustrated in Figure (4.3).

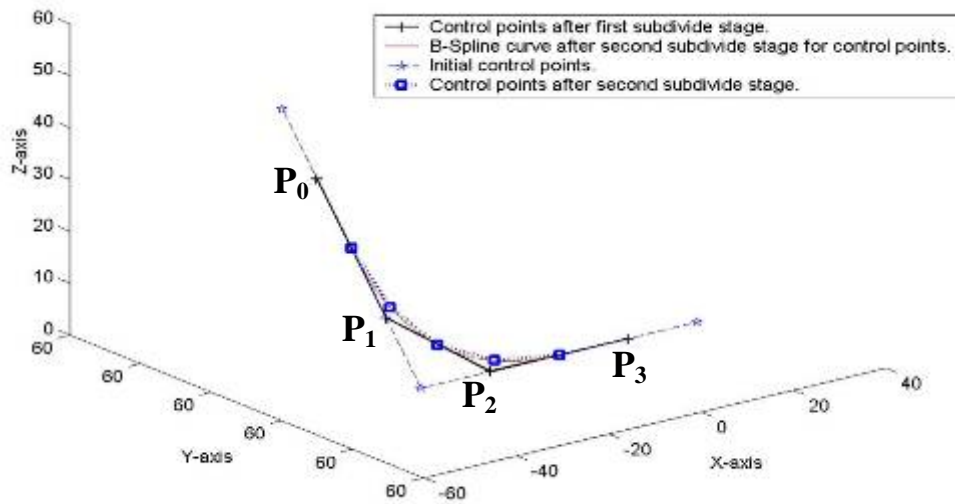


Figure (4.3) The Second subdivides stage for the control points to Uniform B-spline Curve [30].

In the case of the quadratic curve, one is able to state exactly a single procedure for the points of the refinement. In this case, it is not so easy. However, if one examines the rows of the (5×4) matrix used in the refinement, it is seen that they have two distinct forms. This motivates us to classify the points of the refinement as vertex and edge points; this classification makes the description of the refinement process quite straightforward [30].

For the Quartic Uniform B-spline Curve $\mathbf{k=5}$, the equation for this curve with the matrix notation is calculated in chapter three in equation (3.44) and it could be rewritten in another form as shown in equation (4.14):

$$p(u) = \frac{1}{24} \begin{bmatrix} 1 & u & u^2 & u^3 & u^4 \end{bmatrix} \begin{bmatrix} 1 & -4 & 5 & 0 & 0 \\ -4 & 12 & -8 & 0 & 0 \\ 6 & -6 & 9 & 0 & 0 \\ -4 & -12 & -60 & 1 & 0 \\ 1 & 1 & 75 & 0 & 1 \end{bmatrix} \begin{bmatrix} p_k \\ p_{k+1} \\ p_{k+2} \\ p_{k+3} \\ p_{k+4} \end{bmatrix} \dots\dots\dots (4.14)$$

For $k = 0, 1, \dots, n - 4$, and $0 \leq t \leq 1$, and where

$$M_{(\text{quartic B-spline})} = \frac{1}{24} \begin{bmatrix} 1 & -4 & 5 & 0 & 0 \\ -4 & 12 & -8 & 0 & 0 \\ 6 & -6 & 9 & 0 & 0 \\ -4 & -12 & -60 & 1 & 0 \\ 1 & 1 & 75 & 0 & 1 \end{bmatrix} \dots\dots\dots (4.15)$$

And the splitting matrix for the Quartic B-spline curve:

is illustrated in equation (4.16):

$$S_{(\text{quartic B-spline})} = \frac{1}{16} \begin{bmatrix} 5 & 10 & 1 & 0 & 0 \\ 1 & 10 & 5 & 0 & 0 \\ 0 & 5 & 10 & 1 & 0 \\ 0 & 1 & 10 & 5 & 0 \\ 0 & 0 & 5 & 10 & 1 \\ 0 & 0 & 1 & 10 & 5 \end{bmatrix} \dots\dots\dots (4.16)$$

So, the new control points after making the third iteration for subdivision is the Quartic Uniform B-spline curve defined by equation (4.17) which is defined by Pascal triangle..

$$\begin{bmatrix} P_0^1 \\ P_1^1 \\ P_2^1 \\ P_3^1 \\ P_4^1 \\ P_5^1 \end{bmatrix} = \frac{1}{16} \begin{bmatrix} 5 & 10 & 1 & 0 & 0 \\ 1 & 10 & 5 & 0 & 0 \\ 0 & 5 & 10 & 1 & 0 \\ 0 & 1 & 10 & 5 & 0 \\ 0 & 0 & 5 & 10 & 1 \\ 0 & 0 & 1 & 10 & 5 \end{bmatrix} \begin{bmatrix} P_0 \\ P_1 \\ P_2 \\ P_3 \\ P_4 \end{bmatrix} \dots\dots\dots (4.17)$$

A new control polygon is generated which serves as the refinement of the original. The six control points of this new control polygon specify the two subdivision halves of the curve-and therefore specify the curve itself as shown in Figure (4.4).

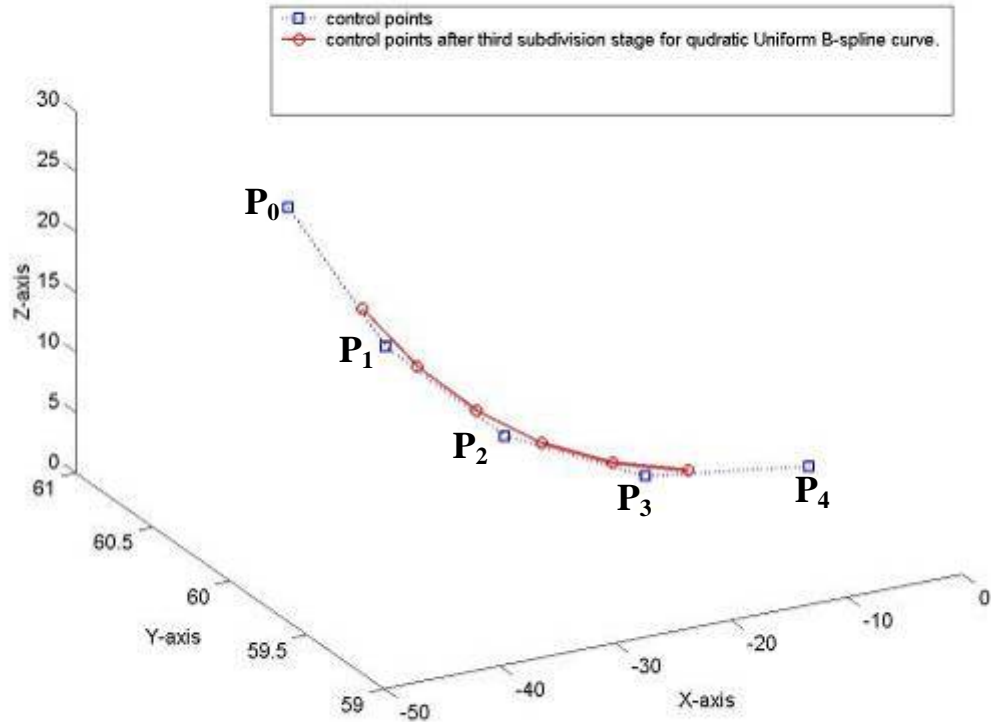


Figure (4.4) The Third subdivides stage for the control points to quadratic Uniform B-spline curve.

For the Quartic Uniform B-spline Curve $k=6$, the equation for this curve is written as shown in equation (4.18).

$$p(u) = \frac{1}{24} [1 \quad u \quad u^2 \quad u^3 \quad u^4 \quad u^5] M \begin{bmatrix} p_k \\ p_{k+1} \\ p_{k+2} \\ p_{k+3} \\ p_{k+4} \\ p_{k+5} \end{bmatrix} \dots\dots\dots (4.18)$$

For $k = 0, 1, \dots, n - 5$, and $0 \leq t \leq 1$, and where

And the splitting matrix for the Quartic B-spline curve:

is illustrated in equation (4.19) which is defined by Pascal triangle.

$$S_{(quartic \ B-spline)} = \frac{1}{32} \begin{bmatrix} 6 & 20 & 6 & 0 & 0 & 0 \\ 1 & 15 & 15 & 1 & 0 & 0 \\ 0 & 6 & 20 & 6 & 0 & 0 \\ 0 & 1 & 15 & 15 & 1 & 0 \\ 0 & 0 & 6 & 20 & 6 & 0 \\ 0 & 0 & 1 & 15 & 15 & 1 \\ 0 & 0 & 0 & 6 & 20 & 6 \end{bmatrix} \dots\dots\dots (4.19)$$

So, the new control points after the fourth iteration for subdivision for the Quintic Uniform B-spline curve are defined by Pascal triangle and by the following equation

$$\begin{bmatrix} P_0^1 \\ P_1^1 \\ P_2^1 \\ P_3^1 \\ P_4^1 \\ P_5^1 \\ P_6^1 \end{bmatrix} = \frac{1}{32} \begin{bmatrix} 6 & 20 & 6 & 0 & 0 & 0 \\ 1 & 15 & 15 & 1 & 0 & 0 \\ 0 & 6 & 20 & 6 & 0 & 0 \\ 0 & 1 & 15 & 15 & 1 & 0 \\ 0 & 0 & 6 & 20 & 6 & 0 \\ 0 & 0 & 1 & 15 & 15 & 1 \\ 0 & 0 & 0 & 6 & 20 & 6 \end{bmatrix} \begin{bmatrix} P_0 \\ P_1 \\ P_2 \\ P_3 \\ P_4 \\ P_5 \end{bmatrix} \dots\dots\dots (4.20)$$

Anew control polygon is generated which serves as the refinement of the original. The seven control points of this new control polygon specify the two subdivision halves of the curve-and therefore specify the curve itself as shown in Figure (4.5).

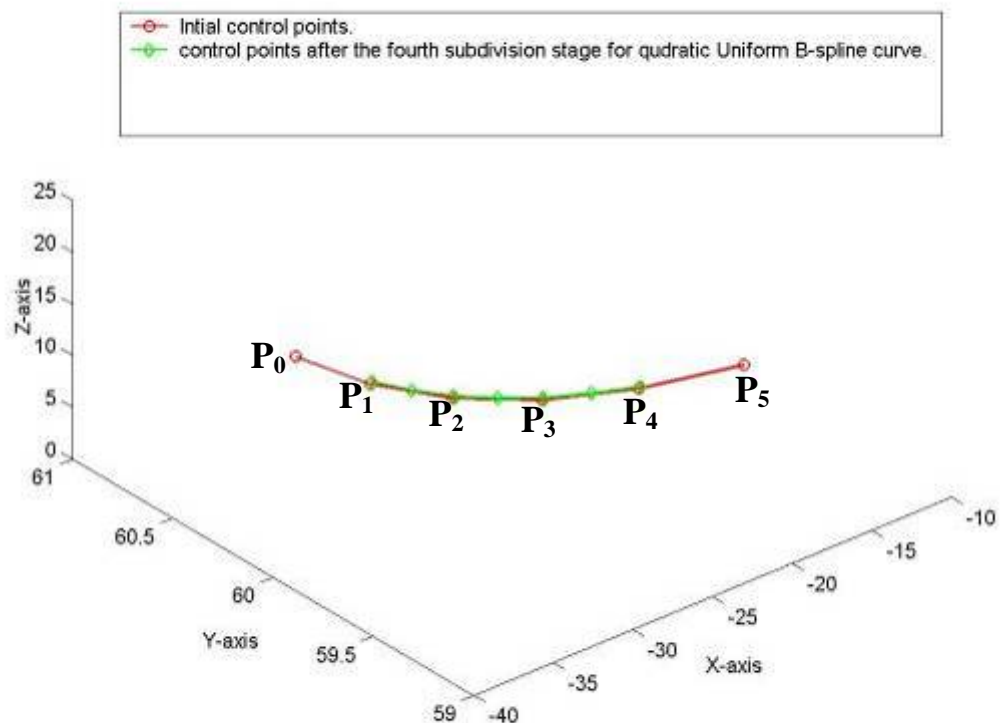


Figure (4.5) The Fourth subdivides stage for the control points to quintic Uniform B-spline Curve.

4.2.2 Subdivision and Refinement of Bezier Curve:

The Bezier curve representation is one that is utilized most frequently in computer graphics and geometric modeling. The curve is defined geometrically, which means that the parameters have geometric meaning - they are just points in three-dimensional space. It was developed by two competing European engineers in the late 1960s in an attempt to draw automotive components ^[24].

Refinement for the Cubic Bezier Curve:

A cubic Bezier patch has a useful representation when written in matrix form. This form allows us to specify many operations with Bezier patches as matrix operations which can be performed quickly on computer systems optimized for geometry operations with matrices.

This is an unusual representation for many entrepreneurs as it is not frequently shown in basic books. So if you have not seen this before it is suggested that you begin with the section on matrix representations for Bezier curves in which the equations are simpler and easier to understand ^[33].

The matrix formulation for cubic Bezier curve which is introduced in chapter three in equation (3.12) builds the foundation for our refinement curve and is rewritten as ^[34].

$$p(u) = [1 \quad u \quad u^2 \quad u^3] \begin{bmatrix} 1 & 0 & 0 & 0 \\ -3 & 3 & 0 & 0 \\ 3 & -6 & 3 & 0 \\ -1 & 3 & -3 & 1 \end{bmatrix} \begin{bmatrix} p_0 \\ p_1 \\ p_2 \\ p_3 \end{bmatrix} \dots\dots\dots (4.21)$$

And the refinement process for Bezier curve is illustrated as follows ^[33]:

1. When divide the (u) direction from [0-1/2],(as illustrated in equations (4.22) and (4.23)):

$$p\left(\frac{u}{2}\right) = \begin{bmatrix} 1 & \frac{u}{2} & \left(\frac{u}{2}\right)^2 & \left(\frac{u}{2}\right)^3 \end{bmatrix} \begin{bmatrix} 1 & 0 & 0 & 0 \\ -3 & 3 & 0 & 0 \\ 3 & -6 & 3 & 0 \\ -1 & 3 & -3 & 1 \end{bmatrix} \begin{bmatrix} p_0 \\ p_1 \\ p_2 \\ p_3 \end{bmatrix} \dots\dots\dots (4.22)$$

$$p(u) = \begin{bmatrix} 1 & u & u^2 & u^3 \end{bmatrix} \begin{bmatrix} 1 & 0 & 0 & 0 \\ 0 & \frac{1}{2} & 0 & 0 \\ 0 & 0 & \frac{1}{4} & 0 \\ 0 & 0 & 0 & \frac{1}{8} \end{bmatrix} \begin{bmatrix} 1 & 0 & 0 & 0 \\ -3 & 3 & 0 & 0 \\ 3 & -6 & 3 & 0 \\ -1 & 3 & -3 & 1 \end{bmatrix} \begin{bmatrix} p_0 \\ p_1 \\ p_2 \\ p_3 \end{bmatrix} \dots (4.23)$$

So, the left splitting matrix is shown in equation (4.24).

$$S_L(\text{cubic Bezier curve}) = M^{-1} \begin{bmatrix} 1 & 0 & 0 & 0 \\ 0 & \frac{1}{2} & 0 & 0 \\ 0 & 0 & \frac{1}{4} & 0 \\ 0 & 0 & 0 & \frac{1}{8} \end{bmatrix} M \dots\dots\dots (4.24)$$

It can be rewritten as :

$$\therefore S_L(\text{cubic Bezier curve}) = \begin{bmatrix} 1 & 0 & 0 & 0 \\ \frac{1}{2} & \frac{1}{2} & 0 & 0 \\ \frac{1}{4} & \frac{1}{2} & \frac{1}{4} & 0 \\ \frac{1}{8} & \frac{3}{8} & \frac{3}{8} & \frac{1}{8} \end{bmatrix} \dots\dots\dots (4.25)$$

2. When you divide the (u) direction from [1/2-1]:

the right splitting matrix is shown in equation (4.26):

$$S_R(\text{cubic Bezier curve}) = \begin{bmatrix} \frac{1}{8} & \frac{3}{8} & \frac{3}{8} & \frac{1}{8} \\ 0 & \frac{1}{4} & \frac{1}{2} & \frac{1}{4} \\ 0 & 0 & \frac{1}{2} & 0 \\ 0 & 0 & 0 & 1 \end{bmatrix} \dots\dots\dots (4.26)$$

The Bezier curve before using the splitting matrixes is shown in Figure (4.6).

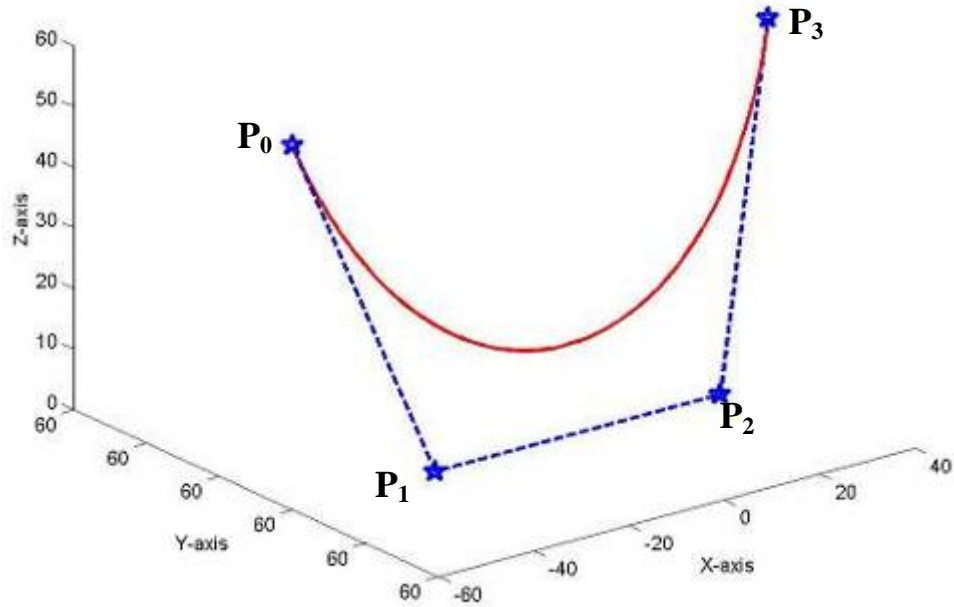


Figure (4.6) Bezier curve before using the splitting matrixes to subdivide the control points.

The matrix from the equation (4.25) has been used and multiplied with the initial control points as shown in equation (4.21),so the result is shown in equation (4.27) and illustrated in Figure (4.7).

$$P'_L = S_L P \quad \dots\dots\dots (4.27)$$

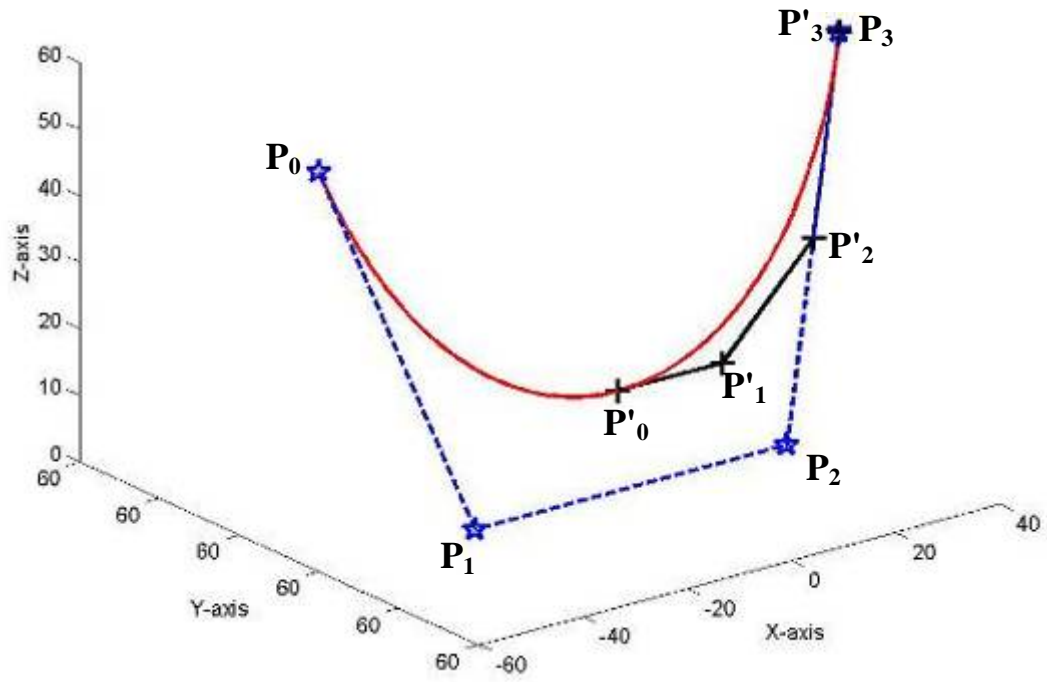


Figure (4.8) Bezier curve after using the right splitting matrixes to subdivide the control points.

When both splitting matrix are used and multiplied with initial control points the result is shown in Figure (4.9).

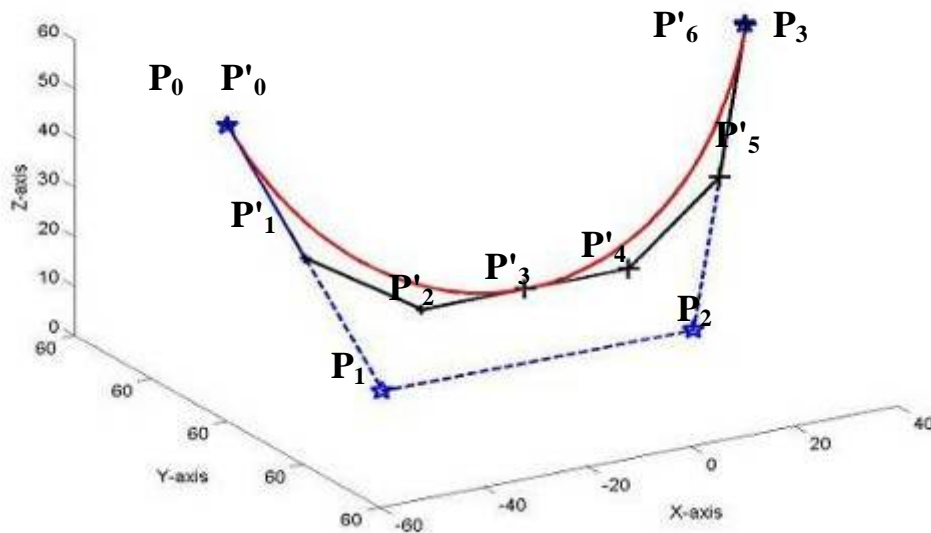


Figure (4.9) Bezier curve after using both (right and left) splitting matrixes to subdivide the control points.

4.3 Uniform B-spline Surface Refinement:

Recursive subdivision is the process of repeatedly refining an initial control polygon P_0 in order to produce a sequence of increasingly more refined polygons $P_0, P_1, P_2, P_3, \dots$ hence approaching a limit polygon, actually a curve [35].

Subdivision surfaces are based upon the binary subdivision of the uniform B-spline surface. In general, they are defined by initial polygonal mesh, along with a subdivision (or refinement) operation which, given a polygonal mesh, will generate a new mesh that has a greater number of polygonal elements, and is hopefully “closer” to some resulting surface. By repetitively applying the subdivision procedure to the initial mesh, a sequence of meshes, has been generated that (hopefully) converges to a resulting surface.

As it turns out, this is a well known process when the mesh has a “rectangular” structure and the subdivision procedure is an extension of binary subdivision for uniform B-spline surfaces [36].

The Matrix Equation for the Quadratic Uniform B-spline Surface:

The equation for this surface can be calculated from the general equation for Uniform B-spline surface in chapter three equation (3.45). So the uniform B-spline surface for $K=3$ is shown in equation (4.29).

$$P(u, w) = [1 \quad u \quad u^2] M_p M^T \begin{bmatrix} 1 \\ w \\ w^2 \end{bmatrix} \dots\dots\dots (4.29)$$

And polygon for this surface is illustrated in Figure (4.10) where M is 3×3 matrixes defined by equation (4.30) and (p) is the initial control points shown in equation (4.31).

$$M_{(Uniform\ quadratic\ B-spline)} = \frac{1}{2} \begin{bmatrix} 1 & -2 & 1 \\ -2 & 2 & 0 \\ 1 & 1 & 0 \end{bmatrix} \dots\dots\dots (4.30)$$

$$p = \begin{bmatrix} p_{0,0} & p_{0,1} & p_{0,2} \\ p_{1,0} & p_{1,1} & p_{1,2} \\ p_{2,0} & p_{2,1} & p_{2,2} \end{bmatrix} \dots\dots\dots (4.31)$$

The matrix M (Uniform quadratic B-splie) defines the quadratic Uniform B-spline

blending functions when multiplied by $\begin{bmatrix} 1 \\ w \\ w^2 \end{bmatrix}$ [36].

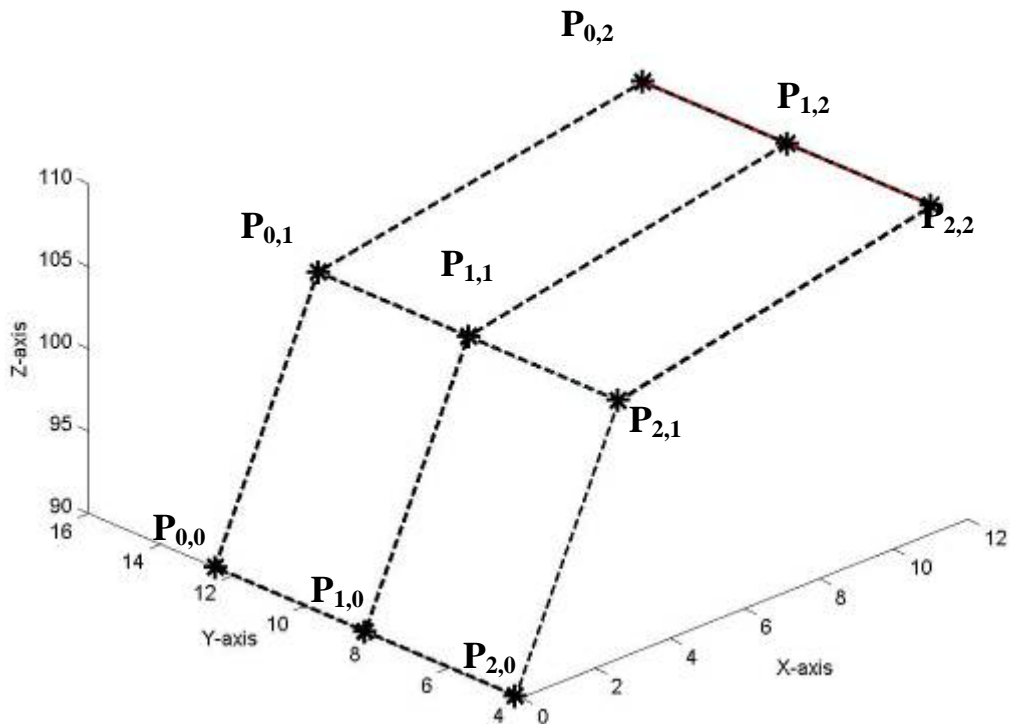


Figure (4.10): Initial control polygon for the quadratic Uniform B-spline

Subdividing the Quadratic Uniform B-spline Surface:

This patch can be subdivided into four sub patches, which are generated from 16 unique sub-control points. It has been focused on the subdivision scheme for only one of the four the sub patch corresponding to $[0 \leq u, w \leq 1/2]$, as the others will follow by symmetry. The Figure (4.11) illustrates the 16 points produced by subdividing into four sub patches. The initial sub patch that is considered below has been outlined. It should be noted that the four “interior” control points are utilized by each of the four sub patch components of the subdivision.

To define new surface $P'(u, w)$, it should be substituted into the equation (4.32) and it yields [36]:

$$P'(u, w) = p\left(\frac{u}{2}, \frac{w}{2}\right) \dots\dots\dots (4.32)$$

$$\begin{aligned}
 &= [1 \quad \frac{u}{2} \quad (\frac{u}{2})^2] M P M^T \begin{bmatrix} 1 \\ \frac{w}{2} \\ (\frac{w}{2})^2 \end{bmatrix} \\
 &= [1 \quad u \quad u^2] \begin{bmatrix} 1 & 0 & 0 \\ 0 & \frac{1}{2} & 0 \\ 0 & 0 & \frac{1}{4} \end{bmatrix} M P M^T \begin{bmatrix} 1 & 0 & 0 \\ 0 & \frac{1}{2} & 0 \\ 0 & 0 & \frac{1}{4} \end{bmatrix}^T \begin{bmatrix} 1 \\ w \\ w^2 \end{bmatrix} \\
 &= [1 \quad u \quad u^2] M M^{-1} \begin{bmatrix} 1 & 0 & 0 \\ 0 & \frac{1}{2} & 0 \\ 0 & 0 & \frac{1}{4} \end{bmatrix} M P M^T \begin{bmatrix} 1 & 0 & 0 \\ 0 & \frac{1}{2} & 0 \\ 0 & 0 & \frac{1}{4} \end{bmatrix}^T (M^{-1})^T M^T \begin{bmatrix} 1 \\ w \\ w^2 \end{bmatrix} \\
 &= [1 \quad u \quad u^2] M \left(M^{-1} \begin{bmatrix} 1 & 0 & 0 \\ 0 & \frac{1}{2} & 0 \\ 0 & 0 & \frac{1}{4} \end{bmatrix} M P M^T \begin{bmatrix} 1 & 0 & 0 \\ 0 & \frac{1}{2} & 0 \\ 0 & 0 & \frac{1}{4} \end{bmatrix}^T \right) (M^{-1})^T M^T \begin{bmatrix} 1 \\ w \\ w^2 \end{bmatrix} \\
 &= [1 \quad u \quad u^2] M \left(M^{-1} \begin{bmatrix} 1 & 0 & 0 \\ 0 & \frac{1}{2} & 0 \\ 0 & 0 & \frac{1}{4} \end{bmatrix} M P M \begin{bmatrix} 1 & 0 & 0 \\ 0 & \frac{1}{2} & 0 \\ 0 & 0 & \frac{1}{4} \end{bmatrix} \right)^T (M^{-1})^T M^T \begin{bmatrix} 1 \\ w \\ w^2 \end{bmatrix}
 \end{aligned}$$

$$P'(u, w) = [1 \quad u \quad u^2] M P' M^T \begin{bmatrix} 1 \\ w \\ w^2 \end{bmatrix}$$

where $P' = S P S^T$ and

$$S = M^{-1} \begin{bmatrix} 1 & 0 & 0 \\ 0 & \frac{1}{2} & 0 \\ 0 & 0 & \frac{1}{4} \end{bmatrix} M \dots\dots\dots (4.33)$$

From this process, the surface $P'(u, w)$ in equation (4.34) can be written as.

$$P'(u, w) = [1 \quad u \quad u^2] M S P S^T M^T \begin{bmatrix} 1 \\ w \\ w^2 \end{bmatrix} \dots\dots\dots (4.34)$$

For (3 x 3) control point array (S) .this implies that $P'(u, w)$ is a uniform quadratic B-spline patch. The matrix (S) is typically called the "Splitting matrix", and is given by (4.33), and is shown in equation (4.35):

$$S = \frac{1}{2} \begin{bmatrix} 2 & -1 & 0 \\ 2 & 1 & 0 \\ 2 & 3 & 4 \end{bmatrix} \begin{bmatrix} 1 & 0 & 0 \\ 0 & 1/2 & 0 \\ 0 & 0 & 1/4 \end{bmatrix} \frac{1}{2} \begin{bmatrix} 1 & 1 & 0 \\ -2 & 2 & 0 \\ 1 & -2 & 1 \end{bmatrix} \dots\dots\dots (4.35)$$

$$= \frac{1}{4} \begin{bmatrix} 3 & 1 & 0 \\ 1 & 3 & 0 \\ 0 & 3 & 1 \end{bmatrix}$$

And so the control point mesh P_0 corresponding to the subdivided patch is related to the original control points mesh by the equation (4.36)

$$P' = S P S^T \dots\dots\dots (4.36)$$

By carrying out the algebra, it has the (P') given the equation (3.38).

$$\begin{aligned}
 P' &= \frac{1}{4} \begin{bmatrix} 3 & 1 & 0 \\ 1 & 3 & 0 \\ 0 & 3 & 1 \end{bmatrix} \begin{bmatrix} p_{0,0} & p_{0,1} & p_{0,2} \\ p_{1,0} & p_{1,1} & p_{1,2} \\ p_{2,0} & p_{2,1} & p_{2,2} \end{bmatrix} \frac{1}{4} \begin{bmatrix} 3 & 1 & 0 \\ 1 & 3 & 0 \\ 0 & 3 & 1 \end{bmatrix}^T \\
 &= \frac{1}{16} \begin{bmatrix} 3p_{0,0} + p_{1,0} & 3p_{0,1} + p_{1,1} & 3p_{0,2} + p_{1,2} \\ p_{0,0} + 3p_{1,0} & p_{0,1} + 3p_{1,1} & p_{0,2} + 3p_{1,2} \\ 3p_{1,0} + p_{2,0} & 3p_{1,1} + p_{2,1} & 3p_{1,2} + p_{2,2} \end{bmatrix} \begin{bmatrix} 3 & 1 & 0 \\ 1 & 3 & 0 \\ 0 & 3 & 1 \end{bmatrix} \dots\dots\dots (4.37)
 \end{aligned}$$

$$= \frac{1}{16} \begin{bmatrix} p'_{0,0} & p'_{0,1} & p'_{0,2} \\ p'_{1,0} & p'_{1,1} & p'_{1,2} \\ p'_{2,0} & p'_{2,1} & p'_{2,2} \end{bmatrix} \dots\dots\dots (4.38)$$

So, the refinement Quadratic Uniform B-spline surface is shown in Figure (4.11).

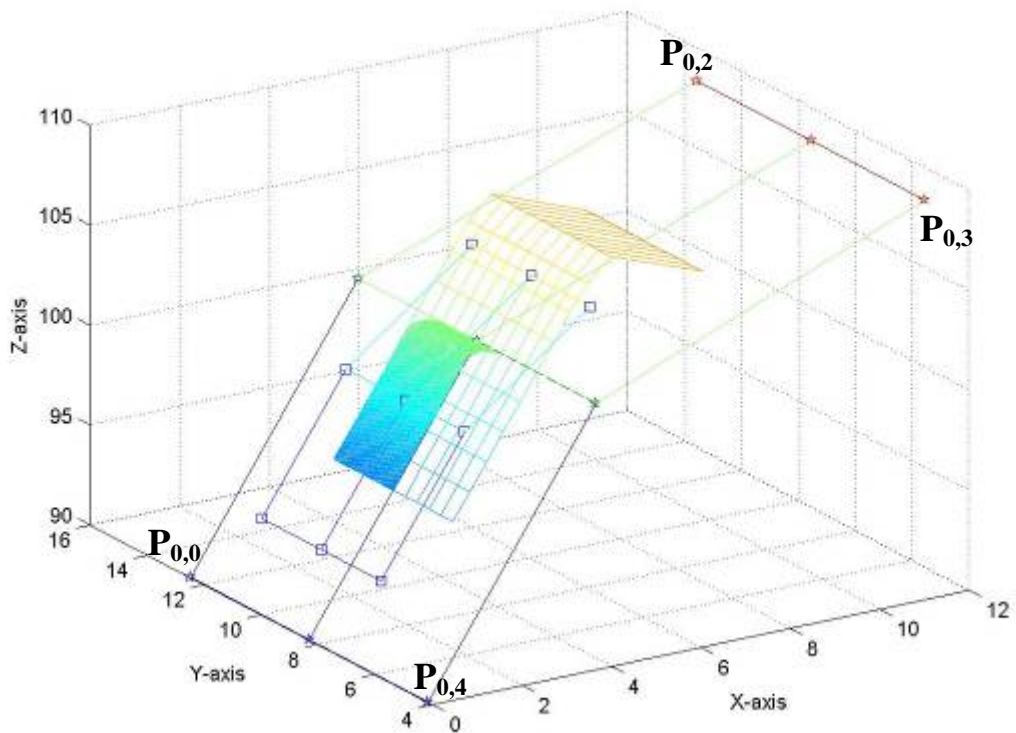


Figure (4.11): Initial control polygon for the quadratic Uniform B-spline surface and the subdivide polygon when $u' = \frac{u}{2}$ and $w' = \frac{w}{2}$.

where the $P'_{i,j}$ from the equation (4.37) is rewritten as

$$\begin{aligned}
 p'_{0,0} &= \frac{1}{16}(3(3p_{0,0} + p_{1,0}) + (3p_{0,1} + p_{1,1})) \\
 p'_{0,1} &= \frac{1}{16}((3p_{0,0} + p_{1,0}) + 3(3p_{0,1} + p_{1,1})) \\
 p'_{0,2} &= \frac{1}{16}(3(3p_{0,1} + p_{1,1}) + (3p_{0,2} + p_{1,2})) \\
 p'_{1,0} &= \frac{1}{16}(3(p_{0,0} + 3p_{1,0}) + (p_{0,1} + 3p_{1,1})) \\
 p'_{1,1} &= \frac{1}{16}((3p_{0,0} + 3p_{1,0}) + 3(3p_{0,1} + 3p_{1,1})) \\
 p'_{1,2} &= \frac{1}{16}(3(p_{0,1} + 3p_{1,1}) + (p_{0,2} + 3p_{1,2})) \\
 p'_{2,0} &= \frac{1}{16}(3(3p_{1,0} + p_{2,0}) + (3p_{1,1} + p_{2,1})) \\
 p'_{2,1} &= \frac{1}{16}((3p_{1,0} + p_{2,0}) + 3(3p_{1,1} + p_{2,1})) \\
 p'_{2,2} &= \frac{1}{16}(3(3p_{1,1} + p_{2,1}) + (3p_{1,2} + p_{2,2}))
 \end{aligned}
 \tag{4.39}$$

These equations can be looked at in two ways:

1. Each of these points $P_{i,j}$ utilizes the four points on a certain face of the rectangular mesh, and calculates a new point by weighing the four points in the ratio of 9-3-3-1. Thus, this algorithm can be specified by using subdivision masks, which specify the ratios of the points on a face to generate the new points. In this case, the subdivision masks are as follows

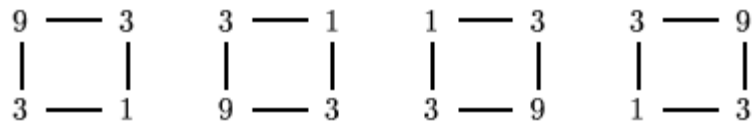


Figure (4.12) Subdivision masks ^[36].

2. Each of these equations is built from weighing the points on an edge in the ratio of 3-1, and then weighing the resulting points in the ratio 3-1. These are exactly the ratios of Chaitin's curve and so this method can be looked upon as an extension of Chaitin's curve to surfaces ^[36].

Generating the Refinement Procedure

To generate the subdivision surface, one has to consider all 16 of the possible points generated through the binary subdivision of the quadratic patch. It is easily seen that each of these points can be generated through considering other subdivisions of the patch $P(u, w)$ and can be defined by the same subdivision masks ^[36].

The Matrix Equation for a Cubic Uniform B-spline Surface

In the same method for the refinement for quadratic B-spline surface, is the refinement for cubic B-spline surface. Catmull and Clark believed that study of the cubic case would lead to a better subdivision surface generation scheme.

The equation for this surface can be calculated from the general equation for Uniform B-spline surface in chapter three equation (3.45), so the Cubic Uniform B-spline surface for $K=4$ is written in equation (4.40) below.

$$P(u, w) = [1 \quad u \quad u^2 \quad u^3] M p M^T \begin{bmatrix} 1 \\ w \\ w^2 \\ w^3 \end{bmatrix} \dots\dots\dots (4.40)$$

And polygon for this surface is illustrated in Figure (4.13) where M is 4×4 matrix defined by equation (4.41) and (p) is the initial control polygons defined by equation (4.42).

$$M_{(\text{Cubic Uniform B-spline})} = \frac{1}{6} \begin{bmatrix} 1 & 4 & 1 & 0 \\ -3 & 0 & 3 & 0 \\ 3 & -6 & 3 & 0 \\ -1 & 3 & -3 & 1 \end{bmatrix} \dots\dots\dots (4.41)$$

$$p = \begin{bmatrix} p_{0,0} & p_{0,1} & p_{0,2} & p_{0,3} \\ p_{1,0} & p_{1,1} & p_{1,2} & p_{1,3} \\ p_{2,0} & p_{2,1} & p_{2,2} & p_{2,3} \\ p_{3,0} & p_{3,1} & p_{3,2} & p_{3,3} \end{bmatrix} \dots\dots\dots (4.42)$$

The matrix M defines the quadratic Uniform B-spline blending functions

when multiplied by $\begin{bmatrix} 1 \\ w \\ w^2 \\ w^3 \end{bmatrix}$

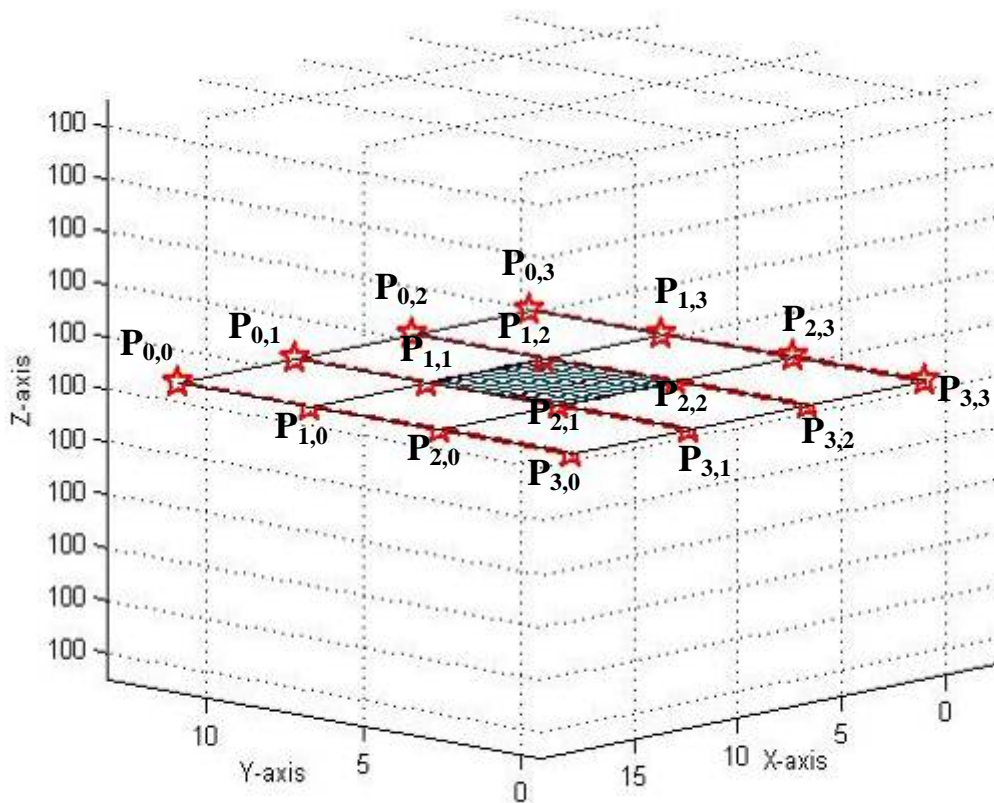


Figure (4.13) Initial control polygon for the cubic Uniform B-spline surface [36].

Subdividing the cubic B-spline Surface:

The cubic uniform B-spline patch can be subdivided into four sub patches, which can be generated from 25 unique sub-control points. It has been focused on the subdivision scheme for only one of the four (the sub patch corresponding to $[0 \leq u, w \leq 1/2]$ as the others will follow by symmetry). Figure (4.9) illustrates the 16 points produced by subdividing into four sub patches. It should be noted that the nine “interior” control points are utilized by each of the four sub patch components of the subdivision.

This sub patch can be generated by reparameterizing the surface by the variables u' and w' where $u' = u/2$ and $w' = w/2$ substituting these into the equation (4.40); one obtains the subdivision polygon and refinement the cubic B-spline surface which are shown in equation (4.43) and illustrated in Figure (4.14) ^[9].

$$P'(u, w) = p\left(\frac{u}{2}, \frac{w}{2}\right) \dots\dots\dots (4.43)$$

$$\begin{aligned}
 &= \begin{bmatrix} 1 & \frac{u}{2} & \left(\frac{u}{2}\right)^2 & \left(\frac{u}{2}\right)^3 \end{bmatrix} \text{MPM}^T \begin{bmatrix} 1 \\ \frac{w}{2} \\ \left(\frac{w}{2}\right)^2 \\ \left(\frac{w}{2}\right)^3 \end{bmatrix} \\
 &= \begin{bmatrix} 1 & u & u^2 & u^3 \end{bmatrix} \begin{bmatrix} 1 & 0 & 0 & 0 \\ 0 & \frac{1}{2} & 0 & 0 \\ 0 & 0 & \frac{1}{4} & 0 \\ 0 & 0 & 0 & \frac{1}{8} \end{bmatrix} \text{MPM}^T \begin{bmatrix} 1 & 0 & 0 & 0 \\ 0 & \frac{1}{2} & 0 & 0 \\ 0 & 0 & \frac{1}{4} & 0 \\ 0 & 0 & 0 & \frac{1}{8} \end{bmatrix}^T \begin{bmatrix} 1 \\ w \\ w^2 \\ w^3 \end{bmatrix} \\
 &= \begin{bmatrix} 1 & u & u^2 & u^3 \end{bmatrix} \text{MM}^{-1} \begin{bmatrix} 1 & 0 & 0 & 0 \\ 0 & \frac{1}{2} & 0 & 0 \\ 0 & 0 & \frac{1}{4} & 0 \\ 0 & 0 & 0 & \frac{1}{8} \end{bmatrix} \text{MPM}^T \begin{bmatrix} 1 & 0 & 0 & 0 \\ 0 & \frac{1}{2} & 0 & 0 \\ 0 & 0 & \frac{1}{4} & 0 \\ 0 & 0 & 0 & \frac{1}{8} \end{bmatrix}^T (\text{M}^{-1})^T \text{M}^T \begin{bmatrix} 1 \\ w \\ w^2 \\ w^3 \end{bmatrix} \\
 &= \begin{bmatrix} 1 & u & u^2 & u^3 \end{bmatrix} \text{M} \left(\text{M}^{-1} \begin{bmatrix} 1 & 0 & 0 & 0 \\ 0 & \frac{1}{2} & 0 & 0 \\ 0 & 0 & \frac{1}{4} & 0 \\ 0 & 0 & 0 & \frac{1}{8} \end{bmatrix} \right) \text{M} \text{P} \left(\text{M}^T \begin{bmatrix} 1 & 0 & 0 & 0 \\ 0 & \frac{1}{2} & 0 & 0 \\ 0 & 0 & \frac{1}{4} & 0 \\ 0 & 0 & 0 & \frac{1}{8} \end{bmatrix}^T \right) (\text{M}^{-1})^T \text{M}^T \begin{bmatrix} 1 \\ w \\ w^2 \\ w^3 \end{bmatrix} \\
 &= \begin{bmatrix} 1 & u & u^2 & u^3 \end{bmatrix} \text{M} \left(\text{M}^{-1} \begin{bmatrix} 1 & 0 & 0 & 0 \\ 0 & \frac{1}{2} & 0 & 0 \\ 0 & 0 & \frac{1}{4} & 0 \\ 0 & 0 & 0 & \frac{1}{8} \end{bmatrix} \right) \text{M} \text{P} \left(\text{M}^T \begin{bmatrix} 1 & 0 & 0 & 0 \\ 0 & \frac{1}{2} & 0 & 0 \\ 0 & 0 & \frac{1}{4} & 0 \\ 0 & 0 & 0 & \frac{1}{8} \end{bmatrix}^T \right) (\text{M}^{-1})^T \text{M}^T \begin{bmatrix} 1 \\ w \\ w^2 \\ w^3 \end{bmatrix} \\
 &= \begin{bmatrix} 1 & u & u^2 & u^3 \end{bmatrix} \text{MP}' \text{M}^T \begin{bmatrix} 1 \\ w \\ w^2 \\ w^3 \end{bmatrix}
 \end{aligned}$$

where $P' = SPS^T$ and (4.44)

$$S = M^{-1} \begin{bmatrix} 1 & 0 & 0 & 0 \\ 0 & \frac{1}{2} & 0 & 0 \\ 0 & 0 & \frac{1}{4} & 0 \\ 0 & 0 & 0 & \frac{1}{8} \end{bmatrix} M \quad \text{..... (4.45)}$$

From this process, the surface $P'(u, w)$ can be written as

$$P'(u, w) = [1 \quad u \quad u^2 \quad u^3] M p' M^T \begin{bmatrix} 1 \\ w \\ w^2 \\ w^3 \end{bmatrix} \quad \text{..... (4.46)}$$

For a (4×4) control point array p' this implies that $P'(u, w)$ is a uniform cubic B-spline patch. The matrix S is typically called the “splitting matrix”, and is straightforward to calculate from equation (4.45), so it is given by equation (4.47) [9].

$$S = \frac{1}{8} \begin{bmatrix} 4 & 4 & 0 & 0 \\ 1 & 6 & 1 & 0 \\ 0 & 4 & 4 & 0 \\ 0 & 1 & 6 & 1 \end{bmatrix} \quad \text{..... (4.47)}$$

By carrying out the algebra, the new polygon array p' has been calculated from equation (4.44) and rewritten in the equation (4.48).

$$P' = \frac{1}{8} \begin{bmatrix} 4 & 4 & 0 & 0 \\ 1 & 6 & 1 & 0 \\ 0 & 4 & 4 & 0 \\ 0 & 1 & 6 & 1 \end{bmatrix} \begin{bmatrix} p_{0,0} & p_{0,1} & p_{0,2} & p_{0,3} \\ p_{1,0} & p_{1,1} & p_{1,2} & p_{1,3} \\ p_{2,0} & p_{2,1} & p_{2,2} & p_{2,3} \\ p_{3,0} & p_{3,1} & p_{3,2} & p_{3,3} \end{bmatrix} \frac{1}{8} \begin{bmatrix} 4 & 4 & 0 & 0 \\ 1 & 6 & 1 & 0 \\ 0 & 4 & 4 & 0 \\ 0 & 1 & 6 & 1 \end{bmatrix}^T \quad \text{..... (4.48)}$$

$$= \frac{1}{8} \begin{bmatrix} 4p_{0,0} + 4p_{1,0} & 4p_{1,0} + 4p_{1,1} & 4p_{0,2} + 4p_{1,2} & 4p_{0,3} + 4p_{1,3} \\ p_{0,0} + 6p_{1,0} + p_{2,0} & p_{0,1} + 6p_{1,1} + p_{2,1} & p_{0,2} + 6p_{1,2} + p_{2,2} & p_{0,3} + 6p_{1,3} + p_{2,3} \\ 4p_{1,0} + 4p_{2,0} & 4p_{1,1} + 4p_{2,1} & 4p_{1,2} + p_{2,2} & p_{1,3} + 6p_{2,3} + p_{3,3} \\ p_{1,0} + 6p_{2,0} + p_{3,0} & p_{1,1} + 6p_{2,1} + p_{3,1} & p_{1,2} + 6p_{2,2} + p_{3,2} & p_{1,3} + 6p_{2,3} + p_{3,3} \end{bmatrix} \begin{bmatrix} 4 & 4 & 0 & 0 \\ 1 & 6 & 1 & 0 \\ 0 & 4 & 4 & 0 \\ 0 & 1 & 6 & 1 \end{bmatrix}$$

Each of these points can be classified into three categories – face points, edge points and vertex points – depending on each point's relationship to the original control point mesh (see Appendix B). The points $p'_{0,0}$, $p'_{0,2}$, $p'_{2,0}$, and $p'_{2,2}$ are shown in Figure (4.14) ^[20].

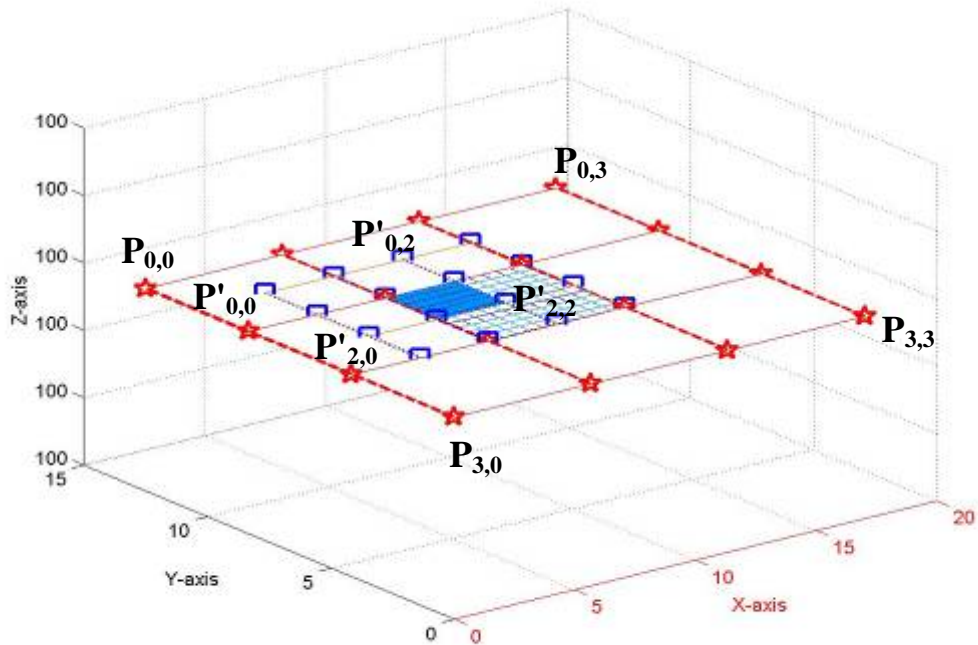


Figure (4.14): Initial control polygon for the cubic Uniform B-spline surface and the splitting control points (control polygon) with subdivide the cubic Uniform B-spline surface ^[9].

To explain the method, the great new polygon point are illustrated by equation (4.49).

$$P'_{i,j} = \frac{Q + 2R + S}{4} \tag{4.49}$$

where Q is the average of the face points of the faces adjacent to the vertex point (see equation (4.50)), R is the average of the midpoints of the edges adjacent to the vertex point (see equation (4.51)) and S is the corresponding vertex from the original mesh (see equation (4.52)).

For example, if the point $P'_{1,3}$ is considered, then

$$Q = \frac{F_{0,1} + F_{0,2} + F_{0,3} + F_{0,4}}{4} \tag{4.50}$$

$$R = \frac{\frac{P_{0,2} + P_{1,2}}{2} + \frac{P_{1,1} + P_{1,2}}{2} + \frac{P_{1,3} + P_{1,2}}{2} + \frac{P_{2,2} + P_{1,2}}{2}}{4} \tag{4.51}$$

$$S = P_{1,2} \tag{4.52}$$

All sixteen points of the subdivision have now been characterized in terms of face points, edge points and vertex points, and a geometric method has been developed to calculate these points ^[9].

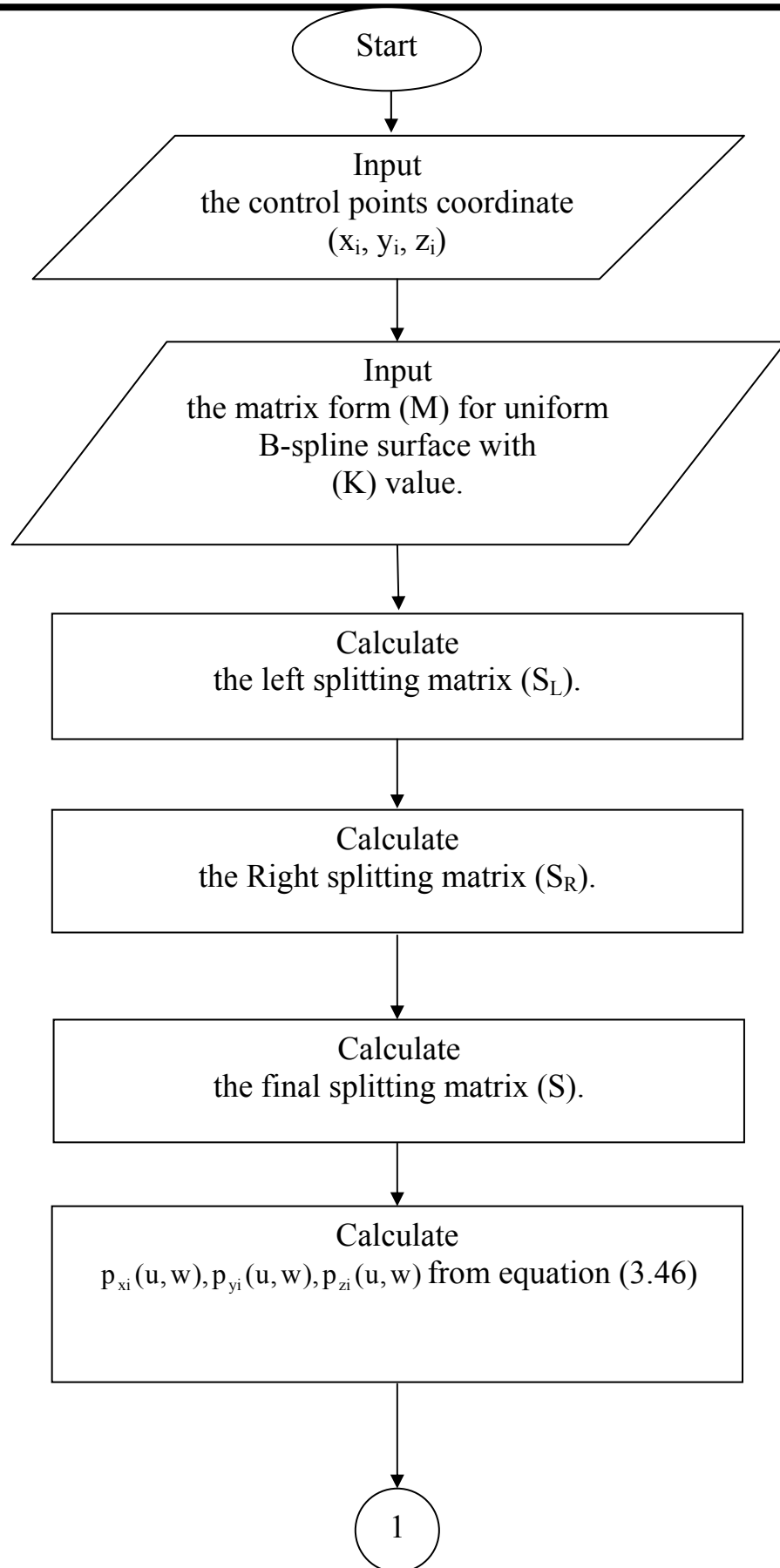
Extending This Subdivision Procedure to the Entire Patch

The process generated from these rules actually extends to arbitrary rectangular meshes. In this case, it has been known that this represents yet another subdivision and that eventually, if it keeps refining, this “limit mesh” will converge to the original uniform B-spline surface.

Thus, this process gives us a sequence of meshes, each of which is a refinement of the mesh directly above, and which converges to the surface in the limit. In the same time the following rules have been reviewed to generate the points for the refinement of the surface:

1. For each face in the original mesh, generate the new face points which are the average of all the original points defining the face.
2. For each internal edge of the original mesh (i.e. an edge not on the boundary), generate the new edge points – which are calculated as the average of four points: the two points which define the edge, and the two new face points for the faces that are adjacent to the edge.
3. For each internal vertex of the original mesh (i.e. a vertex not on the boundary of the mesh), generate the new vertex points – which are calculated as the average of Q , $2R$ and S , where Q is the average of the new face points of all faces adjacent to the original vertex point, R is the average of the midpoints of all original edges incident on the original vertex point, and S is the original vertex point ^[10].

To implement program to build refinement for Uniform B-spline surface needs to drawing the block diagram which is shown in Figure (4.15) and explaining the main steps of the program while the detailed explanation of the proposed program is given in the flowchart shown in Figure (4.16).



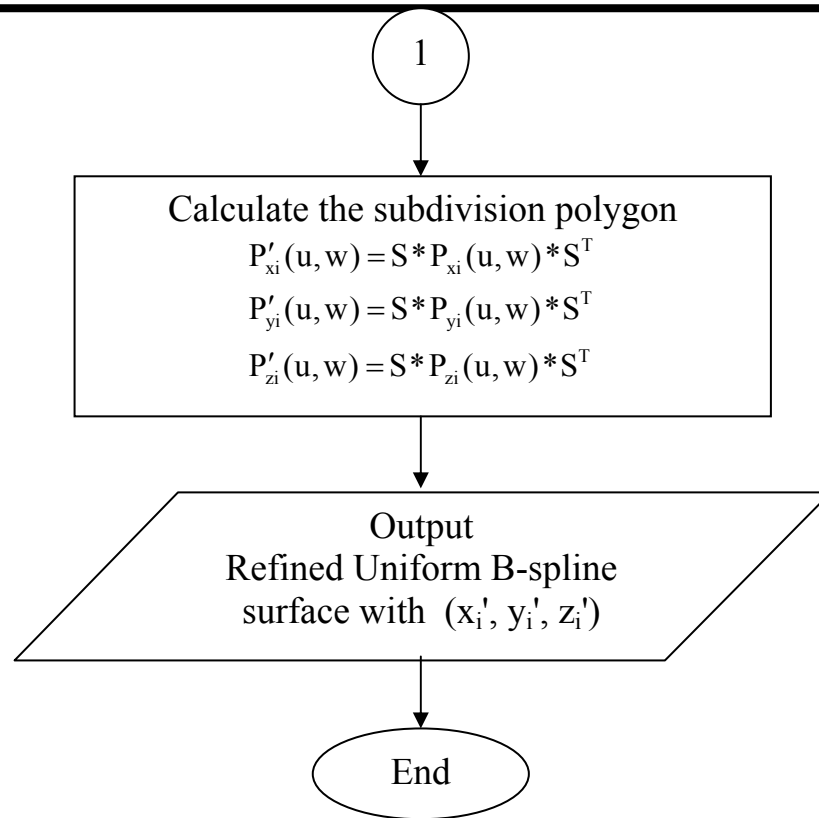
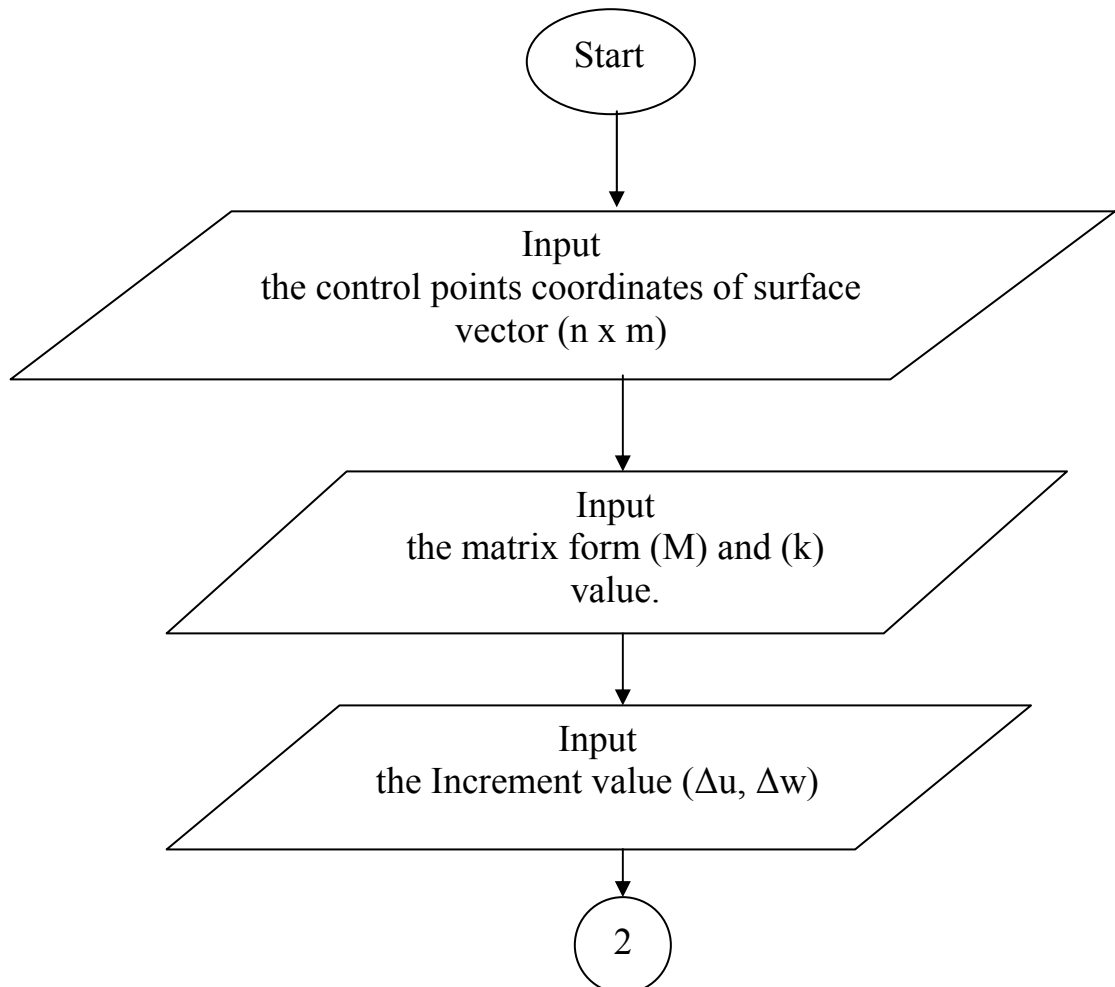


Figure (4.15): Block diagram of the proposed program depending on refinement Uniform B-spline technique.



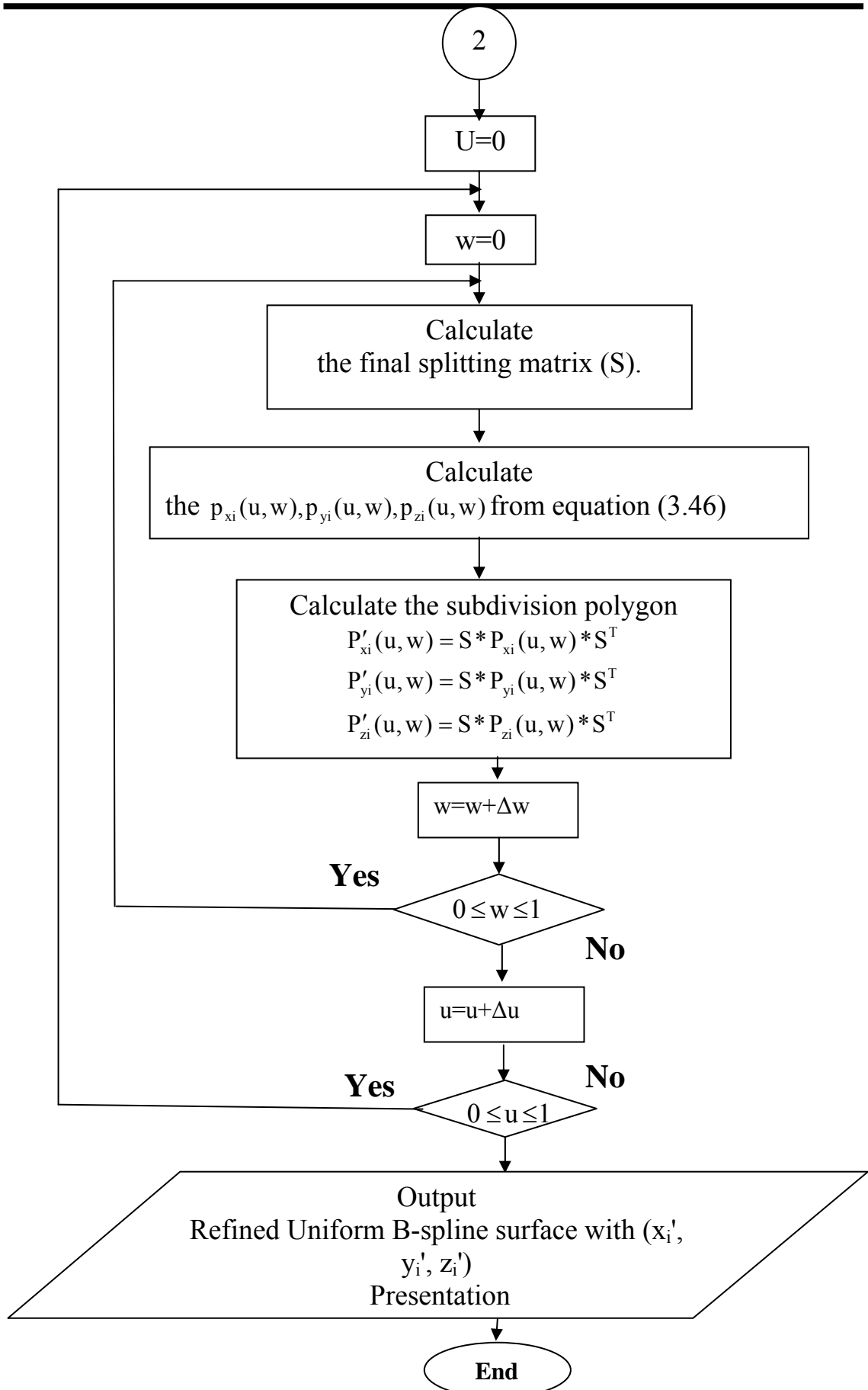


Figure (4.16): Flowchart of the proposed program depending on refinement Uniform B-spline Surfaces.

4.4 Bezier Surface Refinement:

A Bezier patch has a useful representation when written in a matrix form. This form allows us to specify many operations with Bezier patches as matrix operations which can be performed quickly on computer systems optimized for geometry operations with matrices [24].

The Matrix Formulation for a Cubic Bezier Surface:

The equation for this surface can be calculated from the general equation for Cubic Bezier surface in chapter three equation (3.24), so the cubic Bezier surface can be rewritten as equation (4.53) and shown in Figure (4.17):

$$\begin{aligned}
 P(u, w) &= \sum_{j=0}^3 \sum_{i=0}^3 P_{i,j} B_{i,3}(u) B_{j,3}(w) \dots\dots\dots (4.53) \\
 &= \sum_{j=0}^3 \left[\sum_{i=0}^3 p_{i,j} B_{i,3}(u) \right] B_{j,3}(w) \\
 &= \sum_{j=0}^3 [1 \quad u \quad u^2 \quad u^3] \begin{bmatrix} 1 & 0 & 0 & 0 \\ -3 & 3 & 0 & 0 \\ 3 & -6 & 3 & 0 \\ -1 & 3 & -3 & 1 \end{bmatrix} \begin{bmatrix} p_{0,j} \\ p_{1,j} \\ p_{2,j} \\ p_{3,j} \end{bmatrix} B_{j,3}(w) \\
 &= [1 \quad u \quad u^2 \quad u^3] \begin{bmatrix} 1 & 0 & 0 & 0 \\ -3 & 3 & 0 & 0 \\ 3 & -6 & 3 & 0 \\ -1 & 3 & -3 & 1 \end{bmatrix} \begin{bmatrix} p_{0,0} & p_{0,1} & p_{0,2} & p_{0,3} \\ p_{1,0} & p_{1,1} & p_{1,2} & p_{1,3} \\ p_{2,0} & p_{2,1} & p_{2,2} & p_{2,3} \\ p_{3,0} & p_{3,1} & p_{3,2} & p_{3,3} \end{bmatrix} \begin{bmatrix} 1 & 0 & 0 & 0 \\ -3 & 3 & 0 & 0 \\ 3 & -6 & 3 & 0 \\ -1 & 3 & -3 & 1 \end{bmatrix}^T \begin{bmatrix} 1 \\ w \\ w^2 \\ w^3 \end{bmatrix}
 \end{aligned}$$

Patch Subdivision Using the Matrix Forms:

When the patch at the point $u = 1/2$ is subdivided. it reparameterized the matrix equation above (by substituting $u/2$ for u) is reparameterized to cover only the first half of the patch, and simplified to obtain the equation (4.54).

$$\begin{aligned}
 P\left(\frac{u}{2}, w\right) &= \begin{bmatrix} 1 & \left(\frac{u}{2}\right) & \left(\frac{u}{2}\right)^2 & \left(\frac{u}{2}\right)^3 \end{bmatrix} M \begin{bmatrix} p_{0,0} & p_{0,1} & p_{0,2} & p_{0,3} \\ p_{1,0} & p_{1,1} & p_{1,2} & p_{1,3} \\ p_{2,0} & p_{2,1} & p_{2,2} & p_{2,3} \\ p_{3,0} & p_{3,1} & p_{3,2} & p_{3,3} \end{bmatrix} M^T \begin{bmatrix} 1 \\ w \\ w^2 \\ w^3 \end{bmatrix} \dots (4.54) \\
 &= \begin{bmatrix} 1 & u & u^2 & u^3 \end{bmatrix} \begin{bmatrix} 1 & 0 & 0 & 0 \\ 0 & \frac{1}{2} & 0 & 0 \\ 0 & 0 & \frac{1}{4} & 0 \\ 0 & 0 & 0 & \frac{1}{8} \end{bmatrix} M \begin{bmatrix} p_{0,0} & p_{0,1} & p_{0,2} & p_{0,3} \\ p_{1,0} & p_{1,1} & p_{1,2} & p_{1,3} \\ p_{2,0} & p_{2,1} & p_{2,2} & p_{2,3} \\ p_{3,0} & p_{3,1} & p_{3,2} & p_{3,3} \end{bmatrix} M^T \begin{bmatrix} 1 \\ w \\ w^2 \\ w^3 \end{bmatrix} \\
 &= \begin{bmatrix} 1 & u & u^2 & u^3 \end{bmatrix} M S_L \begin{bmatrix} p_{0,0} & p_{0,1} & p_{0,2} & p_{0,3} \\ p_{1,0} & p_{1,1} & p_{1,2} & p_{1,3} \\ p_{2,0} & p_{2,1} & p_{2,2} & p_{2,3} \\ p_{3,0} & p_{3,1} & p_{3,2} & p_{3,3} \end{bmatrix} M^T \begin{bmatrix} 1 \\ w \\ w^2 \\ w^3 \end{bmatrix}
 \end{aligned}$$

where the matrix S_L is defined before in equation (4.55), so the equation result is defined as:

$$S_L = \begin{bmatrix} 1 & 0 & 0 & 0 \\ \frac{1}{2} & \frac{1}{2} & 0 & 0 \\ \frac{1}{4} & \frac{1}{2} & \frac{1}{4} & 0 \\ \frac{1}{8} & \frac{3}{8} & \frac{3}{8} & \frac{1}{8} \end{bmatrix} \dots (4.55)$$

and is identical to the left subdivision matrix for the curve case. So in particular, the sub patch $P(u/2)$ is again Bezier patch and the quantity is defined by the equation (4.56).

$$P'(u, w) = \begin{bmatrix} 1 & 0 & 0 & 0 \\ \frac{1}{2} & \frac{1}{2} & 0 & 0 \\ \frac{1}{4} & \frac{1}{2} & \frac{1}{4} & 0 \\ \frac{1}{8} & \frac{3}{8} & \frac{3}{8} & \frac{1}{8} \end{bmatrix} \begin{bmatrix} p_{0,0} & p_{0,1} & p_{0,2} & p_{0,3} \\ p_{1,0} & p_{1,1} & p_{1,2} & p_{1,3} \\ p_{2,0} & p_{2,1} & p_{2,2} & p_{2,3} \\ p_{3,0} & p_{3,1} & p_{3,2} & p_{3,3} \end{bmatrix} \dots (4.56)$$

$P'(u, w)$ forms the new polygon points of this patch illustrated in Figure (4.18).

Calculation of the Second Half of the Patch

In the same way, the subdivision matrix for the second half of the patch has been obtained. First the original surface is reparameterized, and then simplified to obtain the equation (5.57).

$$\begin{aligned}
 P\left(\frac{1+u}{2}, w\right) &= \begin{bmatrix} 1 & \left(\frac{1+u}{2}\right) & \left(\frac{1+u}{2}\right)^2 & \left(\frac{1+u}{2}\right)^3 \end{bmatrix} M \begin{bmatrix} p_{0,0} & p_{0,1} & p_{0,2} & p_{0,3} \\ p_{1,0} & p_{1,1} & p_{1,2} & p_{1,3} \\ p_{2,0} & p_{2,1} & p_{2,2} & p_{2,3} \\ p_{3,0} & p_{3,1} & p_{3,2} & p_{3,3} \end{bmatrix} M^T \begin{bmatrix} 1 \\ w \\ w^2 \\ w^3 \end{bmatrix} \quad (4.57) \\
 &= \begin{bmatrix} 1 & \frac{1}{2} & \frac{1}{4} & \frac{1}{8} \\ 0 & \frac{1}{2} & \frac{1}{2} & \frac{3}{8} \\ 0 & 0 & \frac{1}{4} & \frac{3}{8} \\ 0 & 0 & 0 & \frac{1}{8} \end{bmatrix} M \begin{bmatrix} p_{0,0} & p_{0,1} & p_{0,2} & p_{0,3} \\ p_{1,0} & p_{1,1} & p_{1,2} & p_{1,3} \\ p_{2,0} & p_{2,1} & p_{2,2} & p_{2,3} \\ p_{3,0} & p_{3,1} & p_{3,2} & p_{3,3} \end{bmatrix} M^T \begin{bmatrix} 1 \\ w \\ w^2 \\ w^3 \end{bmatrix} \\
 &= \begin{bmatrix} 1 & u & u^2 & u^3 \end{bmatrix} M S_R \begin{bmatrix} p_{0,0} & p_{0,1} & p_{0,2} & p_{0,3} \\ p_{1,0} & p_{1,1} & p_{1,2} & p_{1,3} \\ p_{2,0} & p_{2,1} & p_{2,2} & p_{2,3} \\ p_{3,0} & p_{3,1} & p_{3,2} & p_{3,3} \end{bmatrix} M^T \begin{bmatrix} 1 \\ w \\ w^2 \\ w^3 \end{bmatrix}
 \end{aligned}$$

where the matrix S_R is defined in equation (4.58).

$$S_R = \begin{bmatrix} 1 & \frac{1}{2} & \frac{1}{4} & \frac{1}{8} \\ 0 & \frac{1}{2} & \frac{1}{2} & \frac{3}{8} \\ 0 & 0 & \frac{1}{4} & \frac{3}{8} \\ 0 & 0 & 0 & \frac{1}{8} \end{bmatrix} \dots\dots\dots (4.58)$$

which is identical to the right subdivision matrix in the curve case and a matrix has been obtained that can be applied to a set of control points to produce the control points for the second half of the patch as illustrated in Figure (4.19), and figures out the splitting control polygon for the left and the right sides to the cubic Bezier surface in the Figure (4.20).

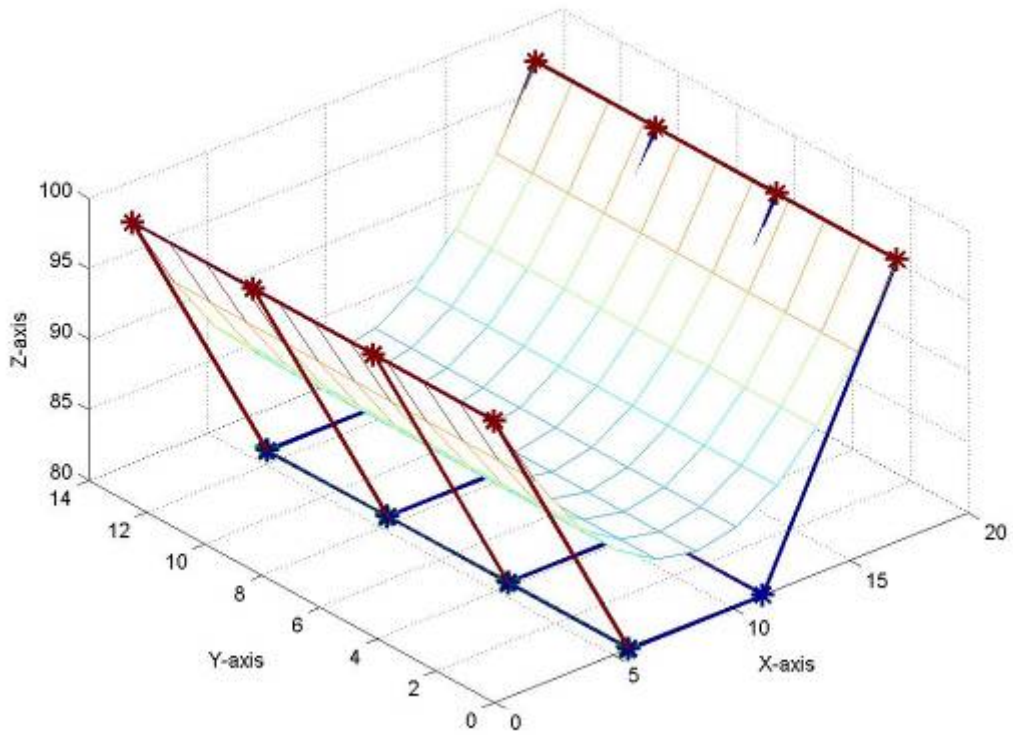


Figure (4.17) Initial control polygon for the cubic Bezier surface.

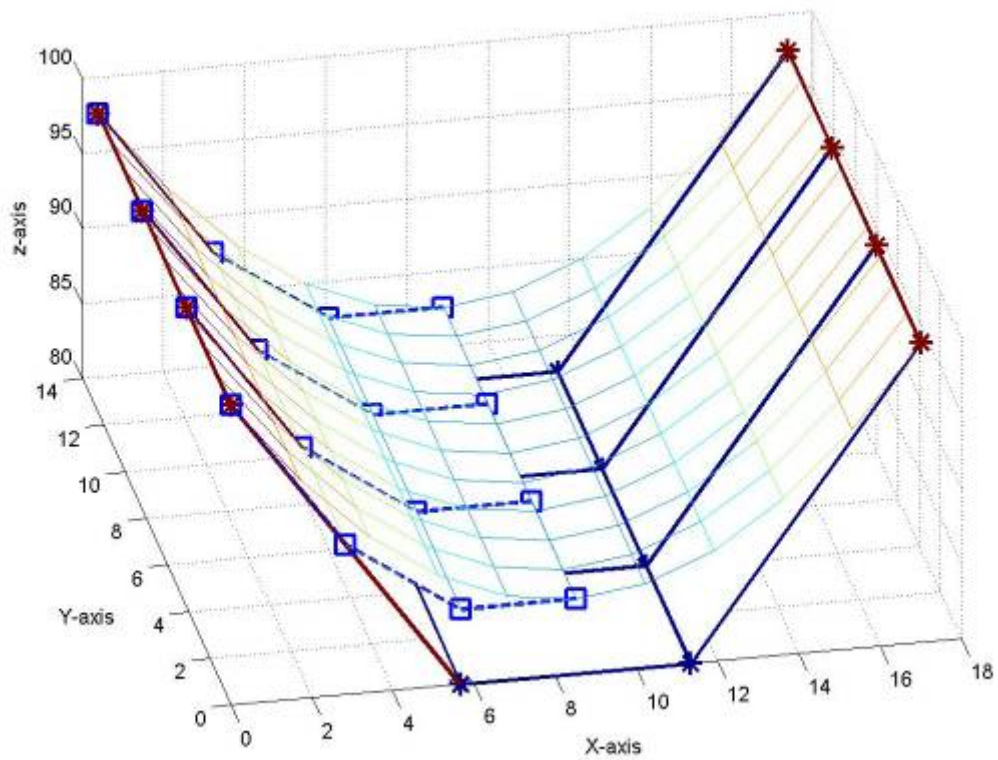


Figure (4.18) Initial control polygon for the cubic Bezier surface, and the splitting the left control polygon when used S_L matrix.

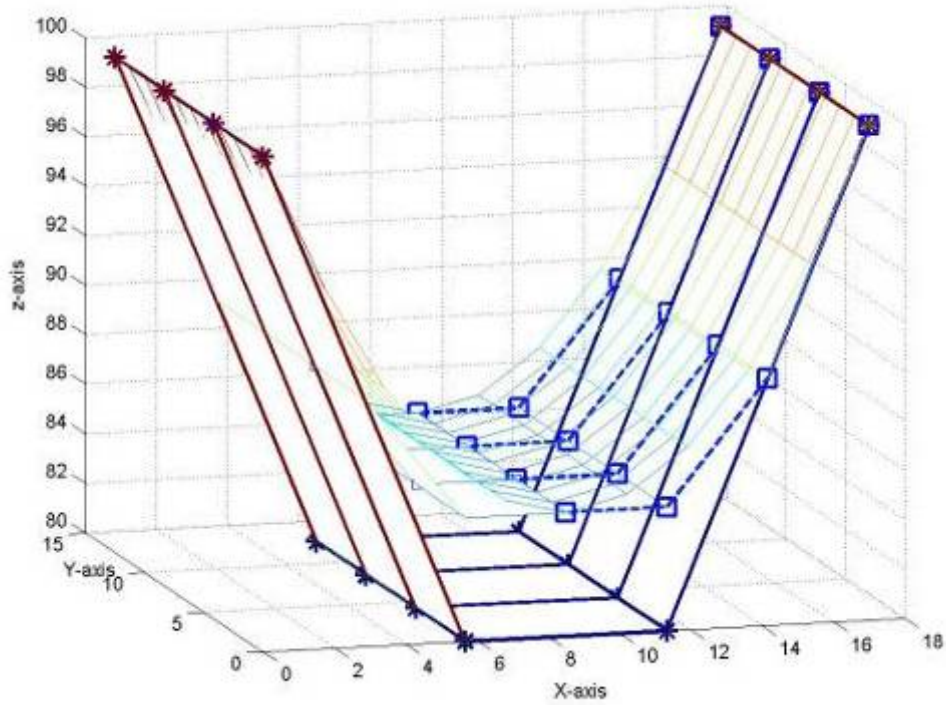


Figure (4.19) Initial control polygon for the cubic Bezier surface, and the splitting the right control polygon when used S_R matrix.

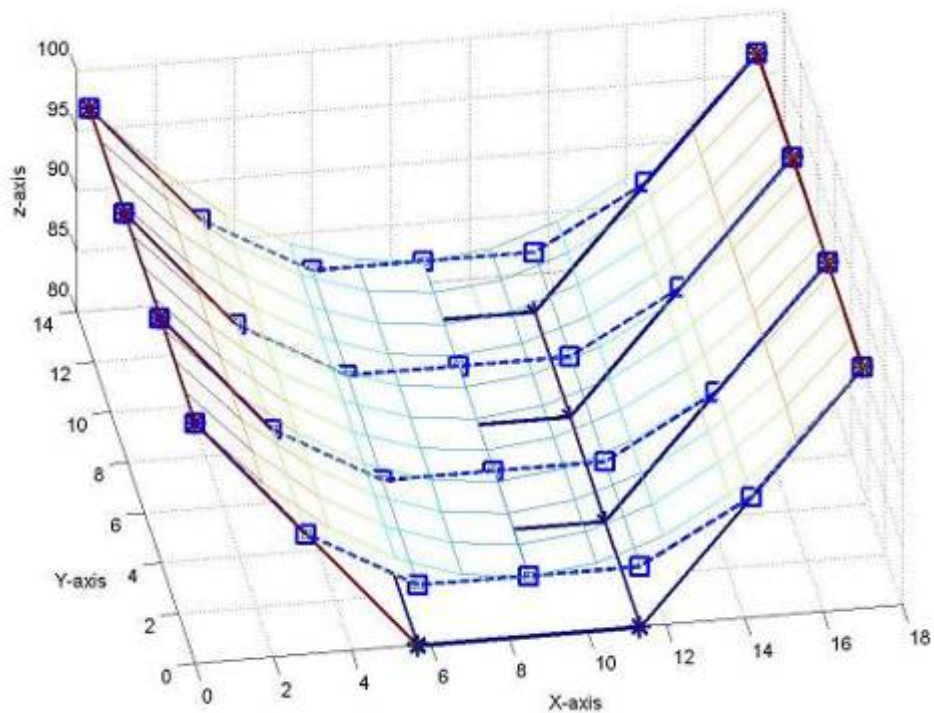
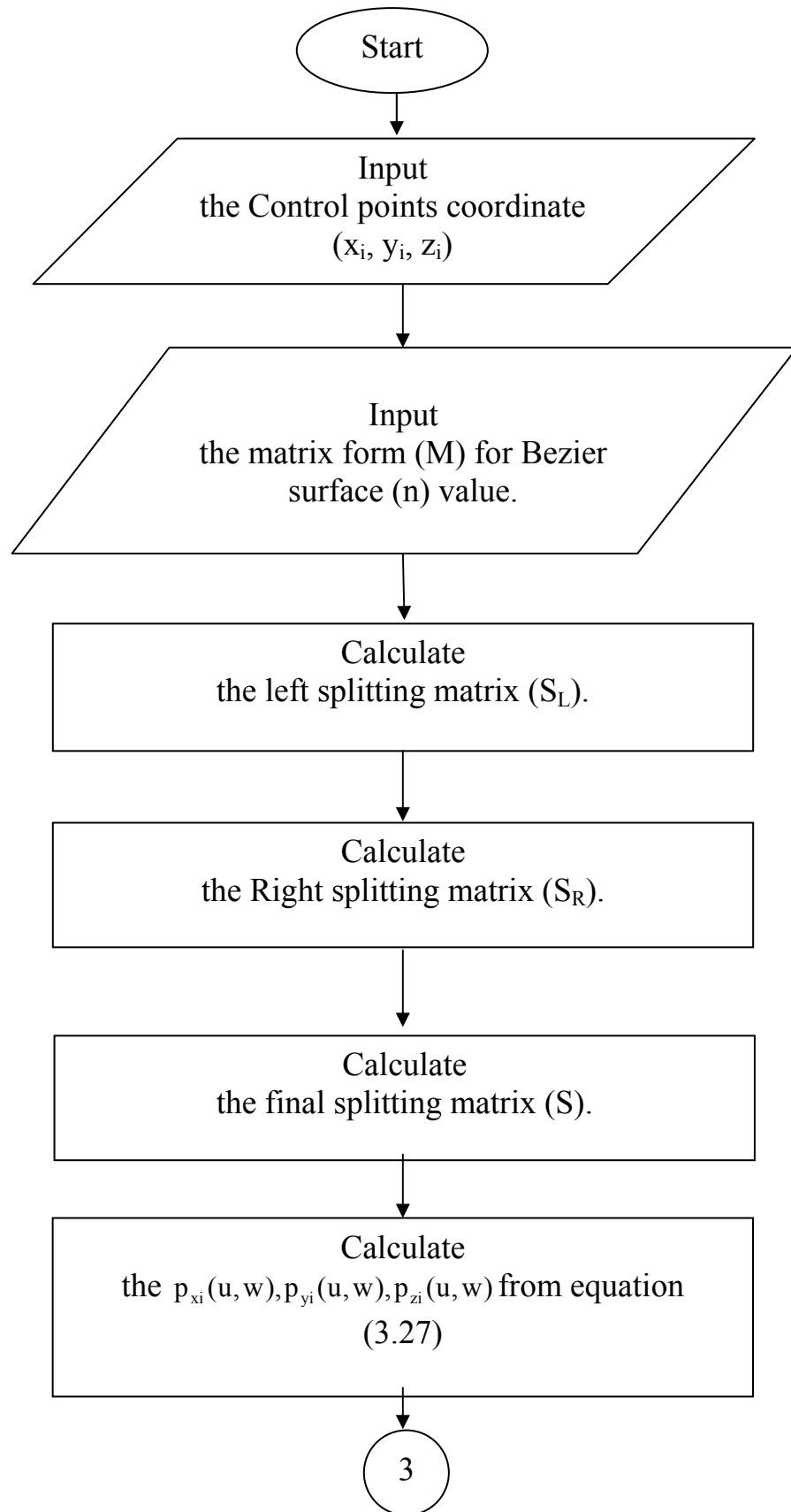


Figure (4.20) Initial control polygon for the cubic Bezier surface, and the splitting the right and left control polygon when used S_L and S_R matrix.

Implement program to build refinement for Bezier surface needs drawing the block diagram which is shown in Figure (4.21) and explaining the main

steps of the program while the detailed explanation of the proposed program has been given in the flowchart t shown in Figure (4.22).



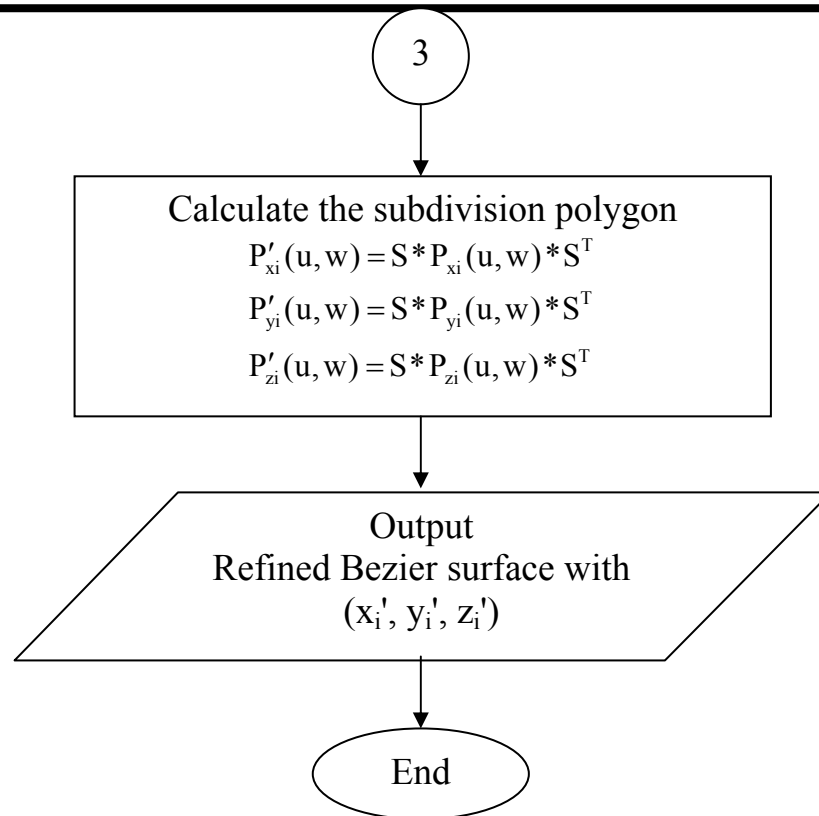
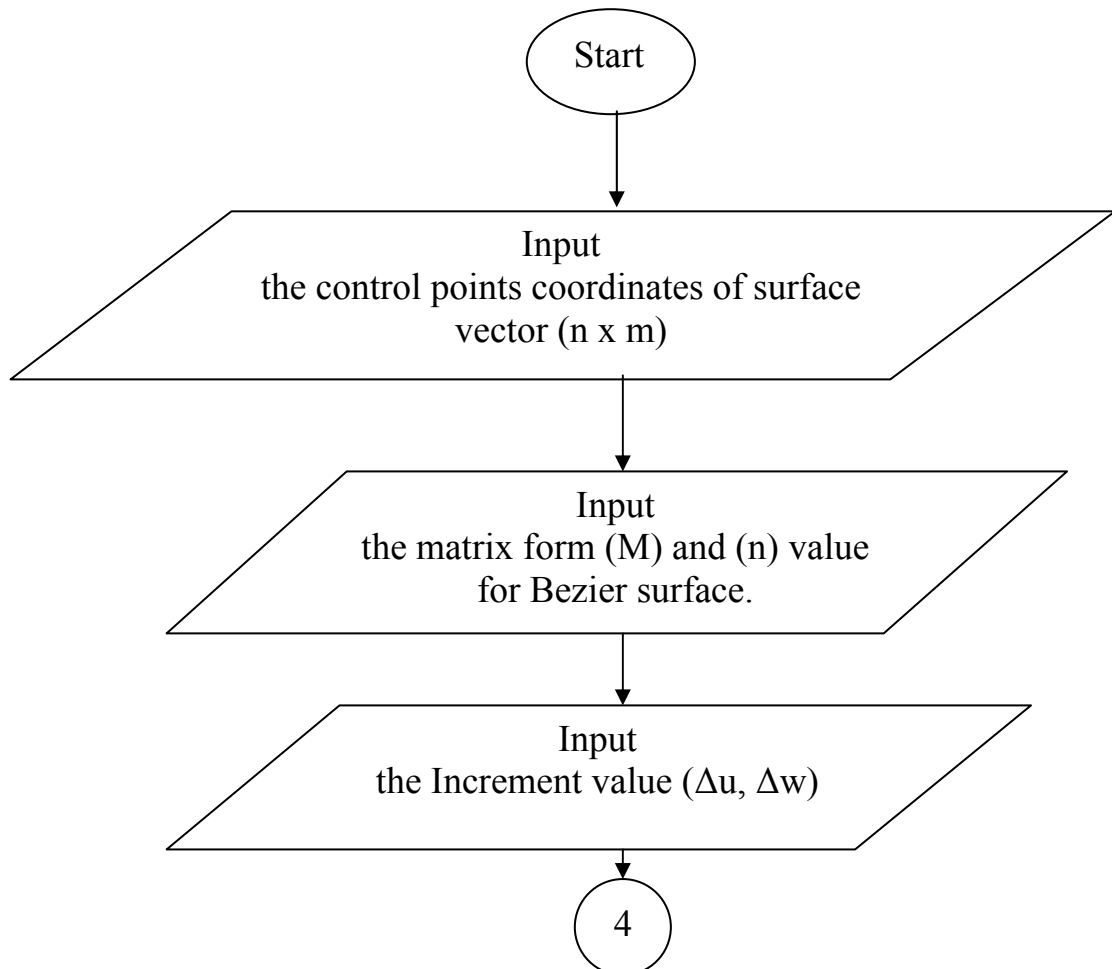


Figure (4.21): Block diagram of the proposed program depending on refinement Bezier technique.



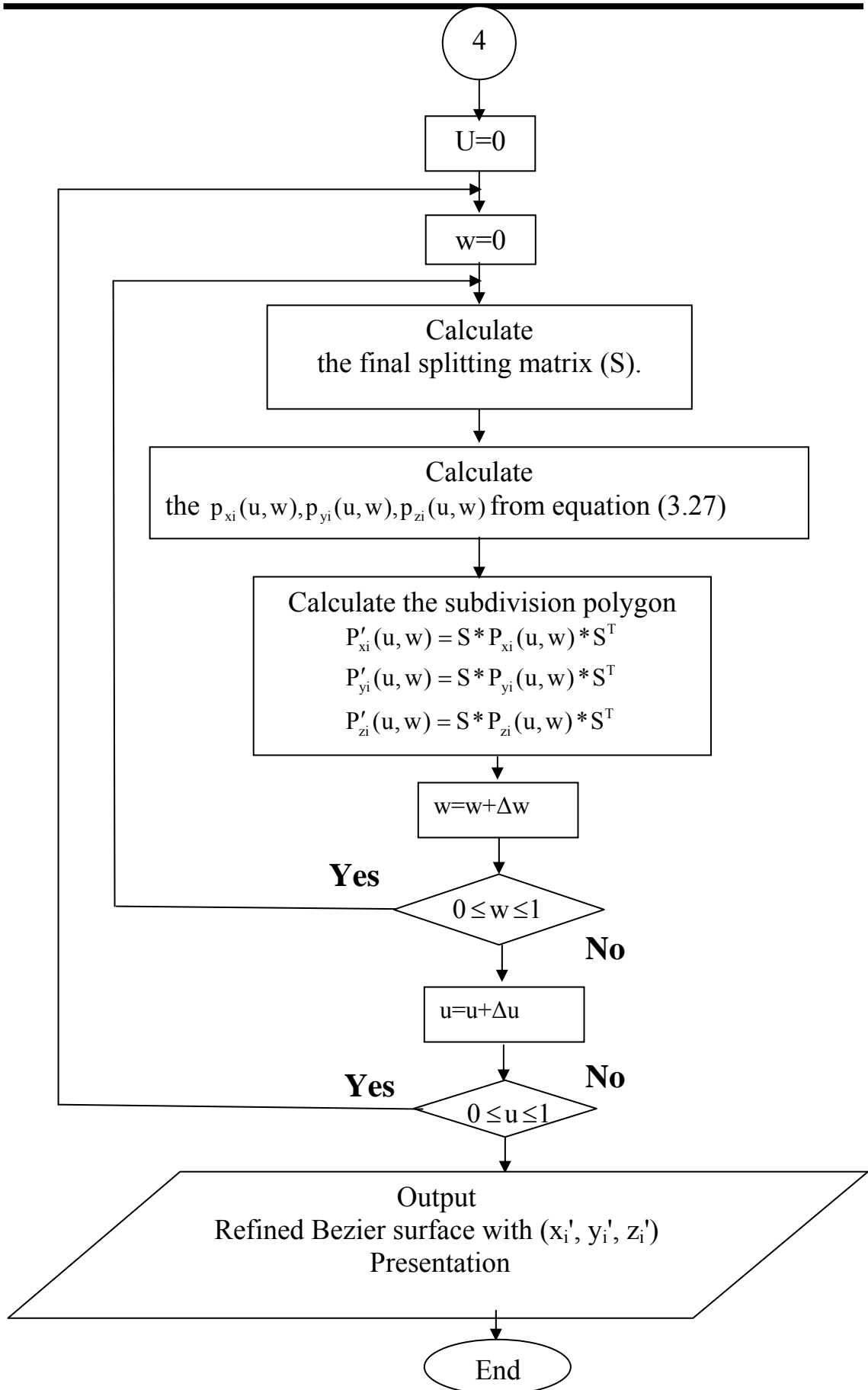


Figure (4.22): Flowchart of the proposed program depending on refinement Bezier Surfaces.

4.5 Loop Subdivision Scheme

Charles Loop generalized the subdivision rules of a symmetric quadratic box-spline over a regular triangulation to include rules to be applied in the vicinity of extraordinary points. The limit surface is C_2 continuous everywhere except at the extraordinary points, where it is only C_1 . The extraordinary point at the surface exhibits a continuous tangent plane, as long as the weighting factors stay between certain limits. Although part of Loop's motivations were based on intuition, it turned out that the rules that he considered as optimal still survive today as being the most suited for stationary triangular subdivision [37].

In Figure (4.23), four consecutive steps of the Loop subdivision scheme of a triangle are shown. Each time all existing triangles are divided into four smaller triangles.

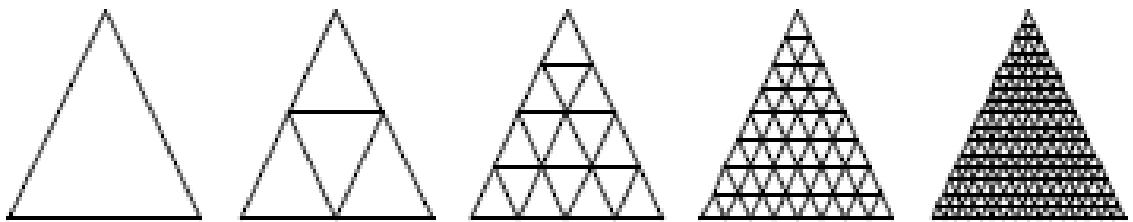


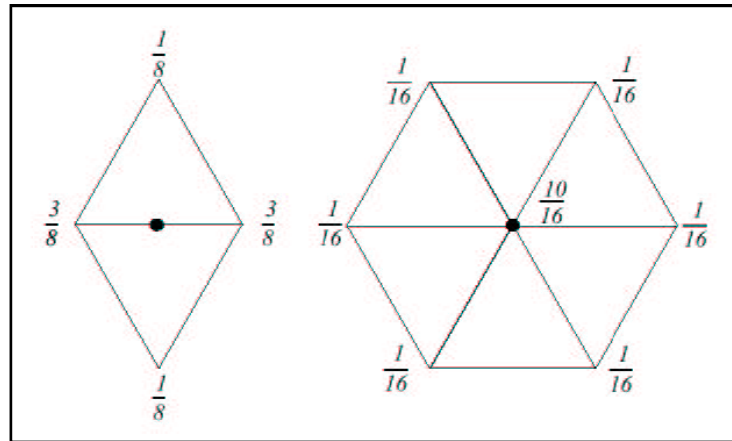
Figure (4.23) Four steps in the subdivision of a triangle [14].

The mathematics for this method is can be explained briefly by choosing locations for new vertices as weighted average β of original vertices in local neighborhood in equations (4.59) and (4.60).

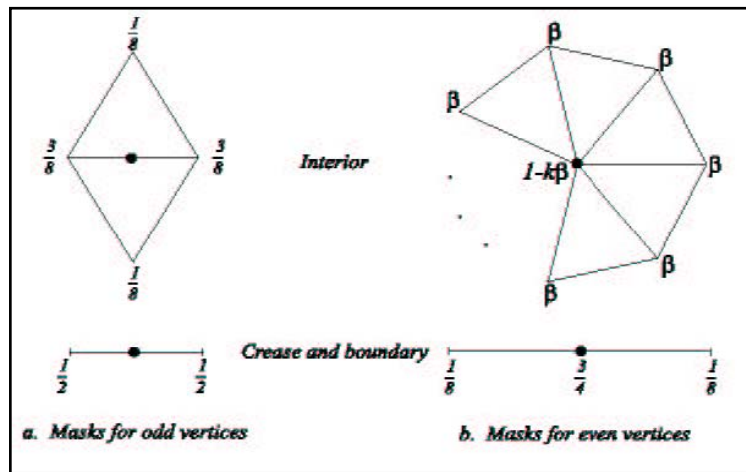
$$\beta = \frac{1}{n} \left(\frac{5}{8} - \left(\frac{3}{8} + \frac{1}{4} \cos \frac{2\pi}{n} \right)^2 \right) \dots\dots\dots (4.59)$$

$$\beta = \begin{cases} \frac{3}{8n} & n > 3 \\ \frac{3}{16} & n = 3 \end{cases} \dots\dots\dots (4.60)$$

n is the vertex of valances in loop scheme, the rules for extraordinary vertices and boundaries are illustrated in Figure (4.24:a,b)



(a)



(b)

Figure (4.24: a, b): Rules for extraordinary vertices and boundaries ^[13].

4.6 The Butterfly Scheme

The structure of the meshes created by the Butterfly algorithm is very similar to the meshes created by Loop's scheme. It also creates new points by splitting the edges into two, followed by a relaxing step. The averaging masks used are quite different, however. The vertex-points always stay in their original position, which causes this scheme to be an interpolating one. The averaging mask for the newly inserted edge-points is depicted in Figure (4.25) the form of this mask resembles a butterfly, hence the name of the scheme. The limit surface is differentiable everywhere except at extraordinary points of valence $n = 3$ and $n \geq 8$. Although the surface is tangent plane continuous at extraordinary points of valence $n \geq 8$, the

surface is not regular as it has self-intersections, the algorithm is illustrated in Figure (4.25) and equation (4.59).

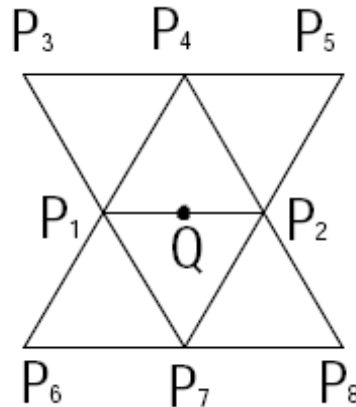


Figure (4.25): Situation around a newly inserted edge point for the interpolator Butterfly scheme.

And the main formula to determine the new points Q is determined by the equation (4.61) [5].

$$Q = \frac{1}{2}(P_1 + P_2) + 2w(P_3 + P_4) - w(P_5 + P_6 + P_7 + P_8) \quad \dots\dots\dots (4.61)$$

4.7 Hexagon Subdivision Surface:

In order to search for the most interesting values for the subdivision weights, the following considerations are regarded. Firstly, the support area should be small such that every control point exhibits only a local influence. Therefore, one gets solutions that are restricted to using the points of the polygon in which the new points are created. Furthermore, just as in existing schemes, it makes sense to look for a symmetrical scheme, invariant to the order in which the points are considered and let all points play an equal role. For the standard mesh (hexagons where every point has valence 3), these considerations lead to the existence of three different weights (see Figure 4 .26):

- one for the two points closest to the new point (a),
- another weight for the two points in the middle (b),
- and a third weight for the two furthest points (c).

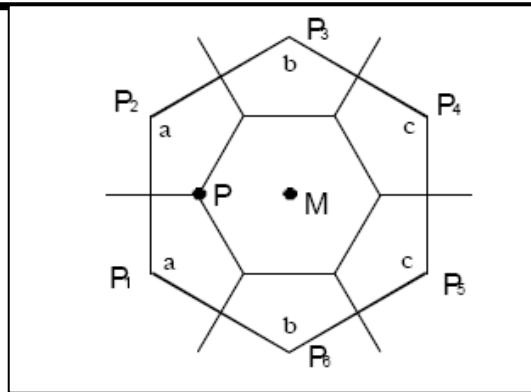


Figure (4.26): The position of the new point P is a weighted average of the points of the surrounding hexagon.

Expressed using these factors, the equation for the new point is then written in equation (4.62).

$$P = ap_1 + ap_2 + bp_3 + bp_4 + cp_5 + cp_6 \dots\dots\dots (4.62)$$

Another consideration is that for an input configuration of all equal regular hexagons, the new points should be located such that all newly created small hexagons are again exactly equally sized. As for each input hexagon, three new hexagons are created, and the area of the new hexagons has to be equal to one third of the area of the original ones. To obtain this, the sides of the hexagons have to be divided by a factor of $(1/\sqrt{3})$. Due to the symmetry of the regular hexagons, this is only possible if the weight is $(c = a - 1/3)$.

For the scheme to be invariant under affine transformations, the sum of these weights should be equal to one: $(2a + 2b + 2c = 1)$. So, together with the condition on (c) , this condition leads to $(b = 5/6 - 2a)$. Putting all this in a matrix, and getting the subdivision matrix S'' it's defined by equation (4.63) [14]:

$$S'' = \begin{bmatrix} a & a & 5/6-2a & a-1/3 & a-1/3 & 5/6-2a \\ 5/6-2a & a & a & 5/6-2a & a-1/3 & a-1/3 \\ a-1/3 & 5/6-2a & a & a & 5/6-2a & a-1/3 \\ a-1/3 & a-1/3 & 5/6-2a & a & a & 5/6-2a \\ 5/6-2a & a-1/3 & a-1/3 & 5/6-2a & a & a \\ a & 5/6-2a & a-1/3 & a-1/3 & 5/6-2a & a \end{bmatrix} \dots\dots\dots (4.63)$$

4.8 Catmull-Clark

The subdivision scheme for cubic B-splines a tensor-product definition. This approach is nicely defined on regular quadrilateral meshes and can be executed in two separate passes. First, the curve scheme is executed in one direction, followed by a second pass in the orthogonal direction. Catmull and Clark's most important innovation was the extension of the scheme allowing it to cope with non-regular meshes. In the regular setting, the mesh consists solely of quadrilaterals and all vertices have a valence of four, they observed that they could split faces that are not quadrilaterals in a similar way as the faces that are split in the regular case. Just a point is added in the center of the face and connected it to the center of every edge. This ensures that starting from the first subdivision step, all generated faces are quadrilaterals. Also newly generated points at the centers of the edges nicely get a valence of four. Only the centers of input faces that were not quadrilaterals lead to the creation of an extraordinary vertex. This implies that the number of extraordinary vertices stays constant, namely one for each extraordinary vertex in the input mesh and one for each face that was not a quadrilateral; Figure (4.27) illustrates this subdivision algorithm.

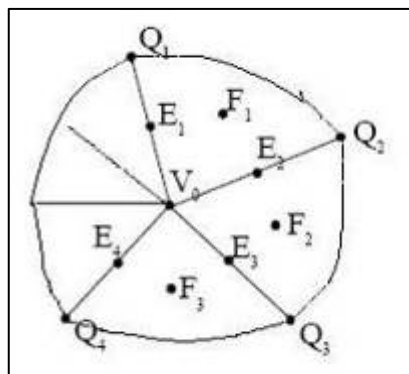


Figure (4.27): Subdivision around a central vertex V_0 , showing surrounding control points (Q_i), edge points (E_i) and face points (F_i)^[7].

An initial vertex V_0 is surrounded by n edges, leading to n neighbor vertices Q_i . A first step in the subdivision process is to insert so-called face points F_i at the centers of the faces.

Then, for every edge a so-called edge point E_i is calculated as the mean between the two vertices and the two face points of the faces that make up the edge.

Finally, the positions of the existing vertices are relaxed by averaging them with their neighbors in the following way. V_i is the position of V_0 after the first subdivision step and is calculated from the formula (4.64):

$$V_i = \frac{n-2}{n} V_0 + \frac{1}{n^2} \sum Q_i + \frac{1}{n^2} \sum F_i \quad \dots\dots\dots (4.64)$$

After using these rules for face points, edge points and vertex points, new faces are formed. First the existing edges are split using the edge points and the new vertex points, and then new faces are formed by connecting the edge points to the face points ^[7].

4.9 Doo-Sabin

This scheme, is also based on a tensor product for subdivision curves. Instead of cubic curves, Doo and Sabin used quadratic curves. This leads to quite simple rules. Only one type of new point is introduced, at the center of a quadrilateral formed by an existing vertex, two edge points and the center of the face. This effectively shrinks the existing faces to half their original size. In order to close the mesh again, also new faces are put around the old vertices and edges. This has the visual effect of cutting away the corners of the polygonal mesh. The mesh obtained is the dual of the mesh from the Catmull-Clark scheme, interchanging the roles of points and faces. In Figure (4.28) the Doo-Sabin subdivision process is illustrated for a polygon with five vertices ^[5].

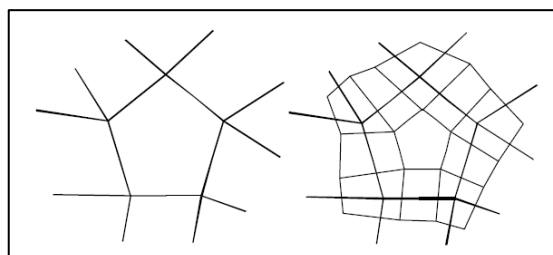


Figure (4.28): Left: An input polygon with surrounding edges. Right: The new faces created by one subdivision step of the Doo-Sabin algorithm.

4.10 Chapter Summary

This chapter has focused on the Chaitin's subdivision algorithm, Linear Algebra, is the mathematical basis for Catmull Clark and Doo-Sabin subdivision method.

Firstly it explains the curve refinement by Chaitin's algorithm, So it has been concentrated on Subdivided the Uniform B-spline curve starting from subdivide the Uniform quadratic B-spline curve to arrive to Quintic Uniform B-spline curve, because it will be the basis for our practical principles to generate the profile shape for extrusion process in chapter five, after that it explains refinement for Bezier curve and it lets cubic Bezier curve be the case study to explain this method.

Secondly the work continues with Chaitin's algorithm to demonstrate the Uniform B-spline surface refinement ,and Bezier surface refinement, by taking Cubic polynomials for both surfaces (Bezier and Uniform B-spline), and the case study explains subdivision algorithm, then Block diagram, and Flowchart for Bezier and Uniform B-spline surfaces are built.

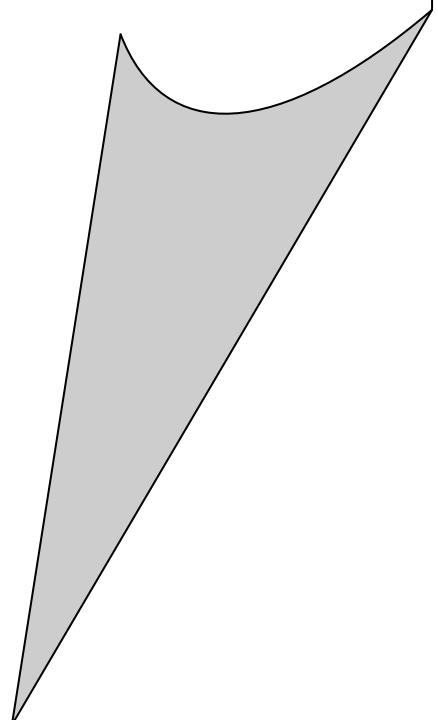
Thirdly it gives the guidelines for the more complex subdivision algorithm (Loop Subdivision Scheme, Butterfly scheme, Hexagon subdivision surface, Catmull-Clark algorithm, and Doo-Sabin algorithm). And these subdivisions algorithms are summarized in the table (4.1) Note that Chaitin's algorithm is omitted in this table because it's implied in Catmull-Clark , and Doo-Sabian algorithm.

Table (4.1) Classification of the subdivision surface algorithm.

	Primitive (face-split)		Dual (vertex-split)
	Triangles	Quadrilaterals	Quadrilaterals
Approximating (not interpolating original vertices)	Loop Scheme	Catmull-Clark	Doo Sabian Midedge
Interpolating The original vertices	Butterfly Scheme	Kobbelt	

CHAPTER FIVE

TESTING SUBDIVISION ALGORITHM IN PRODUCTION FIELD



CHAPTER FIVE

Testing the Subdivision Algorithm in Production Field

This chapter investigates and evaluates the proposed CAD, CAM, and theoretical die design profile, there is no doubt that any developed method or technique that tries to solve any kind of problem should be tested. In our case the subdivision algorithm is developed and employed in production field.

The practical part of this research has been done in these listed points:

1. The die design theory of Constant Ratios of Successive Generalized Homogeneous Strain Increments (CRHS) was implemented on one problem as case study (in order to design the optimum die profile), then a asymptotical die profile was made which was designed via CRHS, by using two approximation techniques after modifying it by subdivision algorithm .

The First approximation technique is the quartic Uniform B-spline curve (with six control points) which is developed from cubic Uniform B-spline curve after third iteration, and the second is Quintic Uniform B-spline curve (with seven control points) which is developed from cubic Uniform B-spline curve after fourth iteration .The reason for developing this subdivision algorithm is to increase the degree for the curve and get the control points set on the curve especially after the second iteration, so that will reduce the chance to get the error for identity. These curves with the curve result from the CRHS method.

2. Create surfaces from the curves proposed; these surfaces are half die for direct extrusion die process.
3. Find the mean curvature and the radius of curvature for each case.
4. Find the minimum radius of curvature (to find the optimum tool radius for finishing process theoretically).

5. Find the deviation for each surface proposed above (the deviation between the surface before exposure by machining process and after this process).
6. Find the maximum and the minimum deviation for each surface.
7. Create toolpath for each surface, which generates the interior data of the desired surfaces by Matlab (V7.0) software to represent the desired surface in graphical mode.
8. Import the toolpath from Matlab (V7.0) software to Surfcam software as DXF extension (Design Matlab software to make the converter from Matlab Software to Surfcam Software).
9. Make simulation by surfcam software to manufacture these surfaces with the manufacturing parameters which are calculated before (like the cutter radius).
10. Obtain the G-codes from the surfcam software.
11. Design software to import the G-code result from surfcam program as NCC file to Matlab program (the reason for this software is to shifting the zero coordinate to the stock (block) corners or out of the stock coordinate with defined value, because the surfcam program fails to do this option) that greatly simplifies the machining process for the operator.
12. Import the modified NCC file to surfcam software then make simulation depend on the G-codes modified.
13. Implement the final G-codes result for these three surfaces generated by Matlab program, on CNC machine (Hermle C30U dynamic, 5-axis AC-kinematics, with specification of linear motor drives (60.000 m/min), motor spindle 37kw 28.000 rpm) and controlled by Siemens 840D, and the position error was below 0.002mm This machine belongs to the Technical University Darmstadt (Germany).

5.1 Dies Designed According Rational Concepts

In this concept, the design of tool is directly linked with the lessening of the severity of the operation to ensure the flow lines of the metal are smooth and do not suffer unnecessary discontinuities. In any forming process the pattern of the deformation depends either on the order in which the magnitude of the successive ratios of generalized strain increments varies along the pass, or on the variation in the strain rate itself. Therefore if a constant rate of either of these parameters can be maintained throughout the operation, the likelihood of the incidence of flow discontinuities will be reduced. The characteristics of the worked material and the mechanics of the process will dictate which of the two parameters is likely to be of greater importance in any given case.

The possible basis of tool design can be associated with two modes of flow:

1. Constant Ratios of Successive Generalized Homogeneous Strain Increments (CRHS).

The geometry of the pass in this concept depends on the variation in the dimensions of the workpiece and consequently on that of the generalized homogenous strain ϵ_H . The manipulation of this variation affords means of controlling the flow.

2. The Constancy of the Mean Strain Rate (CMSR)

The concept of constancy of the mean strain rate is defined analytically as

$$\dot{\epsilon}_1 = \dot{\epsilon}_2 = \dots = \dot{\epsilon}_{n-1} = \dot{\epsilon}_n = \text{Constant}$$

Where is $\dot{\epsilon}$ the mean strain rate. Since many engineering materials are susceptible to the effects of the strain rate at both low and elevated temperatures, the use of strain rate as a basis for tool design could be potentially advantageous [6].

This thesis has focused on (CRHS) concepts to make the die profile for extrusion process, and build the theoretical side for this thesis.

5.1.1 Constant Ratios of Successive Generalized Homogeneous Strain Increments (CRHS)

This concept depends on the following assumption which says "the ideal geometric shape for the extrusion die is the geometric shape which was designed to get the effect for resultant homogenous strain (which is needed to make forming process) from the total plastic strain (that means there is no resultant for non-homogenous strain),and in another words: is the ideal geometric shape which does not generate any sheared deformed in the sample formed and that is the main aim for any design to the die forming process.

So, the CRHS concept depends on the general resultant homogenous strain for the forming process, for that reason equation (5.1) has been used to calculate the general homogenous strain, which it is assumed neglects the value for the elastic strain especially when it is compared with the plastic strain value.

$$d\epsilon_h = \frac{\sqrt{2}}{3} \left[(d\epsilon_x - d\epsilon_y)^2 + (d\epsilon_y - d\epsilon_z)^2 + (d\epsilon_z - d\epsilon_x)^2 \right]^{1/2} \dots (5.1)$$

$d\epsilon_h$ = total homogenous strain

And assume the volume for the material is staying constant before and after the forming process.

$$d\epsilon_x + d\epsilon_y + d\epsilon_z = 0 \dots\dots\dots (5.2)$$

Or:

$$\epsilon_x + \epsilon_y + \epsilon_z = 0 \dots\dots\dots (5.3)$$

And substitute equation (5.2) in equation (5.1), then integral it, so the equation result is (5.4):

$$\epsilon_h = \sqrt{\frac{2}{3}} (\epsilon_x^2 + \epsilon_y^2 + \epsilon_z^2)^{1/2} \dots\dots\dots (5.4)$$

Equation (5.4) is the mathematical expression used to calculate the total homogenous strain. This expression is used principally in die

design depending on CRHS concept, and this equation contains three components for the homogeneous strain:

- a. Longitudinal Strain ϵ_x .
- b. Radial Strain ϵ_y .
- c. Circumferential Strain ϵ_z .

The condition constant homogenous strain rate can be verified by equation (5.5) [39]:

$$\frac{\epsilon_{h_2} - \epsilon_{h_1}}{\epsilon_{h_1} - \epsilon_{h_0}} = \frac{\epsilon_{h_3} - \epsilon_{h_2}}{\epsilon_{h_2} - \epsilon_{h_1}} = \dots = \frac{\epsilon_{h_n} - \epsilon_{h_{n-1}}}{\epsilon_{h_{n-1}} - \epsilon_{h_{n-2}}} = S \quad \dots\dots\dots (5.5)$$

where:

ϵ_{h_n} =is the homogeneous strain at any section (n) for die profile.

S: constant, which determines the rate of deformation.

Three basic rates are adopted for this they are S= 0.8, S =1, and S =1.2.but in this thesis S=0.8 is value which is used. That means the rate of deformation is Decelerated (D), and the profile shape result which appear is the same as that of DCRHS (as shown in Figure (5.1)).

In any specific physical situation, equation (5.4), when integrated can be represented as logarithmic equation (5.6)

$$\epsilon_{h_n} = \ln(Z_n). \quad \dots\dots\dots (5.6)$$

Z_n = is a function that reflects the dimensions of the workpiece in section (n) of the pass (bar with rounded section has been used in the case study). It is clear that in section 0, which corresponds to the entry to the pass, $\epsilon_{h_0} = 0$ and therefore $Z_0 = 1$.

When use the bar with rounded section at the section (n) is used as a workpiece in deformation area, the value of $\epsilon_x, \epsilon_y, \epsilon_z$ for the bar with rounded section can be calculated as follows:

$$d\epsilon_x = \frac{dA}{A} \quad \dots\dots\dots (5.7)$$

where A is the area at any section:

$$\therefore d\epsilon_x = \frac{2\pi.R.dR}{\pi.R^2} = \frac{2.dR}{R} \dots\dots\dots (5.8)$$

And integration is made for the equation (5.8) along all the profile length:

$$\epsilon_{x_n} = \int_{R_0}^{R_n} d\epsilon_x = 2.\ln\left(\frac{R_0}{R_n}\right) \dots\dots\dots (5.9)$$

where

R_0 : is the initial radius for the bar which we need to formed it (the entire for die profile) see figure (5.2).

R_n : is the bar radius at (n) section along all die profile.

ϵ_{x_n} : the Longitudinal Strain at the (n) section along all die profile.

Assume the volume for the material is constant:

$$\epsilon_{x_n} + \epsilon_{y_n} + \epsilon_{z_n} = 0 \dots\dots\dots (5.10)$$

For the bar (rounded section):

$$\therefore \epsilon_{y_n} = \epsilon_{z_n} \dots\dots\dots (5.11)$$

And that means

$$\therefore \epsilon_{x_n} = -2.\epsilon_{y_n} \Rightarrow \epsilon_{y_n} = -\frac{\epsilon_{x_n}}{2} \dots\dots\dots (5.12)$$

And substituting equation (5.9) in equation (5.12) gives:

$$\epsilon_{y_n} = \epsilon_{z_n} = -\ln\left(\frac{R_0}{R_n}\right) \dots\dots\dots (5.13)$$

And substituting equation (5.13) in equation (5.4) yields:

$$\epsilon_{h_n} = \ln\left(\frac{R_0}{R_n}\right)^2 \dots\dots\dots (5.14)$$

By make comparison between the equation (5.6) and the equation (5.14):

$$Z_n = \left(\frac{R_0}{R_n}\right)^2 ; (Z_n \text{ at the section } n). \dots\dots\dots (5.15)$$

$$\text{and } Z_1 = \left(\frac{R_0}{R_1}\right)^2 ; (Z_1 \text{ at the section } n=1). \dots\dots\dots (5.16)$$

$$\text{And } C = \frac{R_1}{R_0} \dots\dots\dots (5.17)$$

$$R_1 = CR_0$$

C: is a constant value always ($C < 1$) and the range for this value is (0.9-0.99)

So, from equations (5.16) and (5.17)

$$Z_1 = \left(\frac{R_0}{R_1}\right)^2 = \left(\frac{1}{C}\right)^2 \dots\dots\dots (5.18)$$

And when we substitute the equation (5.6) in equation (5.5) ^[39]:

$$\frac{\ln(Z_2) - \ln(Z_1)}{\ln(Z_1) - \ln(Z_0)} = S \dots\dots\dots (5.19)$$

$$Z_2 = Z_1^{s^{(n-1)} + s^{(n-2)}} \dots\dots\dots (5.20)$$

$$\frac{Z_3}{Z_2} = Z_1^{s^2}$$

$$\therefore \frac{Z_n}{Z_{n-1}} = Z_1^{s^{n-1}} \dots\dots\dots (5.21)$$

$$Z_3 = Z_1^{s^2 + s + 1} \dots\dots\dots (5.22)$$

$$\therefore Z_n = Z_1^{s^{(n-1)} + s^{(n-2)} + s^{(n-3)} + \dots\dots\dots + s^{(n-n)}} \dots\dots\dots (5.23)$$

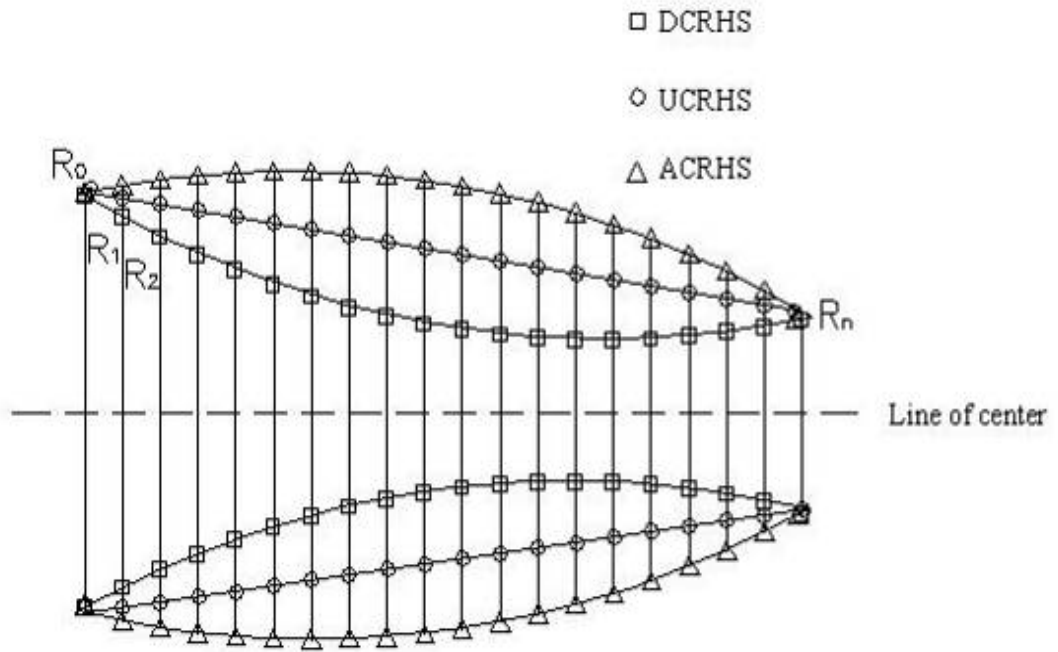


Figure (5.1): The geometric shape (for the Forward Extrusion) dies profile designed by CRHS [6].

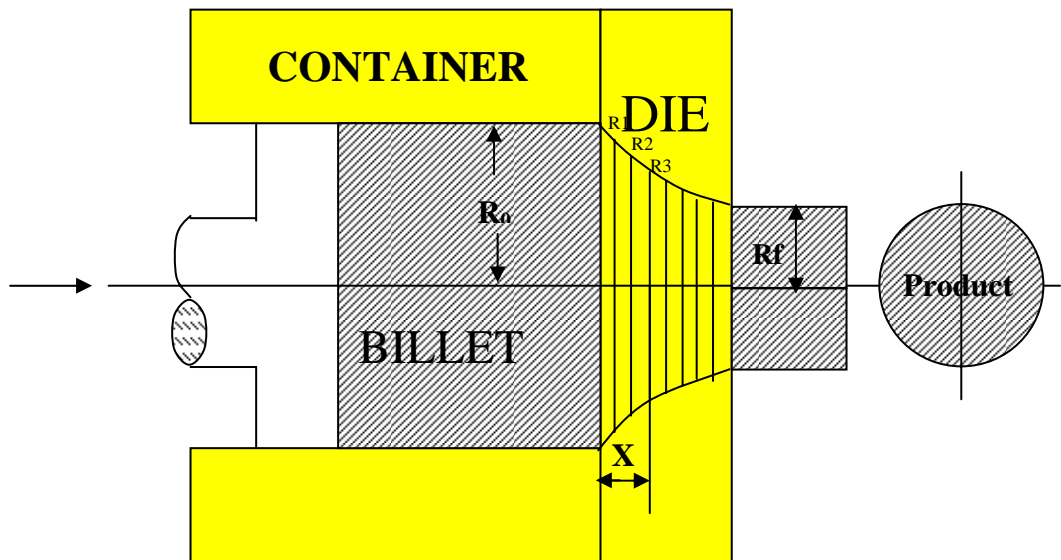


Figure (5.2): The shape for the Die, and the way to divide the Die profile to (n) sections (for Forward Extrusion), to design the Geometric shape for the Die by CRHS concepts [6].

5.2 Curvature Algorithm

The curvature of the surface may be expressed as the rate of change in the direction of the tangent vector with respect to the arc length. So there are many different ways to calculate the curvature for the surfaces, which are widely used in designing and manufacturing free form surfaces.

Let k_1 and k_2 be the principal curvatures, then their mean is

$$H = \frac{1}{2}(k_1 + k_2) \dots\dots\dots (5.24)$$

H: is called the mean curvature.

Let R_1 and R_2 be the radii corresponding to the principal curvatures, then the multiplicative inverse of the mean curvature H is given by the multiplicative inverse of the harmonic mean

$$H = \frac{1}{2} \left(\frac{1}{R_1} + \frac{1}{R_2} \right) = \frac{R_1 + R_2}{2R_1R_2} \dots\dots\dots (5.25)$$

To calculate the curvature in regular patch (let $x : U \rightarrow R^3$)

$$H = \frac{eG - 2fF + gE}{2(EG - F^2)} \dots\dots\dots (5.26)$$

where E, F and G are coefficients of the first fundamental form and e, f and g are coefficients of the second fundamental form ^[40].

The best test for the curvature equation is the sphere shape; the curvature value should be equated at any radius for circle in this sphere. So, the logical explanation for the constant color in any radius of circles, and difference from another radius is the curvature which is equal for the same radius of circles and different when the radius is different (decrease or increase the radius) as shown in Figure (5.3).

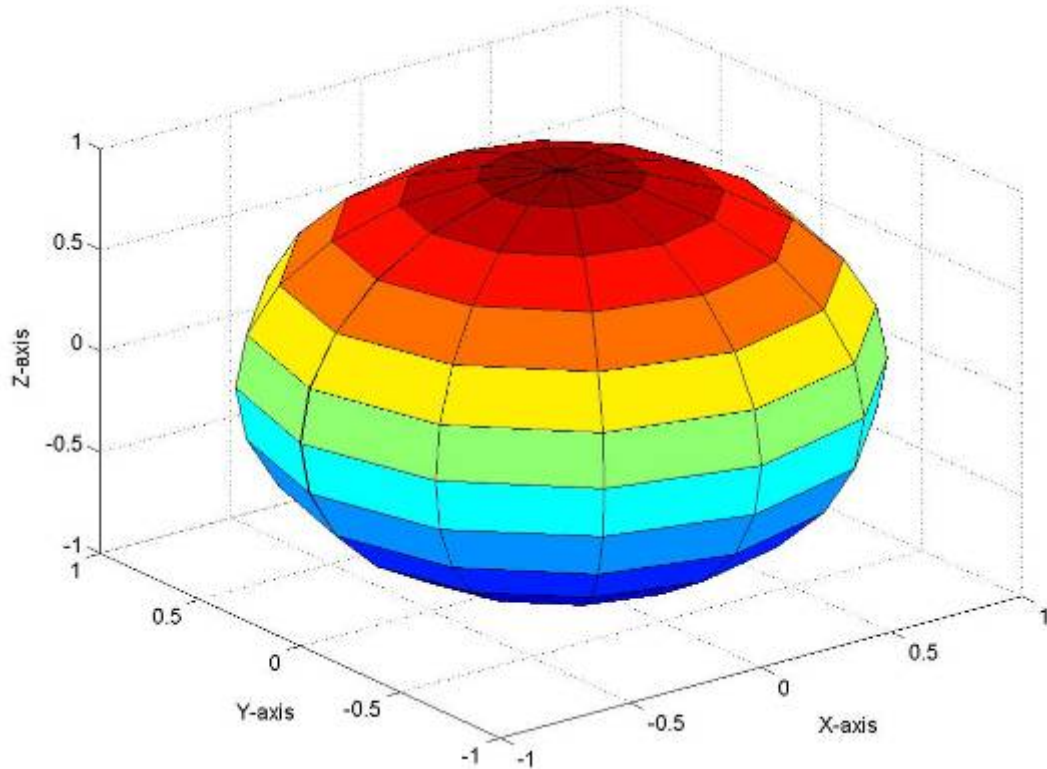


Figure (5.3): The sphere shape which explains the difference in the curvature value when the circles radius is different and the curvature has constant value at the same radius value.

5.3 Radius of Curvature

To calculate the radius of curvature for the curves or surfaces, means we should calculate the radius of curvature for all the surface points.

For the tool with ball tip, we will talk about the sphere tip, given a set of points; we find the center and radius of a sphere that fits the points best

In n dimension, points $x \in \mathbb{R}^n$ on a sphere with center $c \in \mathbb{R}^n$ and radius $r > 0$ are characterized by

$$r^2 = \|x - c\|^2 \quad \dots\dots\dots (5.27)$$

Equivalently,

$$\sum 2x_i c_i + r^2 - \sum c_i^2 = \sum x_i^2 = \|x\|^2 \quad \dots\dots\dots (5.28)$$

where the summations are over $j=1, 2, 3 \dots n$. Now, only consider the cases $n=2$ and $n=3$, and given a set of m points

$$\{x^k = (x_1^k, \dots, x_n^k) \in \mathbb{R}^n : k = 1, 2, \dots, m\}$$

To obtain the center of the fitting sphere $c = (c_1 \dots c_n)$, the following system has been solved for linear equations in the least square sense [41]

$$\begin{pmatrix} 2x_1^1 & \dots & 2x_n^1 & 1 \\ \vdots & & \vdots & \\ \vdots & & \vdots & \\ 2x_1^m & \dots & 2x_n^m & 1 \end{pmatrix} \cdot \begin{pmatrix} c_1 \\ \vdots \\ c_n \\ \dots \\ R \end{pmatrix} = \begin{pmatrix} \|x^1\|^2 \\ \vdots \\ \|x^m\|^2 \end{pmatrix} \dots\dots\dots (5.29)$$

Then, the radius of the sphere is

$$r = \sqrt{R + \|c\|^2} \dots\dots\dots (5.30)$$

If the matrix above does not have maximum rank, we define $r = \infty$ [42].

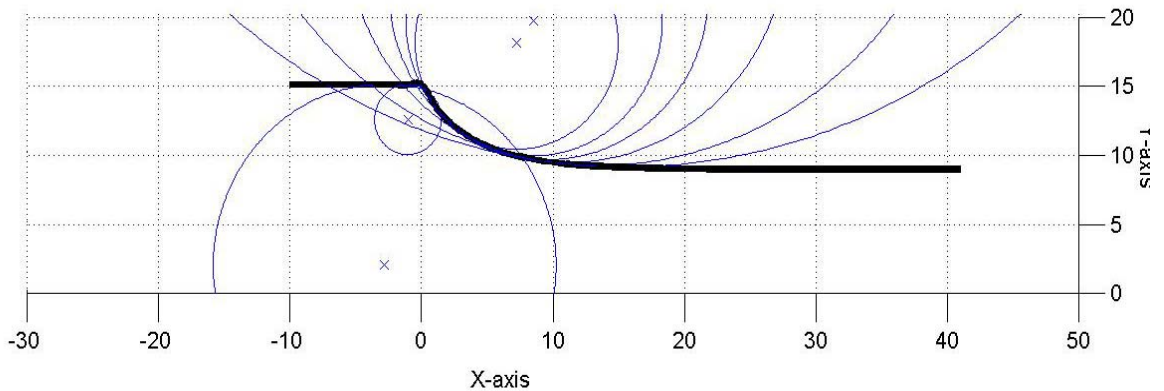


Figure (5.4): The radius of curvature for some points on the designed profile.

5.4 Toolpath Design

A vertical three-axis CNC milling machine is the appropriate system for machining the surfaces. In order to generate the desired shape, the cutter must be moved so as to remain tangent to the surface created by the sliding of the profile curve along the trajectory curve. A tool commonly used for generating free-form surfaces is a spherical end-milling cutter, which has the convenient property that the center of its spherical end remains at a constant distance from the generated surface, while the tool axis maintains a vertical orientation.

A convenient tool center path, corresponding to one pass in the machining process, consists of a series of small lines of prescribed length along the profile's offset, followed by offset motion along the entire length of the trajectory curve, until the end of the profile curve is reached, see Figure (5.5) ^[43].

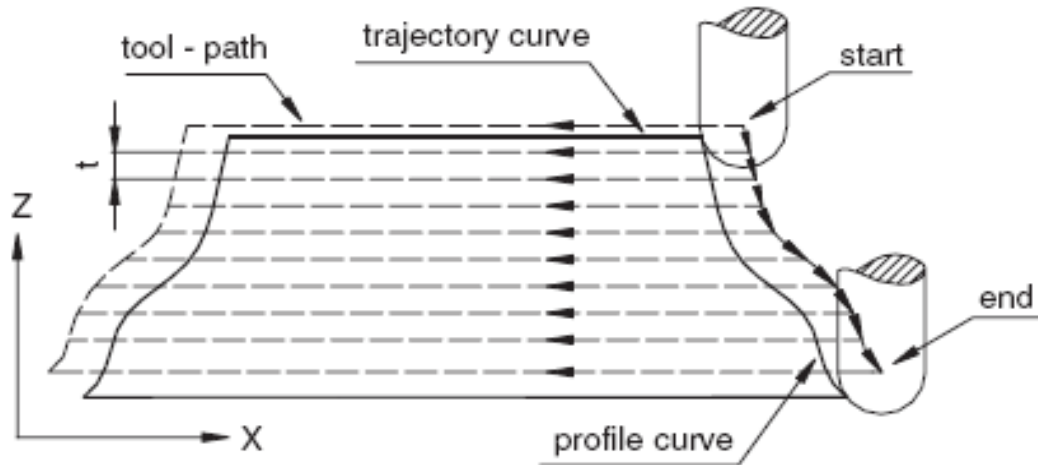


Figure (5.5):The tool-paths in XZ-plan (Front View) ^[42].

The necessary steps for this motion are generated, using as data input the following:

- the coordinates of the surface defining the profile curve.
- the tool-radius,
- the step size,
- the distance between scallops.
- the federate

The programmed distance between scallops is used to determine when to switch from motion generation along the profile curve to the motion generation along the trajectory curve ^[43].

A spherical cutter permits gouge-free machining of nonconvex surfaces if the cutter radius is less than the minimum concave principal radius of curvature on the surface obviously ^[44], as shown in equation (5.31) ^[45].

$$R_f \leq \rho_{\min} \quad \dots\dots\dots (5.31)$$

ρ_{\min} : the minimum radius of curvature of the over all surface.

R_f : radius of finishing cutter.

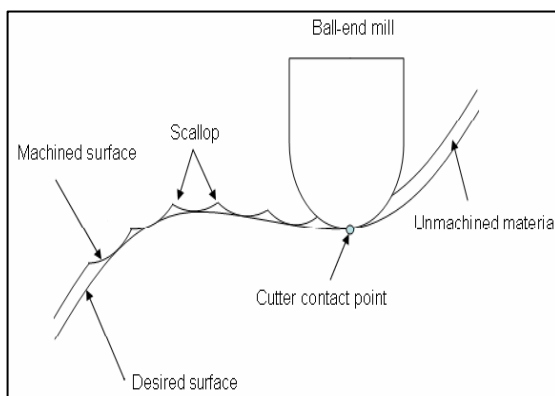
The cutter radius and the updated offset distance should be less than the minimum concave radius of curvature on the profile and the trajectory curves, respectively. By choosing a tool with a sufficiently small radius, the program can accommodate the considered surfaces [tool-path].

In fact, given information about cutter deflection, machine tool chatter and tool breakage will increase the tool life and surface integrity can be optimized in selecting appropriate cutting conditions. In milling, a lot of parameters are saved to be considered for any optimization attempt. These parameters concern the tool (geometry material), the tool path (path description, path length, and accessibility), and the tool engagement in workpiece (depths of cut, cutting modes), the kinematics (spindle frequency, feed velocity) and the lubrication conditions (lubricant type and flow or no lubrication) ^[43].

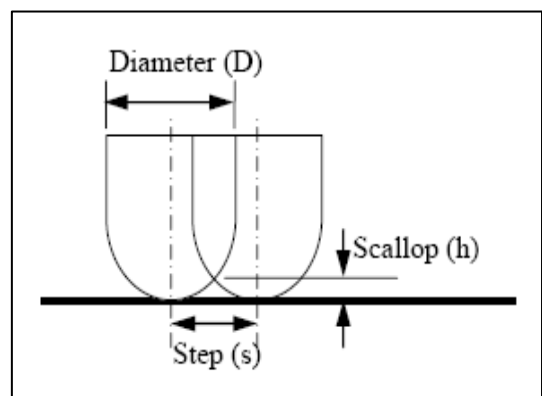
The tool center points are offsets of the tool surface, contact points in the surface normal directions by the tool radius. Coordinates of the tool tip points can then be obtained by translating the center points in the tool axis direction. The uncut region between successive tool cut is usually called scallop [39]. Scallops are the main factor which influences machining quality. Finishing operation process generally requires that the scallop height does not exceed 0.05 millimeters. With a given diameter of ball-end mill, the distance between two tool paths is computed in terms of the value of scallop height. For example, in the case of planar ball-end milling (see Figure (5.6)) the value of stepover can be calculated according to the formula in equation (5.32) [46].

$$s = 2\sqrt{Dh - h^2} \quad \dots\dots\dots (5.32)$$

s: The value of stepover, D: The diameter of ball mill, and h: Scallop height .Therefore, using a ball-end mill with given diameter dimension, produces much higher density of tool paths in convex regions than in concave regions when making the finish cut. This means that the overall productivity and material removal rate of ball-end mill finish surface machining is very low [46].



(a) Ball-end milling



(b) Step, scallop and diameter for ball-end milling

Figure (5.6): Ball-end mill surface machining [46].

This thesis has used scallop height value exceed 0.05 millimeters (approximately 0.4 millimeters) so that means the process which adopted is semi finishing process to reduce the milling process time and it is positively affects on milling process cost.

Most complex shapes fall within categories of 3D it is requiring movement of three axes in machining process. So to draw the toolpath for the shape which is shown in Figure (5.7), the toolpath has been designed in U-direction or in W-direction. Artificially the tool path should be designed for the longer dimension, but in some special cases (like making some experiments in laboratory), they need to design the tool path in another direction for special reasons of research ^[47], Figure (5.8: a, b) illustrates the tool path in U and W direction.

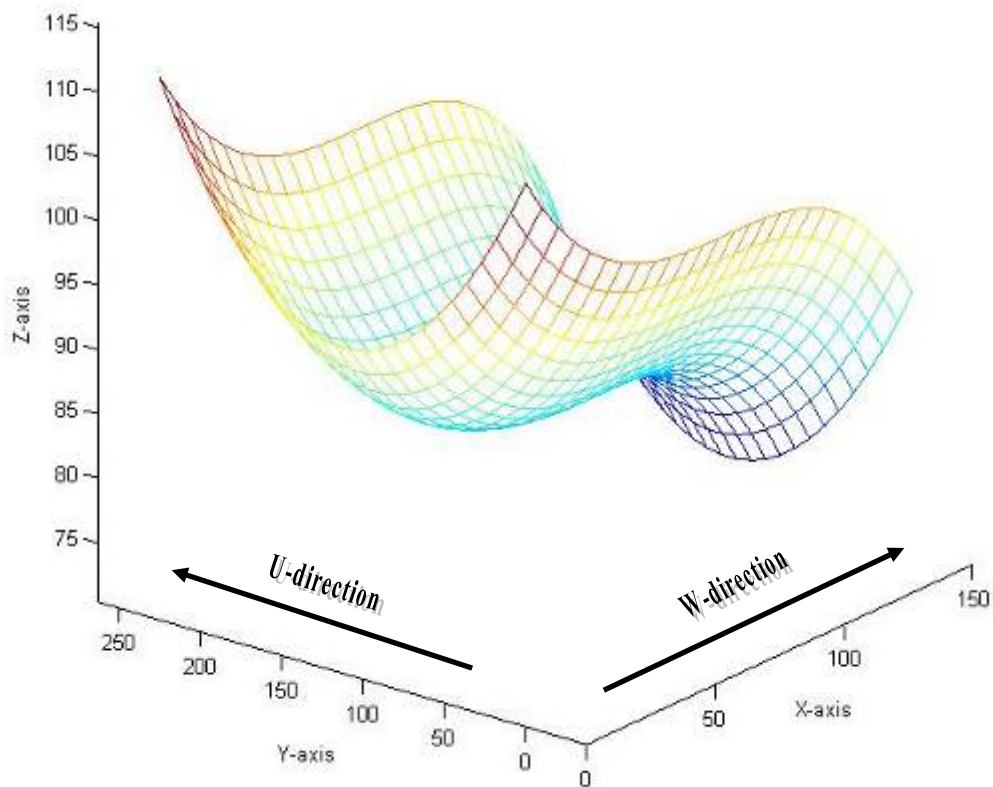
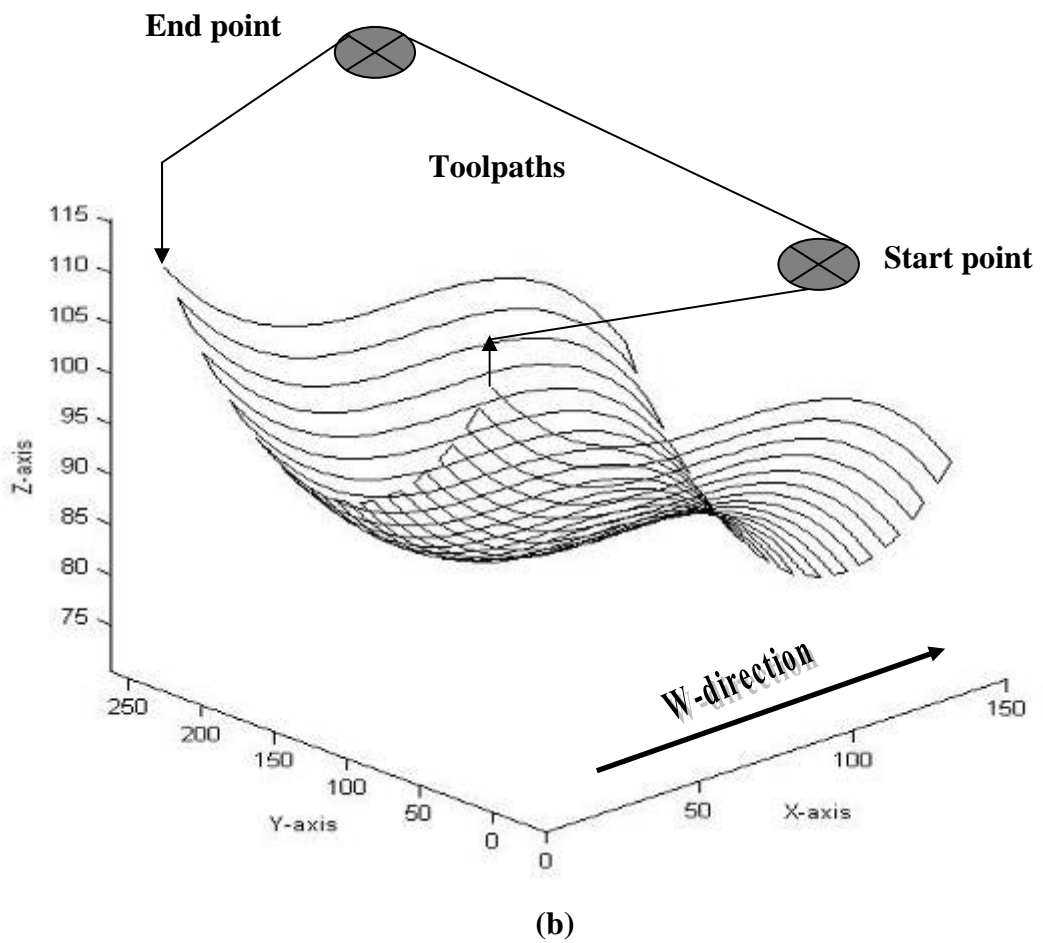
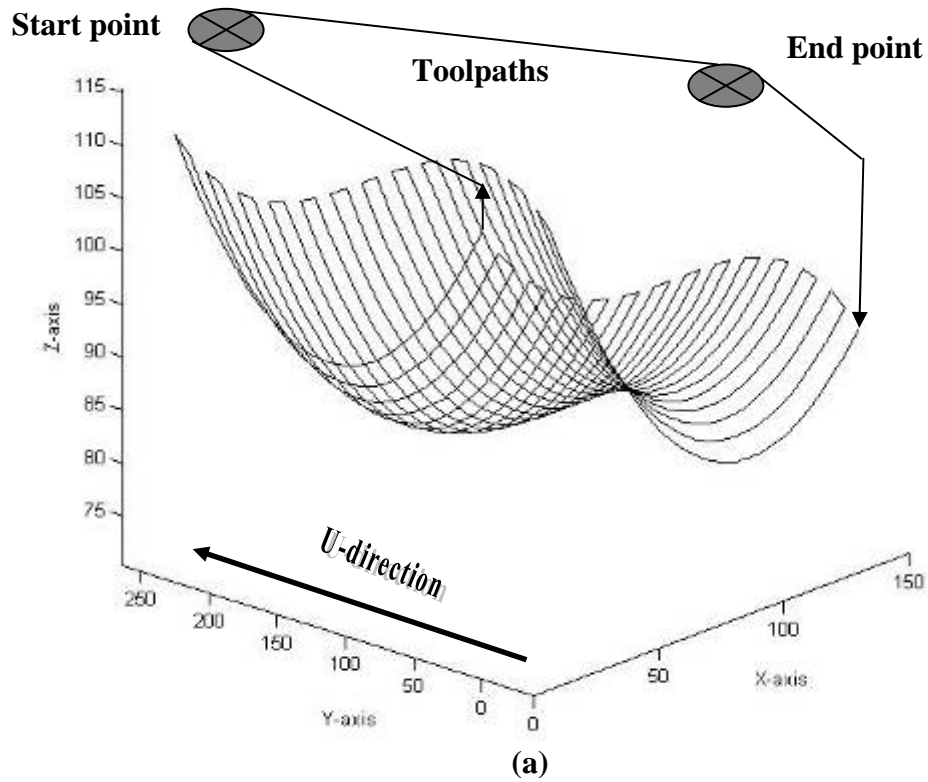


Figure (5.7): Bezier surface $n=3$, ^[48].



(b)
Figure (5.8: a, b): Three dimension toolpath
a- In U-direction.
b- In w-direction.

Case study:

Design the extrusion die depending on the theoretical concept (CRHS) and explain which type of CRHS will result with the information listed below:

$$R_o = 22.5\text{mm}; R_f = 15$$

$$L = 13\text{mm} \quad (\text{Distance from die inlet}).$$

$$S = 0.8$$

Depending on the CRHS concept:

To find Z_n at the point ($n=13$), we should use equation (5.15)

$$Z_{12} = \left[\frac{22.5}{15} \right]^2$$

$$Z_{12} = 2.25$$

And the Z_1 is calculated from the equation (5.23)

$$Z_1 = 1.18723$$

And again from the equation (5.15) we calculate R_1

$$R_1 = \frac{R_o}{Z_1^{1/2}}$$

$$\therefore R_1 = 20.65\text{mm}$$

So, we continue in the same calculation to find Z_2 from equation (5.23).

$$Z_2 = Z_1^{0.8^{(2-1)} + 0.8^{(2-2)}}$$

$$Z_2 = 1.36195$$

And to calculate R_2 from equation (5.15)

$$Z_2 = \left(\frac{R_o}{R_2} \right)^2$$

$$R_2 = \frac{22.5}{1.36195^{1/2}}$$

$$\therefore R_2 = 19.28\text{mm}$$

So, we continue in this calculation to find Z , R , at every L (Distance from Die inlet).

Table (5.1): Calculate the R, Z, at every L for Forward Extrusion Die Profile by CRHS concept

n	X(mm)	Z _n	R _n (mm)
1	1	Z ₀	22.5
2	2	Z ₁	20.65
3	3	Z ₂	19.28
4	4	Z ₃	18.249
5	5	Z ₄	17.465
6	6	Z ₅	16.862
7	7	Z ₆	16.394
8	8	Z ₇	16.03
9	9	Z ₈	15.744
10	10	Z ₉	15.519
11	11	Z ₁₀	15.341
12	12	Z ₁₁	15.2
13	13	Z ₁₂	15.089

From this table we find that is

$$Z_n = 2.25$$

R_f: 15.089mm (Final radius for die Profile)

L_n: 13mm (Distance from die inlet)

And n: 13 (number of sections for die profile for forward extrusion process).

The die profile results from this R mm and L mm is shown in Figure (5.9).

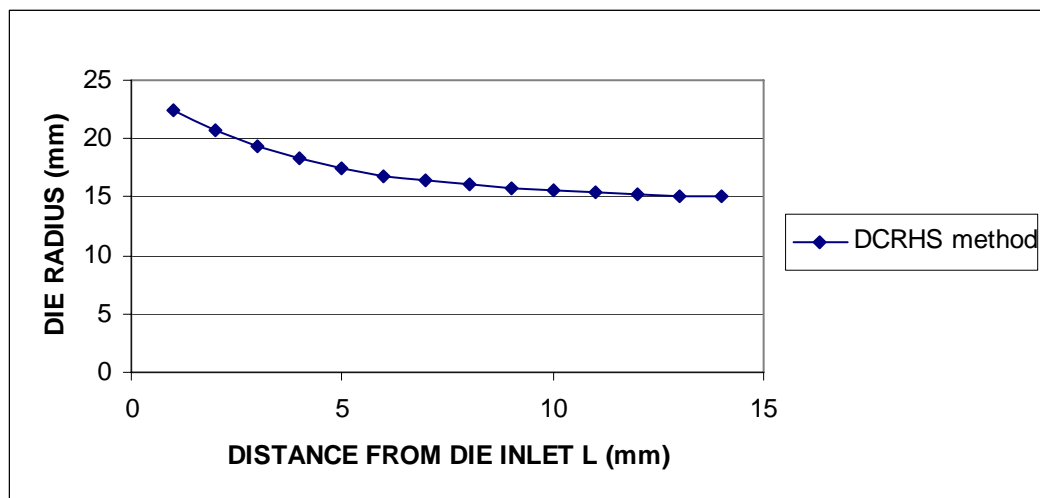


Figure (5.9): Design the Geometric shape for the Die profile by CRHS concepts, the shape result is **DCRHS**, (for Forward Extrusion).

From the comparison between the curve result in Figure (5.9) and the curves in Figure (5.1) is noted that the curve in Figure (5.9) is DCRHS type and note the die geometry which was designed before in Figure (5.9) see Figure (5.10).

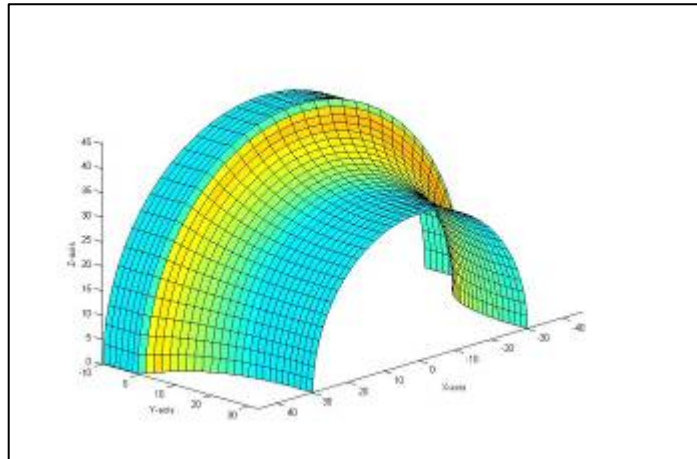


Figure (5.10) Geometric Die design for Forward Extrusion process depends on CRHS concepts with Die profile length 13mm.

The curve in Figure (5.9) has been drawn again by using Uniform B-spline curve with subdivision iterations to get more control points and to arrive to the same curve geometry by trial and error method, so firstly it is draw with Quartic Subdivision for Uniform B-spline curve (that means 6 control points plotted on the curve) as shown in Figure (5.11) and the surface result is shown in Figure (5.12).

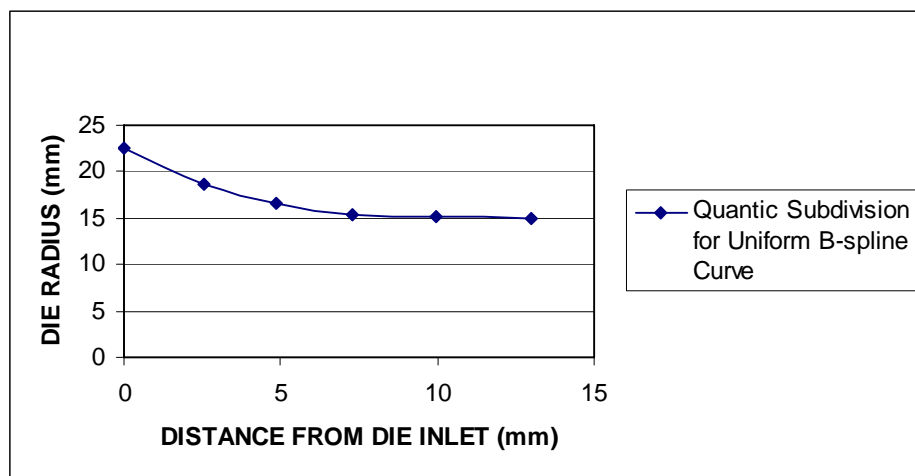


Figure (5.11): Drawing the Geometric shape for the Die profile which is designed by CRHS concepts, the shape result is **DCRHS**, (for Forward Extrusion), drawing by Quartic Subdivision for Uniform B-spline Curve.

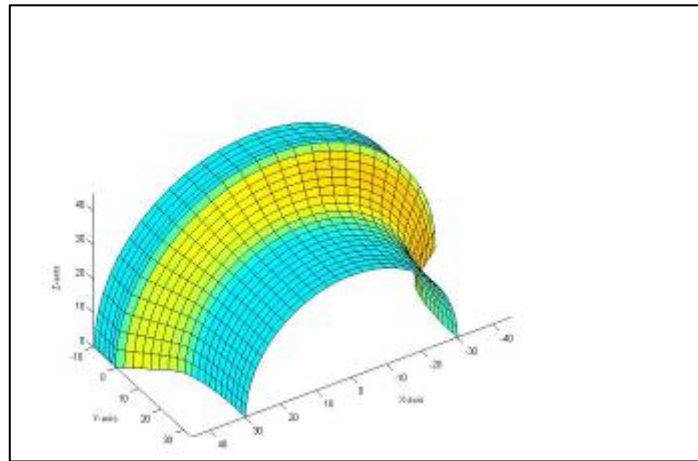


Figure (5.12) Geometric Die design for Forward Extrusion process depends on CRHS concepts with Die profile length 13mm drawing by Quartic Subdivision for Uniform B-spline Curve.

Secondly the same curve in Figure (5.9) is drawn with Quintic Subdivision for Uniform B-spline curve (that means 7 control points plated on the curve) as shown in Figure (5.13) and the surface result is shown in Figure (5.14).

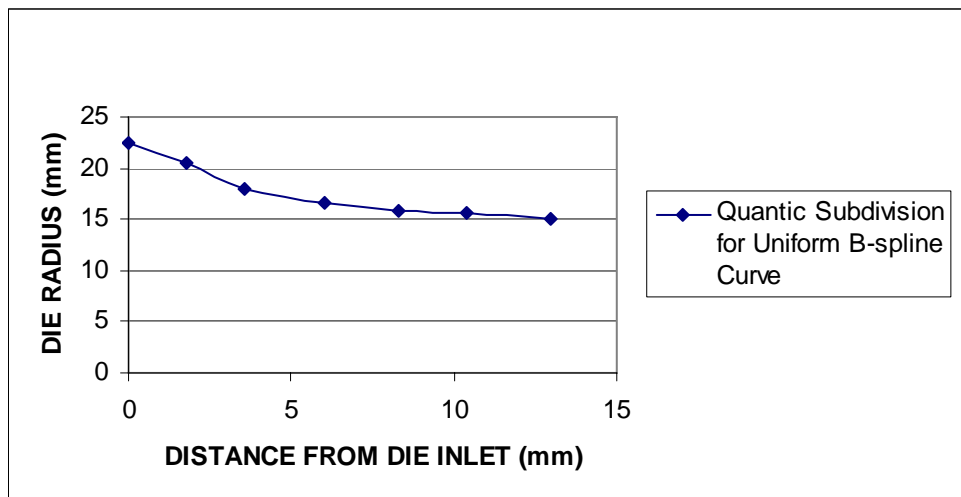


Figure (5.13): Drawing the Geometric shape for the Die profile which is designed by CRHS concepts, the shape result is **DCRHS**, (for Forward Extrusion), drawing by Quintic Subdivision for Uniform B-spline Curve.

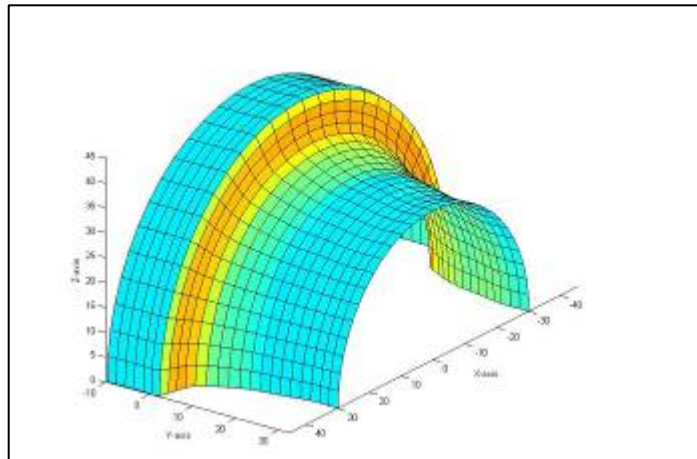


Figure (5.14) Geometric Die design for Forward Extrusion process depends on CRHS concepts with Die profile length 13mm drawing by Quintic Subdivision for Uniform B-spline Curve.

The difference in the shape geometry for these three curves (CRHS curve, Quartic Subdivision for Uniform B-spline Curve, and Quintic Subdivision for Uniform B-spline Curve) for the same design, it is noted in Figure (5.15).

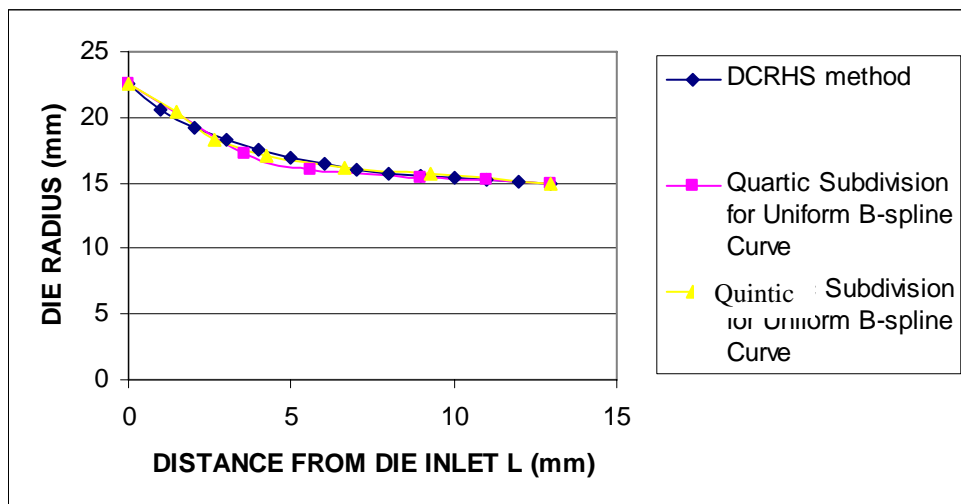


Figure (5.15): Find the difference in the shape geometry for these three curves (CRHS curve, Quartic Subdivision for Uniform B-spline Curve, and Quintic Subdivision for Uniform B-spline Curve).

So the mean curvature for these three proposed technique is shown in Figure (5.16),and Appendix (C), the radius of curvature is shown in Figure (5.17) and Appendix (D) ,and the toolpath generated for each technique is shown in Figure (5.18),and the optimum cutter diameter for each surface machined is illustrated in Figure (5.19), to calculate the maximum and minimum deviations of these three shapes after calculating the deviation shown in Figure (5.20),and deviation in three x-axis section in Figures (5.21),(5.22),and (5.23).

$$\text{Deviation} = Z_f - Z_a$$

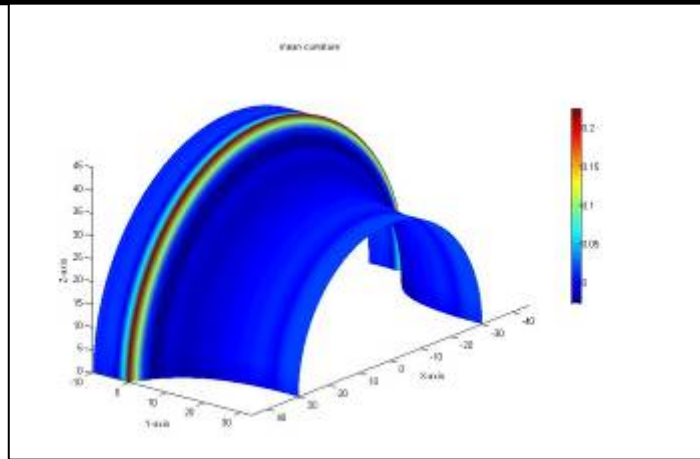
Z_f =value for the desired surface in (z-dir).

Z_a =value for machined surface in (z-dir).

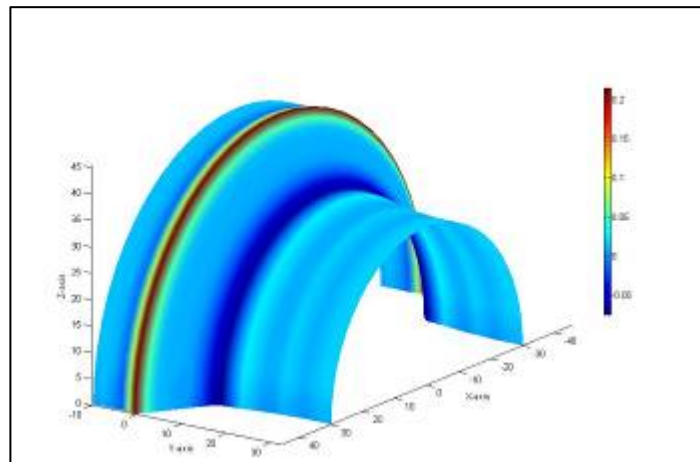
In the same time it has been shown the line segments in Figures (5.24), (5.25), and (5.26) for these three surfaces submitted before.

Table (5.2): The result Comparison between the surfaces presented above

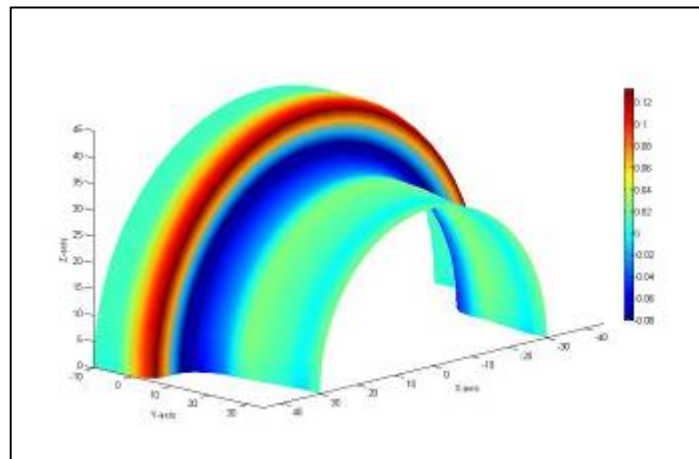
Results Comparison				
NO#	Parameters	CRHS	Quartic subdivision for Uniform B-spline.	Quintic subdivision for Uniform B-spline.
1	Max deviation(between the deserved surface and surface machined)	inf	inf	inf
2	Min deviation(between the deserved surface and surface machined)	-5.0935	-12.4576	-4.6505
3	Max mean curvature	0.22	0.22	0.575
4	Min mean curvature	-0.02	-0.08	-0.15
5	Suitable cutter radius for semi finished process.	4 mm	5 mm	3 mm
6	Number for segment of toolpath interpolator	850	512	942
7	Points in domain	5992	5985	5992
8	Length of segment for toolpath interpolator (total toolpath length).	1780.291	1433.2474	2015.7892



(a)



(b)



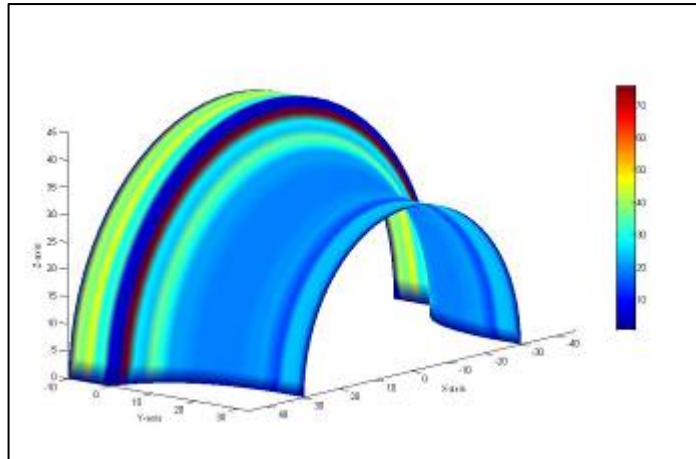
(c)

Figure (5.16: a, b, and c): The mean curvature.

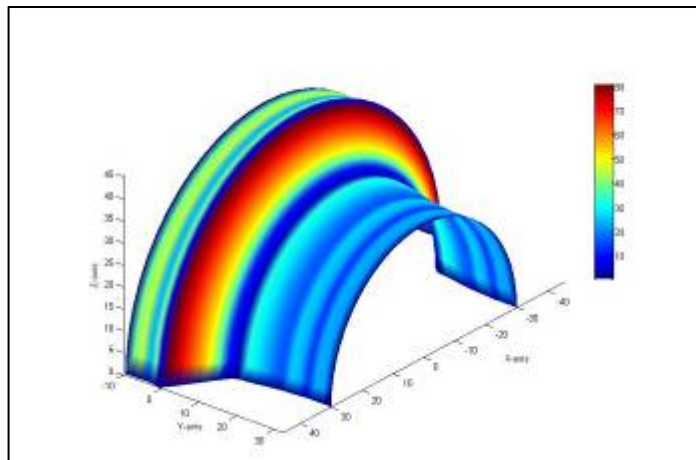
a- Main curvature for CRHS method.

b- Main curvature for Quartic Subdivision for Uniform B-spline technical.

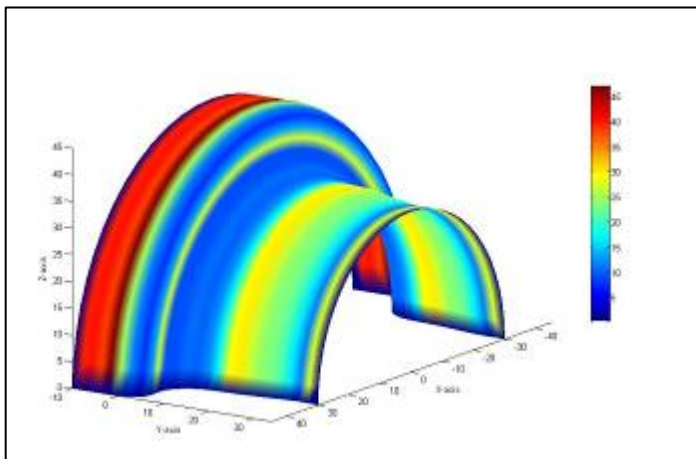
c- Main curvature for Quintic Subdivision for Uniform B-spline technical.



(a)



(b)



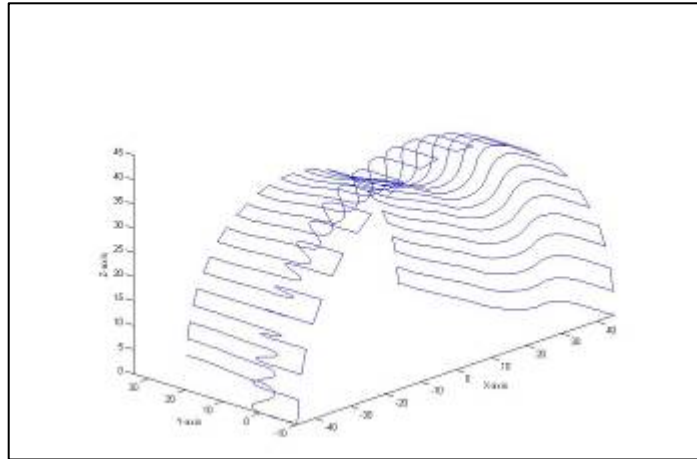
(c)

Figure (5.17: a, b, and c): The radius of curvature drawing.

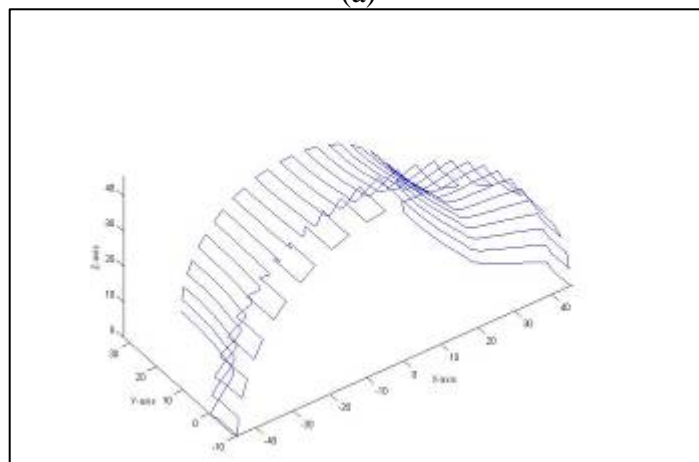
a- The radius of curvature for CRHS method.

b- The radius of curvature for Quartic Subdivision for Uniform B-spline technical.

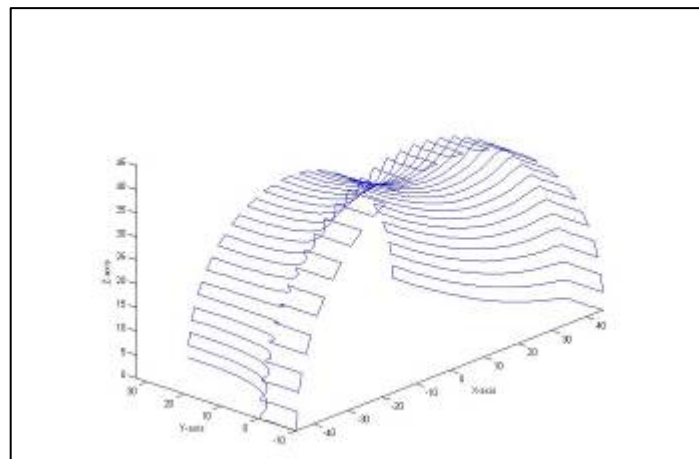
c- The radius of curvature for Quintic Subdivision for Uniform B-spline technical.



(a)



(b)



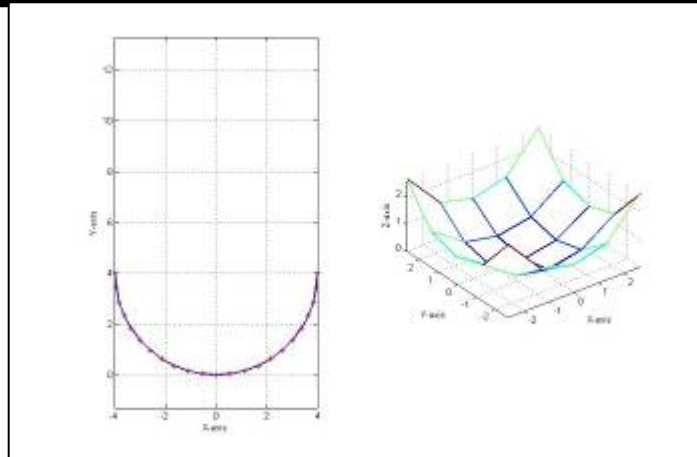
(c)

Figure (5.18: a, b, and c): The toolpath generated.

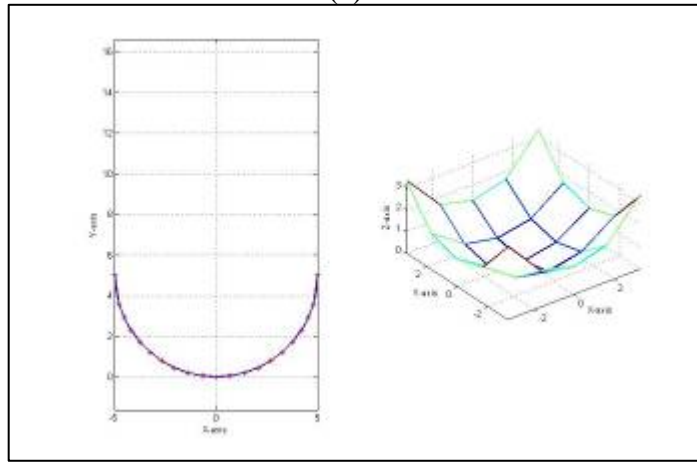
a- The toolpath for CRHS method.

b- The toolpath for Quartic Subdivision for Uniform B-spline technical.

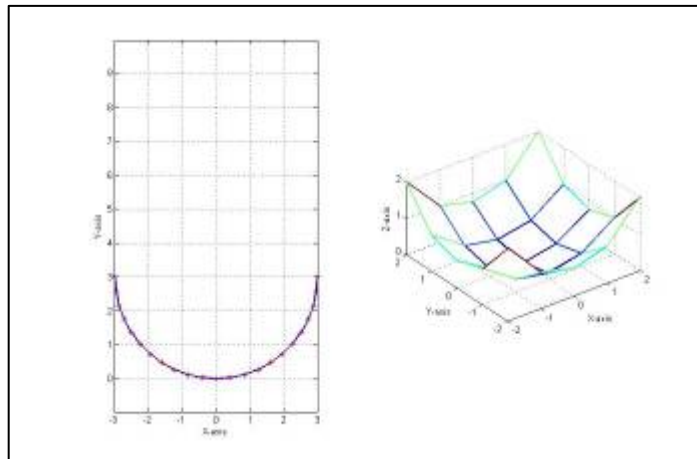
c- The toolpath for Quintic Subdivision for Uniform B-spline technical.



(a)



(b)



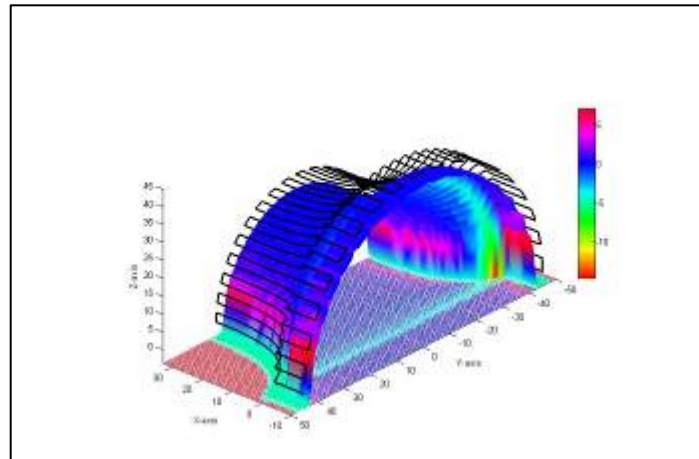
(c)

Figure (5.19: a, b, and c): The cutter ball dimension.

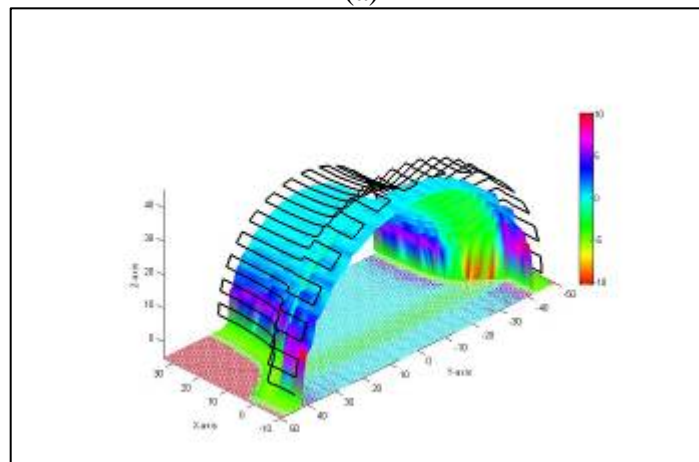
a- The cutter dimension for CRHS method.

b- The cutter dimension for Quartic Subdivision for Uniform B-spline technical.

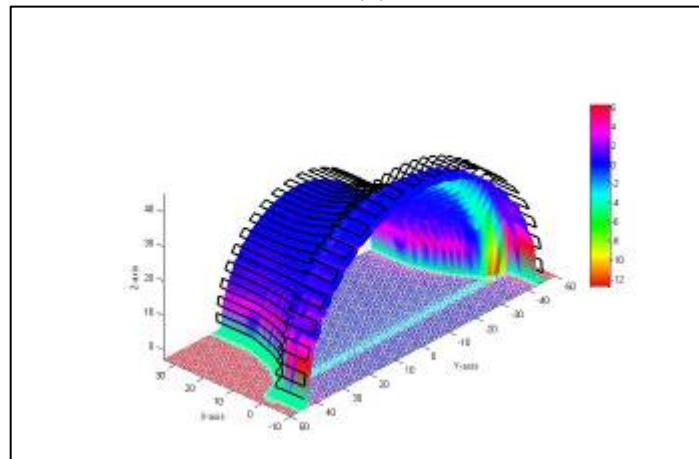
c- The cutter dimension for Quintic Subdivision for Uniform B-spline technical.



(a)



(b)



(c)

Figure (5.20: a, b, and c): The deviation between the desired surface and surface after machined.

- a- The Deviation for surface generated by CRHS method.
- b- The Deviation for surface generated by Quartic Subdivision for Uniform B-spline technical.
- c- The Deviation for surface generated by Quintic Subdivision for Uniform B-spline technical.

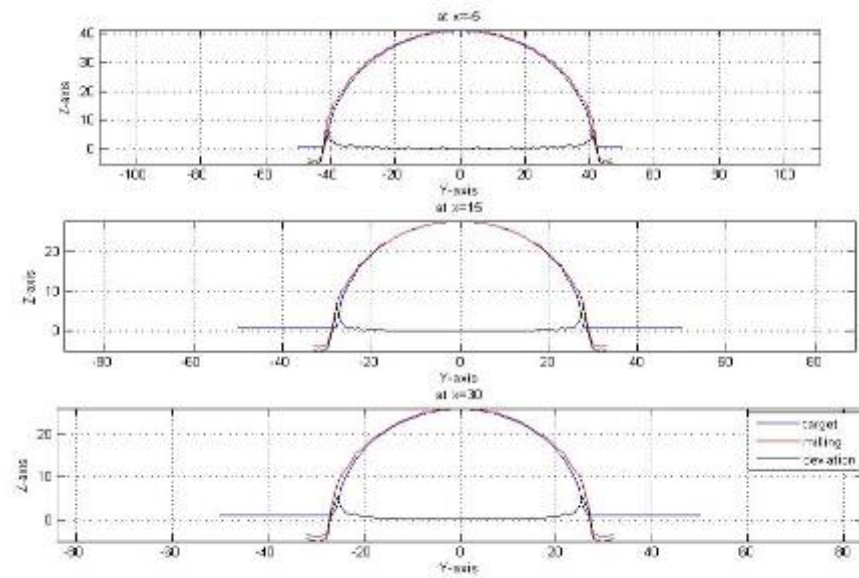


Figure (5.21): The deviation between the desired surface and the machined surface at $x=5$, 15, and 30 for surface generated by CRHS method.

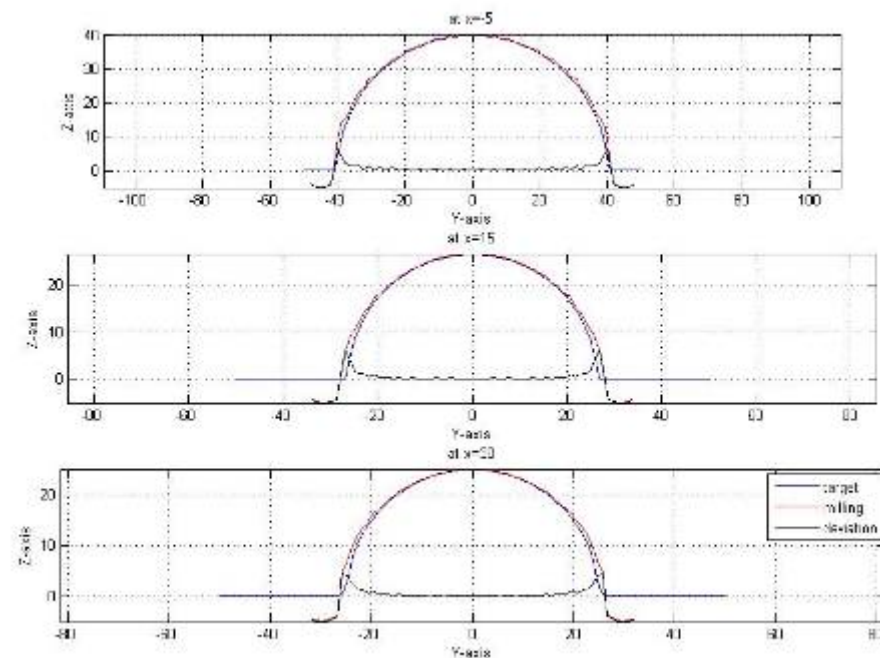


Figure (5.22): The deviation between the desired surface and the machined surface at $x=5$, 15, and 30 for surface generated by using Quartic subdivision algorithm to Uniform B-spline technical.

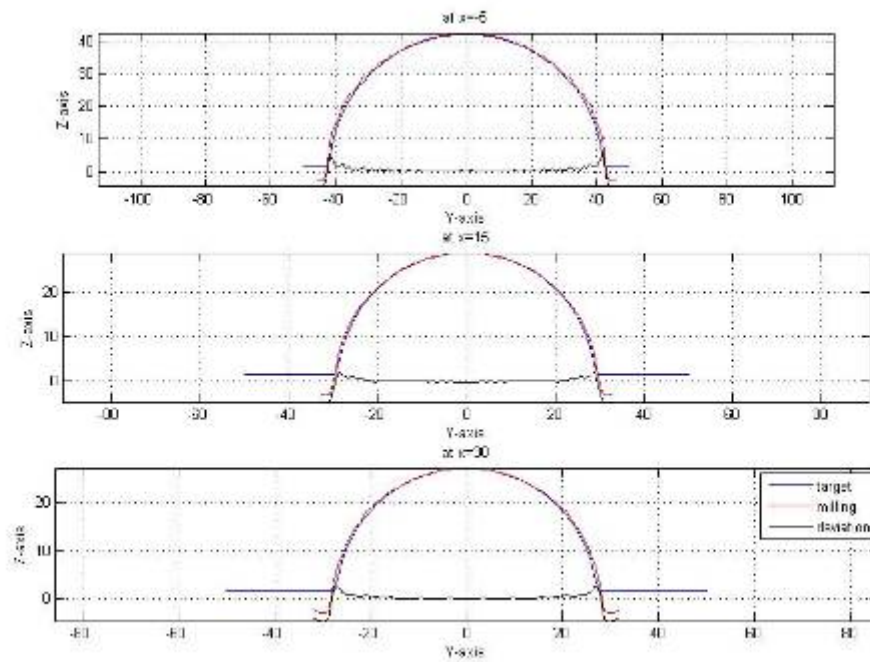


Figure (5.23): The deviation between the desired surface and the machined surface at $x=5$, 15, and 30 for surface generated by using Quintic subdivision algorithm to Uniform B-spline technical.

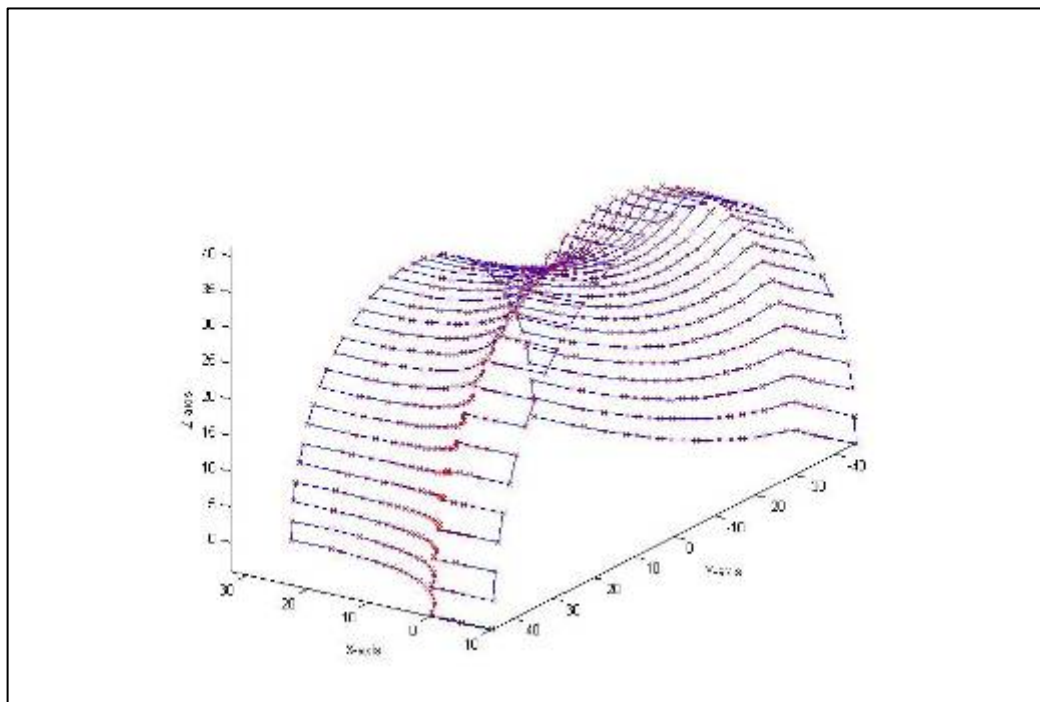


Figure (5.24): The line segment for toolpath generated by CRHS method.

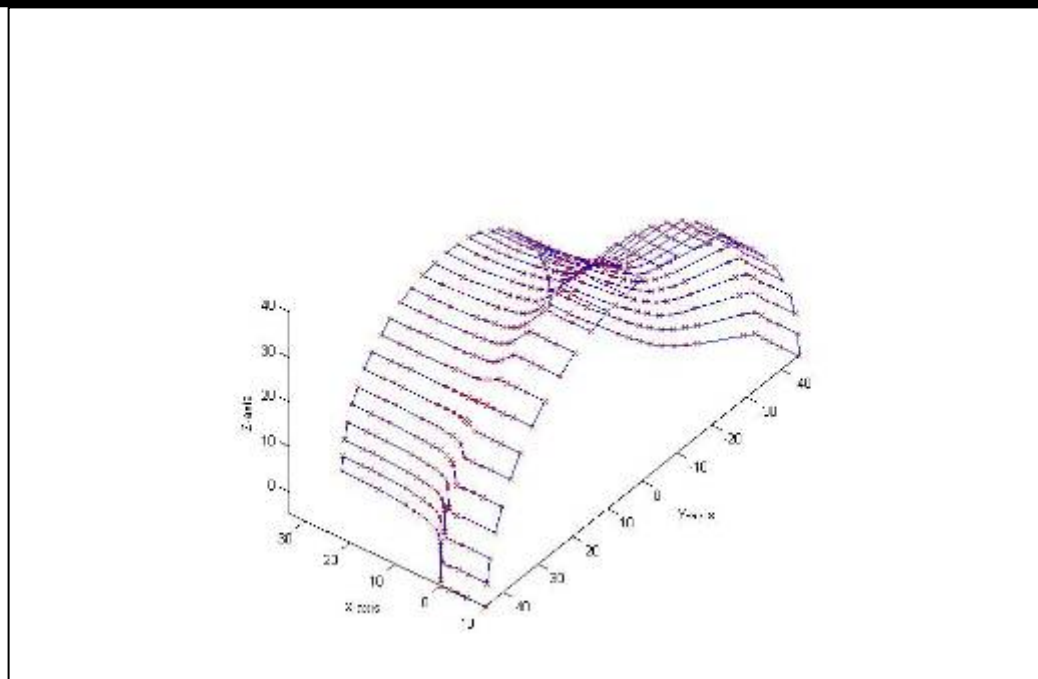


Figure (5.25): The line segment for toolpath generated by Quartic subdivision algorithm to uniform B-spline technical.

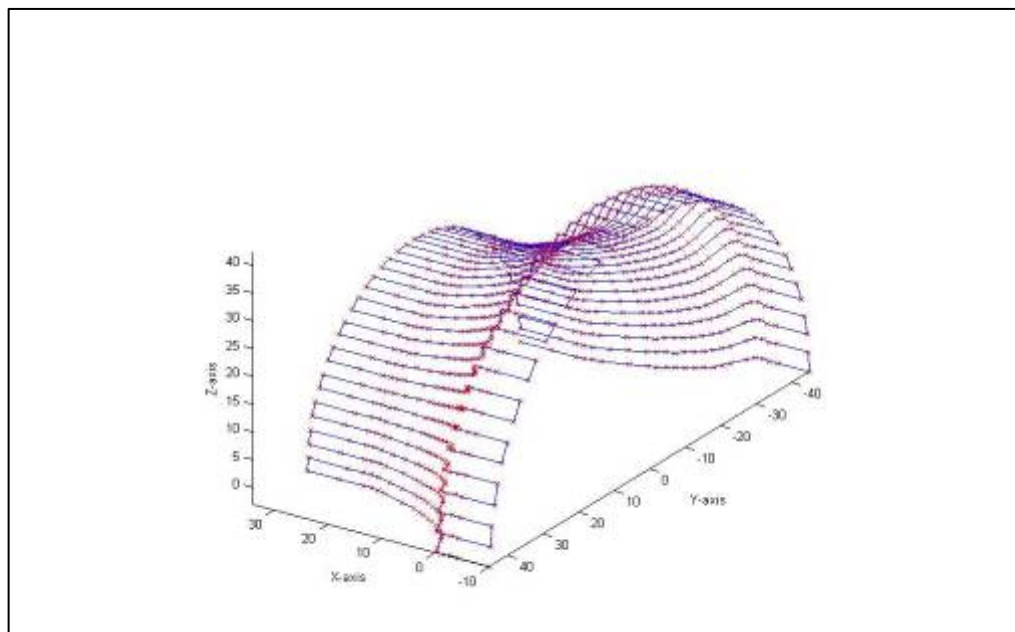


Figure (5.26): The line segment for toolpath generated by Quintic subdivision algorithm to uniform B-spline technical.

After designing the toolpath by using Matlab (V7.0) software, with DXF file extension (after converting it from m file extension by Matlab software), it has been exported to surfcam program as shown in Figure (5.27).

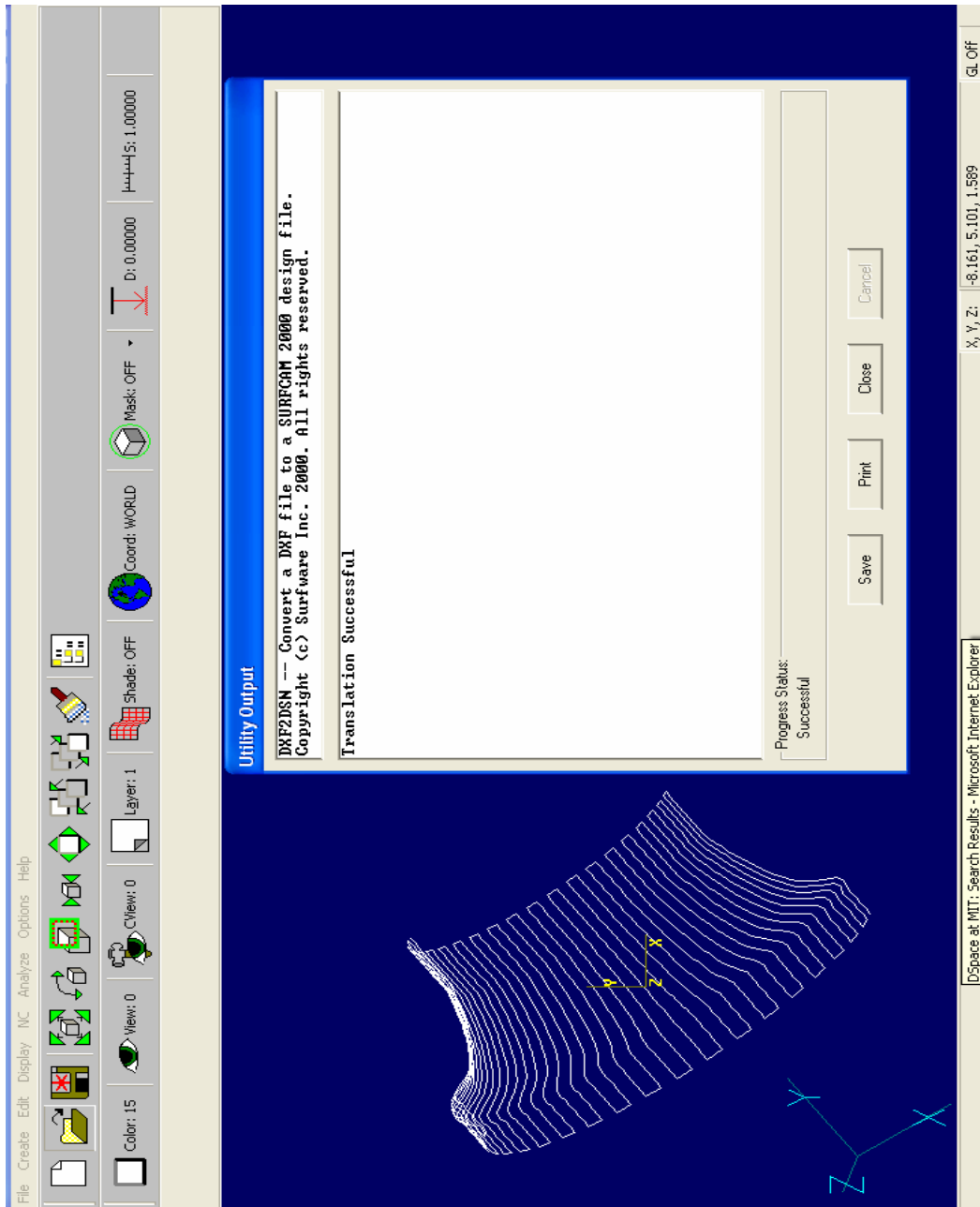


Figure (5.27): Import the DXF file extension to Surfam design file.

Field

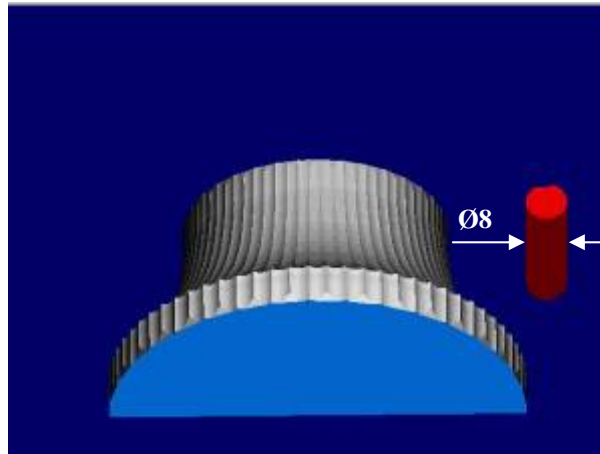
The machining parameters for this process (roughing and semi-finishing) are illustrated in Table (5.3).

Table (5.3): Surfcam cutting options summary sheet

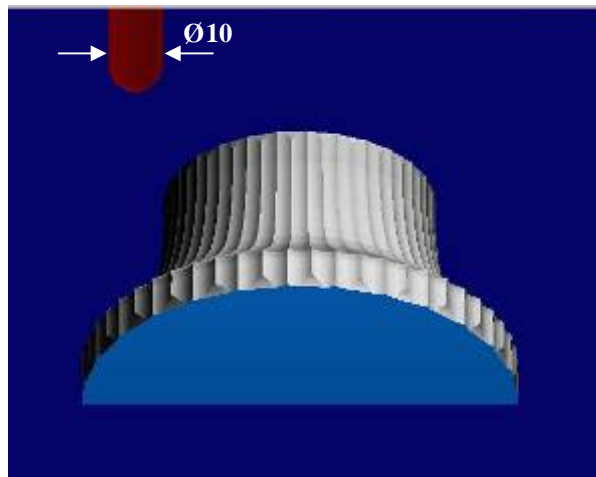
Stock material :UREOL (EPOXY RESIN)				
NO#	Machining parameters	CRHS	Quartic Subdivision for Uniform B-spline.	Quintic Subdivision for Uniform B-spline.
1	Cutter radius for semi finishing process.	4 mm	5 mm	3 mm
2	Cutter radius for roughing process.	4 mm	5 mm	3 mm
3	Cutter travel length (m)	327	208	363.5
4	Spindle speed	14000	14000	18000
5	Feed rate (m/min)	Min:0.382	Min:0.5073	Min:0.1432
		Max:10.000	Max: 10.000	Max: 10.000
6	Cutter material (ball nose)	HSS	HSS	HSS
7	Flutes	2	2	2
8	Min X for stock (mm)	0		
9	Min Y stock (mm)	0		
10	Min Z stock (mm)	0		
11	Max X for stock (mm)	90		
12	Max Y for stock (mm)	42		
13	Max Z for stock (mm)	45		
14	Block number	4970	3204	5459
15	Program size (byte)	128742	81902	143092
16	Toolpath type (cutting strategy)	Zig-Zag toolpath for roughing and semi finishing process.		
17	Axial in feed (mm)	5		

The main problem for surfcam software is the zero coordinate for the stock will be in the middle of the stock (because the shapes are symmetrical) which is illustrated in Figure (5.26), and that the machining side fails, because the zero coordinate should be in the out of the stock (with defined value) or in the any corner for the stock. For that reason Matlab program has been used to shift the zero coordinate to the defined corner (the surfcam software fails to do this option), and define the base for stock as xy-plan and the Z-direction is the cutting direction (note: the result

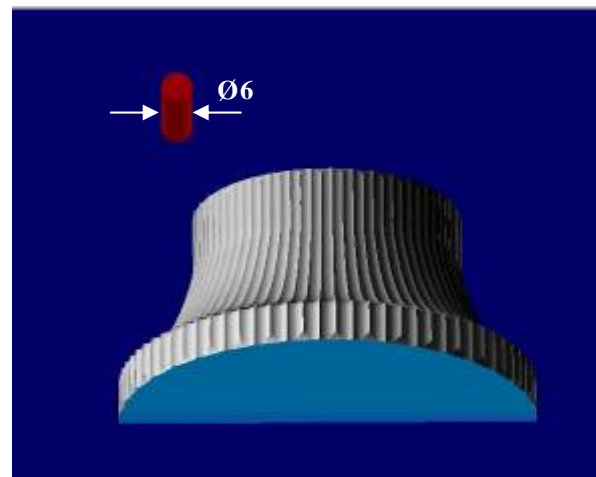
The shapes result from the Surfcam software is shown if Figure (5.30).



(a)



(b)



(c)

Figure (5.30: a, b, and c): The semi finishing for the surfaces machined by Surfcam Software.
a- The semi finishing surface generated by CRHS method.
b- The semi finishing surface generated by Quartic Subdivision to Uniform B-spline technical.
c- The semi finishing surface generated by Quintic Subdivision to Uniform B-spline technical.

5.5 Cutting Conditions for Experimental part

According to the conditions of the experimental work, the type of material that was used is Ureol (an Epoxy Resin) .The tool used in this work is tip ball mill cutter, tool material is (HSS) with $\text{Ø}8$ for CRHS method, $\text{Ø}10$ for Quartic Uniform B-spline technical, and $\text{Ø}6$ for Quintic Uniform B-spline technical, the machining was achieved on CNC machine (Hermle C30U dynamic, 5-axis AC-kinematics, with specification of linear motor drives (60.000 m/min), motor spindle 37kw 28.000 rpm) , the control is Siemens 840D,and the position error was below 0.002mm The machine is operated in Technical University Darmstadt (Germany) as shown in Figure (5.31), and the G-codes imported to this CNC machine was achieved by Surfcam software and modified by Matlab (V7.0) software. The G-code designed is 3-axis FANUC 15 MB system, and the machining process was done without Lubricant.

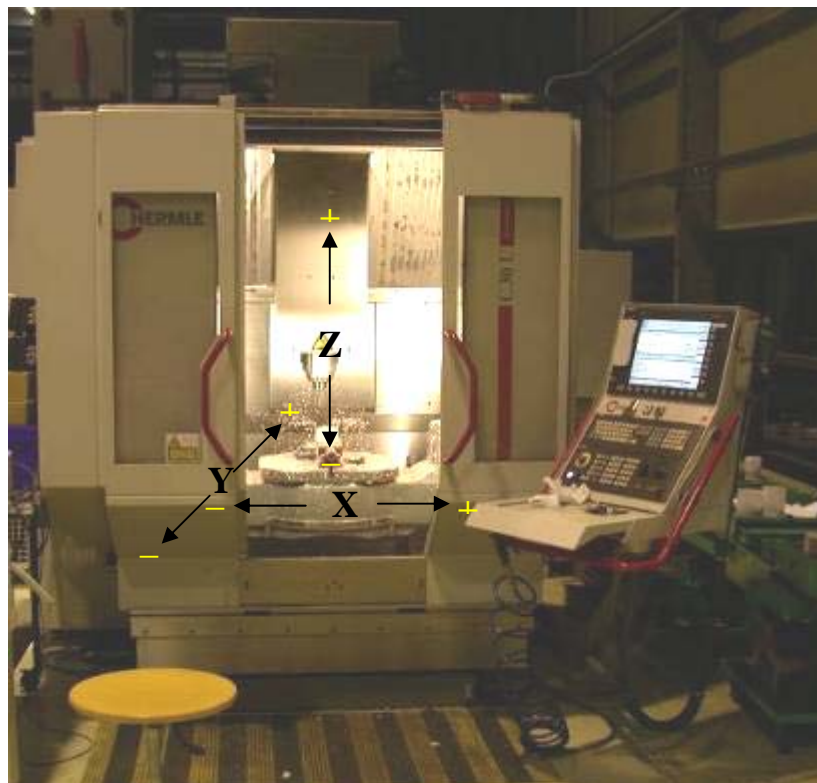


Figure (5.31): CNC machine (Hermle C30U dynamic, 5-axis AC-kinematics) which belongs to Technical University Darmstadt (Germany)

The other cutting conditions are written in Table (5.3), and the surfaces samples results from machining process are shown in Figure (5.32) and Figure (5.33).

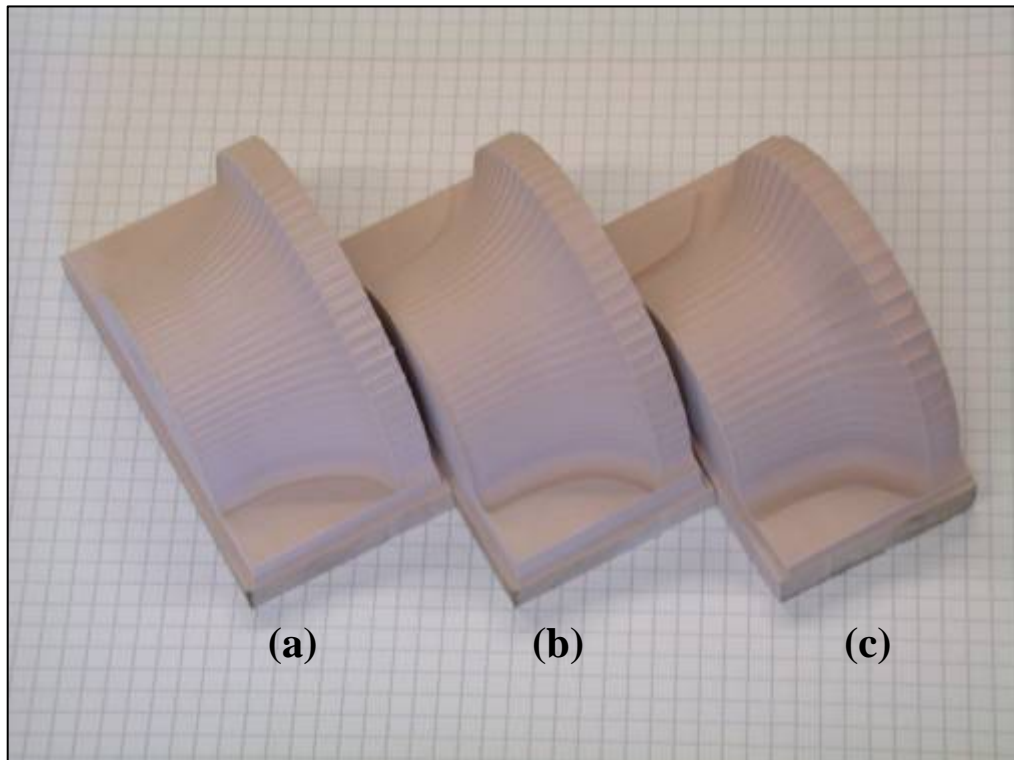
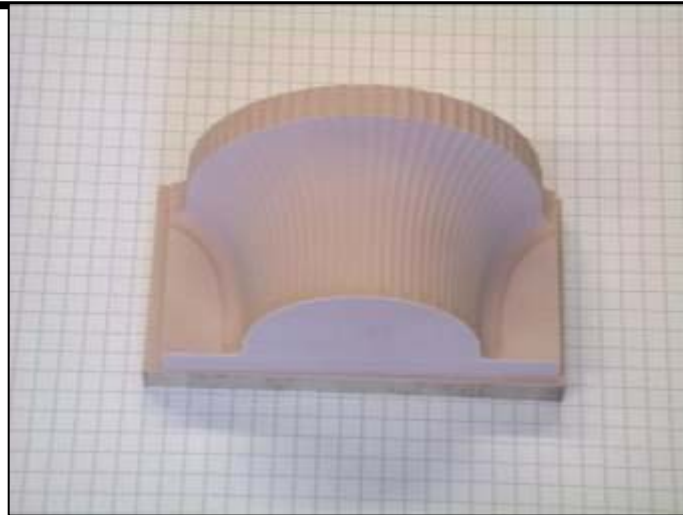
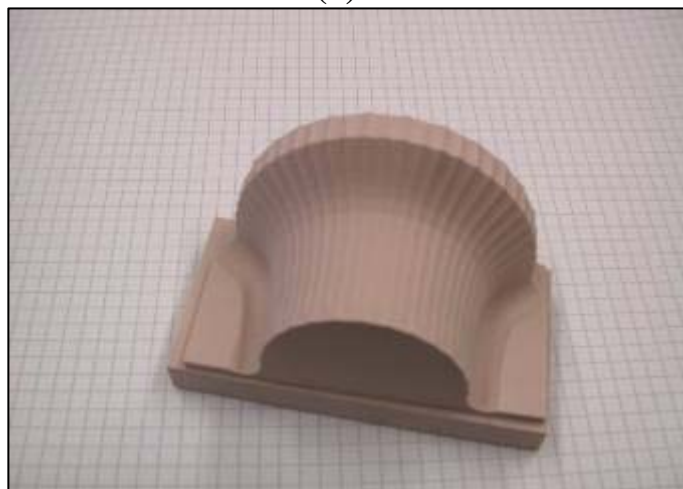


Figure (5.32): The samples result from Machining process by CNC milling machine.
a- Sample designed by CRHS method and machined with cutter radius R 4mm.
b- Sample designed by Quintic Subdivision for Uniform B-spline technical and machined with cutter radius R 3mm.
b- Sample designed by Quartic Subdivision for Uniform B-spline technical and machined with cutter radius R 5mm.

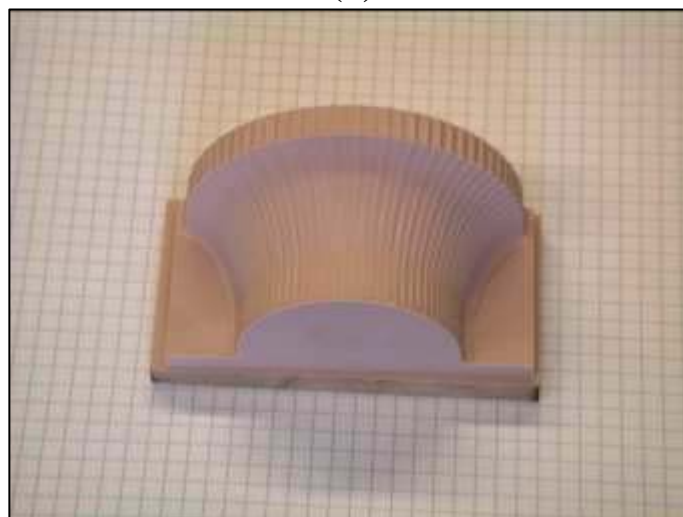
Field



(a)



(b)

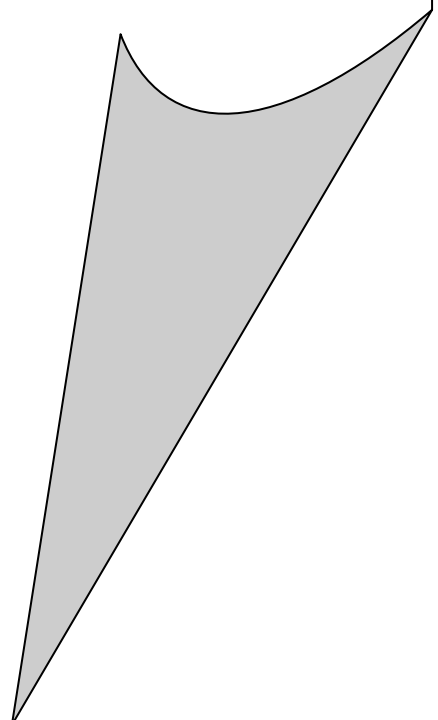


(c)

Figure (5.33): The samples result from Machining process by CNC milling machine.
a- Sample designed by CRHS method and machined with cutter radius R 4mm.
b- Sample designed by Quartic Subdivision for Uniform B-spline technical and machined with cutter radius R 5mm.
c- Sample designed by Quintic Subdivision for Uniform B-spline technical and machined with cutter radius R 3mm.

CHAPTER SIX

CONCLUSIONS AND SUGGESTIONS FOR FUTURE WORK.



CHAPTER SIX

Conclusions and Suggestions for Future Work

This chapter summarizes the results of the work done within the framework of the adopted subdivision technique with different subdivision iterations, and compares the result surfaces with the surface generated by CRHS method, described in this thesis.

The surfaces are designed using Matlab (V7.0) software package, while the program used to make machining simulation and G-code programs are designed by using Surfcam software. These G-code programs are implemented on a CNC machine (Hermle C30U dynamic, 5-axis AC-kinematics, with specification of linear motor drives (60.000 m/min), motor spindle 37kw 28.000 rpm) , the control is Siemens 840D, and the position error was below 0.002mm this machine is operated in the Technical University Darmstadt (Germany).

6.1 Conclusions:

1. The proposed technique of optimum cutter radius selection based on the minimum of cutter radius of curvature proves to be efficient enough in the prevention of cutter interference with the part geometric.
2. The proposed graphical simulation is an important step in preprocessing to submit an assessing, for the correctness of the surface presented before applying real cutting process (by generating the G-code by Surfcam software and show up the final shape resulting from implementing the G-codes).
3. Generation of G-code program could be achieved by uncomplicated method which is utilizing the capability of (PC) in saving the large data and processing facility .to allow machining of complicated parts that require multi processes that means a very large number of G-code block.

4. The toolpath could be obtained in two directions (U-direction and W-direction) for the roughing and semi finishing processes and the optimum toolpath (the optimum one is accompanied with the lower time milling process) can be chosen.
5. The proposed subdivision algorithm that is developed (subdividing the cubic Uniform B-Spline curve to Quartic Uniform B-Spline curve after three iterations of subdivision and Quintic B-spline curve after four iterations of subdivision) is successful in representing the die profile which is designed by CRHS method, and the effect of the subdivision iteration is shown in choose the cutter radius, toolpath design, and the surface deviation in roughing and semi finishing processes.
6. The CNC machine (Hermle C30U) with position error below 0.002mm facilitated obtaining the accurate results when the samples were machined by this CNC machine.
7. The sample shapes resulting from the experimental work by using CNC machine (Hermle C30U), was superposed with the samples shapes resulting from Simulation which is done by using Surfcam software prove the accuracy work to design the G-code .
8. The Matlab program which is invented to transfer the zero coordinate of the stocks on the stocks corner is successful, because the G-code result was run successful on this CNC machine, and the sample shapes results identify the samples shapes which result from simulation program.
9. The difference in cutter radius, and the toolpath length (see table 5.3) was affects directly the surface roughing results (recognize by vision).
10. The conversion of the file extension from Matlab file to DXF file was done successfully, that is because the commercial program

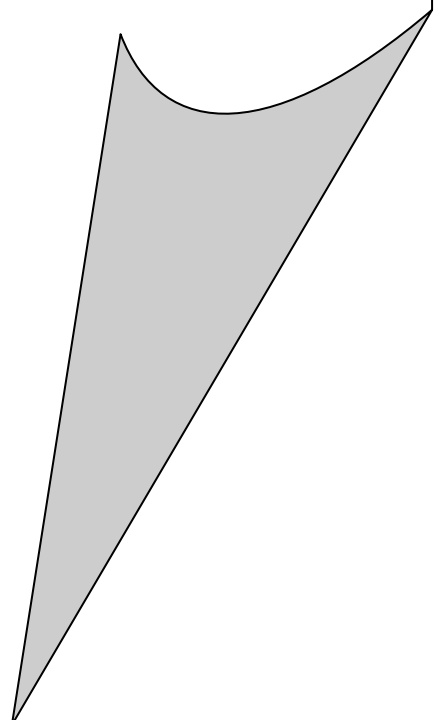
which is used to make simulation of our samples imports this DXF file extension successfully.

11. In all the fields which use subdivision algorithms (like subdivision for the polygon, subdivision for the vertex boundary, or subdivision for mesh node of the surface), the main reason for using these algorithms is to increase the resolution (in image processing), and increase the surface smoothness. In this thesis the cutter radius result for the surface generated by Quintic Uniform B-spline surface is (3mm), and the cutter used for surface generated by CRHS method is (5mm). As widely known the cutter radius is the most important indicator of the smoothness of surfaces, and that means the resulting surface from the subdivision algorithm is smoother than the surface resulting from the CRHS method.

6.2 Suggestions for Future Work:

1. Using more Subdivision iterations in Uniform B-spline technique and making comparison with the surfaces (die profile) designed by using DCRHS, CRHS, and ACRHS method, with Zig-Zag toolpath type.
2. Drawing the die profile by using Bezier, Non-Uniform B-spline technique, and comparison it with the die designed by using CRHS or CMSR method.
3. Drawing the Die profile by approximation method with different machining types (Iso-parametric machining, Iso-scallop machining, and Iso-planar machining) and making comparing between the results.
4. Studying the splitting matrix for Subdivision algorithm, and developing the way to find the splitting matrixes.

REFERENCES



References

1. Groover, P.M. "CAD/CAM Computer Aided Design and Manufacturing" Prentice Hall International inc, (1984).
2. Manley, G.D. "Assembly Differentiation in CAD Systems" M.Sc thesis, University of Pittsburgh", (2006).
3. Kwon, T.H. "Geometric modeling", <http://amp.postech.ac.kr/> (2001).
4. Holmstram, P. "Modeling Manufacturing Systems Capability" M.Sc thesis, KTH Industrial Engineering and Management, (2006).
5. Schweitzer, J. E. "Analysis and Application of Subdivision Surfaces" Ph.D thesis, University of Washington, (1996).
6. Shahab, A. F. "Investigation of the pass Geometry in compound backward– Forward Extrusion Process" Ph.D thesis, University of Technology, (2005).
7. Hoppe, H. "Surface Reconstruction from Unorganized Points" Ph.D thesis, University of Washington, (1994).
8. Zorin, D., and Kristjansson, D. " Evaluation of Piecewise Smooth Subdivision Surfaces", mrl.nyu.edu/~kristja/eval.pdf, (2000).
9. Joy, K. I. "Bicubic Uniform B-Spline Surface Refinement", Visualization and Graphics Research Group, University of California, (2000).
10. Joy, K. I. "Control Polygons for Cubic Curves", Visualization and Graphics Research Group, University of California, (2000).
11. Vlachos, A., Peters, J., Boyd, C., and Mitchell, J.L. "Curved PN Triangles", NSF NYI CCR-9457806, (2001).
12. Amresh, A., Farin, G., and Razdan, A., "Adaptive Subdivision Schemes for Triangular Meshes" Arizona State University, Tempe AZ 85287-5106, (2001).

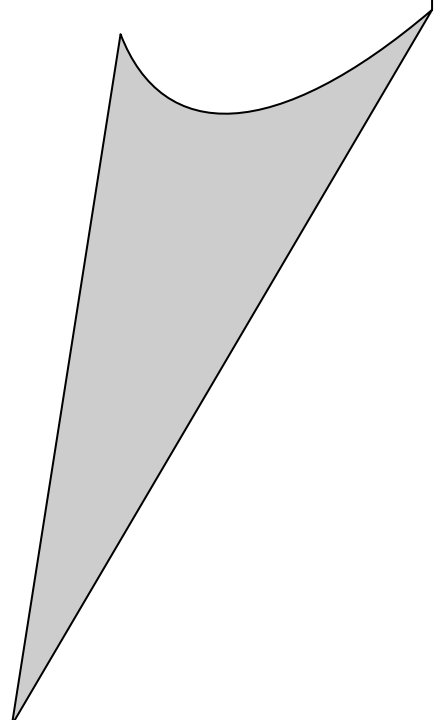
13. Bertram, M., and Hagen, H., "Subdivision Surfaces for Scattered-data Approximation", Eurographics; Proceedings, pp. 131–138, (2001).
14. Claes, J., "New approaches in the modeling of subdivision surfaces" Ph.D thesis, University of Limburg, (2001).
15. Stam, J. and Loop, C. "Quad/Triangle Subdivision", Microsoft Research, Volume xx (200y), Number z, pp. 1–5, (2002).
16. Gross, N. "Applications of Subdivision Techniques in Product Development", Ph.D thesis, Technical University Bonn, (German), (2004).
17. Barthe, L., and Kobbelt, L. "Subdivision Scheme Tuning Around Extraordinary Vertices", Computer Graphics Group, Rwth Aachen Ahornstrasse 55, 52074 Aachen, Germany, (2004).
18. Yvonnet, J. "New Approaches without grid bases on the method of the natural elements for the digital simulation working." Ph.D thesis, Ecole Nationale (French), (2004).
19. Hakenberg, J. P. "Smooth Subdivision for Mixed Volumetric Meshes", M.Sc thesis, Rice University, (2004).
20. Seeger, S., Hormann, K., Hausler, G., and Greiner, G. "A Sub-Atomic Subdivision Approach", Euro graphics Symposium on Geometry Processing (2005).
21. Schaefer, S., Levin, D., and Goldman, R. "Subdivision Schemes and Attractors", Eurographics Symposium on Geometry Processing, (2005).
22. Lounsbery, J. M. "Multiresolution Analysis for Surfaces of Arbitrary Topological Type", Ph.D thesis, Washington University, (1994).
23. Stephen Manna "Surface approximation using geometric patches", Ph.D thesis, Washington University, (1992).

24. Marco Paluszny, Wolfgang Boehm, and Hartmut Prautzsch "Bezier and B-spline techniques", Karlsruhe University, (2002).
25. Qiulin, D., and Davies, B. J. "Surface Engineering Geometry for Computer-Aided Design and Manufacture" British Library Cataloguing, (1989).
26. Rogers, D. F. "Mathematical Elements for Computer Graphics" Singapore, Mc.Graw-Hill, (1990).
27. Fisher, H. "Summary of Bezier curve properties ",
<http://escience.anu.edu.au/lecture/cg/Spline/printCG.en.html> , (2004)
28. Wang, S. L. "Introduction Fundamentals of Computer Graphics Using Matlab" North Carolina A and T State University, Greensboro, NC 27411, (1996).
29. Musra, H. K. "Development of the Free Form Surface Construction Approach by Using Computer" M.Sc Thesis, University of Technology, (2002).
30. Joy, K. I. "Cubic Uniform B-spline Curve Refinement", Visualization and Graphics Research Group, University of California, Davis, (2000).
31. Bartels, R.H., and Samavite, F.F. "Reversing Subdivision Rules", Computer Science Department, University of Waterloo (2001).
32. Joy, K. I. "Quadratic Uniform B-spline Curve Refinement", Visualization and Graphics Research Group, University of California, Davis, (2000).
33. Joy, K. I. "A Matrix Formulation of the Cubic Bezier Curve", Visualization and Graphics Research Group, University of California, Davis, (2000).
34. Joy, K. I. "Cubic Bezier Curves", Visualization and Graphics Research Group, University of California, Davis, (2000).
35. Zeiler, J. D. "Subdivision Surfaces" Computer Graphics CS 446, (2000).

36. Joy, K. I. "Bi-Quadratic Uniform B-spline Surface Refinement" Visualization and Graphics Research Group, University of California, Davis, (2000).
37. Joy, K. I. "A Matrix Representation of a Cubic Bezier Patch", Visualization and Graphics Research Group, University of California, Davis, (2000).
38. Loop, C. T. "Smooth Subdivision Surfaces Based on Triangles", M.Sc thesis, Utah University, (1990).
39. Kadhim, A.J. "Assessment of Die design and Manufacturing preparation for the Extrusion of elliptical sections from round billets", Ph.D thesis, University of Technology, (2004).
40. Gray, A. "The Gaussian and Mean Curvatures." Boca Raton, FL: CRC Press, pp. 373-380, (1997).
41. Meyer, C.D. "Matrix Analysis and Applied Linear Algebra", published by SIAM organization, (2001).
42. Hakenberg, J. P., www.hakenberg.de, Rice University, (2007).
43. Omirou, S. L., and Nearc, A.C. "A CNC machine tool interpolator for surfaces of cross-sectional design", Robotics and Computer-Integrated Manufacturing 23- 257–264, (2007).
44. Fontaine, M., Moufki, A.; Devillez, A.; and Dudzinski, D., " Modeling of cutting forces in ball-end milling with tool–surface inclination", Journal of Materials Processing Technology 189- 73–84,(2007).
45. Hamdan, W.K. "Three axes Interpolation and Emulation for Computerized Numerically Controlled Milling Machines", M.Sc thesis, University of Technology, (2001).
46. Wang, J. "Global Finish Curvature Matched Machining" M.Sc thesis, University of Brigham Young, (2005).

-
- 47.**Kim, T. "Time-optimal tool paths-A mathematical model of machining" Ph.D thesis, University of Massachusetts [institute of Technology] (2001).
- 48.**Choi, Y. K. "Tool Path Generation and 3D Tolerance Analysis for Free-Form Surfaces" Ph.D thesis, University of Texas A and M, (2004).

APPENDICES



Appendix A

Derivative of the Uniform B-Spline Basis Functions with $k=5$:

The uniform B-spline basis function is determined by the general equation (A.1):

$$N_{i,1}(u) = \begin{cases} 1 & \text{if } t_i \leq u \leq t_{i+1} \\ 0 & \text{otherwise} \end{cases} \dots\dots\dots (A.1)$$

And other equation:

$$N_{i,k}(u) = \frac{(u-t_i)N_{i,k-1}(u)}{t_{i+k-1}-t_i} + \frac{(t_{i+k}-u)N_{i+1,k-1}(u)}{t_{i+k}-t_{i+1}} \dots\dots\dots (A.2)$$

while k: is equation order (degree=k-1), t_i =knot vector and symbolized by (T).

In the beginning calculate the functions when (k=5) which is represented in $(N_{i,5}, N_{i+1,5}, N_{i+2,5})$, and select the range for the (i) value from the relation $(k \leq i \leq n)$, and calculate the knot (t_i) from the relation $t_i = i - (k - 1)$, then calculate (t_i) when (k=5):

$$t_i = i - (5 - 1) = i - 4$$

By using the equations (A.1) and (A.2) it's easy to calculate the knot vector (T):

$$T = \{i - 4, i - 3, i - 2, i - 1, i, i + 1, i + 2, i + 3, i + 4, i + 5, i + 6\}$$

And calculate the values from (t_i) to (t_{i+10}):

$$t_i = i - 4; t_{i+1} = i - 3; t_{i+2} = i - 2; t_{i+3} = i - 1; t_{i+4} = i; t_{i+5} = i + 1; t_{i+6} = i + 2; t_{i+7} = i + 3; t_{i+8} = i + 4; t_{i+9} = i + 5; t_{i+10} = i + 6.$$

When $k = 1$:

$$\begin{aligned}
 N_{i,1}(u) &= 1 && \text{for } i-4 \leq u < i-3 \\
 &= 0 && \text{otherwise} \\
 N_{i+1,1}(u) &= 1 && \text{for } i-3 \leq u < i-2 \\
 &= 0 && \text{otherwise} \\
 N_{i+2,1}(u) &= 1 && \text{for } i-2 \leq u < i-1 \\
 &= 0 && \text{otherwise} \\
 N_{i+3,1}(u) &= 1 && \text{for } i-1 \leq u < i \\
 &= 0 && \text{otherwise} \\
 N_{i+4,1}(u) &= 1 && \text{for } i \leq u < i+1 \\
 &= 0 && \text{otherwise} \\
 N_{i+5,1}(u) &= 1 && \text{for } i+1 \leq u < i+2 \\
 &= 0 && \text{otherwise} \\
 N_{i+6,1}(u) &= 1 && \text{for } i+2 \leq u < i+3 \\
 &= 0 && \text{otherwise} \\
 N_{i+7,1}(u) &= 1 && \text{for } i+3 \leq u < i+4 \\
 &= 0 && \text{otherwise} \\
 N_{i+8,1}(u) &= 1 && \text{for } i+4 \leq u < i+5 \\
 &= 0 && \text{otherwise} \\
 N_{i+9,1}(u) &= 1 && \text{for } i+5 \leq u < i+6 \\
 &= 0 && \text{otherwise}
 \end{aligned}
 \tag{A.3}$$

Then calculate the equations when $k = 2$:

$$\begin{aligned}
 N_{i,2}(u) &= (u-i+4)N_{i,1} + (i-2-u)N_{i+1,1}(u) \\
 N_{i+1,2}(u) &= (u-i+3)N_{i+1,1} + (i-1-u)N_{i+2,1}(u) \\
 N_{i+2,2}(u) &= (u-i+2)N_{i+2,1} + (i-u)N_{i+3,1}(u) \\
 N_{i+3,2}(u) &= (u-i+1)N_{i+3,1} + (i+1-u)N_{i+4,1}(u) \\
 N_{i+4,2}(u) &= (u-i)N_{i+4,1} + (i+2-u)N_{i+5,1}(u) \\
 N_{i+5,2}(u) &= (u-i-1)N_{i+5,1} + (i+3-u)N_{i+6,1}(u)
 \end{aligned}
 \tag{A.4}$$

When $k = 3$:

$$N_{i,3}(u) = \frac{(u-i+4)[(u-i+4)N_{i,1}(u) + (i-2-u)N_{i+1,1}(u)]}{(i-2)-(i-4)} + \frac{(i-1-u)[(u-i+3)N_{i+1,1}(u) + (i-1-u)N_{i+2,1}(u)]}{(i-1)-(i-3)}$$

$$\therefore N_{i,3}(u) = \frac{1}{2}[(u-i+4)^2 N_{i,1}(u) + (u-i+4)(i-2-u) N_{i+1,1}(u) + (i-1-u)(u-i+3)N_{i+1,1}(u) + (i-1-u)^2 N_{i+2,1}(u)].$$

$$N_{i+1,3}(u) = \frac{1}{2}[(u-i+3)^2 N_{i+1,1}(u) + (u-i+3)(i-1-u) N_{i+2,1}(u) + (i-u)(u-i+2)N_{i+2,1}(u) + (i-u)^2 N_{i+3,1}(u)].$$

$$N_{i+2,3}(u) = \frac{1}{2}[(u-i+2)^2 N_{i+2,1}(u) + (u-i+2)(i-u) N_{i+3,1}(u) + (i+1-u)(u-i+1)N_{i+3,1}(u) + (i+1-u)^2 N_{i+4,1}(u)].$$

$$N_{i+3,3}(u) = \frac{1}{2}[(u-i+1)^2 N_{i+3,1}(u) + (u-i+1)(i+1-u) N_{i+4,1}(u) + (i+2-u)(u-i)N_{i+4,1}(u) + (i+2-u)^2 N_{i+5,1}(u)].$$

$$N_{i+4,3}(u) = \frac{1}{2}[(u-i)^2 N_{i+4,1}(u) + (u-i)(i+2-u) N_{i+5,1}(u) + (i+3-u)(u-i-1)N_{i+5,1}(u) + (i+3-u)^2 N_{i+6,1}(u)].$$

... (A.5)

if $k=4$

$$N_{i,4} = \frac{(u-i+4)}{3} * \frac{1}{2} * [(u-i+4)^2 N_{i,1}(u) + (u-i+4)(i-2-u) N_{i+1,1}(u) + (i-1-u)(u-i+3) N_{i+1,1}(u) + (i-1-u)^2 N_{i+2,1}(u)] + \frac{(i-u)}{3} * \frac{1}{2} * [(u-i+3)^2 N_{i+1,1}(u) + (u-i+3)(i-1-u) N_{i+2,1}(u) + (i-u)(u-i+2) N_{i+2,1}(u) + (i-u)^2 N_{i+3,1}(u)].$$

$$\therefore N_{i,4} = \frac{1}{6} [(u-i+4)^3 N_{i,1}(u) + (u-i+4)^2 (i-2-u) N_{i+1,1}(u) + (u-i+4)(i-1-u)(u-i+3) N_{i+1,1}(u) + (u-i+4)(i-1-u)^2 N_{i+2,1}(u) + (i-u)(u-i+3)^2 N_{i+1,1}(u) + (i-u)(u-i+3)(i-1-u) N_{i+2,1}(u) + (i-u)^2 (u-i+2) N_{i+2,1}(u) + (i-u)^3 N_{i+3,1}(u)].$$

$$N_{i+1,4} = \frac{(u-i+3)}{3} * \frac{1}{2} * [(u-i+3)^2 N_{i+1,1}(u) + (u-i+3)(i-1-u) N_{i+2,1}(u) + (i-u)(u-i+2) N_{i+2,1}(u) + (i-u)^2 N_{i+3,1}(u)] + \frac{(i+1-u)}{3} * \frac{1}{2} * [(u-i+2)^2 N_{i+2,1}(u) + (u-i+2)(i-u) N_{i+3,1}(u) + (i+1-u)(u-i+1) N_{i+3,1}(u) + (i+1-u)^2 N_{i+4,1}(u)].$$

$$\therefore N_{i+1,4} = \frac{1}{6} [(u-i+3)^3 N_{i+1,1}(u) + (u-i+3)^2 (i-1-u) N_{i+2,1}(u) + (u-i+3)(i-u)(u-i+2) N_{i+2,1}(u) + (u-i+3)(i-u)^2 N_{i+3,1}(u) + (i+1-u)(u-i+2)^2 N_{i+2,1}(u) + (i+1-u)(u-i+2)(i-u) N_{i+3,1}(u) + (i+1-u)^2 (u-i+1) N_{i+3,1}(u) + (i+1-u)^3 N_{i+4,1}(u)].$$

(A.6)

$$\begin{aligned}
 N_{i+2,4} &= \frac{1}{6}[(u-i+2)^3 N_{i+2,1}(u) + (u-i+2)^2(i-u)N_{i+3,1}(u) + \\
 &\quad (u-i+2)(i+1-u)(u-i+1)N_{i+3,1}(u) + (u-i+2)(i+1-u)^2 \\
 &\quad N_{i+4,1}(u) + (i+2-u)(u-i+1)^2 N_{i+3,1}(u) + (i+2-u)(u-i+1) \\
 &\quad (i+1-u)N_{i+4,1}(u) + (i+2-u)^2(u-i)N_{i+4,1}(u) + \\
 &\quad (i+2-u)^3 N_{i+5,1}(u)].
 \end{aligned}
 \tag{A.6}$$

$$\begin{aligned}
 N_{i+3,4} &= \frac{1}{6}[(u-i+1)^3 N_{i+3,1}(u) + (u-i+1)^2(i+1-u)N_{i+4,1}(u) + \\
 &\quad (u-i+1)(i+2-u)(u-i)N_{i+4,1}(u) + (u-i+1)(i+2-u)^2 \\
 &\quad N_{i+5,1}(u) + (i+3-u)(u-i)^2 N_{i+4,1}(u) + (i+3-u)(u-i) \\
 &\quad (i+2-u)N_{i+5,1}(u) + (i+3-u)^2(u-i-1)N_{i+5,1}(u) + \\
 &\quad (i+3-u)^3 N_{i+6,1}(u)].
 \end{aligned}$$

When $k=5$:

$$\begin{aligned}
 N_{i,5} &= \frac{1}{24}[(u-i+4)^4 N_{i,1}(u) + (u-i+4)^3(i-2-u)N_{i+1,1}(u) + \\
 &\quad (u-i+4)^2(i-1-u)(u-i+3)N_{i+1,1}(u) + (u-i+4)^2(i-1-u)^2 \\
 &\quad N_{i+2,1}(u) + (u-i+4)(i-u)(u-i+3)^2 N_{i+1,1}(u) + (u-i+4) \\
 &\quad (i-u)(u-i+3)(i-1-u)N_{i+2,1}(u) + (u-i+4)(i-u)^2(u-i+2) \\
 &\quad N_{i+2,1}(u) + (u-i+4)(i-u)^3 N_{i+3,1}(u) + (i+1-u)(u-i+3)^3 \\
 &\quad N_{i+1,1}(u) + (i+1-u)(u-i+3)^2(i-1-u)N_{i+2,1}(u) + (i+1-u) \\
 &\quad (u-i+3)(i-u)(u-i+2)N_{i+2,1}(u) + (i+1-u)(u-i+3)(i-u)^2 \\
 &\quad N_{i+3,1}(u) + (i+1-u)^2(u-i+2)^2 N_{i+2,1}(u) + (i+1-u)^2 \\
 &\quad (u-i+2)(i-u)N_{i+3,1}(u) + (i+1-u)^3(u-i+1)N_{i+3,1}(u) + \\
 &\quad (i+1-u)^4 N_{i+4,1}(u)].
 \end{aligned}
 \tag{A.7}$$

$$\begin{aligned}
 N_{i+1,5} &= \frac{1}{24} [(u-i+3)^4 N_{i+1,1}(u) + (u-i+3)^3 (i-1-u) \\
 &\quad N_{i+2,1}(u) + (u-i+3)^2 (i-u)(u-i+2) N_{i+2,1}(u) + \\
 &\quad (u-i+3)^2 (i-u)^2 N_{i+3,1}(u) + (u-i+3)(i+1-u) \\
 &\quad (u-i+2)^2 N_{i+2,1}(u) + (u-i+3)(i+1-u)(u-i+2)(i-u) \\
 &\quad N_{i+3,1}(u) + (u-i+3)(i+1-u)^2 (u-i+1) N_{i+3,1}(u) + \\
 &\quad (u-i+3)(i+1-u)^3 N_{i+4,1}(u) + (i+2-u)(u-i+2)^3 \\
 &\quad N_{i+2,1}(u) + (i+2-u)(u-i+2)^2 (i-u) N_{i+3,1}(u) + \\
 &\quad (i+2-u)(u-i+2)(i+1-u)(u-i+1) N_{i+3,1}(u) + \\
 &\quad (i+2-u)^2 (u-i+2)(i+1-u)^2 N_{i+4,1}(u) + (i+2-u)^2 \\
 &\quad (u-i+1)^2 N_{i+3,1}(u) + (i+2-u)^2 (u-i+1)(i+1-u) \\
 &\quad N_{i+4,1}(u) + (i+2-u)^3 (u-i) N_{i+4,1}(u) + \\
 &\quad (i+2-u)^4 N_{i+5,1}(u)]. \tag{A.7}
 \end{aligned}$$

$$\begin{aligned}
 N_{i+2,5} &= \frac{1}{24} [(u-i+2)^4 N_{i+2,1}(u) + (u-i+2)^3 (i-u) N_{i+3,1}(u) + \\
 &\quad (u-i+2)^2 (i+1-u)(u-i+1) N_{i+3,1}(u) + (u-i+2)^2 \\
 &\quad (i+1-u)^2 N_{i+4,1}(u) + (u-i+2)(i+2-u)(u-i+1)^2 \\
 &\quad N_{i+3,1}(u) + (u-i+2)(i+2-u)(u-i+1)(i+1-u) N_{i+4,1}(u) + \\
 &\quad (u-i+2)(i+2-u)^2 (u-i+2) N_{i+4,1}(u) + (u-i+2)(i+2-u)^3 \\
 &\quad N_{i+5,1}(u) + (i+3-u)(u-i+1)^3 N_{i+3,1}(u) + (i+3-u) \\
 &\quad (u-i+1)^2 (i+1-u) N_{i+4,1}(u) + (i+3-u)(u-i+1)(i+2-u) \\
 &\quad (u-i) N_{i+4,1}(u) + (i+3-u)(u-i+1)(i+2-u)^2 N_{i+4,1}(u) + \\
 &\quad (i+3-u)^2 (u-i+2)^2 N_{i+4,1}(u) + (i+3-u)^2 (u-i+2)(i+2-u) \\
 &\quad N_{i+5,1}(u) + (i+3-u)^3 (u-i-1) N_{i+5,1}(u) + \\
 &\quad (i+3-u)^4 N_{i+6,1}(u)].
 \end{aligned}$$

From the equation above it's easy to calculate $(p(u))$ for any piece of the curve with the enclosed period $(i \leq u < i+1)$ depending on the function $N_{i,1}(u) = 1$, and from notified the equations above, we note that the function $(N_{i+4,1} = 1)$ just in this period, and making summation of this functions in one equation will yield $(p(u))$:

$$\begin{aligned}
 p(u) = & \frac{1}{24}(i+1-u)^4 p_i + \frac{1}{24}[(u-i+3)(i+1-u)^3 p_{i+1} + \\
 & (i+2-u)(u-i+2)(i+1-u)^2 p_{i+1} + (i+2-u)^2(u-i+1) \\
 & (i+1-u)p_{i+1} + (i+2-u)^3 u-i)p_{i+1}] + \frac{1}{24}[(u-i+2)^2 \\
 & (i+1-u)^2 p_{i+2} + (u-i+2)(i+2-u)(u-i+1)(i+1-u)p_{i+2} + \\
 & (u-i+2)(i+2-u)^2(u-i+2)p_{i+2} + (i+3-u)(u-i+1)^2 \\
 & (i+1-u)p_{i+2} + (i+3-u)(u-i+1)(i+2-u)(u-i)p_{i+2} + \\
 & (i+3-u)(u-i+1)(i+2-u)^2 p_{i+2} + (i+3-u)^2 \\
 & (u-i+2)^2 p_{i+2}].
 \end{aligned} \tag{A.8}$$

and it could be written in another form :

$$\begin{aligned}
 p_i(u) = & \frac{1}{24}[((1-2u+u^2)(1-2u+u^2))p_i + ((u+3)(1-u) \\
 & (1-2u+u^2) + (2-u)(u+2)(1-2u+u^2) + (4-4u+u^2) \\
 & (u+1)(1-u) + (2-u)(4-4u+u^2)u)p_{i+1} + ((u^2+4u+4) \\
 & (1-2u+u^2) + (u+2)(2-u)(u+1)(1-u) + (u+2) \\
 & (4-4u+u^2)(u+2) + (3-u)(u^2+2u+1)(1-u) + (3-u) \\
 & (u+1)(2-u)u + (3-u)(u+1)(4-4u+u^2) + (9-6u+u^2) \\
 & (u^2-4u+4)p_{i+2}].
 \end{aligned} \tag{A.9}$$

where $(0 \leq u \leq 1)$, $p_i(u)$ is the function for the curve $[p_i, p_{i+1}, p_{i+2}]$: is the control points.

$$p_i(u) = \frac{1}{24}[(u^4 - 4u^3 + 6u^2 - 4u + 1)p_i + (-4u^4 + 12u^3 - 6u^2 - 12u + 1)p_{i+1} + (5u^4 - 8u^3 + 9u^2 - 60u + 75)p_{i+2}]. \quad \dots\dots\dots (A.10)$$

From equation(A.10)theMatrix form(M)is the result.

$$M = \frac{1}{24} \begin{vmatrix} 1 & -4 & 5 & 0 & 0 \\ -4 & 12 & -8 & 0 & 0 \\ 6 & -6 & 9 & 0 & 0 \\ -4 & -12 & -60 & 1 & 0 \\ 1 & 1 & 75 & 0 & 1 \end{vmatrix} \quad \dots\dots\dots (A.11)$$

$$P_i(u) = \frac{1}{24} [u^4 \quad u^3 \quad u^2 \quad u \quad 1] \begin{bmatrix} 1 & -4 & 5 & 0 & 0 \\ -4 & 12 & -8 & 0 & 0 \\ 6 & -6 & 9 & 0 & 0 \\ -4 & -12 & -60 & 1 & 0 \\ 1 & 1 & 75 & 0 & 1 \end{bmatrix} \begin{bmatrix} p_{i-1} \\ p_i \\ p_{i+1} \\ p_{i+2} \\ p_{i+3} \end{bmatrix} \quad \dots\dots (A.12)$$

Appendix B

Subdividing the cubic B-spline surface

$$p'_{0,0} = \frac{p_{0,0} + p_{1,0} + p_{0,1} + p_{1,1}}{4}$$

$$p'_{0,1} = \frac{p_{0,0} + p_{1,0} + 6(p_{0,1} + p_{1,1}) + p_{0,2} + p_{1,2}}{16}$$

$$p'_{0,2} = \frac{p_{0,1} + p_{1,1} + p_{0,2} + p_{1,2}}{4}$$

$$p'_{0,3} = \frac{p_{0,1} + p_{1,1} + 6(p_{0,2} + p_{1,2}) + p_{0,3} + p_{1,3}}{16}$$

$$p'_{1,0} = \frac{p_{0,0} + p_{0,1} + 6(p_{1,0} + p_{1,1}) + p_{2,0} + p_{2,1}}{16}$$

$$p'_{1,1} = \frac{p_{0,0} + 6p_{1,0} + p_{2,0} + 6(p_{0,1} + 6p_{1,1} + p_{2,1}) + p_{0,2} + 6p_{1,2} + p_{2,2}}{64}$$

$$p'_{1,2} = \frac{p_{0,1} + p_{0,2} + 6(p_{1,1} + p_{1,2}) + p_{2,1} + p_{2,2}}{16}$$

$$p'_{1,3} = \frac{p_{0,1} + 6p_{1,1} + p_{2,1} + 6(p_{0,2} + 6p_{1,2} + p_{2,2}) + p_{0,3} + 6p_{1,3} + p_{2,3}}{64}$$

$$p'_{2,0} = \frac{p_{1,0} + p_{2,0} + p_{1,1} + p_{2,1}}{4}$$

$$p'_{2,1} = \frac{p_{1,0} + p_{2,0} + 6(p_{1,1} + p_{2,1}) + p_{1,2} + p_{2,2}}{16}$$

$$p'_{2,2} = \frac{p_{1,1} + p_{2,1} + p_{1,2} + p_{2,2}}{4}$$

$$p'_{2,3} = \frac{p_{1,1} + p_{2,1} + 6(p_{1,2} + p_{2,2}) + p_{1,3} + p_{2,3}}{16}$$

$$p'_{3,0} = \frac{p_{1,0} + p_{1,1} + 6(p_{2,0} + p_{2,1}) + p_{3,0} + p_{3,1}}{16}$$

$$p'_{3,1} = \frac{p_{1,0} + 6p_{2,0} + p_{3,0} + 6(p_{1,1} + 6p_{2,1} + p_{3,1}) + p_{1,2} + 6p_{2,2} + p_{3,2}}{64}$$

$$p'_{3,2} = \frac{p_{1,1} + p_{1,2} + 6(p_{2,1} + p_{2,2}) + p_{3,1} + p_{3,2}}{16}$$

$$p'_{3,3} = \frac{p_{1,1} + 6p_{2,1} + p_{3,1} + 6(p_{1,2} + 6p_{2,2} + p_{3,2}) + p_{1,3} + 6p_{2,3} + p_{3,3}}{64}$$

Each of these points can be classified into three categories-face point, edge point and vertex point –depending on each point relationship to the original control point mesh. The points $p'_{0,0}$, $p'_{0,2}$, $p'_{2,0}$ and $p'_{2,2}$, which are shown in the Figure (4.14).

Rewrite the equation with these face point substituted on the right –hand side, and obtain

$$p'_{0,0} = F_{0,0}$$

$$p'_{0,1} = \frac{4F_{0,0} + 4F_{0,1} + 4p_{0,1} + 4p_{1,1}}{16}$$

$$p'_{0,2} = F_{0,1}$$

$$p'_{0,3} = \frac{4F_{0,1} + 4F_{0,2} + 4p_{0,2} + 4p_{1,2}}{16}$$

$$p'_{1,0} = \frac{4F_{0,0} + 4F_{1,0} + 4p_{1,0} + 4p_{1,1}}{16}$$

$$p'_{1,1} = \frac{4F_{0,0} + 4F_{0,1} + 4F_{1,0} + 4F_{1,1} + 4p_{1,0} + 4p_{0,1} + 32p_{1,1} + 4p_{2,1} + 4p_{1,2}}{64}$$

$$p'_{1,2} = \frac{4F_{0,1} + 4F_{1,1} + 4p_{1,1} + 4p_{1,2}}{16}$$

$$p'_{1,3} = \frac{4F_{0,1} + 4F_{0,2} + 4F_{1,1} + 4F_{1,2} + 4p_{1,1} + 4p_{0,2} + 32p_{1,2} + 4p_{2,2} + 4p_{1,3}}{64}$$

$$p'_{2,0} = F_{1,0}$$

$$p'_{2,1} = \frac{4F_{1,0} + 4F_{1,1} + 4p_{1,1} + 4p_{2,1}}{16}$$

$$p'_{2,2} = F_{1,1}$$

$$p'_{2,3} = \frac{4F_{1,1} + 4F_{1,2} + 4p_{1,2} + 4p_{2,2}}{16}$$

$$p'_{3,0} = \frac{4F_{1,0} + 4F_{2,0} + 4p_{2,0} + 4p_{2,1}}{16}$$

$$p'_{3,1} = \frac{4F_{1,0} + 4F_{2,0} + 4F_{1,1} + 4F_{2,1} + 4p_{2,0} + 4p_{1,1} + 32p_{2,1} + 4p_{3,1} + 4p_{2,2}}{64}$$

$$p'_{3,2} = \frac{4F_{1,1} + 4F_{2,1} + 4p_{2,1} + 4p_{2,2}}{16}$$

$$p'_{3,3} = \frac{4F_{1,1} + 4F_{2,1} + 4F_{1,2} + 4F_{2,2} + 4p_{2,1} + 4p_{1,2} + 32p_{2,2} + 4p_{3,2} + 4p_{2,3}}{64}$$

Simplifying these equations we obtain

$$p'_{0,0} = F'_{0,0}$$

$$p'_{0,1} = \frac{F_{0,0} + F_{0,1} + p_{0,1} + p_{1,1}}{4}$$

$$p'_{0,2} = F_{0,1}$$

$$p'_{0,3} = \frac{F_{0,1} + F_{0,2} + p_{0,2} + p_{1,2}}{4}$$

$$p'_{1,0} = \frac{F_{0,0} + F_{1,0} + p_{1,0} + p_{1,1}}{4}$$

$$p'_{1,1} = \frac{F_{0,0} + F_{0,1} + F_{1,0} + F_{1,1} + p_{1,0} + p_{0,1} + 8p_{1,1} + p_{2,1} + p_{1,2}}{16}$$

$$p'_{1,2} = \frac{F_{0,1} + F_{1,1} + p_{1,1} + p_{1,2}}{4}$$

$$p'_{1,3} = \frac{F_{0,1} + F_{0,2} + F_{1,1} + F_{1,2} + p_{1,1} + p_{0,2} + 8p_{1,2} + p_{2,2} + p_{1,3}}{16}$$

$$p'_{2,0} = F_{1,0}$$

$$p'_{2,1} = \frac{F_{1,0} + F_{1,1} + p_{1,1} + p_{2,1}}{4}$$

$$p'_{2,2} = F_{1,1}$$

$$p'_{2,3} = \frac{F_{1,1} + F_{1,2} + p_{1,2} + p_{2,2}}{4}$$

$$p'_{3,0} = \frac{F_{1,0} + F_{2,0} + p_{2,0} + p_{2,1}}{4}$$

$$p'_{3,1} = \frac{F_{1,0} + F_{2,0} + F_{1,1} + F_{2,1} + p_{2,0} + p_{1,1} + 8p_{2,1} + p_{3,1} + p_{2,2}}{16}$$

$$p'_{3,2} = \frac{F_{1,1} + F_{2,1} + p_{2,1} + p_{2,2}}{4}$$

$$p'_{3,3} = \frac{F_{1,1} + F_{2,1} + F_{1,2} + F_{2,2} + p_{2,1} + p_{1,2} + 8p_{2,2} + p_{3,2} + p_{2,3}}{16}$$

In examining these equation ,we see that the points $p'_{0,1}, p'_{0,3}, p'_{1,0}, p'_{1,2}, p'_{2,3}, p'_{3,0}$ and $p'_{3,2}$, which are called "edge" points , are given as the average of four point –the two point that define the original edge and the two new face point of the face sharing the edge . This is shown in the following figure

Side of the equation above, we obtain

$$p'_{0,0} = F_{0,0}$$

$$p'_{0,1} = E_{0,1}$$

$$p'_{0,2} = F_{0,1}$$

$$p'_{0,3} = E_{0,2}$$

$$p'_{1,0} = E_{1,0}$$

$$p'_{1,1} = \frac{F_{0,0} + F_{0,1} + F_{1,0} + F_{1,1} + p_{1,0} + p_{0,1} + 8p_{1,1} + p_{2,1} + p_{1,2}}{16}$$

$$p'_{1,2} = E_{1,2}$$

$$p'_{1,3} = \frac{F_{0,1} + F_{0,2} + F_{1,1} + F_{1,2} + p_{1,1} + p_{0,2} + 8p_{1,2} + p_{2,2} + p_{1,3}}{16}$$

$$p'_{2,0} = F_{1,0}$$

$$p'_{2,1} = E_{2,1}$$

$$p'_{2,2} = F_{1,1}$$

$$p'_{2,3} = E_{2,2}$$

$$p'_{3,0} = E_{3,0}$$

$$p'_{3,1} = \frac{F_{1,0} + F_{2,0} + F_{1,1} + F_{2,1} + p_{2,0} + p_{1,1} + 8p_{2,1} + p_{3,1} + p_{2,2}}{16}$$

$$p'_{3,2} = E_{3,2}$$

$$p'_{3,3} = \frac{F_{1,1} + F_{2,1} + F_{1,2} + F_{2,2} + p_{2,1} + p_{1,2} + 8p_{2,2} + p_{3,2} + p_{2,3}}{16}$$

The remaining four points, $p'_{1,1}$, $p'_{1,3}$, $p'_{3,1}$ and $p'_{3,3}$, as shown in the figure below

Appendix E

Part program of the adopted technique

CRHS method:

N1 G17 G40 G80 G90
 N2 T7 M6
 N3 M3 S14000
 N4 G00 G54 X90. Y-10.
 N5 G43 Z67. H7
 N6 M8
 N7 G00 Z43.Z7206
 N8 G01 Z41.2206 F382.0
 N9 X90.0207 Y4.8906 F10000.0
 N10 X89.9527 Y6.5312
 N11 X90.0409 Y8.1406
 N12 X90.2206 Y9.7031
 N13 X88.964 Y10.7031
 N14 X86.013 Y12.1562
 N15 X84.6696 Y13.0469
 N16 X83.4401 Y14.1094
 N17 X82.2581 Y15.2188
 N18 X81.1381 Y16.4062
 N19 X80.135 Y17.7031
 N20 X79.2527 Y19.0625
 N21 X78.4669 Y20.5
 N22 X77.7944 Y21.9844
 N23 X77.2257 Y23.5
 N24 X76.7391 Y25.0625
 N25 X76.332 Y26.6406
 N26 X75.9919 Y28.2344
 N27 X75.4697 Y31.4531
 N28 X75.1037 Y34.6875
 N29 X74.9901 Y36.3125
 N30 X75.0003 Y42.8438
 N31 X74.8862
 N32 X74.876 Y36.3125
 N33 X74.9891 Y34.6875
 N34 X75.3537 Y31.4531
 N35 X75.874 Y28.2344
 N36 X76.2127 Y26.6406
 N37 X76.6183 Y25.0625
 N38 X77.103 Y23.5
 N39 X77.6696 Y21.9844
 N40 X78.3396 Y20.5
 N41 X79.1224 Y19.0625
 N42 X80.0013 Y17.7031
 N43 X81.0006 Y16.4062
 N44 X82.1164 Y15.2188
 N45 X83.2938 Y14.1094
 N46 X84.5186 Y13.0469
 N47 X85.857 Y12.1562
 N48 X88.7967 Y10.7031
 N49 X90.0485 Y9.7031
 N50 X89.8695 Y8.1406
 N51 X89.7816 Y6.5312
 N52 X89.8493 Y4.8906
 N53 X89.8288 Y0
 N54 X89.3163
 N55 X89.3367 Y4.8906
 N56 X89.2697 Y6.5312
 N57 X89.3566 Y8.1406
 N58 X89.5336 Y9.7031
 N59 X88.2961 Y10.7031
 N60 X85.39 Y12.1562
 N61 X84.0669 Y13.0469
 N62 X82.8561 Y14.1094
 N63 X81.6921 Y15.2188
 N64 X80.5891 Y16.4062
 N65 X79.6012 Y17.7031
 N66 X78.7323 Y19.0625
 N67 X77.9585 Y20.5
 N68 X77.2962 Y21.9844
 N69 X76.7361 Y23.5
 N70 X76.2569 Y25.0625
 N71 X75.856 Y26.6406
 N72 X75.5211 Y28.2344

 N4785 X19.6129 Y28.2344 Z13.7762
 N4786 X19.3344 Y26.6406 Z13.9713
 N4787 X19.0008 Y25.0625 Z14.2048
 N4788 X18.6023 Y23.5 Z14.4839
 N4789 X18.1364 Y21.9844 Z14.8101
 N4790 X17.5855 Y20.5 Z15.1958
 N4791 X16.9418 Y19.0625 Z15.6465
 N4792 X16.2191 Y17.7031 Z16.1526
 N4793 X15.3974 Y16.4062 Z16.728
 N4794 X14.4799 Y15.2188 Z17.3704
 N4795 X13.5117 Y14.1094 Z18.0483
 N4796 X12.5046 Y13.0469 Z18.7535
 N4797 X11.4041 Y12.1562 Z19.5241
 N4798 X8.9868 Y10.7031 Z21.2167
 N4799 X7.9574 Y9.7031 Z21.9375
 N4800 X8.1047 Y8.1406 Z21.8344
 N4801 X8.1769 Y6.5312 Z21.7838
 N4802 X8.1212 Y4.8906 Z21.8228
 N4803 X8.1382 Y0 Z21.8109
 N4804 X6.0289 Z18.5
 N4805 X6.011 Y4.8906 Z18.5103
 N4806 X6.0698 Y6.5312 Z18.4763
 N4807 X5.9934 Y8.1406 Z18.5204
 N4808 X5.8378 Y9.7031 Z18.6103
 N4809 X6.926 Y10.7031 Z17.982
 N4810 X9.4817 Y12.1562 Z16.5065
 N4811 X10.6451 Y13.0469 Z15.8348
 N4812 X11.7099 Y14.1094 Z15.22
 N4813 X12.7335 Y15.2188 Z14.6291
 N4814 X13.7034 Y16.4062 Z14.0691
 N4815 X14.5722 Y17.7031 Z13.5675
 N4816 X15.3363 Y19.0625 Z13.1264
 N4817 X16.0168 Y20.5 Z12.7335
 N4818 X16.5992 Y21.9844 Z12.3972
 N4819 X17.0918 Y23.5 Z12.1128
 N4820 X17.5131 Y25.0625 Z11.8696
 N4821 X17.8657 Y26.6406 Z11.666
 N4822 X18.1602 Y28.2344 Z11.496
 N4823 X18.6125 Y31.4531 Z11.2348
 N4824 X18.9294 Y34.6875 Z11.0518
 N4825 X19.0278 Y36.3125 Z10.9951
 N4826 X19.0189 Y42.8438 Z11.0002
 N4827 X17.8105 Z8.6787
 N4828 X17.8197 Y36.3125 Z8.6744
 N4829 X17.7168 Y34.6875 Z8.7224
 N4830 X17.3851 Y31.4531 Z8.877
 N4831 X16.9118 Y28.2344 Z9.0978
 N4832 X16.6036 Y26.6406 Z9.2415
 N4833 X16.2346 Y25.0625 Z9.4135
 N4834 X15.7936 Y23.5 Z9.6192
 N4835 X15.2782 Y21.9844 Z9.8595
 N4836 X14.6687 Y20.5 Z10.1437
 N4837 X13.9565 Y19.0625 Z10.4758
 N4838 X13.1569 Y17.7031 Z10.8487
 N4839 X12.2477 Y16.4062 Z11.2726
 N4840 X11.2327 Y15.2188 Z11.746
 N4841 X10.1614 Y14.1094 Z12.2455
 N4842 X9.0471 Y13.0469 Z12.7651
 N4843 X7.8296 Y12.1562 Z13.3329
 N4844 X5.1551 Y10.7031 Z14.58
 N4845 X4.0162 Y9.7031 Z15.1111
 N4846 X4.1791 Y8.1406 Z15.0351
 N4847 X4.259 Y6.5312 Z14.9978
 N4848 X4.1974 Y4.8906 Z15.0266
 N4849 X4.2161 Y0 Z15.0178
 N4850 X2.7138 Z11.3909
 N4851 X2.6944 Y4.8906 Z11.398
 N4852 X2.7583 Y6.5312 Z11.3747
 N4853 X2.6754 Y8.1406 Z11.4049
 N4854 X2.5065 Y9.7031 Z11.4664
 N4855 X3.6873 Y10.7031 Z11.0366
 N4856 X6.4603 Y12.1562 Z10.0273
 N4857 X7.7228 Y13.0469 Z9.5678
 N4858 X8.8781 Y14.1094 Z9.1473
 N4859 X9.9888 Y15.2188 Z8.743
 N4860 X11.0413 Y16.4062 Z8.36
 N4861 X11.9839 Y17.7031 Z8.0169
 N4862 X12.813 Y19.0625 Z7.7151
 N4863 X13.5514 Y20.5 Z7.4464
 N4864 X14.1833 Y21.9844 Z7.2164
 N4865 X14.7178 Y23.5 Z7.0218
 N4866 X15.175 Y25.0625 Z6.8554
 N4867 X15.5576 Y26.6406 Z6.7162
 N4868 X15.8771 Y28.2344 Z6.5999
 N4869 X16.3679 Y31.4531 Z6.4212
 N4870 X16.7118 Y34.6875 Z6.2961
 N4871 X16.8185 Y36.3125 Z6.2572
 N4872 X16.8089 Y42.8438 Z6.2607
 N4873 X16.0219 Z3.7647
 N4874 X16.0318 Y36.3125 Z3.762
 N4875 X15.9221 Y34.6875 Z3.7914
 N4876 X15.5685 Y31.4531 Z3.8861
 N4877 X15.0641 Y28.2344 Z4.0213
 N4878 X14.7356 Y26.6406 Z4.1093
 N4879 X14.3424 Y25.0625 Z4.2147
 N4880 X13.8724 Y23.5 Z4.3406
 N4881 X13.323 Y21.9844 Z4.4878
 N4882 X12.6734 Y20.5 Z4.6619
 N4883 X11.9144 Y19.0625 Z4.8653
 N4884 X11.0622 Y17.7031 Z5.0936
 N4885 X10.0932 Y16.4062 Z5.3532
 N4886 X9.0114 Y15.2188 Z5.6431
 N4887 X7.8697 Y14.1094 Z5.949
 N4888 X6.6821 Y13.0469 Z6.2672
 N4889 X5.3844 Y12.1562 Z6.615
 N4890 X2.534 Y10.7031 Z7.3787
 N4891 X1.3202 Y9.7031 Z7.704
 N4892 X1.4938 Y8.1406 Z7.6574
 N4893 X1.5791 Y6.5312 Z7.6346
 N4894 X1.5134 Y4.8906 Z7.6522
 N4895 X1.5333 Y0 Z7.6469
 N4896 X0.6837 Z3.8142
 N4897 X0.6633 Y4.8906 Z3.8178
 N4898 X0.7303 Y6.5312 Z3.8059
 N4899 X0.6434 Y8.1406 Z3.8213
 N4900 X0.4664 Y9.7031 Z3.8525
 N4901 X1.7039 Y10.7031 Z3.6343
 N4902 X4.61 Y12.1562 Z3.1218
 N4903 X5.9331 Y13.0469 Z2.8886
 N4904 X7.1439 Y14.1094 Z2.6751
 N4905 X8.3079 Y15.2188 Z2.4698
 N4906 X9.4109 Y16.4062 Z2.2753
 N4907 X10.3988 Y17.7031 Z2.1011
 N4908 X11.2677 Y19.0625 Z1.9479
 N4909 X12.0415 Y20.5 Z1.8115
 N4910 X12.7038 Y21.9844 Z1.6947
 N4911 X13.2639 Y23.5 Z1.5959
 N4912 X13.7431 Y25.0625 Z1.5114
 N4913 X14.144 Y26.6406 Z1.4407
 N4914 X14.4789 Y28.2344 Z1.3817
 N4915 X14.9932 Y31.4531 Z1.291
 N4916 X15.3537 Y34.6875 Z1.2275
 N4917 X15.4655 Y36.3125 Z1.2077
 N4918 X15.4554 Y42.8438 Z1.2095
 N4919 X15.1138 Z-1.3853
 N4920 X15.124 Y36.3125 Z-1.3862
 N4921 X15.0109 Y34.6875 Z-1.3763
 N4922 X14.6463 Y31.4531 Z-1.3444
 N4923 X14.126 Y28.2344 Z-1.2989
 N4924 X13.7873 Y26.6406 Z-1.2692
 N4925 X13.3817 Y25.0625 Z-1.2338
 N4926 X12.897 Y23.5 Z-1.1913
 N4927 X12.3304 Y21.9844 Z-1.1418
 N4928 X11.6604 Y20.5 Z-1.0832
 N4929 X10.8776 Y19.0625 Z-1.0147
 N4930 X9.9987 Y17.7031 Z-0.9378
 N4931 X8.9994 Y16.4062 Z-0.8504
 N4932 X7.8836 Y15.2188 Z-0.7527
 N4933 X6.7062 Y14.1094 Z-0.6497
 N4934 X5.4814 Y13.0469 Z-0.5426
 N4935 X4.143 Y12.1562 Z-0.4255
 N4936 X1.2033 Y10.7031 Z-0.1683
 N4937 X-0.0485 Y9.7031 Z-0.0588
 N4938 X0.1305 Y8.1406 Z-0.0744
 N4939 X0.2184 Y6.5312 Z-0.0821
 N4940 X0.1507 Y4.8906 Z-0.0762
 N4941 X0.1712 Y0 Z-0.078
 N4942 X0 Z-4.
 N4943 X-0.0207 Y4.8906
 N4944 X0.0473 Y6.5312
 N4945 X-0.0409 Y8.1406
 N4946 X-0.2206 Y9.7031
 N4947 X1.036 Y10.7031
 N4948 X3.987 Y12.1562
 N4949 X5.3304 Y13.0469
 N4950 X6.5599 Y14.1094
 N4951 X7.7419 Y15.2188
 N4952 X8.8619 Y16.4062
 N4953 X9.865 Y17.7031
 N4954 X10.7473 Y19.0625
 N4955 X11.5331 Y20.5
 N4956 X12.2056 Y21.9844
 N4957 X12.7743 Y23.5
 N4958 X13.2609 Y25.0625
 N4959 X13.668 Y26.6406
 N4960 X14.0081 Y28.2344
 N4961 X14.5303 Y31.4531
 N4962 X14.8963 Y34.6875
 N4963 X15.0099 Y36.3125
 N4964 X14.9997 Y42.8438
 N4965 G00 Z43.7206
 N4966 M9
 N4967 G90 G00 G49 Z0 M5
 N4968 X0 Y0
 N4969 M30
 N4970 %

Appendix E
Part program of the adopted (Subdivision algorithm)
Quartic Uniform B-spline technique:

N1 G17 G40 G80 G90
N2 T8 M6
N3 M3 S14000
N4 G00 G54 X90. Y-10 .
N5 G43 Z66. H8
N6 M8
N7 G00 Z42.764
N8 G01 Z40.264 F324.7
N9 X90.0128 Y4.2118 F10000.0
N10 X89.941 Y6.2977
N11 X90.264 Y8.169
N12 X90.2599 Y9.7494
N13 X88.6689 Y11.115
N14 X81.9677 Y16.1909
N15 X80.3208 Y17.5535
N16 X78.8341 Y19.0175
N17 X77.6446 Y20.7304
N18 X76.9275 Y22.668
N19 X76.4142 Y24.7055
N20 X76.0002 Y26.7743
N21 X75.6844 Y28.8578
N22 X75.0799 Y35.1018
N23 X74.9652 Y37.1973
N24 X75.0069 Y39.2953
N25 X75.0005 Y43.4974
N26 X74.8119
N27 X74.8182 Y39.2953
N28 X74.7768 Y37.1973
N29 X74.8908 Y35.1018
N30 X75.4915 Y28.8578
N31 X75.8053 Y26.7743
N32 X76.2167 Y24.7055
N33 X76.7268 Y22.668
N34 X77.4393 Y20.7304
N35 X78.6213 Y19.0175
N36 X80.0987 Y17.5535
N37 X81.7353 Y16.1909
N38 X88.3943 Y11.115
N39 X89.9754 Y9.7494
N40 X89.9794 Y8.169
N41 X89.6584 Y6.2977
N42 X89.7298 Y4.2118
N43 X89.717 Y0
N44 X88.8718
N45 X88.8842 Y4.2118
N46 X88.8142 Y6.2977
N47 X89.1292 Y8.169
N48 X89.1252 Y9.7494
N49 X87.574 Y11.115
N50 X81.0409 Y16.1909
N51 X79.4352 Y17.5535
N52 X77.9858 Y19.0175
N53 X76.8261 Y20.7304
N54 X76.127 Y22.668
N55 X75.6266 Y24.7055
N56 X75.223 Y26.7743
N57 X74.9151 Y28.8578
N58 X74.3257 Y35.1018
N59 X74.2139 Y37.1973
N60 X74.2546 Y39.2953
N61 X74.2484 Y43.4974
N62 X73.317
N63 X73.323 Y39.2953
N64 X73.2836 Y37.1973
N65 X73.3919 Y35.1018
N66 X73.9625 Y28.8578
N67 X74.2606 Y26.7743
N68 X74.6514 Y24.7055
N69 X75.1359 Y22.668
N70 X75.8127 Y20.7304
N71 X76.9354 Y19.0175
N72 X78.3387 Y17.5535
.....
N3019 X29.0387 Z20.4022
N3020 X29.0354 Y39.2953 Z20.4076
N3021 X29.0576 Y37.1973 Z20.3722
N3022 X28.9965 Y35.1018 Z20.4694
N3023 X28.6749 Y28.8578 Z20.9812
N3024 X28.5069 Y26.7743 Z21.2486
N3025 X28.2866 Y24.7055 Z21.5992
N3026 X28.0135 Y22.668 Z22.0338
N3027 X27.632 Y20.7304 Z22.641
N3028 X26.9992 Y19.0175 Z23.6481
N3029 X26.2082 Y17.5535 Z24.907
N3030 X25.332 Y16.1909 Z26.3015
N3031 X21.7668 Y11.115 Z31.9755
N3032 X20.9203 Y9.7494 Z33.3227
N3033 X20.9181 Y8.169 Z33.3262
N3034 X21.09 Y6.2977 Z33.0526
N3035 X21.0518 Y4.2118 Z33.1134
N3036 X21.0586 Y0 Z33.1026
N3037 X16.943 Z30.1824
N3038 X16.935 Y4.2118 Z30.1924
N3039 X16.9798 Y6.2977 Z30.1363
N3040 X16.7783 Y8.169 Z30.3888
N3041 X16.7809 Y9.7494 Z30.3856
N3042 X17.7729 Y11.115 Z29.1417
N3043 X21.951 Y16.1909 Z23.9025
N3044 X22.9779 Y17.5535 Z22.6149
N3045 X23.9048 Y19.0175 Z21.4525
N3046 X24.6464 Y20.7304 Z20.5226
N3047 X25.0935 Y22.668 Z19.9619
N3048 X25.4135 Y24.7055 Z19.5606
N3049 X25.6717 Y26.7743 Z19.2369
N3050 X25.8686 Y28.8578 Z18.99
N3051 X26.2455 Y35.1018 Z18.5174
N3052 X26.317 Y37.1973 Z18.4277
N3053 X26.291 Y39.2953 Z18.4603
N3054 X26.295 Y43.4974 Z18.4554
N3055 X23.7864 Z16.2136
N3056 X23.7819 Y39.2953 Z16.2181
N3057 X23.8114 Y37.1973 Z16.1886
N3058 X23.7303 Y35.1018 Z16.2697
N3059 X23.3028 Y28.8578 Z16.6972
N3060 X23.0795 Y26.7743 Z16.9205
N3061 X22.7868 Y24.7055 Z17.2132
N3062 X22.4238 Y22.668 Z17.5762
N3063 X21.9168 Y20.7304 Z18.0832
N3064 X21.0757 Y19.0175 Z18.9243
N3065 X20.0244 Y17.5535 Z19.9756
N3066 X18.8599 Y16.1909 Z21.1401
N3067 X14.1214 Y11.115 Z25.8786
N3068 X12.9964 Y9.7494 Z27.0036
N3069 X12.9935 Y8.169 Z27.0065
N3070 X13.2219 Y6.2977 Z26.7781
N3071 X13.1711 Y4.2118 Z26.8289
N3072 X13.1802 Y0 Z26.8198
N3073 X9.8176 Z23.057
N3074 X9.8076 Y4.2118 Z23.065
N3075 X9.8637 Y6.2977 Z23.0202
N3076 X9.6112 Y8.169 Z23.2217
N3077 X9.6144 Y9.7494 Z23.2191
N3078 X10.8583 Y11.115 Z22.2271
N3079 X16.0975 Y16.1909 Z18.049
N3080 X17.3851 Y17.5535 Z17.0221
N3081 X18.5475 Y19.0175 Z16.0952
N3082 X19.4774 Y20.7304 Z15.3536
N3083 X20.0381 Y22.668 Z14.9065
N3084 X20.4394 Y24.7055 Z14.5865
N3085 X20.7631 Y26.7743 Z14.3283
N3086 X21.01 Y28.8578 Z14.1314
N3087 X21.4826 Y35.1018 Z13.7545
N3088 X21.5723 Y37.1973 Z13.683
N3089 X21.5397 Y39.2953 Z13.709
N3090 X21.5446 Y43.4974 Z13.705
N3091 X19.5978 Z10.9614
N3092 X19.5924 Y39.2953 Z10.9646
N3093 X19.6278 Y37.1973 Z10.9424
N3094 X19.5306 Y35.1018 Z11.0035
N3095 X19.0188 Y28.8578 Z11.3251
N3096 X18.7514 Y26.7743 Z11.4931
N3097 X18.4008 Y24.7055 Z11.7134
N3098 X17.9662 Y22.668 Z11.9865
N3099 X17.359 Y20.7304 Z12.368
N3100 X16.3519 Y19.0175 Z13.0008
N3101 X15.093 Y17.5535 Z13.7918
N3102 X13.6985 Y16.1909 Z14.668
N3103 X8.0245 Y11.115 Z18.2332
N3104 X6.6773 Y9.7494 Z19.0797
N3105 X6.6738 Y8.169 Z19.0819
N3106 X6.9474 Y6.2977 Z18.91
N3107 X6.8866 Y4.2118 Z18.9482
N3108 X6.8974 Y0 Z18.9414
N3109 X4.4564 Z14.5248
N3110 X4.4449 Y4.2118 Z14.5303
N3111 X4.5096 Y6.2977 Z14.4992
N3112 X4.2185 Y8.169 Z14.6393
N3113 X4.2222 Y9.7494 Z14.6376
N3114 X5.6557 Y11.115 Z13.9472
N3115 X11.6932 Y16.1909 Z11.0397
N3116 X13.1771 Y17.5535 Z10.3251
N3117 X14.5166 Y19.0175 Z9.68
N3118 X15.5882 Y20.7304 Z9.164
N3119 X16.2343 Y22.668 Z8.8528
N3120 X16.6968 Y24.7055 Z8.6301
N3121 X17.0698 Y26.7743 Z8.4505
N3122 X17.3543 Y28.8578 Z8.3135
N3123 X17.8989 Y35.1018 Z8.0512
N3124 X18.0023 Y37.1973 Z8.0014
N3125 X17.9647 Y39.2953 Z8.0195
N3126 X17.9704 Y43.4974 Z8.0167
N3127 X16.683 Z4.9086
N3128 X16.677 Y39.2953 Z4.9106
N3129 X16.7164 Y37.1973 Z4.8969
N3130 X16.6081 Y35.1018 Z4.9348
N3131 X16.0375 Y28.8578 Z5.1344
N3132 X15.7394 Y26.7743 Z5.2387
N3133 X15.3486 Y24.7055 Z5.3755
N3134 X14.8641 Y22.668 Z5.545
N3135 X14.1873 Y20.7304 Z5.7818
N3136 X13.0646 Y19.0175 Z6.1747
N3137 X11.6613 Y17.5535 Z6.6657
N3138 X10.1068 Y16.1909 Z7.2097
N3139 X3.7817 Y11.115 Z9.4229
N3140 X2.2799 Y9.7494 Z9.9484
N3141 X2.276 Y8.169 Z9.9498
N3142 X2.581 Y6.2977 Z9.8431
N3143 X2.5132 Y4.2118 Z9.8668
N3144 X2.5252 Y0 Z9.8626
N3145 X1.1282 Z5.0134
N3146 X1.1158 Y4.2118 Z5.0163
N3147 X1.1858 Y6.2977 Z5.0003
N3148 X0.8708 Y8.169 Z5.0722
N3149 X0.8748 Y9.7494 Z5.0713
N3150 X2.426 Y11.115 Z4.7172
N3151 X8.9591 Y16.1909 Z3.2261
N3152 X10.5648 Y17.5535 Z2.8596
N3153 X12.0142 Y19.0175 Z2.5288
N3154 X13.1739 Y20.7304 Z2.2641
N3155 X13.873 Y22.668 Z2.1045
N3156 X14.3734 Y24.7055 Z1.9903
N3157 X14.777 Y26.7743 Z1.8982
N3158 X15.0849 Y28.8578 Z1.8279
N3159 X15.6743 Y35.1018 Z1.6934
N3160 X15.7861 Y37.1973 Z1.6679
N3161 X15.7454 Y39.2953 Z1.6772
N3162 X15.7516 Y43.4974 Z1.6757
N3163 X15.1881 Z-1.641
N3164 X15.1818 Y39.2953 Z-1.6403
N3165 X15.2232 Y37.1973 Z-1.645
N3166 X15.1092 Y35.1018 Z-1.6321
N3167 X14.5085 Y28.8578 Z-1.5644
N3168 X14.1947 Y26.7743 Z-1.5291
N3169 X13.7833 Y24.7055 Z-1.4827
N3170 X13.2732 Y22.668 Z-1.4253
N3171 X12.5607 Y20.7304 Z-1.345
N3172 X11.3787 Y19.0175 Z-1.2118
N3173 X9.9013 Y17.5535 Z-1.0453
N3174 X8.2647 Y16.1909 Z-0.8609
N3175 X11.6057 Y11.115 Z-0.1106
N3176 X0.0246 Y9.7494 Z0.0675
N3177 X0.0206 Y8.169 Z0.068
N3178 X0.3416 Y6.2977 Z0.0318
N3179 X0.2702 Y4.2118 Z0.0398
N3180 X0.283 Y0 Z0.0384
N3181 X0 Z-5 .
N3182 X-0.0128 Y4.2118
N3183 X0.059 Y6.2977
N3184 X-0.264 Y8.169
N3185 X-0.2599 Y9.7494
N3186 X1.3311 Y11.115
N3187 X8.0323 Y16.1909
N3188 X9.6792 Y17.5535
N3189 X11.1659 Y19.0175
N3190 X12.3554 Y20.7304
N3191 X13.0725 Y22.668
N3192 X13.5858 Y24.7055
N3193 X13.9998 Y26.7743
N3194 X14.3156 Y28.8578
N3195 X14.9201 Y35.1018
N3196 X15.0348 Y37.1973
N3197 X14.9931 Y39.2953
N3198 X14.9995 Y43.4974
N3199 G00 Z42.764
N3200 M9
N3201 G90 G00 G49 Z0 M5
N3202 X0 Y0
N3203 M30
N3204%

Part program of the adopted (Subdivision algorithm)

Quintic Uniform B-spline technique:

N1 G17 G40 G80 G90
 N2 T6 M6
 N3 M3 S18000
 N4 G00 G54 X90. Y-10.
 N5 G43 Z68. H6
 N6 M8
 N7 G00 Z44.8595
 N8 G01 Z42.3595 F143.2
 N9 X90.007 Y5.9216 F10000.0
 N10 X89.8818 Y7.3961
 N11 X90.3595 Y8.7803
 N12 X89.9118 Y10.0666
 N13 X88.6244 Y10.7569
 N14 X85.8721 Y11.9494
 N15 X84.5872 Y12.6131
 N16 X83.3761 Y13.4794
 N17 X82.338 Y14.5491
 N18 X81.4732 Y15.7126
 N19 X80.6452 Y16.9854
 N20 X79.8961 Y18.2515
 N21 X79.2059 Y19.5302
 N22 X78.5456 Y20.8836
 N23 X77.9587 Y22.2375
 N24 X76.9398 Y25.0183
 N25 X75.6179 Y29.2512
 N26 X75.2323 Y30.6596
 N27 X74.9888 Y32.1135
 N28 X74.9362 Y33.5976
 N29 X75.0166 Y38.04
 N30 X75.0001 Y43.9498
 N31 X74.9076
 N32 X74.918 Y36.5818
 N33 X74.8439 Y33.5976
 N34 X74.8964 Y32.1135
 N35 X75.1391 Y30.6596
 N36 X75.9545 Y27.8362
 N37 X76.8413 Y25.0183
 N38 X77.8571 Y22.2375
 N39 X78.4422 Y20.8836
 N40 X79.1004 Y19.5302
 N41 X79.7885 Y18.2515
 N42 X80.5354 Y16.9854
 N43 X81.3608 Y15.7126
 N44 X82.2229 Y14.5491
 N45 X83.2578 Y13.4794
 N46 X84.4652 Y12.6131
 N47 X85.7461 Y11.9494
 N48 X88.4899 Y10.7569
 N49 X89.7733 Y10.0666
 N50 X90.2197 Y8.7803
 N51 X89.7434 Y7.3961
 N52 X89.8683 Y5.9216
 N53 X89.8613 Y0
 N54 X89.446
 N55 X89.4529 Y5.9216
 N56 X89.3292 Y7.3961
 N57 X89.8011 Y8.7803
 N58 X89.3588 Y10.0666
 N59 X88.0873 Y10.7569
 N60 X85.3689 Y11.9494
 N61 X84.0998 Y12.6131
 N62 X82.9036 Y13.4794
 N63 X81.8783 Y14.5491
 N64 X81.0242 Y15.7126
 N65 X80.2064 Y16.9854
 N66 X79.4664 Y18.2515
 N67 X78.7847 Y19.5302
 N68 X78.1326 Y20.8836
 N69 X77.553 Y22.2375
 N70 X76.5466 Y25.0183
 N71 X75.241 Y29.2512
 N72 X74.8601 Y30.6596

 N5274 X19.2228 Y30.6596 Z12.7963
 N5275 X18.5254 Y27.8362 Z13.2237
 N5276 X17.7668 Y25.0183 Z13.6885
 N5277 X16.8981 Y22.2375 Z14.2209
 N5278 X16.3976 Y20.8836 Z14.5275
 N5279 X15.8347 Y19.5302 Z14.8725
 N5280 X15.2462 Y18.2515 Z15.2331
 N5281 X14.6074 Y16.9854 Z15.6246
 N5282 X13.9015 Y15.7126 Z16.0572
 N5283 X13.1641 Y14.5491 Z16.5091
 N5284 X12.279 Y13.4794 Z17.0514
 N5285 X11.2464 Y12.6131 Z17.6843
 N5286 X10.1508 Y11.9494 Z18.3556
 N5287 X7.8041 Y10.7569 Z19.7937
 N5288 X6.7064 Y10.0666 Z20.4663
 N5289 X6.3246 Y8.7803 Z20.7003
 N5290 X6.732 Y7.3961 Z20.4507
 N5291 X6.6252 Y5.9216 Z20.5161
 N5292 X6.6312 Y0 Z20.5124
 N5293 X4.9047 Z17.4296
 N5294 X4.8985 Y5.9216 Z17.4328
 N5295 X5.01 Y7.3961 Z17.3759
 N5296 X4.5844 Y8.7803 Z17.5928
 N5297 X4.9833 Y10.0666 Z17.3895
 N5298 X6.1304 Y10.7569 Z16.805
 N5299 X8.5827 Y11.9494 Z15.5555
 N5300 X9.7275 Y12.6131 Z14.9722
 N5301 X10.8067 Y13.4794 Z14.4224
 N5302 X11.7316 Y14.5491 Z13.9511
 N5303 X12.5021 Y15.7126 Z13.5585
 N5304 X13.2399 Y16.9854 Z13.1826
 N5305 X13.9074 Y18.2515 Z12.8425
 N5306 X14.5223 Y19.5302 Z12.5291
 N5307 X15.1106 Y20.8836 Z12.2294
 N5308 X15.6336 Y22.2375 Z11.9629
 N5309 X16.5414 Y25.0183 Z11.5004
 N5310 X17.7192 Y29.2512 Z10.9002
 N5311 X18.0629 Y30.6596 Z10.7252
 N5312 X18.2798 Y32.1135 Z10.6146
 N5313 X18.3266 Y33.5976 Z10.5908
 N5314 X18.255 Y38.04 Z10.6273
 N5315 X18.2697 Y43.9498 Z10.6198
 N5316 X17.2835 Z8.4805
 N5317 X17.2739 Y36.5818 Z8.4845
 N5318 X17.3425 Y33.5976 Z8.4561
 N5319 X17.294 Y32.1135 Z8.4762
 N5320 X17.069 Y30.6596 Z8.5694
 N5321 X16.3134 Y27.8362 Z8.8824
 N5322 X15.4915 Y25.0183 Z9.2228
 N5323 X14.5501 Y22.2375 Z9.6128
 N5324 X14.0079 Y20.8836 Z9.8374
 N5325 X13.3979 Y19.5302 Z10.09
 N5326 X12.7602 Y18.2515 Z10.3541
 N5327 X12.0681 Y16.9854 Z10.6408
 N5328 X11.3032 Y15.7126 Z10.9577
 N5329 X10.5042 Y14.5491 Z11.2886
 N5330 X9.5452 Y13.4794 Z11.6859
 N5331 X8.4262 Y12.6131 Z12.1494
 N5332 X7.2391 Y11.9494 Z12.6411
 N5333 X4.6963 Y10.7569 Z13.6943
 N5334 X3.5069 Y10.0666 Z14.187
 N5335 X3.0933 Y8.7803 Z14.3583
 N5336 X3.5346 Y7.3961 Z14.1755
 N5337 X3.4189 Y5.9216 Z14.2234
 N5338 X3.4254 Y0 Z14.2208
 N5339 X2.2025 Z10.9058
 N5340 X2.1958 Y5.9216 Z10.9079
 N5341 X2.3149 Y7.3961 Z10.8692
 N5342 X1.8605 Y8.7803 Z11.0169
 N5343 X2.2864 Y10.0666 Z10.8785
 N5344 X3.5108 Y10.7569 Z10.4807
 N5345 X6.1283 Y11.9494 Z9.6302
 N5346 X7.3503 Y12.6131 Z9.2331
 N5347 X8.5022 Y13.4794 Z8.8589
 N5348 X9.4894 Y14.5491 Z8.5381
 N5349 X10.3119 Y15.7126 Z8.2708
 N5350 X11.0994 Y16.9854 Z8.015
 N5351 X11.8119 Y18.2515 Z7.7835
 N5352 X12.4683 Y19.5302 Z7.5702
 N5353 X13.0962 Y20.8836 Z7.3662
 N5354 X13.6544 Y22.2375 Z7.1848
 N5355 X14.6234 Y25.0183 Z6.8699
 N5356 X15.8806 Y29.2512 Z6.4615
 N5357 X16.2474 Y30.6596 Z6.3423
 N5358 X16.4789 Y32.1135 Z6.2671
 N5359 X16.529 Y33.5976 Z6.2508
 N5360 X16.4525 Y38.04 Z6.2756
 N5361 X16.4682 Y43.9498 Z6.2705
 N5362 X15.8288 Z4.0034
 N5363 X15.8186 Y36.5818 Z4.0058
 N5364 X15.8909 Y33.5976 Z3.9885
 N5365 X15.8398 Y32.1135 Z4.0007
 N5366 X15.6031 Y30.6596 Z4.0576
 N5367 X14.8078 Y27.8362 Z4.2485
 N5368 X13.9427 Y25.0183 Z4.4562
 N5369 X12.9519 Y22.2375 Z4.6941
 N5370 X12.3812 Y20.8836 Z4.8311
 N5371 X11.7392 Y19.5302 Z4.9852
 N5372 X11.0681 Y18.2515 Z5.1463
 N5373 X10.3396 Y16.9854 Z5.3212
 N5374 X9.5346 Y15.7126 Z5.5145
 N5375 X8.6936 Y14.5491 Z5.7164
 N5376 X7.6843 Y13.4794 Z5.9587
 N5377 X6.5066 Y12.6131 Z6.2415
 N5378 X5.2572 Y11.9494 Z6.5414
 N5379 X2.581 Y10.7569 Z7.1839
 N5380 X1.3291 Y10.0666 Z7.4844
 N5381 X0.8938 Y8.7803 Z7.589
 N5382 X1.3583 Y7.3961 Z7.4774
 N5383 X1.2365 Y5.9216 Z7.5067
 N5384 X1.2434 Y0 Z7.505
 N5385 X0.554 Z4.0396
 N5386 X0.5471 Y5.9216 Z4.0406
 N5387 X0.6708 Y7.3961 Z4.0211
 N5388 X0.1989 Y8.7803 Z4.0958
 N5389 X0.6412 Y10.0666 Z4.0257
 N5390 X1.9127 Y10.7569 Z3.8244
 N5391 X4.6311 Y11.9494 Z3.3938
 N5392 X5.9002 Y12.6131 Z3.1928
 N5393 X7.0964 Y13.4794 Z3.0033
 N5394 X8.1217 Y14.5491 Z2.841
 N5395 X8.9758 Y15.7126 Z2.7057
 N5396 X9.7936 Y16.9854 Z2.5761
 N5397 X10.5336 Y18.2515 Z2.4589
 N5398 X11.2153 Y19.5302 Z2.351
 N5399 X11.8674 Y20.8836 Z2.2477
 N5400 X12.447 Y22.2375 Z2.1559
 N5401 X13.4534 Y25.0183 Z1.9965
 N5402 X14.759 Y29.2512 Z1.7897
 N5403 X15.1399 Y30.6596 Z1.7294
 N5404 X15.3804 Y32.1135 Z1.6913
 N5405 X15.4323 Y33.5976 Z1.6831
 N5406 X15.353 Y38.04 Z1.6956
 N5407 X15.3693 Y43.9498 Z1.693
 N5408 X15.0924 Z-0.6462
 N5409 X15.082 Y36.5818 Z-0.6454
 N5410 X15.1561 Y33.5976 Z-0.6512
 N5411 X15.1036 Y32.1135 Z-0.6471
 N5412 X14.8609 Y30.6596 Z-0.628
 N5413 X14.0455 Y27.8362 Z-0.5638
 N5414 X13.1587 Y25.0183 Z-0.494
 N5415 X12.1429 Y22.2375 Z-0.4141
 N5416 X11.5578 Y20.8836 Z-0.368
 N5417 X10.8996 Y19.5302 Z-0.3162
 N5418 X10.2115 Y18.2515 Z-0.2621
 N5419 X9.4646 Y16.9854 Z-0.2033
 N5420 X8.6392 Y15.7126 Z-0.1383
 N5421 X7.7771 Y14.5491 Z-0.0705
 N5422 X6.7422 Y13.4794 Z0.011
 N5423 X5.5348 Y12.6131 Z0.106
 N5424 X4.2539 Y11.9494 Z0.2068
 N5425 X1.5101 Y10.7569 Z0.4227
 N5426 X0.2267 Y10.0666 Z0.5237
 N5427 X-0.2197 Y8.7803 Z0.5589
 N5428 X0.2566 Y7.3961 Z0.5214
 N5429 X0.1317 Y5.9216 Z0.5312
 N5430 X0.1387 Y0 Z0.5307
 N5431 X0 Z-3.
 N5432 X-0.007 Y5.9216
 N5433 X0.1182 Y7.3961
 N5434 X-0.3595 Y8.7803
 N5435 X0.0882 Y10.0666
 N5436 X1.3756 Y10.7569
 N5437 X4.1279 Y11.9494
 N5438 X5.4128 Y12.6131
 N5439 X6.6239 Y13.4794
 N5440 X7.662 Y14.5491
 N5441 X8.5268 Y15.7126
 N5442 X9.3548 Y16.9854
 N5443 X10.1039 Y18.2515
 N5444 X10.7941 Y19.5302
 N5445 X11.4544 Y20.8836
 N5446 X12.0413 Y22.2375
 N5447 X13.0602 Y25.0183
 N5448 X14.3821 Y29.2512
 N5449 X14.7677 Y30.6596
 N5450 X15.0112 Y32.1135
 N5451 X15.0638 Y33.5976
 N5452 X14.9834 Y38.04
 N5453 X14.9999 Y43.9498
 N5454 G00 Z44.8595
 N5455 M9
 N5456 G90 G00 G49 Z0 M5
 N5457 X0 Y0
 N5458 M30
 N5459 %

الخلاصة

تركز هذه الأطروحة على التصميم والتصنيع بمساعدة الحاسوب (CAM/CAD)، وحوارزمية التقسيم الى اجزاء صغيرة، والمفهوم النظري المعتمد في تصميم القوالب، مفهوم ثبات نسب الانفعال المتجانس (CRHS).

إنّ تكوين ثوابت السطوح الناعمة لها الأهمية المركزية في الهندسة الميكانيكية. ولتشغيل شكل باستعمال الحاسوب فانه يجب انتاج وصف حاسوب متوافق لذلك الشكل.

تمت مقارنة بين سطح ولد بطريقة CRHS وسطوح ولدت بتقنيات التقريب (Quartic Uniform B-spline technique and Quantic Uniform B-spline technique).

ان شكل قالب البثق هو مثال تمهيدي صنع بواسطة عملية تصنيع مؤتمتة (CNC). كما ان السطح الناتج من طريقة حوارزمية التقسيم (Chaitian) التي وضفت في هذه الاطروحة هو سطح دقيق وكفوء خصوصا في السطوح الثلاثية الابعاد.

في هذا البحث تبنيت وطورت حوارزمية التقسيم (Chaitian) في حالة تقنيه ال (Uniform B-spline) لتحديد نصف قطر الاداة الامثل (شبه عملية انهاء سطحي)، وفتيجة نصف قطر الاداة في حاله سطح شكل القالب المصمم بطريقة (CRHS) هو (4mm) بينما في حالة السطح المولد بطريق (B-spline Quartic Uniform) هو (5mm)، وللسطح المولد بطريق (Quantic Uniform B-spline) هو (3mm)، هذه النتائج تحسن دقة السطوح المشغلة مع زيادة تكرار التقسيم وذلك يؤثر مباشرة على تصميم (side step) والذي يقود الى تغيير طول وتصميم مسار الاداة.

ان البيانات التصميمية للسطوح المطلوبة صممت بواسطة برنامج (Matlab) والتي نقلت الى برنامج (Surfcam) للحصول على محاكاة عملية التشغيل وبرامج (G-code) لثلاث عينات (صممت بواسطة CRHS وتقنية التقريب) ان برامج (G-code) صممت لنظام

(FANUC 15 MB system ثلاثي المحاور)، كما انها نفذت على ماكينة القطع المبرمج

(Hermle C30U dynamic) ذات خمس محاور حركية ومعدن العينات هو UREOL

(Epoxy Resin) لذلك فان هذه العملية انجزت بدون استخدام سوائل تبريد.



جمهورية العراق
وزارة التعليم العالي والبحث العلمي
الجامعة التكنولوجية
قسم هندسة الانتاج والمعادن

تحليلات السطوح المقسمة وتطبيقها

اطروحة تقدم بها

مقدم حبيب شمعون

الى قسم هندسة الانتاج والمعادن-الجامعة التكنولوجية
وهي جزء من متطلبات درجة الماجستير في
علوم هندسة الانتاج

بأشراف

د.قاسم عبد الحسن خلف

د.ليث عبد الله محمد

تموز ٢٠٠٧